THE UNIVERSITY OF ASTON IN BIRMINGHAM

(Department of Chemical Engineering)

OXYGEN MASS-TRANSFER IN TOWER FERMENTERS

by

ALAN WALTER DOWEN

being a thesis submitted in support of an application for the degree of Doctor of Philosophy.

February 1979

SUMMARY

Oxygen Mass-Transfer in Tower Fermenters

Alan Walter Dowen

Ph.D. Thesis · 1979

The research described in this thesis is concerned with tower fermenters and the measurement of the rate of oxygen mass-transfer in such systems using fast-response oxygen electrodes.

Consideration has been given to ways of modelling the behaviour of fast-response probes and to the evaluation of mass-transfer coefficients from the results of unsteady-state experiments. The effects of gas flow-rate, nutrient concentration, antifoams and microbial concentration on mass-transfer have been studied in detail: superficial air velocity and the presence of anti-foams are shown to be the most important factors. Measurements with the oxygen electrode have also been used to estimate microbial respiration rates during work on the batch growth of the filamentous fungus Aspergillus niger.

Gas holdup in tower fermenters has been investigated since this provides valuable information about the behaviour of the gas phase. A manometric method of measurement was used except when the fermenters were run aseptically: in such cases a light-transmittance technique was employed. The factors found to have the greatest effect on gas holdup were the superficial gas velocity and the presence of nutrients and anti-foams. It was not possible to make meaningful estimates of average bubble size using photographic methods: nevertheless, valuable qualitative information was obtained and this has been used to interpret both the mass-transfer and gas holdup measurements.

Keywords : OXYGEN MASS-TRANSFER

TOWER-FERMENTERS

LIST OF CONTENTS

LIST OF FIGURES

LIST OF TABLES

ACKNOWLEDGMENTS.

The author wishes to express his thanks to:

(1) The Science Research Council for financial assistance in the form of a Research Studentship.

(2) Professor G.V. Jeffreys and the staff of the Chemical Engineering Department for their assistance.

(3) Dr. E.L. Smith for his supervision and guidance throughout the course of this research.

(4) Dr. R.N. Greenshields, Dr. M. Fidgett, Dr. S.D. Pannell, Dr. R.A. Spensley and all other members of the Tower Fermentation Group for their helpful suggestions.

(5) Mrs. J. Heath for her help with the typing of this thesis.

(6) My wife for her moral support and patience.

1. INTRODUCTION

1 Introduction.

During the last decade an increasing amount of attention has been given to continuous fermentation systems for both the production of metabolites and single cell protein (SCP). Maximum microbial growth theoretically occurs in well mixed systems, whereas maximum metabolite production may require a plug-flow or multi-stage system (1). The A.P.V. Co. Ltd. of Sussex were first to use a tower fermenter commercially for the production of beer, but it may be operated in such a way as to fulfil either of the above conditions. Essentially this type of fermenter consists of a vertical reactor, usually without baffles, and it has been described in several papers (2,3,4).

The design of such fermentation systems and their applications are the subjects of research at the University of Aston in Birmingham. The work was initiated by Dr. R. N. Greenshields in the Department of Biological Sciences, and his collaboration with Dr. E. L. Smith led to the formation of the Tower Fermentation Research Group, which consists of both biological scientists and chemical engineers. The microbiological aspects of the research involve studies of possible applications of tower fermenters: beer and vinegar fermentations and bio-mass production using moulds have been given special attention (5, 6,7). The chemical engineering aspects are concerned with the design, scale-up and operation of tower fermenters for both aerobic and anaerobic conditions.

The overall engineering experimental programme has been divided into several projects:-

(1) properties of suspensions of micro-organisms,

(2) behaviour of single bubbles in suspensions of micro-organisms,

(3) behaviour of bubble swarms in tower fermenters,

(4) properties of microbial aggregates and their behaviour in tower fermenters,

(5) mass-transfer in gas-liquid-solid systems in towers,

(6) heat transfer studies in gas-liquid-solid systems in towers,

and (7) development of mathematical models to aid design, scale-up and operation of tower systems.

The author's research is concerned with project 5. The aim is to look at the engineering aspects of oxygen mass-transfer with particular reference to the estimation of transfer rates. Oxygen transfer has long been a challenging problem to fermentation technologists. Unlike most of the other microbial nutrients which can be dissolved in the substrate in large amounts, oxygen, limited by its low solubility in aqueous broths, has to be supplied continuously. The rate of oxygen supply can be, and often is, the controlling factor of the overall fermentation process. In such cases it is generally agreed that the best scale-up method is to maintain a constant volumetric oxygen mass-transfer coefficient (8).

The majority of previously documented work has been concerned with stirred fermenters, although many of the techniques used for measuring oxygen transfer and the theories involved still hold for tower systems after only minor modifications.

This thesis is divided into six main sections. Following a description of the experimental programme in section 2 the techniques available for measuring gas hold-up and oxygen mass-transfer rates are outlined in section 3. In section 4 the experimental apparatus is described and a summary of the experimental methods is given. The results obtained in the experimental work are presented in section 5 and are then discussed and compared with those of other workers in

section 6. Finally, the conclusions and recommendations for future work are presented in section 7.

The literature survey has been spread throughout the thesis, articles being drawn upon at the point where they are of most interest for either descriptive or comparative reasons. A list of references has also been included separately for each section.

The experimental results obtained during this work have been included in Appendix 2 as a complete record for the benefit and for the use of other members of the Tower Fermentation Research Group.

References (Section 1)

(1) GRIEVES, R.B., PIPES, W.O, MILBURY, W.F. and WOOD, R.K., J. Appl. Chem., 14, 478 (1964)

(2) ROYSTON, M.G., Process Biochem., July, 215 (1966)

(3) GREENSHIELDS, R.N. and SMITH, E.L., Chem. Engr., (249), 182 (1971)

(4) MORRIS, G.G., GREENSHIELDS, R.N. and SMITH, E.L., Biotechnol. Bioeng. Symp. No. 4, 535 (1973)

(5) COOTE, S.D.J., Ph.D. Thesis, University of Aston in Birmingham (1974)

(6) PANNELL, S.D., Ph.D. Thesis, University of Aston in Birmingham (1976)

(7) SPENSLEY, R.A., Ph.D. Thesis, University of Aston in Birmingham (1977)

(8) BANDYOPADHYAY, B., HUMPHREY, A.E. and TAGUCHI, H., Biotechnol. Bioeng., 9, 533 (1967)

2. EXPERIMENTAL PROGRAMME

2 Experimental Programme.

The experimental programme may be divided into three areas:-

(1) Gas holdup

(2) Oxygen mass transfer in tower fermenters

(3) A qualitative study of the action of antifoams.

In this section details are given of the experimental programme and the procedures used.

In all areas the complexity of the experimental system was increased gradually. Air-water dispersions were used first: then studies were made of a two-phase system of air and substrate (M1SM), before a three-phase fermentation system was investigated. The effect of antifoams was also considered at each stage.

The air-water system was used to obtain an understanding of the overall problem of holdup and oxygen transfer measurement without the need for sterilization of either equipment or other materials used. Also, because of the existence of published data for this system, it was possible to check that the basic equipment was operating satisfactorily. Unlike other workers who used distilled water, for example Heineken (1), Birmingham tap water was used.

The liquid fermentation medium used, M1SM, was developed by Pannell (2) for his work with Aspergillus niger. It was a solution of molasses, salts and sugars and it was used at concentrations of 0.5%, 2.75% and 5% w/w. Further details of the medium are given in Appendix 1.

On completion of the ground work with the above systems the procedures which had been developed were used in the study of an A. niger fermentation. The fermentation was usually run for three days

Table 2.1 - The Experimental Programme.

System.	Measurements.	Col.d. (mm)	T. (°C)	Comments.
Air-water.	ε	152	ambient	Confirmation of work by Shayegan-Salek.
	ε, k_La	102	25-35	Preliminary information on two phase system.
Air-MlSM (0.5, 2.75, 5.0% $^{w}/_{w}$)	ε, k_La	102	30	Three concentrations of MlSM. Experiments to provide background data for fermentations.
Air-MlSM-Silcolapse. Air-MiSM-P2000.	ε, k_La	102	30	Effect of antifoams on measured parameters.
Air-A.niger-MlSM	k_La, R	102	30	Measurements of parameters in a fermentation situation.

and measurements were made every hour.

A summary of the overall experimental programme is given in table 2.1.

2.1 Gas Holdup.

This section of the programme was undertaken to confirm the results reported by Shayegan-Salek (3) in his work with a similar fermenter and to develop a method for measuring gas holdup compatible with an aseptic system. Gas holdup is an important parameter in a fermentation system because, for a dispersion of bubbles of a uniform size, it provides an estimate of the area available for mass transfer between the gas and the liquid.

A manometric method of measurement, described in a later section, was used first. Superficial gas velocities between 10 and 50 mm s^{-1} were considered. At about 50 mm s^{-1} gas slugs began to develop. In a fermentation this would be detrimental due to the possible carry over of micro-organism from the system and to the decrease in the surface area available for oxygen mass-transfer. Preliminary experiments, which were used to develop the method fully, were made in a 152 mm diameter column. Here, a range of liquid superficial velocities was also used; the maximum liquid velocity was limited to 20 mm s^{-1} by the pumping capability of the rig.

Later experiments were made using a 102 mm diameter column. This column was equipped as a fermentation unit and further experimentation was planned accordingly. Whilst a similar range of superficial gas velocities was used, only a stationary liquid phase was considered. This was because in fermentations carried out in the laboratory the rate of liquid addition was so low as to be negligible. However, a range of operating temperatures, 25 - 35°C, was included; the larger column mentioned previously had no facilities for temperature control. During the work with fermentation media, and indeed the fermentation itself, the temperature was maintained at 30°C, this being the optimum temperature for growth of A. niger (4).

Unfortunately, during a fermentation the manometric technique for the measurement of gas holdup could not be used for two reasons. Firstly, the manometers were open to the atmosphere, a situation which would allow the ingress of contaminants. Secondly, the sample tubes, which are inserted into the column to make the connection between the system and the manometers, would quickly become blocked with organism from within the fermenter. Consequently, a second method of holdup measurement based on the transmittance of light was sought and developed. A calibration of this method was made against the manometric technique so that it could be used independently when aseptic conditions were required.

2.2 Oxygen Mass-transfer in Tower Fermenters.

The transfer of oxygen during a fermentation from a gas bubble to a living cell via a liquid medium may be described by a series of steps. Arnold and Steel (5) list seven such steps, each with its own resistance to transfer. The overall resistance is equal to the sum of the individual resistances, but it is often the transfer of oxygen across the gas-liquid interface which limits the rate of the overall transfer process (6). When material is transferred across an interface the resistance to transfer causes a concentration gradient in each phase (figure 2.1). The concentrations of the transferring material in the two phases at the interface are generally unequal but are related by the laws of thermodynamic equilibrium. If the equilibrium relationship between the concentration in the gas phase and that in the liquid phase is linear, it it not necessary to consider individual interfacial compositions in order to calculate transfer rates; indeed these would be very difficult to measure. Rather, by using an overall mass-transfer coefficient in these cases, the rate of transfer may be calculated from the product of the mass-transfer coefficient and the difference between the concentration in one phase and the concentration of the solute which

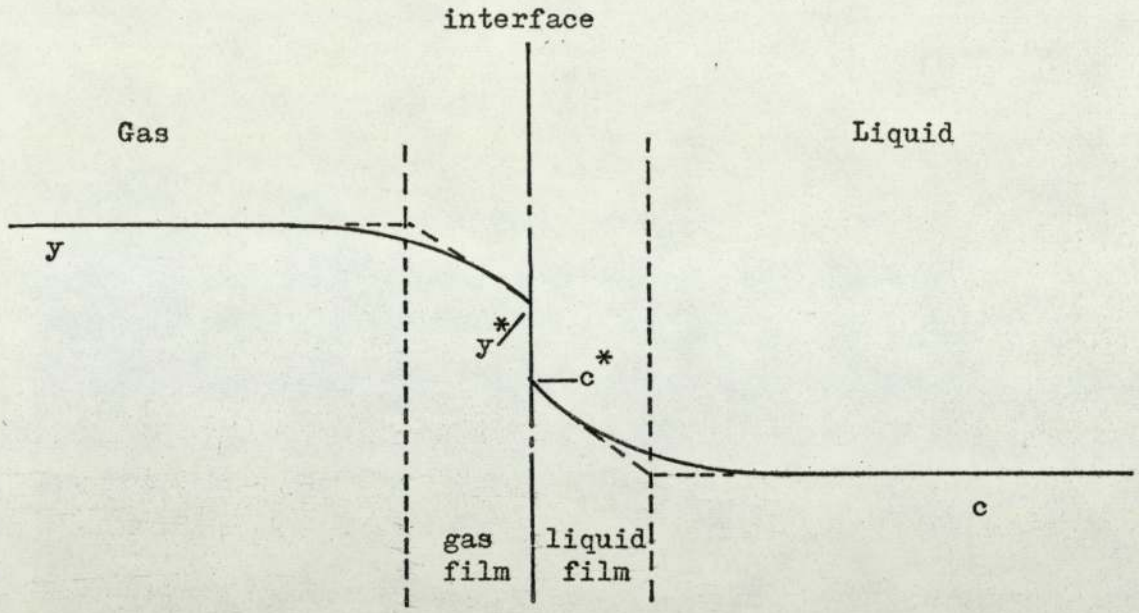

Figure 2.1 Schematic Diagram of the Concentration Gradient Between a Liquid and Gas During Mass-Transfer.

would be in equilibrium with the second phase. Hence

$$N = k_L (c^* - c) \qquad (1)$$

More commonly, the transfer rate is based on unit volume of the system. Thus we arrive at the expression

$$\frac{dc}{dt} = k_L a (c^* - c) \qquad (2)$$

where a is the specific surface of the gaseous phase. It is this equation which forms the basis for much of the work described here.

Oxygen mass-transfer rates were measured using fast response oxygen electrodes (refer to section 3). This is acceptable, provided that the response rate of the electrode is greater than the rate limiting step controlling the transfer of oxygen. Calibration experiments were made to measure the response rate of two types of electrode. These electrodes were based on the designs of Clark (7) and Johnson et alia (8). However, because of the results obtained, only the electrode based on the design of Clark was used in further series of experiments. The effect of temperature was also considered so that adjustments could be made if they were found to be necessary.

Mass-transfer experiments in the tower system were based on a method for the dynamic measurement of the overall mass-transfer coefficient reported by Taguchi and Humphrey (9). This technique is described in detail in section 4. However, in their original work no attempt was made to account for the response characteristics of the oxygen electrode. They evaluated the method by experimentation with systems containing either a yeast, Saccharomyces cerevisiae, or a mould, Aspergillus niger, in stirred vessels with volumes of 5 and 14 l. The work progressed further in collaboration with Bandyopadhyay (10), who investigated the effect of prolonged oxygen starvation on living organisms when dynamic measurements were being made. Their conclusions were that a critical dissolved oxygen concentration exists above which there is no effect on the organism. At concentrations below this there is a temporary effect on the organism which exhibits exponential recovery with time. For this reason they recommended that prolonged oxygen starvation should be avoided.

In later work (11) an allowance was made for the response of the oxygen electrode. Having assumed that the electrode exhibits a first order response, the following expression was developed for the variation of the concentration of dissolved oxygen, corresponding to the sensor reading (c_p), with time in response to a step change in the dissolved oxygen level.

$$c_p = c^* \left[1 + \frac{k_L a}{(k - k_L a)} \cdot \exp(-kt) - \frac{k}{(k - k_L a)} \cdot \exp(-k_L a t) \right] \qquad (3)$$

This expression is similar in part to that developed at an earlier date by Heineken (12), and later simplified by Linek (13). Heineken tested his model by experimentation with Bacillus subtilis in stirred fermenters of 5 and 120 l capacities. It was found that the faster the electrode response the simpler the model to describe it became.

Respiration data for B. subtilis obtained using an electrode manufactured by the Lee Scientific Company of Chelsea, Massachusetts, compared favorably with growth rates determined by turbidity measurements, thus further confirming the validity of the dynamic measurement technique.

Having arrived at a measurement technique and a method to allow for electrode response rates and their effect on mass-transfer measurements, one problem still remained in relation to work with a tower fermenter system. All of the work reported above was done using stirred fermenters. In such systems interruption of aeration, a requirement of the dynamic measurement technique, has no effect on the homogeneneity of the suspension of micro-organisms. With a tower fermenter interruption of aeration removes all source of mixing from the system and leads to the separation of the micro-organism due to the effect of gravity. Hsu et alia (14) used a sieve-tray column as a fermenter, and in order to prevent settling of the organism during their mass-transfer studies the air flow was not discontinued but reduced. The organism was then allowed to reduce the concentration of dissolved oxygen so providing a step change effect when the aeration rate was returned to its original level. The method was found to work satisfactorily but a direct assessment of respiration levels of the organism could not be made. It was found, however, that the respiration level could be calculated from the saturated oxygen concentration when equilibrium existed between the transfer of oxygen from the gas bubbles to the liguid phase and the rate of usage by the organism.

In many of the experiments contained in this thesis it was necessary to operate the apparatus without organisms present in order to obtain transfer data for the simpler two-phase systems. The dissolved oxygen level was therefore reduced by blowing an inert

gas (oxygen - free nitrogen) through the column. This method of operation was also used during fermentations but care had to be taken to ensure that the period of oxygen starvation of the organism was kept to a minimum.

2.3 Qualitative Study of The Action of Antifoams.

Many fermentations require high rates of aeration and mixing. These conditions, together with the types of nutrient used, provide an ideal situation for foam formation: if pure liquids were used foam formation would not be favoured on thermodynamic grounds. In an aseptic situation, if the foam remains uncontrolled, the exit air filter may become wetted leading to a risk of infection. Foams may also cause the preferential removal of the micro-organism by floatation and an effective decrease in the available volume of the fermenter. Consequently, in fermentation technology, it is the prevention or destruction of foams that is important.

A true foam is a coarse dispersion of a gas in a liquid such that the bulk density approaches that of the gas rather than that of the liquid. This occurs when the liquid between two bubbles thins down to a lamella instead of rupturing at the point of closest approach. Metastability may be conferred on a foam by a solute that is positively adsorbed to the liquid surface and requires work to remove it from there to the liquid bulk.

Surfactants of this type impart film elasticity. Surface activity in aqueous solutions arises from the possession of hydrophilic and hydrophobic groups by one molecule. The hydrophobe is squeezed out of solution whilst the hydrophilic portion is retained by the attraction between it and the water molecules. If this occurs at the surfaces of a lamella which is then stretched, the concentration of the surfactant

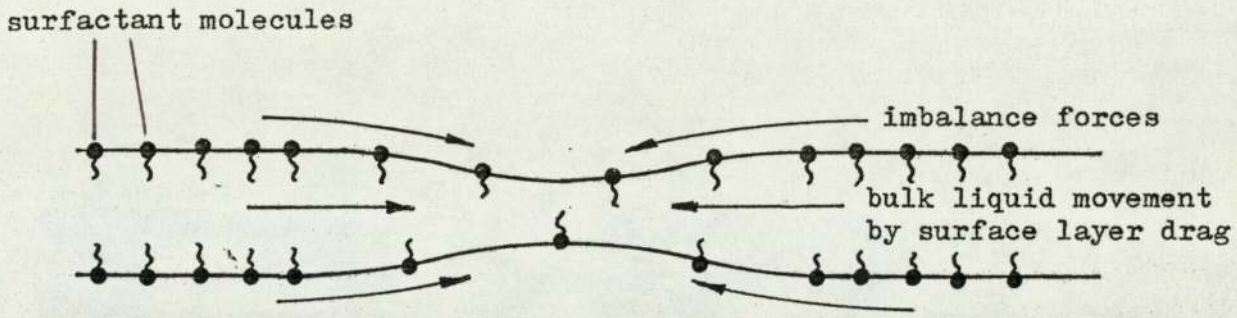

Figure 2.2 Gibbs-Marangoni Elasticity - Film Elasticity Due to the Presence of Surfactant Molecules.

is decreased at the thinnestspot, which is most likely to rupture (see figure 2.2). The resulting imbalance of forces causes the surface surrounding that region to move towards the thinned spot to equalise the surface tensions. This movement of the surface layer drags along layers of the underlying bulk so preventing further thinning, an effect often referred to as Gibbs-Marangoni elasticity.

Surface tension is not the sole factor affecting foam stability; high bulk and surface viscosities also retard drainage from the lamellae within a foam. In fact surface viscosity and foam stability show a good correlation (15). Protein solutions exhibit both high surface viscosity and surface tension and produce stable foams.

Foam breakdown may either be obtained mechanically or by the addition of a chemical 'anti-foam'. Mechanical foam-breakers have included rotating paddles, ultrasonic whistles and devices based on fluid acceleration through nozzles: hot-wire grids suspended above the liquid level have also been used. Whilst these methods have been shown to be effective, their application to the simple tower fermenter

layout is limited and so they have not been considered further in this work.

Chemical antifoams, which can prevent foam formation or destroy an existing foam, are in wide use in the fermentation industry and are themselves surface active. They appear to act by competitively replacing the surface active compounds causing the foaming, whilst being unable themselves to produce stable foams due to surface tension or viscosity effects. Many types of antifoams are used commercially although few possess the features listed by Solomons (16) viz:

1. fast knock down of an existing foam
2. long lasting action to prevent reformation of the foam
3. high efficiency i.e. active in low concentrations
4. non-toxic to the micro-organisms, animals or humans
5. no effect on start-up procedures
6. low flammability
7. cheapness
8. minimal effect on oxygen-transfer rates
9. non-metabolisable by the micro-organism

The ideal antifoam should also have low surface and interfacial tensions, have a low water solubility and be capable of being dispersed readily and quickly throughout a foaming system with the minimum of agitation. Commercial antifoams include oils, alcohols, fatty acids, fatty acid esters, amines, ethers, phosphate esters, and polyorgano-siloxanes or silicones. Many require the presence of a 'carrier' if they are to be effective, the carrier acting as a reservoir from which the antifoam is liberated (16).

Two anti-foams were used during the course of the work described in this thesis. They were "Silcolapse", a propriatory silicone-based

antifoam from which the carrier was removed due to its precipitation on autoclaving, and "P2000",polypropylene glycol with molecular weight of around 2000. Solomons (16) has reported that silicone antifoams are particularly suitable for bacterial fermentations at an alkaline pH but do not perform as well in mould fermentations. It is not clear whether this was a pH effect or whether it was due to the presence of mycelium. However, in mould fermentations P2000 has proved particularly useful, and it has been reported (16) that less than 20 ml of P2000 added to a 10 l batch of medium was sufficient to supress foaming during the whole of a fermentation run.

The effect of Silcolapse and P2000 on aeration was recorded photographically and, as mentioned earlier in this section, antifoams were also used during holdup and mass-transfer experiments.

Nomenclature (Section 2)

Symbol	Explanation	Units
a	specific surface area	cm^2/cm^3
c	concentration of dissolved oxygen in the liquid medium	g/l
c_p	oxygen concentration detected by the oxygen electrode	g/l
c^*	equilibrium concentration of dissolved oxygen in the liquid	g/l
k	probe calibration constant	s^{-1}
k_L	mass transfer coefficient	cm/s
N	mass flux based on unit specific area	cm g/l s
R	organism respiratory rate	$(g\ O_2)/(g\ org)\ s$
t	time	
y	oxygen concentration in gas	atm
y^*	oxygen concentration in gas which is in equilibrium with the liquid	atm

Greek

ε	gas holdup	-

References (Section 2)

(1) HEINEKEN, F.G., Biotechnol. Bioeng., 13, 599 (1971)

(2) PANNELL, S.D., Ph.D. Thesis, University of Aston in Birmingham (1976)

(3) SHAYEGAN-SALEK, J., Ph.D. Thesis, University of Aston in Birmingham (1974)

(4) MORRIS, G.G., Ph.D. Thesis, University of Aston in Birmingham (1972)

(5) ARNOLD, B.H. and STEEL, R., "Biochemical Engineering", Ed. STEEL, R. (Macmillan Co., New York) 1958

(6) CALDERBANK, P.H., "Biochemical and Biological Engineering Science", 1,102, Ed. BLAKEBROUGH, N. (Academic Press, London) 1967

(7) CLARK, Jr., L.C., Trans. Am. Soc. Artificial Internal Organs, 2, 41 (1956)

(8) JOHNSON, M.J., BORKOWSKI, J. and ENGBLOM, C., Biotechnol. Bioeng., 6, 457 (1964)

(9) TAGUCHI, H. and HUMPHREY, A.E., J. Ferment. Technol. Japan, 44, 881 (1966)

(10) BANDYOPADHYAY, B., HUMPHREY, A.E. and TAGUCHI, H., Biotechnol. Bioeng., 9, 533 (1967)

(11) AIBA, S., HUMPHREY, A.E. and MILLIS, N.F., "Biochemical Engineering", 2nd. Edn. (Academic Press, New York)(1973)

(12) HEINEKEN, F.G., Biotechnol. Bioeng., 12, 145 (1970)

(13) LINEK, V., Biotechnol. Bioeng., 14, 285 (1972)

(14) HSU, K.H., ERICKSON, L.E. and FAN, L.T., Biotechnol. Bioeng., 17, 499 (1975)

(15) KITCHENER, J.A. and COOPER, C.F., Quart. Rev. Chem. Soc., 13, 71 (1959)

(16) SOLOMONS, G.L., Process Biochem., October, 47 (1967)

3. MEASUREMENT TECHNIQUES

3 Measurement Techniques.

3.1 Gas Holdup Measurements.

The methods available for the measurement of gas holdup in bubble columns have been documented by Shayegan-Salek (1). These techniques fall into four catagories which may be summarized as follows:-

(1) Separation of the two phases

(2) Manometric techniques

(3) Radiation attenuation

(4) Measurement of resistivity.

Each of these techniques will now be described further.

3.1.1 Phase Separation Technique.

This is the simplest of the techniques mentioned above and has been used by several investigators (2-5). The method relies on the instantaneous isolation of the experimental system from both liguid and gaseous feeds. This is achieved by the use of quick-action isolation valves on both inlets. The gas holdup may be determined by noting the volume of both phases after they have separated.

3.1.2 Pressure Measurement.

This is another popular technique (1,6-8) in which the gas holdup is determined by measuring the pressure at one or several points in the column using a manometric system.

A and B in figure 3.1 represent two manometers positioned

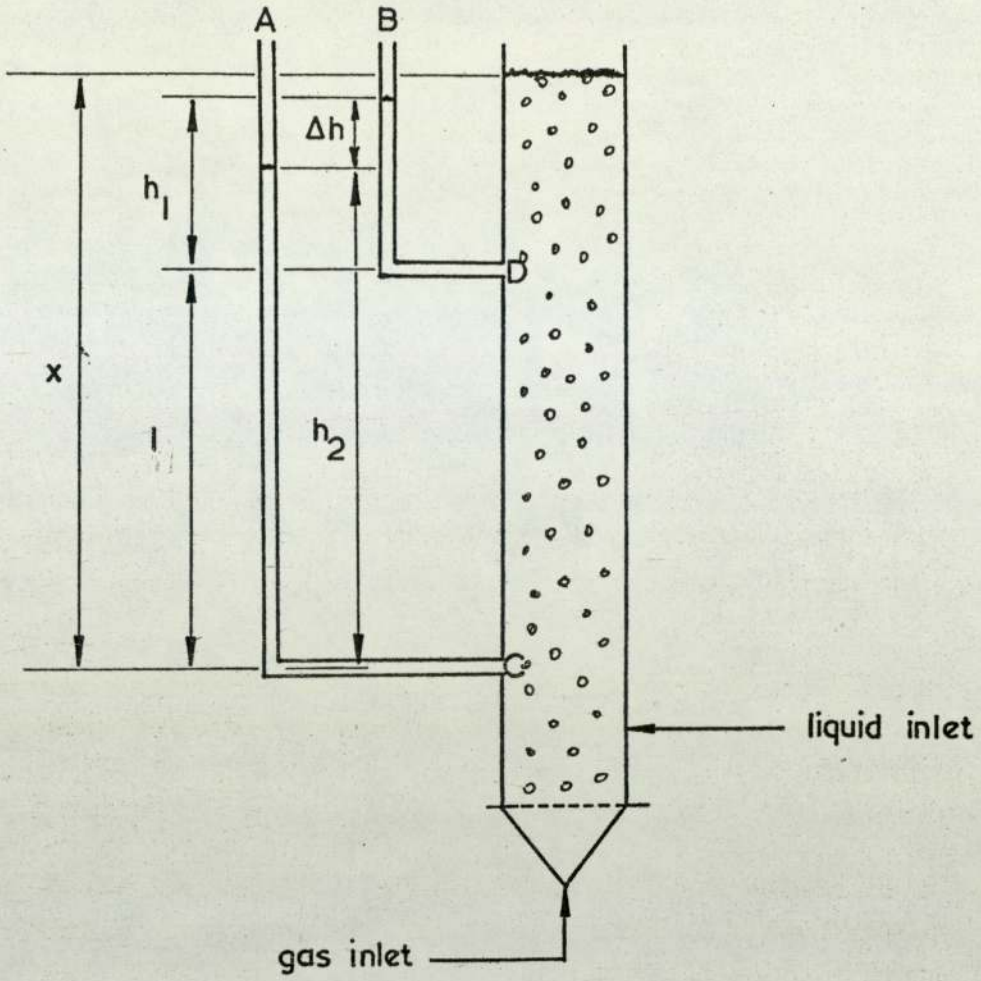

Figure 3.1 Diagramatic Representation of the System for Measurement of Gas Holdup.

at arbitrary distances along the column length. The difference in the manometer levels, Δh, gives a direct indication of the holdup in the section contained between the two tappings. This is also true for the case where more than two manometers are used.

By definition,

$$\text{Average Gas Holdup} = \varepsilon = \frac{l\,s - l_o\,s}{l\,s} \qquad (1)$$

where l_o = height of liquid in the tower if all of the air were excluded, s = cross-sectional area, and

l = height of aerated liquid.

The density of the gas/liquid mixture may also be defined by:

$$\rho = \rho_L - (\rho_L - \rho_G)(1 - \frac{l_o}{l}) \qquad (2)$$

Thus from the above equations

$$\varepsilon = \frac{\rho_L - \rho}{\rho_L - \rho_G} \qquad (3)$$

Now $\rho_L >> \rho_G$ and so equation (3) may be simplified further with negligible error:

$$\varepsilon = \frac{\rho_L - \rho}{\rho_L} \qquad (4)$$

Considering the pressures due to the hydrostatic head in the system:

At C $\quad P_C = \rho x = \rho_L h_2 \qquad (5)$

At D $\quad P_D = \rho(x - l) = \rho_L h_1 \qquad (6)$

and $\quad \Delta p = \rho l \qquad (7)$

or $\quad \Delta p = \rho_L(h_2 - h_1) = \rho_L(l - \Delta h) \qquad (8)$

Therefore, combining equations (7) and (8)

$$\frac{\Delta h}{l} = \frac{\rho_L - \rho}{\rho_L} \qquad (9)$$

Thus comparing equations (4) and (9)

$$\varepsilon = \frac{\Delta h}{l} \qquad (10)$$

The advantage of this technique over that of phase separation is that by careful positioning of the manometers end effects may be eliminated: it is also possible to estimate ε over short lengths of the tower.

3.1.3 Radiation Attenuation.

This technique is based on the differential absorption of radiation by the components of a system due to differences in their densities. Previous investigators have used γ (9,10) and β (11) radiation. Visible light has been used by Calderbank (12) to measure the interfacial area of suspensions: this is a related measurement.

The choice between γ and β radiation depends on the sensitivity required and the distance to be traversed by the radiation, although in a system containing living organisms the possibility of cell mutation (and even death) must also be considered. Both γ and β radiation may cause mutation but this is a function of the dose and the complexity of the organism. In general the simpler the organism the less likely it is to mutate (13). β radiation is absorbed more readily than γ radiation, and so small density differences can be detected using β rays: for the same reason β radiation can only be used to traverse a short distance. This distance, or range, depends on the material through which the radiation must pass and the initial energy. There are however no problems due to screening of high energy β radiation.

Calderbank (12) has determined interfacial areas by passing a parallel beam of light through a dispersion and measuring the transmittance using a light sensitive cell, placed opposite the source, at the end of a blackened tube. Interfacial area and bubble swarm density can be related and so, assuming that the bubble swarm density is uniform, the same technique may be used to estimate gas holdup. Two types of experimental apparatus were used by Calderbank, the choice of which depended on the size of the vessel being used (figure 3.2). Of these only that used with small vessels was directly

Figure 3.2 Light-Transmission Probes for the Measurement of Bubble Swarm Interfacial Areas - Design by Calderbank.

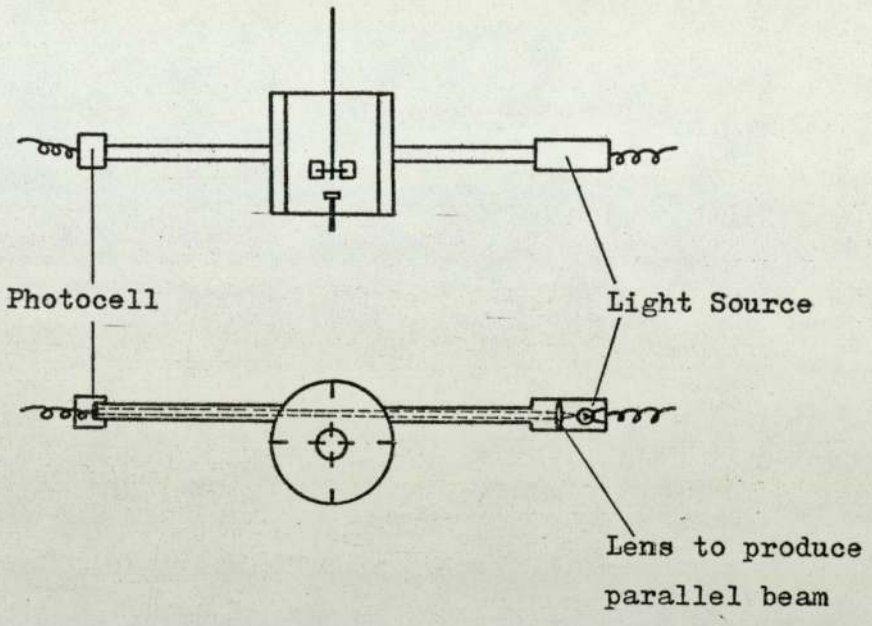

(a) Probes for use with small vessels.

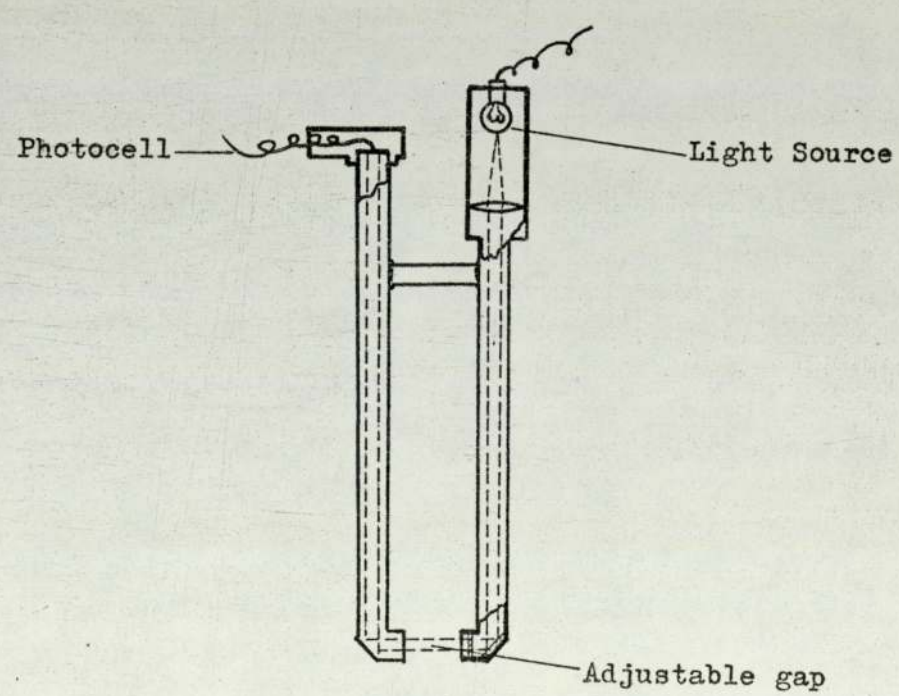

(b) Compound probe for use with large vessels.

applicable in this work due to the design of the tower (see section 4).

3.1.4 Resistivity Measurement.

This method measures local, rather than bulk, void properties and these may only be equated if the system is isotropic. The technique, which has been used by Neal and Bankoff (14) and Hills (15), relies in the difference of the conductivities of the two phases. Since the current will only flow when the resistivity probe is in the liquid, the holdup at any point may be found from the time fraction for which the current flows. However the experimental readings are not easy to interpret.

3.2 Analysis of Oxygen Absorption.

In theory any reaction which utilizes oxygen or any process which may be coupled to such a reaction may be used to measure oxygen uptake rates. These may be broadly classified as Chemical Methods and Physico-Chemical Methods.

3.2.1 Chemical Methods.

These methods may be further sub-divided.

(1) Direct Chemical Analysis

(2) Indirect Chemical Methods

(3) Indirect Biological Methods

Direct Chemical Analysis.

There are several chemical methods available for analysing dissolved oxygen in a sample withdrawn from a fermenter. These methods

tend to be complicated in practice since the sample must be taken and analysed under a nitrogen blanket in order to prevent changes in the concentration being measured.

The Winkler titration is a widely used method of analysis (16). It involves the addition of an excess of a standard solution of manganous ions followed by back-titration to determine the unoxidised portion. Substances contained in most fermentation broths interfere with this method. This interference is less likely to occur with the ascorbic acid oxidase method described by Sharp et alia (17).

Indirect Chemical Methods.

This technique involves the simulation of the fermentation process within the fermenter by using a chemical reaction utilizing oxygen. One such reaction is the catalytic oxidation of sodium sulphite, introduced by Cooper et alia (18). This reaction may only be used for comparative tests because living cells act as autocatalysts. The exact mechanism of the oxidation reaction is still uncertain: and Srivastara et alia (19) have indicated that the reaction may depend on the type of equipment, purity of the sodium sulphite solution, the catalyst used, the pH of the solution and the concentrations of the oxygen and the sodium sulphite. For example, Pirt et alia (20) compared cobalt ions with copper ions as catalysts and found that higher reaction rates could be obtained with cobalt. Comparisons have been made by several investigators between this method and other physico-chemical techniques.

A second indirect chemical technique has been employed by Muchmore, Chen and BeMiller (21) who used elemental copper adsorbed on a weakly basic anion-exchange resin as a solid phase oxygen acceptor.

The solid phase was prepared according to the method described by Mills and Dickinson (22).

Thus techniques allowing the indirect estimation of oxygen mass-transfer rates are available and practicable although, in the opinion of the author, measurements on the actual fermentation system are preferable.

Indirect Biological Measurements.

These methods are based on calculations using metabolic ratios which may then be related to a dissolved oxygen level within the fermenter. An example is provided by the work of Bennett and Kempe (23) who studied the transfer rate of oxygen in the gluconic acid fermentation using Pseudomonas Ovalis by measuring the rate of production of the acid in a nitrogen free, aerated medium. Comparisons were again made with a physico-chemical technique as discussed later in the text.

3.2.2 Physico-Chemical Methods.

The oxygen demand of a culture may be determined directly using these techniques. They require the use of some device, electronic or otherwise, as an intermediate to a direct reading of the oxygen concentration or tension within a system. The literature pertaining to these devices has been reviewed by Ricica (24). In all cases but one, the tubing method, the devices are based on the direct electrochemical reduction of oxygen. These "Oxygen Electrodes" depend on the electrolysis of the dissolved oxygen at a weakly negative cathode. Such electrodes may be sub-classified as:

(1) Uncovered Amperometric Electrodes.

(2) Covered Amperometric Electrodes

(3) Covered Galvanic Electrodes.

The major difference in the above classification is that between amperometric and galvanic devices. Amperometric electrodes require a polarizing voltage to be applied to the cathode and the small current produced requires amplification. Galvanic electrodes are self generating and may be used in conjunction with a micro-ammeter or, via a resistance, with a potentiometric recorder. The current produced is much greater than that of their amperometric counterparts and because of this requires little or no amplification.

The electrode reaction of these devices is still in some doubt. Much of the present information has been inferred from other measurements. Latinen and Kolthoff (25) suggest a two electron reaction:

$$2H^+ + O_2 + 2e^- \longrightarrow H_2O_2$$

whereas Davis and Brink (26) and subsequently Kolthoff and Lingane (27) suggest a two step reaction:

$$2H_2O + O_2 + 2e^- \longrightarrow H_2O_2 + 2OH^-$$

$$H_2O_2 + 2e^- \longrightarrow 2OH^-$$

Amperometric elecrodes, both covered and uncovered, consist of a small area of either platinum or gold, which acts as the cathode, connected to a suitable reference electrode, eg. calomel or silver/silver chloride. One exception to this, the dropping mercury electrode, was used by Bartholomew et alia (28) for the direct measurement of dissolved oxygen within a fermenter. This electrode has, however, several disadvantages and will not be considered further.

The required polarizing voltage for amperometric electrodes usually lies between -0.4v and -0.8v with respect to the reference

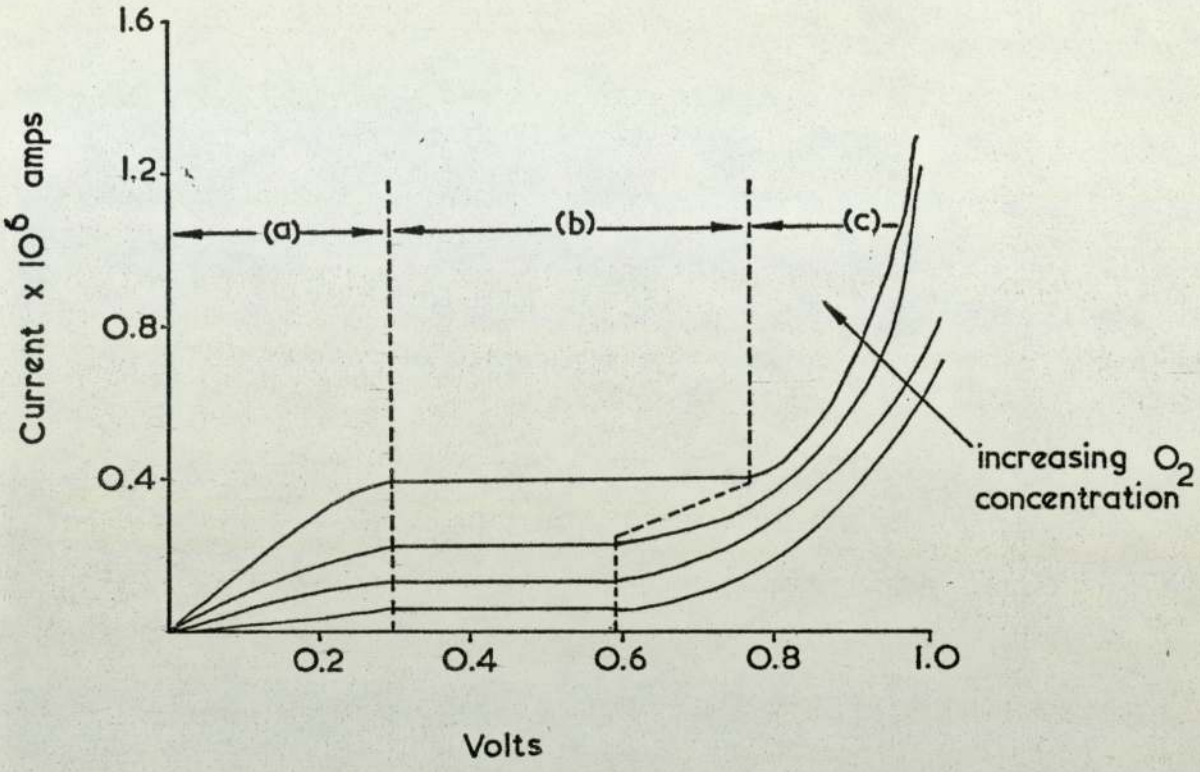

Figure 3.3 Current-Voltage Curves for a Typical Amperometric Electrode.

electrode. The optimum value may be found from a plot of signal current versus applied voltage for solutions with known dissolved oxygen levels. Such plots have a characteristic shape and may be divided into three regions, as shown in figure 3.3. In the lower potential region, a, the electrode current is limited by the availability of oxygen at the electrode surface and the energy required for its reduction. On the plateau, region b, oxygen is diffusing to the electrode at its maximum rate and the current produced is virtually independent of the applied potential difference. In extreme cases the plateau may be very short or indeed non-existent but this does not mean that the response of the electrode is unreliable. At the higher voltages, region c, the electrode current rises rapidly

due to the direct reduction of hydrogen ions. The best working voltage is that giving the least variation in signal current over small changes in applied potential, i.e. on the plateau. The signal current may however be affected by other factors. These include the materials and method of construction of the electrode as well as the properties of the system in which the electrode is used.

Uncovered Amperometric Electrodes.

These were the first type of solid electrode to be developed. There are many designs which vary greatly in size and complexity. Oxygen concentration is measured indirectly in terms of p.p.m. or millimoles per millilitre. In contrast to uncovered electrodes, covered devices measure partial pressure in terms of percentage saturation which, in systems containing living organisms, is preferable since living cells respond to oxygen tension rather than concentration (29). Davis and Brink (30) explored the use of different electrode configurations, including flush, pointed and recessed, for the determination of absolute oxygen tensions.

Simple uncovered probes, usually with gold or platinum electrodes, cannot be used effectively in fermentation systems. If they are used in such systems for periods greater than an hour, the surfaces of the electrode become fouled by proteins and other materials present in the aqueous broth. Conversely, Beechy and Ribbons (31) reported that very clean electrodes tended to give erratic signals and that a small amount of fouling was therefore beneficial as it dampened the noise and stabilized the signal. The great advantage of these simple electrodes, apart from ease of construction and rapid response, is that they are readily steam sterilized. Hybrids were therefore produced which vibrated (31), rotated (32) or were cleaned by a

rotating felt pad (33). Mechanically these electrodes are very complicated especially the latter case.

Covered Amperometric Electrodes.

Another method exploited to combat fouling was the partition of the electrode from the fermentation medium by a semi-permeable membrane. Even so no membrane is entirely effective and some poisoning agents still cause problems. One of the original electrodes of this type was that of Clark et alia (34) who used a platinum cathode covered by a cellophane membrane to measure the oxygen tension of blood. A later modification by Clark (35) incorporated a platinum cathode and a silver/silver chloride anode in the same shell. A polyethylene membrane was used in preference to cellophane.

Apart from the partial pressure of oxygen temperature is the biggest factor affecting the output signal of an oxygen electrode. Vincent (36) has expressed this dependence in the form

$$I_T = A\, e^{-J/T} \qquad (11)$$

where I_T is the signal current at temperature T and A and J are constants. For polyethylene J is approximately 4500K which gives a temperature coefficient of about 5 %/K. For more crystalline materials this value is much lower. Several investigators attempted to adjust their results to allow for this. For example Carrit and Kanwisher (37) incorporated a thermister in their electrode in order to correct their data.

Covered Galvanic Electrodes.

Several galvanic electrodes have been developed which use an oxygen consuming electrochemical cell to generate a signal current proportional to the measured dissolved oxygen concentration. One of the best known of these is the MacKereth electrode (38). It consists of a cell containing a silver cathode and lead anode separated from the external medium by a polyethylene membrane. The internal cavity is filled with saturated potassium hydrogen carbonate solution as the electrolyte. It is large due to its design and quite unsuited to sterilization by heat. In an alteration to this design, Flynn et alia (39) reduced the size of the electrode markedly and improved the stability of the response by using silicone rubber as the membrane instead of polyethylene. Harrison and Melbourne (40) took this design a stage further to produce an autoclavable version.

Heat is the major problem with covered electrodes since the electrolyte, confined within an enclosed space, expands, stretching the thin membrane: as a result the performance of these electrodes alters after each sterilization procedure. This problem was tackled in two ways. Firstly additives were used to supress the boiling point of the electrolyte. Secondly the body of the electrode was left open to the atmosphere so allowing any pressure build up to dissipate.

An electrode which uses these techniques and was developed with biological systems in mind has been described in detail by Johnson et alia (41) with later design improvements by Borkowski and Johnson (42). Again electrodes consisted of silver and lead but an acetate buffer was used as the electrolyte. Teflon was used as the membrane because of its resistance to heat and its chemical

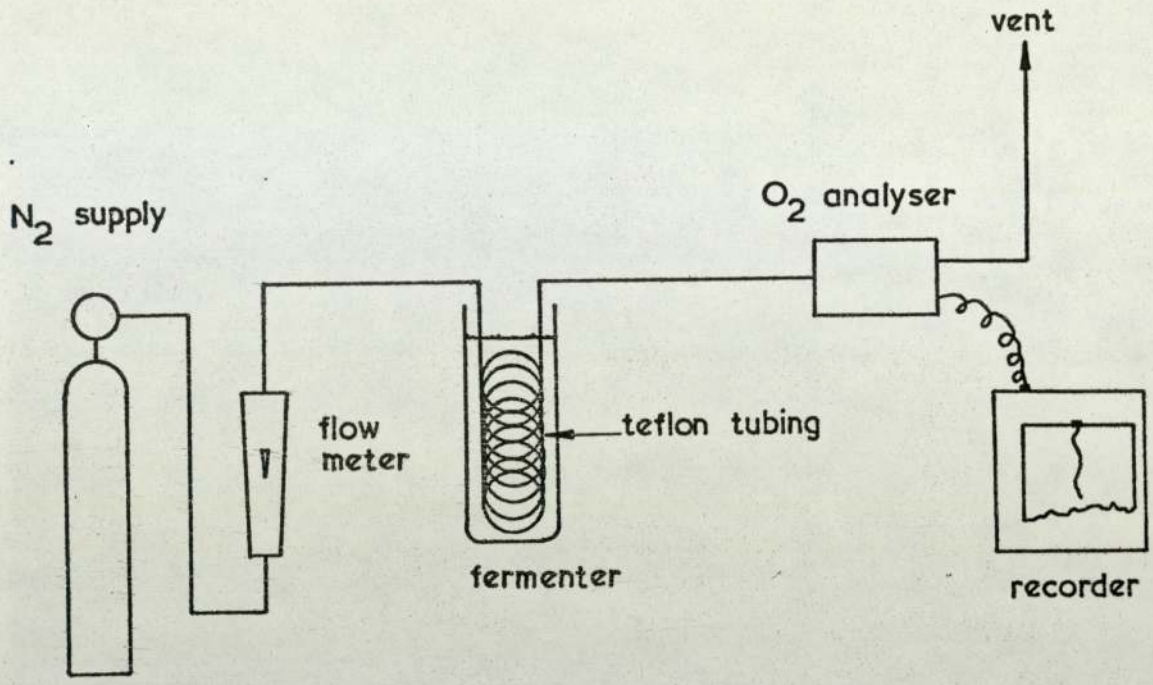

Figure 3.4 Schematic Diagram of the Tubing Method.

inertness. Some models, available commercially, have used polypropylene as a substitute. This type of electrode has been reported as having a life in excess of a year when used intermittently with virtually no maintenance.

The Tubing Method.

The tubing method, which has been mentioned earlier, fits into none of the above classifications. It is a method which makes use of the ability of gases to diffuse through a semi-permeable membrane from a liquid to a gas stream and is described by Phillips and Johnson (43). A coil of teflon tubing (wall thickness 0.25mm) is immersed

in the fermenter (refer to figure 3.4) and a slow stream of oxygen-free nitrogen passed through it. The effluent gas is then analysed and vented to the atmosphere. The sensitivity of the method is a function of the length, diameter and wall thickness of the tubing, the nitrogen flow rate and the sensitvity of the detector.

3.3 The Membranes Used with Covered Electrodes.

During the evolution of membrane covered electrodes many types of membrane film were tried with varying degrees of success. The ultimate choice of any membrane must be based on specific criteria. For example consideration must be given to the permeability of oxygen through the polymer and to its mechanical strength. The polymer properties at elevated temperatures may also be important if it is to be sterilized by steam, as many electrodes are in biological systems. Popular materials include polyethylene, polypropylene and teflon.

Studies into the mechanism of diffusion of molecules through high polymers have shown that, in general, the process is simpler with permanent gases than it is with vapours. The solubility of vapours in polymeric materials is not directly proportional to the pressure of the system (Henry's law is not obeyed). Also the diffusion constants are often dependent on the concentration of the penetrant in the polymer. A partial explanation of the non-ideal behaviour of water vapour in polymer films was proposed by Rogers et alia (44). They suggest that clustering of water molecules at the surface of hydrophobic films, eg. polyethylene, may affect their diffusivity, whilst hydrophilic films are affected by the high degree of interaction between the water and polymer molecules. Tuwiner (45) suggests that the latter may also cause swelling of the membrane.

Permanent gases usually obey Henry's law, and the diffusion constants are independent of concentration. This reflects the lack of interaction between the diffusing molecule and the polymer. Mixtures of gases permeate in an additive fashion, each component in accordance with its partial pressure.

The diffusion mechanism itself involves the formation of "holes" through which the penetrating molecule passes. Hole formation may be depicted by the rotation of the polymer chains about each other so forming inter-molecular spaces. Since hole formation requires a certain amount of energy, diffusion through polymer films may be regarded as an activated process. Hence Barrer (46) described the temperature dependence of diffusion by the relationship:

$$D = D_o \exp - \frac{E_d}{RT} \qquad (12)$$

Where D_o and E_d are the pre-exponential factor and the activation energy respectively.

Diffusion rates through films may be affected by several factors. The size of the penetrant molecule is important. Since the diffusion process depends on hole formation, the greater the effective molecular diameter of the penetrant the greater is the activation energy required for the formation of a hole big enough to allow its passage. The solubility of the penetrant in the polymer is also important. Waack et alia (47) obtained data for several gases which illustrate these points. Nitrogen, oxygen and carbon dioxide were found to have diffusivities which increase in that order in a range of test materials. The trend was due to a combination of molecular size and solubility. Oxygen has the smallest molecular size but carbon dioxide was far more soluble in all of the materials tested than

oxygen, which in turn was more soluble than nitrogen.

The ease of hole formation depends on polymer associated factors, for example the segmental chain mobility of the polymer. This in turn is determined by the degree of cross-linking and the chain packing density. In extreme cases the latter may lead to the presence of a certain number of pre-existing holes which will increase the ease of passage.

Polymer composition and crystallinity also have a marked effect on diffusion. The available evidence indicates that crystallites are impenetrable to the permeating gas and that they are randomly distributed throughout the polymer structure. Michaels and Bixler (48) in their study of polyethylene consider the polymer to be a simple mixture of crystals and amorphous solid each having a characteristic specific volume. Their results show a direct proportionality between the solubility of the gas in the plastic film and the volume fraction of the amorphous material. A second paper by the above authors (49) describes diffusion constants in several materials in terms of the molecular size of the penetrant, a geometric impedance factor and a chain immobilization factor which together account for the crystallinity of the material. The former allows for the need of the diffusing molecule to by-pass the impenetrable crystallites whilst the latter reflects the reduction in chain mobility due to the proximity of crystallites.

3.4 A Model Describing the Response of a Covered Oxygen Electrode to a Transient System.

According to Barrer (50) polymeric compounds obey Henry's law for solution, and, for the case of one dimensional

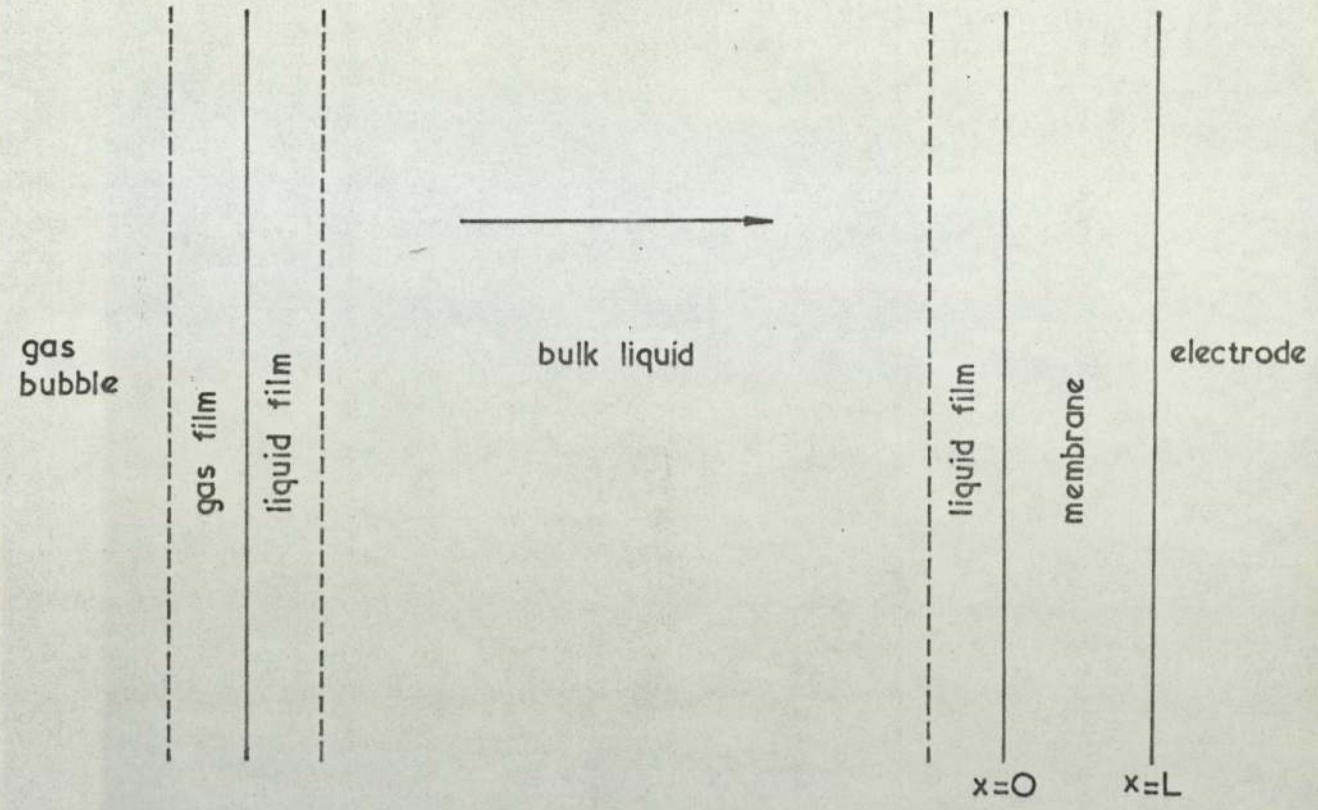

Figure 3.5 Schematic Diagram of the Physical System Involved in the Measurement of Dissolved Oxygen.

diffusion, Fick's law applies. This information was used by Heineken (51) as the starting point for a model describing the response of an oxygen electrode to a system undergoing a step change.

Figure 3.5 shows a simplified diagram of the physical system involved in oxygen transfer studies. There is evidence to suggest that it is the diffusion of oxygen through the probe membrane that is the step controlling the response of the electrode to changes in the bulk liquid dissolved oxygen concentration. Thus, assuming Fick's law of diffusion is valid and that the transfer is one dimensional, the diffusion of oxygen through the membrane may be described by:

$$\frac{\partial C_{Mx}}{\partial t} = D \frac{\partial^2 C_{Mx}}{\partial x^2} \qquad (13)$$

When the gassing in technique of Bandyopadhyay and Humphrey (52), described later in this text, is being used the initial condition for the solution of equation (13) is given by:

$$C_{Mx} = 0 \text{ @ } t = 0 \quad \text{for } 0 < x < L \tag{14}$$

and the boundary condition on the electrode side of the membrane is:

$$C_{ML} = 0 \quad \text{for } t \geq 0 \tag{15}$$

This implies that the rate of chemical reaction at the electrode surface is greater than the rate of transfer through the membrane.

The second boundary condition required for the solution of equation (13) may be derived by considering the transient oxygen concentration on the liquid side of the membrane. Here

$$C_{MO} = \phi(t) \quad \text{for } t > 0 \tag{16}$$

and $\phi(t)$ may be defined by considering the transfer of oxygen from the gas to the liquid phase, assuming that both phases are well mixed. Thus:

$$C_L = C_L^o \left(1 - e^{-\beta t}\right) \tag{17}$$

where

$$\beta = \left\{ k_L a \Big/ \left[1 + \left(\frac{P_t}{H}\right)\left(\frac{V}{Q}\right) k_L a \right] \right\} \tag{18}$$

and

$$C_{MO} = \frac{C_L}{H_M} \quad \text{for } t > 0 \tag{19}$$

Hence the solution of (13) using equations (14), (15), (17) and (19) leads to the expression:

$$E(t) = K_g\left\{1 - \frac{e^{-\beta t}\left[(\beta/D)^{\frac{1}{2}} L\right]}{\sin\left[(\beta/D)^{\frac{1}{2}} L\right]} + 2\sum_{n=1}^{\infty}(-1)^n \cdot \exp\left[\frac{-n^2\pi^2 D}{L^2} t\right] \cdot \left[\frac{\beta}{\beta - (n^2\pi^2 D/L^2)}\right]\right\} \qquad (20)$$

Where $E(t)$ is the millivolt response of the probe and K_g is a constant which allows for the gain factor of the recorder.

Linek (53) simplified the above expression by considering the normalised response of the electrode, $E(t)/E(\infty)$, and by the introduction of a membrane constant, k, where

$$k = \frac{\pi^2 D}{L^2} \cdot \qquad (21)$$

This simplification leads directly to the expression:

$$\Gamma = 1 - \frac{\pi B^{\frac{1}{2}}}{\sin \pi B^{\frac{1}{2}}} \exp(-Bkt) - 2\sum_{n=1}^{\infty}(-1)^n \frac{\exp(-n^2 kt)}{\left[\frac{n^2}{B} - 1\right]} \qquad :(22)$$

where

$$B = \frac{k_L a}{k} \cdot \qquad (23)$$

The membrane constant, k, may be evaluated from an instantaneous step-change in the dissolved oxygen concentration of the liquid in contact with the membrane. In this case the second boundary condition for the solution of equation (13) becomes:

$$C_{MO} = C_{Ms} \quad \text{for} \quad t > 0 \qquad (24)$$

Equation (13) may then be solved together with equations (14), (15) and (24) yeilding the solution:

$$\Gamma' = 1 - 2\exp(-kt) + 2\sum_{n=2}^{\infty} (-1)^n \exp(-n^2 kt) \qquad (25)$$

which is a function of k and t only. A detailed solution for this model is given in Appendix 1.

Nomenclature (Section 3)

Symbol	Explanation	Units
A	constant	
B	$(k_L a/k)$	-
C_L	oxygen concentration in the liquid	g moles/l
C_L^o	initial oxygen concentraion in the liquid	g moles/l
C_{ML}	oxygen concentration in the membrane at position L	g moles/l
C_{MO}	oxygen concentration at the membrane surface - liquid side	g moles/l
C_{Ms}	oxygen concentration at the membrane surface - liquid side - after a step change in the oxygen level	g moles/l
C_{Mx}	oxygen concentration in the membrane at position x	g moles/l
D	membrane diffusivity	cm^2/s
D_o	pre-exponential factor eq. 12	cm^2/s
E_d	activation energy eq. 12	J/g mole
E(t)	response of oxygen electrode as a function of time	mV
h_1	liquid level in manometer 1	cm
h_2	liquid level in manometer 2	cm
h	difference in hydrostatic head	cm
H	Henry's law constant for the liquid phase	atm l/g mole
H_M	Henry's law constant for oxygen in the membrane	
I_T	oxygen electrode signal current at temperature T	mA
J	constant	K
k	oxygen electrode calibration constant	s^{-1}
K_g	constant to allow for gain factor of the recorder	-

Symbol	Explanation	Units
$k_L a$	overall mass-transfer coefficient	s^{-1}
l	distance between manometer tappings	cm
l_o	height of liquid between tappings if all air were excluded	cm
L	membrane thickness	cm
p	pressure due to hydrostatic head	g/cm^2
P_t	total pressure in the fermenter	atm
Q	mass flow rate of gas	g moles/s
R	gas constant	J/g mole K
s	cross-sectional area	cm^2
t	time	s
T	absolute temperature	K
V	volume of liquid in the liquid phase	l

Greek

β	defined by eq. 18	
ε	gas holdup	-
ρ	density of gas-liquid mixture	g/cm^3
ρ_G	gas density	g/cm^3
ρ_L	liquid density	g/cm^3
Γ	normalised probe response following a step change in the oxygen concentration in the gas phase	-
Γ'	normalised probe response following a step change in the oxygen concentration in the liquid phase	-

References (Section 3)

(1) SHAYEGAN-SALEK, J., Ph.D. Thesis, University of Aston in Birmingham (1974)

(2) NICKLIN, D.J., Chem. Engng. Sci., 19, 693 (1962)

(3) HUGHMARK, G.A. and PRESSBURG, B.S., A.I.Ch.E.J., 7, 677 (1961)

(4) KIM, D.S., BAKER, C.G.J. and BERGOUGON, Can. J. Chem. Engng., 50, 695 (1972)

(5) WALLIS, G.B., Trans. Am. Soc. Mech. Engrs., Heat Transfer Conference, 319 (1961/2)

(6) REITH, T., RENKEN, S. and ISRAEL, B.A., Chem. Engng, Sci., 23, 619 (1968)

(7) TOWELL, G.D., STRAND, C.P. and ACKERMAN, G.H., A.I.Ch.E./I. Chem.E. Symposium Series No. 10 (1965)

(8) DOWNIE, J.McC., Ph.D. Thesis, University of Aston in Birmingham (1972)

(9) MARCHATERRE, J.F. and PETRICK, J., Nucl. Sci. Engng., 7, 525 (1960)

(10) ISBIN, H.S., RODRIGUEZ, H.A., LARSON, H.C. and PATTIE, B.D., A.I.Ch.E.J., 5, 427 (1959)

(11) PERKINS, N.C., YUSUF, M. and LEPPERT, G., Nucl. Sci. Engng., 11, 304 (1961)

(12) CALDERBANK, P.H., Trans. Inst. Chem. Engrs., 36, 443 (1958)

(13) THORNBURN, C., Private Communication.

(14) NEAL, L.G. and BANKOFF, S.G., A.I.Ch.E.J., 9, 490 (1963)

(15) HILLS, J.H., Trans. Inst. Chem. Engrs., 52, 1 (1974)

(16) American Public Health Association Inc., Standard Methods for the Examination of Water and Wastewater, 12th. Edn. (1965)

(17) SHARP, P.F., HAND, D.B. and GUTHRIES, E.S., Ind. Engng. Chem. Anal. Ed., 13, 593 (1941)

(18) COOPER, C.M., FERNSTROM, G.A. and MILLER, S.A., Ind. Engng. Chem., 36, 504 (1944)

(19) SRIVASTAVA, R.D., McMILLAN, A.F. and HARRIS, I.J., Can. J. Chem. Engng., 46, 181 (1968)

(20) PIRT, S.J., CALLOW, D.S. and GILLET, W.A., Chem.Ind., 730 (1957)

(21) MUCHMORE, C.B., CHEN, J.W. and BeMILLER, J.N., Biotechnol. Bioeng., 13, 271 (1971)

(22) MILLS, G.F. and DICKINSON, N.B., Ind. Eng. Chem., 41, 2842 (1949)

(23) BENNETT, G.F. and KEMPE, L.L., Biotechnol. Bioeng., 6, 347 (1964)

(24) RICICA, J., "Theoretical and Methodological Bases of Continuous Culture of Micro-Organisms", Ed. MALEK, J. and FENCL, Z., Publishing House of the Academy of Sciences, Prague (1966)

(25) LAITINEN, H.A. and KOLTHOFF, I.M., J. Phys. Chem., 45, 1061 (1941)

(26) DAVIS, P.W. and BRINK, Jr., F., Rev. Sci. Instr., 13, 524 (1942)

(27) KOLTHOFF, I.M. and LINGANE, J.J., "Polography", Interscience, New York (1952)

(28) BARTHOLOMEW, W.H., KAROW, E.O. and SFAT, M.R., Ind. Eng. Chem., 42, 1827 (1950)

(29) SIEGALL, S.D. and GADEN, E.L., Biotechnol. Bioeng., 4, 345 (1962)

(30) DAVIS, P.W. and BRINK, Jr., F., Rev. Sci. Instr., 13, 524 (1942)

(31) BEECHY, R.B. and RIBBONS, D.W., "Methods in Microbiology", Eds. NORRIS, J.R. and RIBBONS, D.W.

(32) STEEL, R. and BRIERLEY, M.R., Appl. Microbiol., 7, 51 (1959)

(33) GUALANDI, G. and MORISI, G., Biotechnol. Bioeng., 8, 621 (1966)

(34) CLARK, L.C.Jr., WOLF, R., GRANGER, D. and TAYLOR, Z., J. Appl. Physiology, 6, 189 (1953)

(35) CLARK, L.C.Jr., Trans. Am. Soc. Artificial Internal Organs, 2, 41 (1956)

(36) VINCENT, A., Process Biochem., April, 19 (1974)

(37) CARRITT, D.E. and KANWISHER, J.W., Analyt. Chem., 31, 5 (1959)

(38) MACKERETH, F.J.H., J. Sci. Instr., 41, 38 (1964)

(39) FLYNN, D.S., KILBURN, D.G., LILLEY, M.D. and WEBB, F.C., Biotechnol. Bioeng., 9, 623 (1967)

(40) HARRISON, D.E.F. and MELBOURNE, K.V., Biotechnol. Bioeng., 12, 633 (1970)

(41) JOHNSON, M.J., BORKOWSKI, J. and ENGBLOM, C., Biotechnol. Bioeng., 6, 457 (1964)

(42) BORKOWSKI, J. and JOHNSON, M.J., Biotechnol. Bioeng., 9, 635 (1967)

(43) PHILLIPS, D.H. and JOHNSON, M.J., J. Biochem. Microbiol. Tech. and Eng., 3, 261 (1961)

(44) ROGERS, C., MEYER, J.A., STANNETT, V. and SZWARC, M., TAPPI, 39, 737 (1956)

(45) TUWINER, S.B., "Diffusion and Membrane Technology", Reinhold Publishing Corp., New York (1962)

(46) BARRER, R.M., "Diffusion in and Through Solids", Cambridge University Press, Cambridge (1951)

(47) WAACK, R., ALEX, N.H., FRISCH, H.L., STANNETT, V. and SZWARC, M., Ind. Eng. Chem., 47, 2524 (1955)

(48) MICHAELS, A.S. and BIXLER, H.J., J. Polymer Sci., 50, 393 (1961)

(49) MICHAELS, A.S. and BIXLER, H.J., J. Polymer Sci., 50, 413 (1961)

(50) BARRER, R.M., "Diffusion in and Through Solids", Cambridge University Press, Cambridge (1951)

(51) HEINEKEN, F.G., Biotechnol. Bioeng., 12, 145 (1970)

(52) BANDYOPADHYAY, B., HUMPHREY, A.E. and TAGUCHI, H., Biotechnol. Bioeng., 9, 533 (1967)

(53) LINEK, V., Biotechnol. Bioeng., 14, 285 (1972)

4. EQUIPMENT AND EXPERIMENTAL METHODS

4. Equipment and Experimental Methods.

4.1 Equipment.

4.1.1 Fermenters and Ancilliary Equipment.

Initial experimentation was carried out using the equipment previously described by Shayegan-Salek (1). This consisted of two towers of 152mm and 305mm diameter, together with ancilliary equipment. Flow diagrams of these systems are shown in figures 4.1 and 4.2.

In later experiments a 10 litre tower, originally developed by Pannell (2) of the Biological Sciences Department, was used in order to facilitate direct comparison of the author's results with those obtained by other members of the Tower Fermentation Research Group.

The tower was constructed from 102mm diameter Q.V.F. glass pipe sections, joints being made across P.T.F.E. gaskets. The aspect ratio (height : diameter ratio) of the tower was approximately 10:1. Side arms were added to the sections to allow easy access for instruments (see figures 4.3 and 4.4).

The liquid feed, except for the case of water, was autoclaved and stored in 20 litre aspirators fitted with anti-bacterial filters. When protected in this way the liquid remained aseptic for many days. A Watson-Marlow peristaltic pump was used to meter and pass the feed into the fermenter through a side port near the base, connections being made with 4mm silicon rubber tubing. Because of the combination of low liquid flow rates and intense liquid-phase mixing within the fermenter, liquid distribution was very rapid; consequently there was no need for a special form of distributer.

Figure 4.1. Process liquid flow diagram.
152mm & 305mm columns.

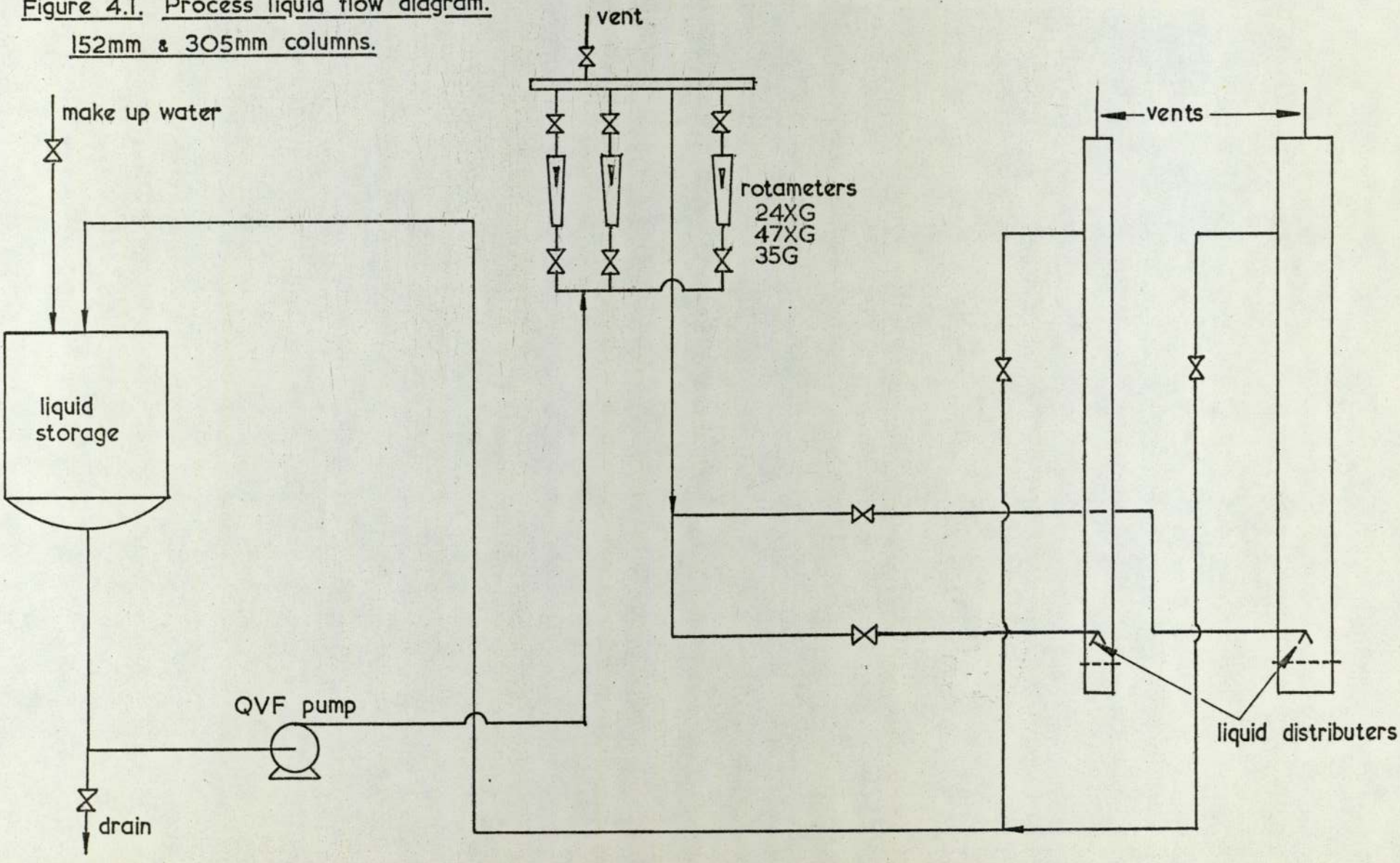

Figure 4.2. Process air & nitrogen flow diagram.
152mm & 305mm columns.

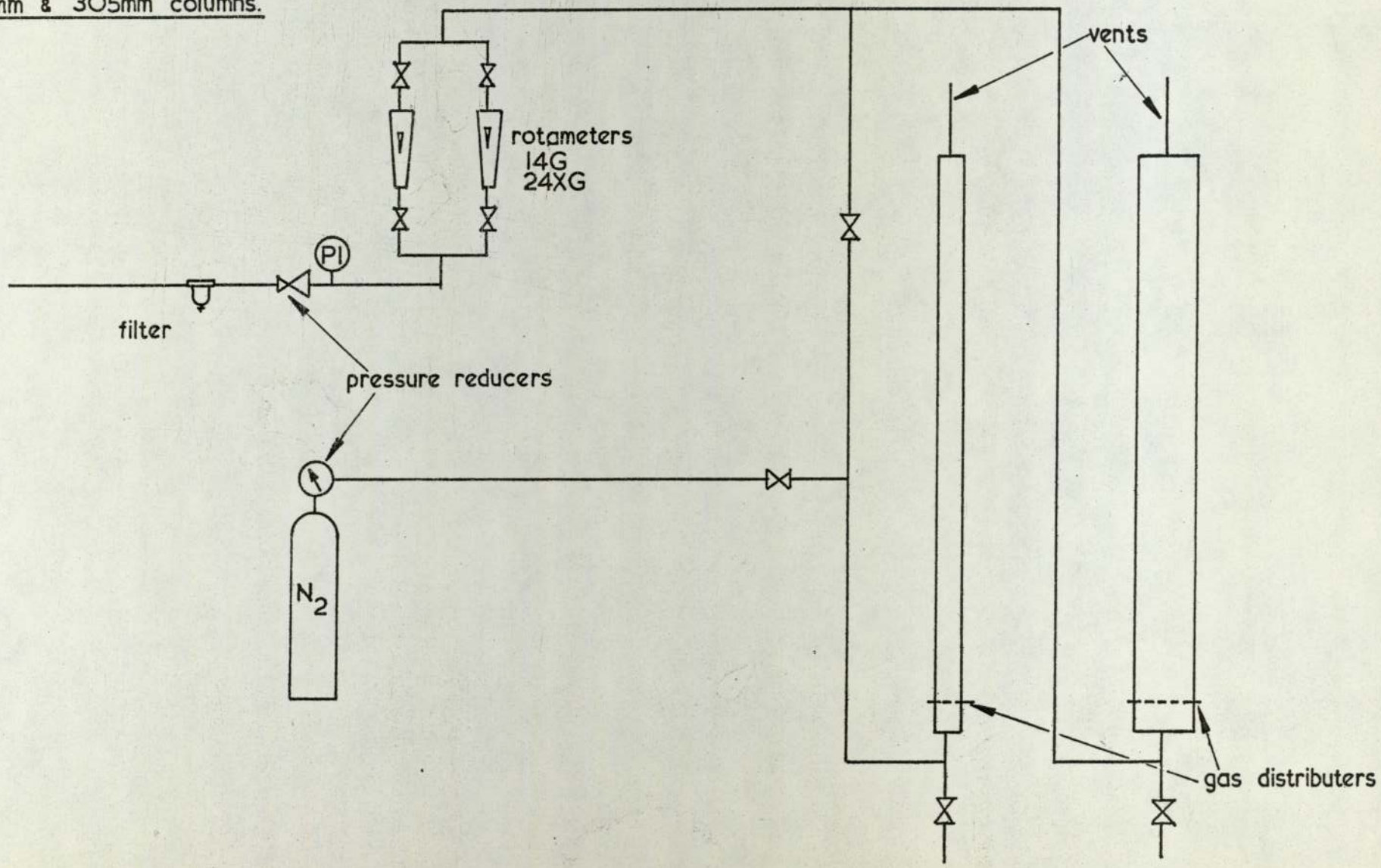

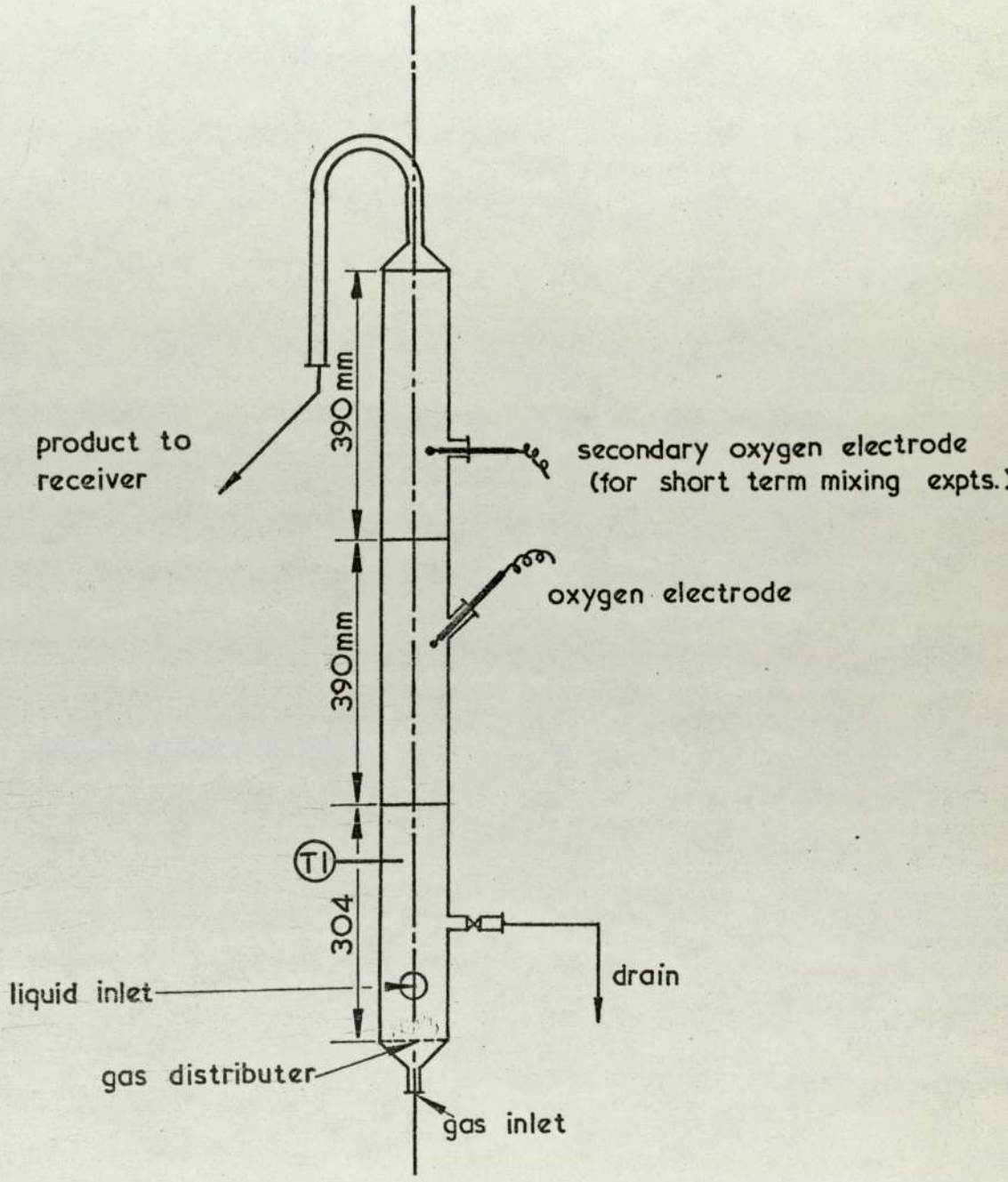

Figure 4.3 The 102 mm Diameter Column.

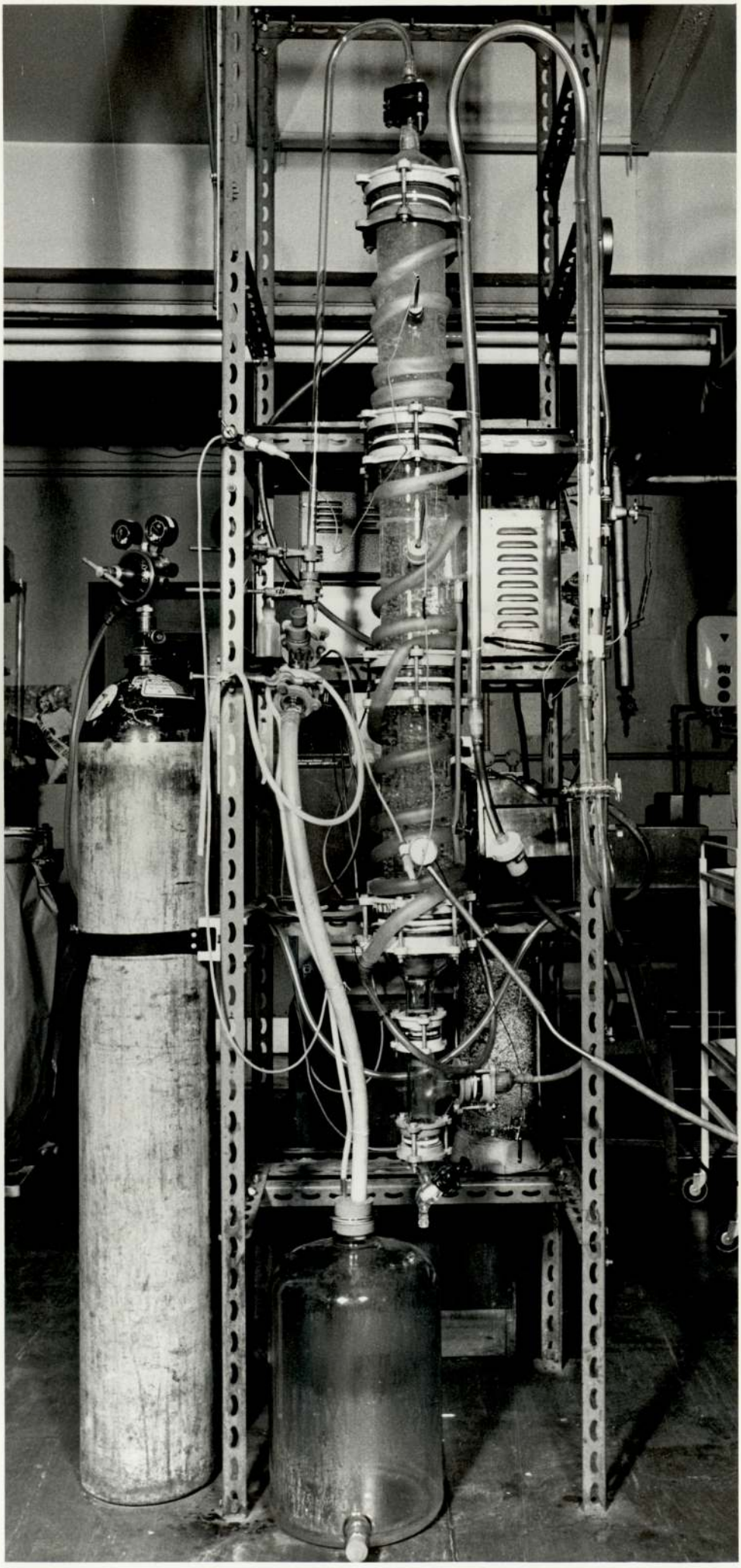

Air, taken from the compressed air service line, was metered using a 10P rotameter, filtered through a Whatman Gamma 12 in-line unit and introduced into the base of the column. The gas flow rate was standardised at the beginning of each set of experiments by setting maximum flow on the rotameter at 5psig at the mains outlet: this was done by adjusting the flow control valve and the pressure reducer similtaneously until the desired conditions were obtained (see figure 4.5). The gas distributer fitted across the base of the column was made of 2mm thick stainless steel. It consisted of a perforated plate with 69 holes of 1mm diameter arranged on a 10mm triangular pitch. The arrangement was such that the distance between the outer holes on the plate and the inner edge of the column section was kept to a minimum: this ensured that stagnant regions, and hence growth of mycellium on the plate, were minimised.

The measurement of oxygen mass-transfer coefficients, using the dynamic measurement technique described previously, required the use of oxygen-free nitrogen (white spot). This was supplied from pressurised cylinders obtained from the British Oxygen Co. Ltd.. A simple switching device was used so that the air metering system could be used for nitrogen flow measurement.

The "spent gas" and the liquid product, which during a fermentation contained microbial aggregates, left the top of the column via an inverted glass 'U' tube. The liquid and product fell into the liquid receiver and the spent gas escaped to atmosphere. The positive pressure within the system made a filter on the outlet unnecessary.

Temperature control was an important feature of the system because of its effect on the functioning of both the organism and

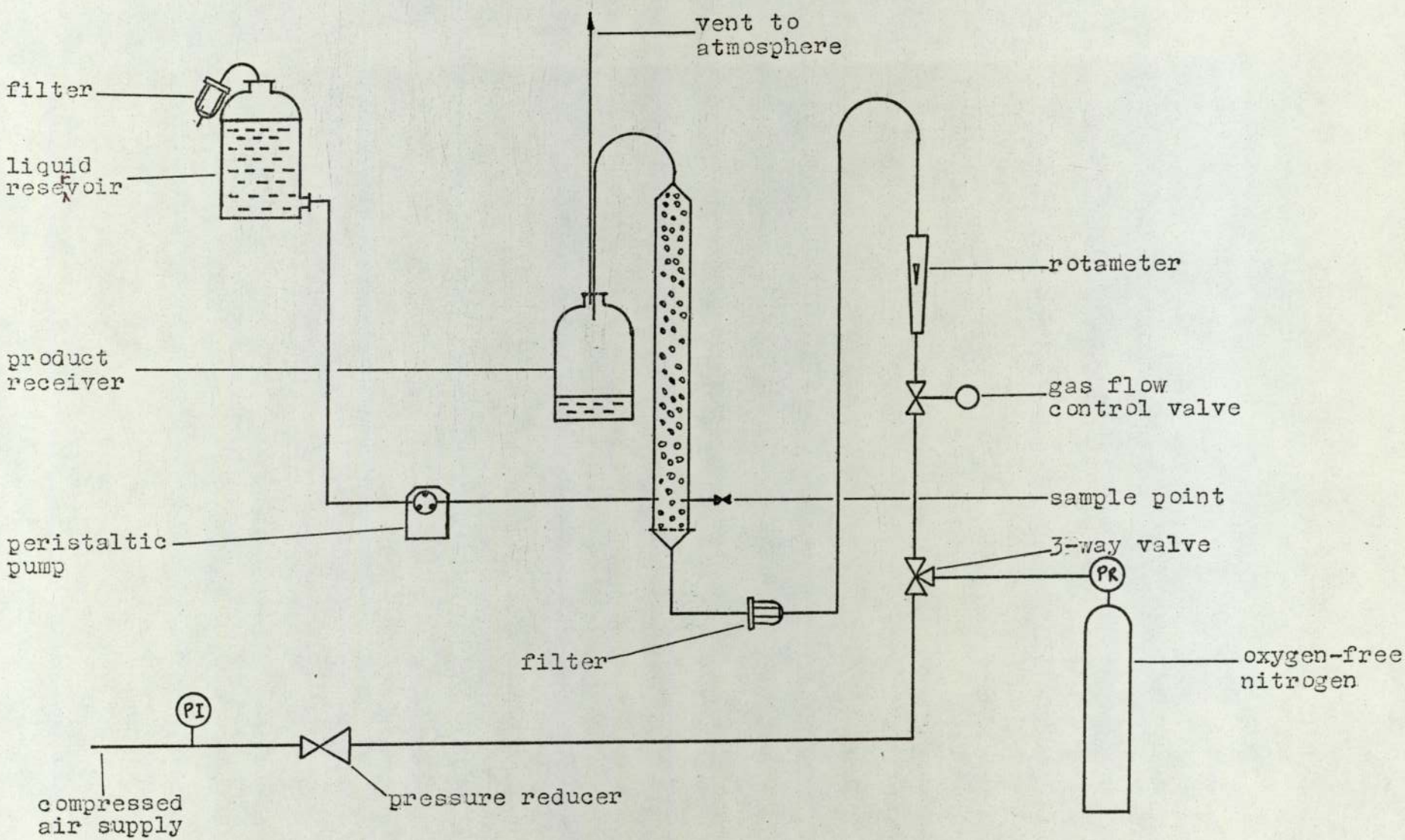

Figure 4.5 Gas and Liquid Flow Diagram -102 mm Diameter Column

the oxygen measuring device. The effect of temperature on microbial growth rate is well known (3); for Aspergillus niger the optimum temperature range is between 30 and 32°C (4). In the case of the Chark oxygen electrodes described below it was found that the probe signal doubled with every 14 degree C rise in temperature: this is a significant effect and illustrates the importance of good temperature control. Finally it should be noted that changes in temperature affect liquid-phase properties as well as the solubility of oxygen. The temperature of the experimental system was maintained by pumping warm water by means of a Churchill Thermocirculator through a length of thin-walled Pauls tubing wound around the fermenter. A thermostat contained within the Thermocirculator allowed feed forward control of the system and enabled the temperature of the fermenter to be kept within the limits of ± 0.5 °C during the course of an experiment. This proved quite satisfactory in the majority of cases.

4.1.2 The Oxygen Electrode.

During early experiments two oxygen electrodes were used. One was based on the design of Johnson et alia (5) and the other, the Chark electrode, on the design of Clark (6). However it soon became clear that the Johnson electrode could not be used in dynamic experiments because the response time was too long.

The Chark Oxygen Electrode, used in most experiments descibed in this thesis, was an electrode manufactured by Chark Electronics of Birmingham. Its advantages included fast response, simplicity of construction, stability of response, availability and low cost.

The electrode, figures 4.6 and 4.7, consisted of a platinum cathode and a silver anode in a perspex case; 5% potassium chloride

Figure 4.6. The Chark Electrode.

Scale: 2 x full size.

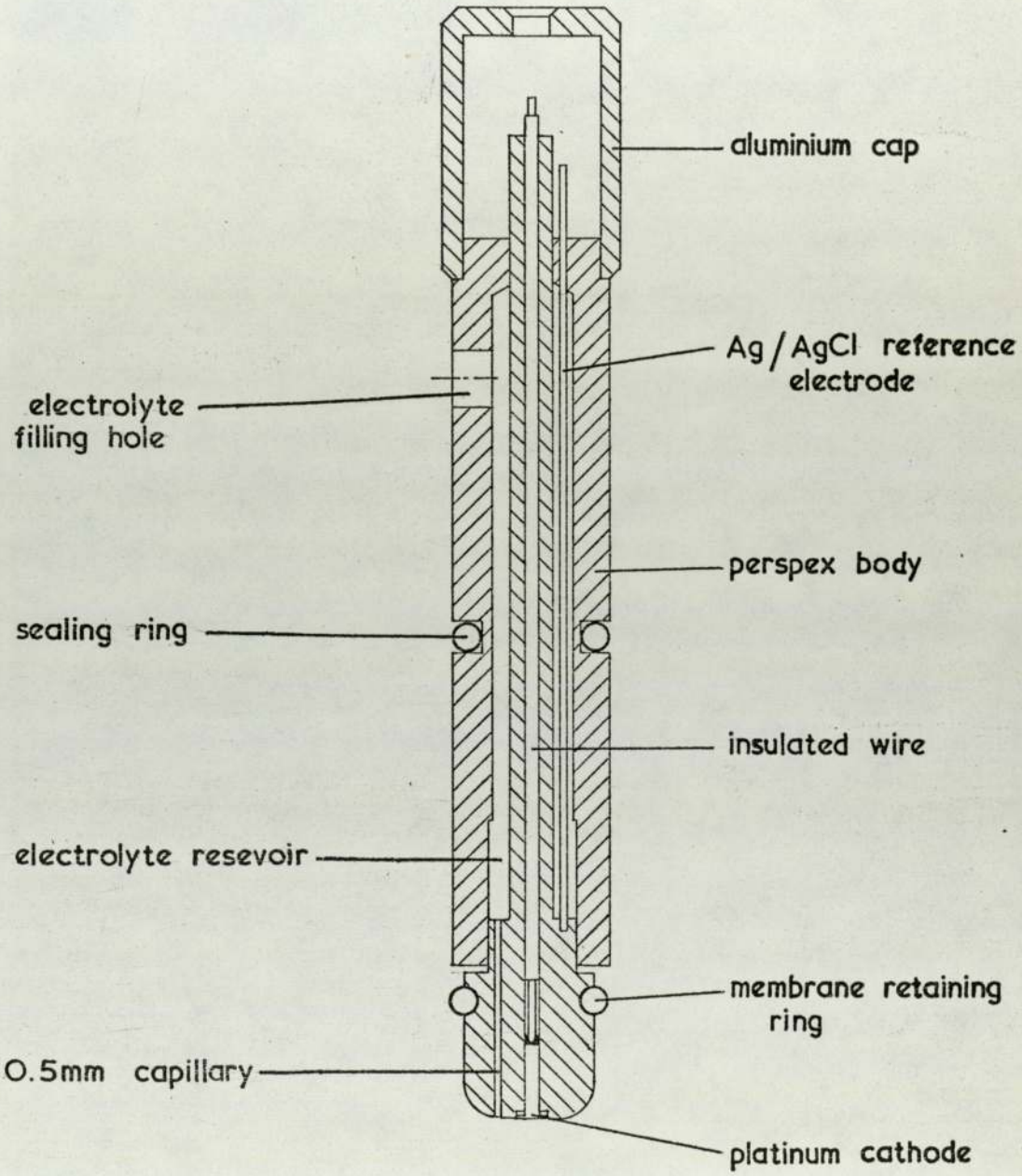

Figure 4.7 The Chark Electrode.

(inset shows the platinum cathode and the 0.5mm capillary)

solution was used as the electrolyte. A 25μm thick polyethylene sheet was stretched across the cathode and held in position by a rubber 'O' ring. During assembly the electrolyte cavity was filled with KCl solution and a few drops of the solution allowed to pass through the capillary onto the membrane before it was fitted. Care was taken not to distort the plastic film by subjecting it to too great a tension. After use the probe was always cleaned out with distilled water to prevent the deposition of KCl in the capillary.

A stainless steel, water tight sheath was designed and manufactured so that the probe could be totally immersed in the fermentation system.

4.2 Experimental Techniques.

4.2.1 The Dynamic Method for the Measurement of $k_L a$.

In the dynamic method originally described by Taguchi and Humphrey (7) $k_L a$ is evaluated by analysis of a dissolved oxygen concentration trace. The trace is produced using a fast response oxygen electrode to measure oxygen concentration during and after a brief interruption of the air flow in a fermenter.

For a perfectly mixed fermenter:

oxygen uptake rate by the organism $= Rx$ (1)

gas-liquid oxygen transfer rate $= k_L a\ (c^* - c)$;(2)

and so for the non-gassing situation

$$-\frac{dc}{dt} = Rx \qquad (3)$$

and for the aeration period immediately following the interruption

$$+\frac{dc}{dt} = k_L a\ (c^*-c) - Rx \qquad (4)$$

At steady state $$\frac{dc}{dt} = 0 \qquad (5)$$

$$Rx = k_L a\ (c^*-c) \qquad (6)$$

It should, therefore, be possible to evaluate $k_L a$ by measuring Rx in the non-gassing period, and on substituting this value into equation (4) to find the oxygen take-up during re-aeration.

The above method has been shown to work quite well with mechanically stirred systems. However, bubble columns rely on the passage of the gas bubbles to provide agitation. Hence termination of aeration stops mixing of the liquid phase and the suspended solid phase separates out. There is also a secondary effect: lack of agitation allows the boundary layer surrounding the oxygen electrode to become depleted of oxygen, and this produces false readings (8).

Instead of a non-gassing period some other method for reducing the oxygen level of the system was therefore sought. Hsu, Erikson and Fan (9) obtained $k_L a$ data by altering the gas throughput without infact interrupting the gas flow completely. Unfortunately using this method it is not possible to measure directly the oxygen uptake rate of the organisms.

During the studies described in this thesis, it was in many cases necessary to run the system without any organism present in order to evaluate probe and system characteristics. A step change in the oxygen level in the fermenter was achieved by purging the

the system with oxygen-free nitrogen. In this way it was hoped that comparison of tower systems with and without organisms would yield some information about organism respiratory rates. The methods for determining the microbial concentration, x, are described on page 65.

4.2.2 Calibration of the Oxygen Electrode.

The oxygen electrodes were calibrated in a simple apparatus consisting of two, 50mm i.d. Q.V.F. glass tubes 300mm long. The tubes were bolted to a twin gas-distributer system (figure 4.8) and immersed in a temperature-controlled water-bath. The tubes were then filled with distilled water and one was aerated whilst the other had oxygen -free nitrogen bubbled through it.

In operation, after setting the water-bath temperature and allowing it to come to equilibrium, the electrode to be calibrated was immersed in the aerated water column. After time had been allowed for the instrument to come to equilibrium the probe was quickly switched to the de-aerated column. The response of the instrument was measured via an amplifier connected to a Servomex chart-recorder. Similarly, after equilibrium had been re-established at the "zero" level the probe was switched back to the aerated tube and the response again recorded. The response of the instrument to this type of experiment was later analysed using the theory of Heineken and Linek outlined in the previous chapter.

4.2.3 Measurement of Average Gas Holdup.

Two methods for the measurement of gas holdup were used; these are referred to as

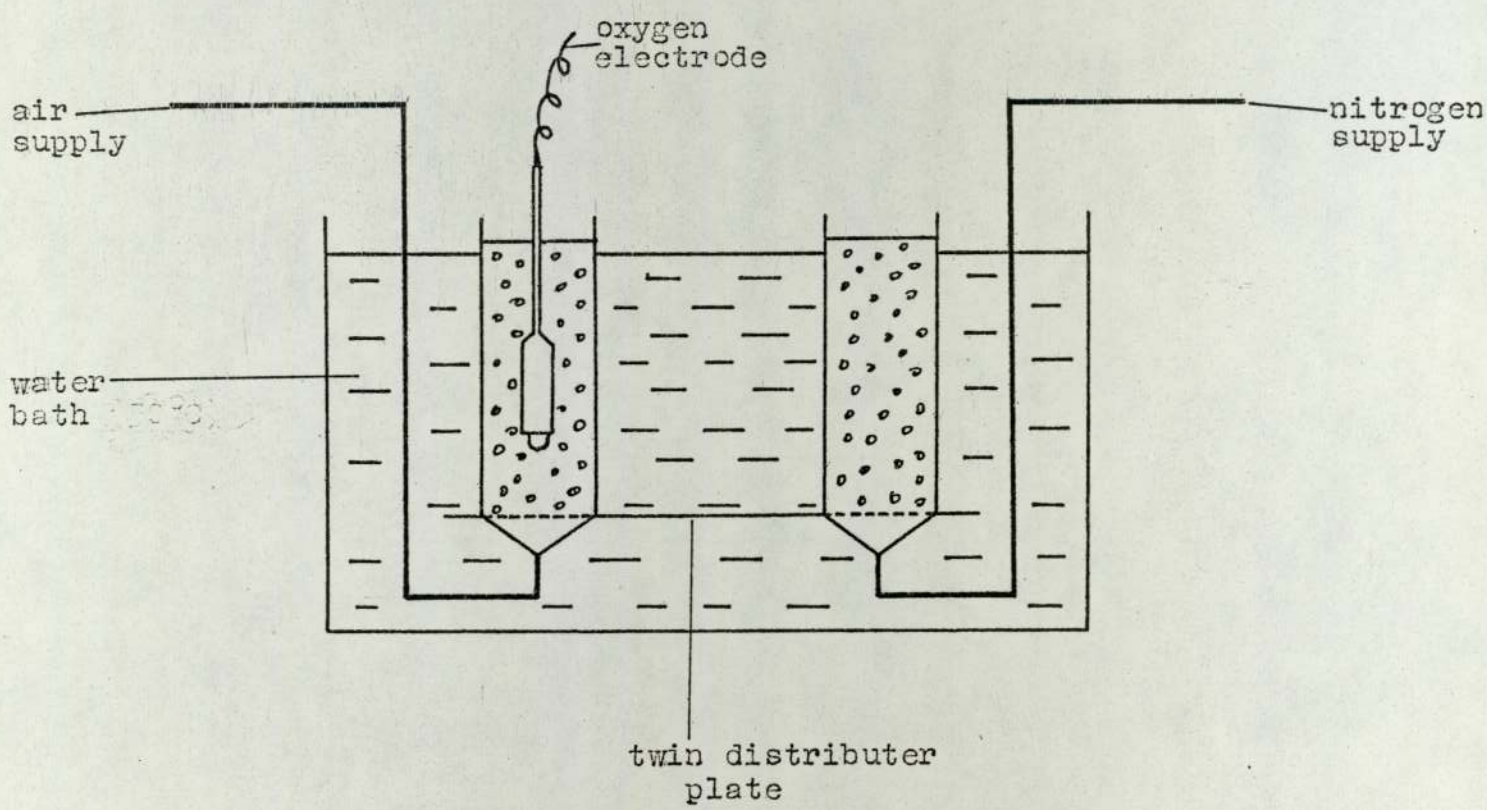

Figure 4.8 Calibration Apparatus.

(i) The Manometric Method and

(ii) The Light Intensity Method.

The latter technique, which was calibrated against the former, was particularly useful when using three-phase systems. During actual fermentations a totally enclosed system was preferred to prevent the ingress of contaminents: also there was a tendency for manometers to become blocked when micro-organisms were present.

4.2.3.1 The Manometric Method.

Two manometers were used to provide an indication of the overall gas-holdup. These were each positioned about two column-diameters away from the top and bottom of the column to avoid end effects. In early experiments the levels indicated by the manometers tended to fluctuate over a wide range. It was found that this fluctuation could be reduced markedly by using smaller diameter stainless steel sampling tubes. The inside diameter of the sample tubes was in fact reduced from 3.2mm to 1.6mm. It was also observed that any further reduction in diameter caused an increase in the occurrence of blockages.

The glass manometer tubes were mounted on a graduated board at the top of the rig in order to overcome the hydrostatic head of the system. They were connected to the sampling tubes using clear P.V.C. tubing. This allowed the lines to be inspected for the presence of air bubbles. Any trapped bubbles were removed by tapping or pinching the lines. During an experiment very few bubbles entered the manometers. Air was, however, drawn in when conditions were altered such that the gas holdup increased.

4.2.3.2 The Light Intensity Method.

This method depended on the variation of the resistance of a light-sensitive cell with light intensity. The resistance of the cell was measured using an Avo-meter. The light source was a photoflood lamp positioned diametrically opposite the light-sensitive cell (see figure 4.9). Distortion due to the curvature of the column wall was corrected using a perspex box filled with water.

The light cell was calibrated in three ways. Firstly, in absolute terms the cell was compared to a Watson IV light meter, light intensities being measured in foot candles. Whilst the accuracy of these measurements may not be high they do provide a convenient standard for purposes of comparison. Secondly, the cell was calibrated against the manometer readings so that in later experiments the gas holdup could be readily found from Avo-meter readings. Thirdly, during a fermentation, the cell was calibrated against microbial dry-weight measurements by taking readings in the absence of aeration. Unfortunately, as the percentage of suspended solid increased the light penetrating the column was reduced drastically and no meaningful results could be obtained.

4.2.4 Fermentation and Aseptic Techniques.

The fermenter body was sterilized using steam at a pressure of one or two pounds above atmospheric pressure, and care was taken to ensure that all side arms were steamed thoroughly. On completion, the air supply to the fermenter was switched on before the steam was switched off in order to maintain a positive pressure within the system and to prevent the ingress of contaminants. After a short cooling period the assembled oxygen electrode, sterilized by washing

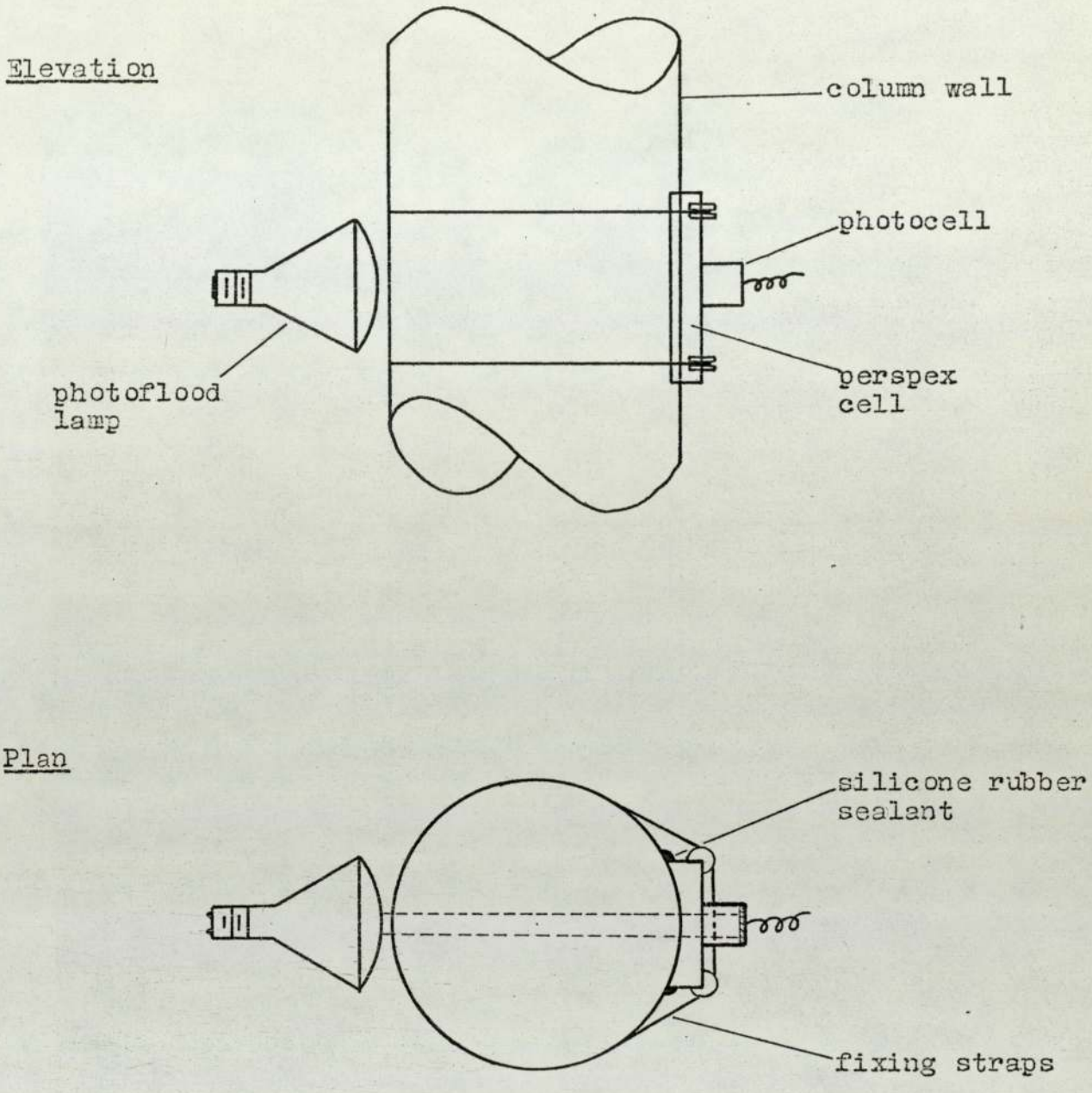

Figure 4.9 Curvature Correction Apparatus to allow for Photographs and Light Transmittance Measurements.

with methyl alcohol, was fixed in position. The column was then filled with liquid medium.

The medium, known as "M1SM", had been formulated by Pannell(2) during his work with Aspergillus niger. It was a medium with a fixed proportion of sugars and salts although the concentration of the solution could be varied (see Appendix 1). M1SM was made up in 20 litre batches and sterilized by autoclaving at a pressure of 15 psig for 45 minutes. In practice this was found to be sufficient to prevent infection even when stored for extended periods of upto a month.

Fermentations were begun using an inoculum of spores prepared from a culture of A. niger grown on molasses agar. The spores, when required, were washed from the fungal mat using a small amount of sterile, weak detergent solution. The suspension formed was totally opaque and inky black. The inoculum was introduced into the column using a hypodermic syringe. A side arm on the fermenter was used almost exclusively for this purpose and was sealed by a rubber septum.

Germination occured whilst the fermenter was being operated batchwise with a reduced gas flow rate (superficial gas velocity $\cong$ 1 cm/s): this was to prevent washout of the spores. In early experiments the gas flow-rate was not low enough and a mat of mycellium was formed on the wall of the fermenter at the gas/liquid interface. This growth tended to separate from the wall later in the fermentation and block side ports and other parts of the system.

Samples for dry weight analysis were withdrawn through a side-arm near the base of the column. The reproducibility of samples was good and the size depended on the estimated concentration: in general

100ml was sufficient. When a sample had been taken the liquid level was made up with fresh medium. Thus the fermenter was operated semi-continuously. Dry weights were obtained by filtering the samples and drying the separated solid in an oven, maintained at 110°C, to constant weight. It should be noted that such dry weight figures do not take account of sample viability. A Light Intensity Method for measuring microbial concentration is described on page 63.

4.2.5 Antifoam: Its Addition and Removal.

Antifoam was added to the column in several experiments both for the study of the action of the antifoam and the prevention of foam during fermentations. In both cases the antifoam was added using a graduated 1ml syringe via the side-arm used for the inoculum.

Once added, the spread of antifoam throughout the column was very quick. Its effect on the bubble size distribution and on the foam itself were marked after only a few seconds. Experience showed that "pure" Birmingham tap-water tended to form a single layer of large cellular bubbles that persisted for a few seconds once the air supply was turned off. Because such small amounts of antifoam had such a marked effect on the system this trace of foam was used to signify the presence or absence of antifoam. On completion of an experiment the rig was flushed with hot tap-water both forwards (filling the column and allowing it to overflow) and backwards (by draining the column through one of the lower ports). This process was repeated with cold water until the thin layer of foam reappeared at the top of the column.

Nomenclature (Section 4)

Symbol	Explanation	Units
c	concentration of oxygen in liquid phase	g/l
c^*	equilibrium concentration of oxygen in the liquid phase	g/l
$k_L a$	overall mass-transfer coefficient	s^{-1}
R	respiratory rate of the micro-organism	$(g\ O_2)/(g\ org)s$
t	time	s
x	micro-organism dry weight	g/l

References (Section 4)

(1) SHAYEGAN-SALEK, J., Ph.D. Thesis, University of Aston in Birmingham (1974)

(2) PANNELL, S.D., Ph.D. Thesis, University of Aston in Birmingham (1976)

(3) PATCHING, J.W. and ROSE, A.H., "Methods in Microbiology", Vol 2, Eds. NORRIS, J.R. and RIBBONS, D.W.

(4) MORRIS, G.G., Ph.D. Thesis, University of Aston in Birmingham (1972)

(5) JOHNSON, M.J., BORKOWSKI, J. and ENGBLOM, C., Biotechnol. Bioeng., 6, 457 (1964)

(6) CLARK, L.C.Jr., Trans. Am. Soc. Artificial Internal Organs, 2, 41 (1956)

(7) TAGUCHI, H. and HUMPHREY, A.E., J. Ferment. Technol. Japan, 44, 881 (1966)

(8) JOHNSON, M.J., BORKOWSKI, J. and ENGBLOM, C., Biotechnol. Bioeng., 6, 457 (1964)

(9) HSU, K.H., ERICKSON, L.E. and FAN, L.T., Biotechnol. Bioeng., 17, 499 (1975)

5. EXPERIMENTAL RESULTS

5. Experimental Results.

5.1 Gas Holdup.

The experimental results obtained for the air-water system have been plotted in figures 5.1 and 5.2. Two columns of different diameters were used, and the data were obtained using the manometric technique. A range of temperatures was used during experiments with the 102 mm diameter column. Figure 5.3 compares data, using the same technique and the above column, for the air-MISM-Silcolapse systems at a temperature of 30°C.

The variation of the resistance of the selenium resistance cell, used in the light transmittance experiments, with luminous flux is recorded in figure 5.4. Gas holdup results obtained in the two phase air-water system, and the effect of the antifoams Silcolapse and P2000 are illustrated in figure 5.5

The effect of superfical gas velocity, anti-foams and MISM concentration on gas holdup has been recorded photographically in figures 5.6 to 5.13. The presence of salts in the liquid phase caused the formation of so-called "ionic" bubbles - small bubbles of less than 1 mm diameter. These bubbles have low rise velocities, and figure 5.14 shows that many are still present in the column sometime after the air supply has been shut off.

Finally figure 5.15 shows holdup data collected during a fermentation. During the early stages of the fermentation it was found that the light transmittance method of measurement could be used quite readily. However, the suspension of micro-organisms soon became too dense for any measurement to be made. With this system the gas holdup was estimated by noting the change in level in the system after an interruption in aeration.

5.2 Oxygen Mass-transfer.

5.2.1. Background to Method of Analysis.

Before the results of the oxygen mass-transfer experiments can be presented it is necessary to outline the development of the method of analysis of the results.

Having found a probe with a rapid response it was hoped that the calibration experiments could be interpreted using the model of Heineken (1) and Linek (2) described previously. However, it was found that plots of $\ln(1 - \Gamma')$ vs. t were not linear (see figures 5.18 and 5.19). Attempts were made to fit straight lines using the Method of Least Squares and a Golden Section Search Method; both proved to be unsatisfactory. This meant that the method used for estimating k_La values from the experimental results had to be modified. An empirical curve-fitting approach was tried using t and $\ln(1 - \Gamma')$ in a polynomial expression of the form

$$t = a + b \ln(1 - \Gamma') + c \ln(1 - \Gamma')^2 + ...$$

where a,b,c .... are constants. To achieve a satisfactory fit to the experimental data a 4th order polynomial with 5 empirical constants was required. Such expressions are cumbersome and difficult to use without much computational effort. Therefore, having accepted that the behaviour of the probe in the calibration tests could not be described by a single-parameter model, it was decided to re-assess the overall oxygen mass-transfer system. It was hoped that this re-assessment would

1) provide a physico-chemical basis for the model,

2) help to account for the "non ideal" behaviour of the probe,

and 3) make it easier to evaluate k_La values from data obtained in bubble columns.

Calderbank (3) has shown that as far as gas-liquid mass-transfer is concerned the liquid-phase resistance is controlling. However, because of the rapid response of some types of electrode and the fact

that the bubbles will pass very close to the probe, interaction between bubbles in the gas-liquid dispersion and the probe cannot be ignored. This aspect of the problem was considered in two papers by Votruka and Sobotka (4) and the same authors in collaboration with Prokop (5): they demonstrated that the dissolved oxygen concentration sensed by the probe can be described by the expression

$$c_p = c^* \varepsilon + c\,(1 - \varepsilon) \qquad (5.1)$$

However, bubble-probe interaction does not account for the results obtained in the probe calibration tests described in this work.

Linek and Vacek (6) made a detailed analysis of the effect of a liquid film resistance at the external probe membrane surface on the probe response. Again this approach cannot explain the results obtained by the author.

Attention was then focused on the probe itself. More detailed consideration was first given to the structure of the membrane. It is likely that, as a result of the manufacturing process, the membrane is not uniform: this could cause changes in the diffusion coefficient for oxygen at different zones across the film. If the membrane diffusivity is a function of position or alternatively of oxygen concentration, the modelling becomes much more difficult. After detailed consideration of the diffusion models described by Crank (7) it became clear that considerable computational effort would be required to develop this approach.

At this stage in the analysis of the results, two papers by Linek and Benes (8,9) showed how a multi-region model of the membrane and the electrolyte-electrode system could be used to account for the

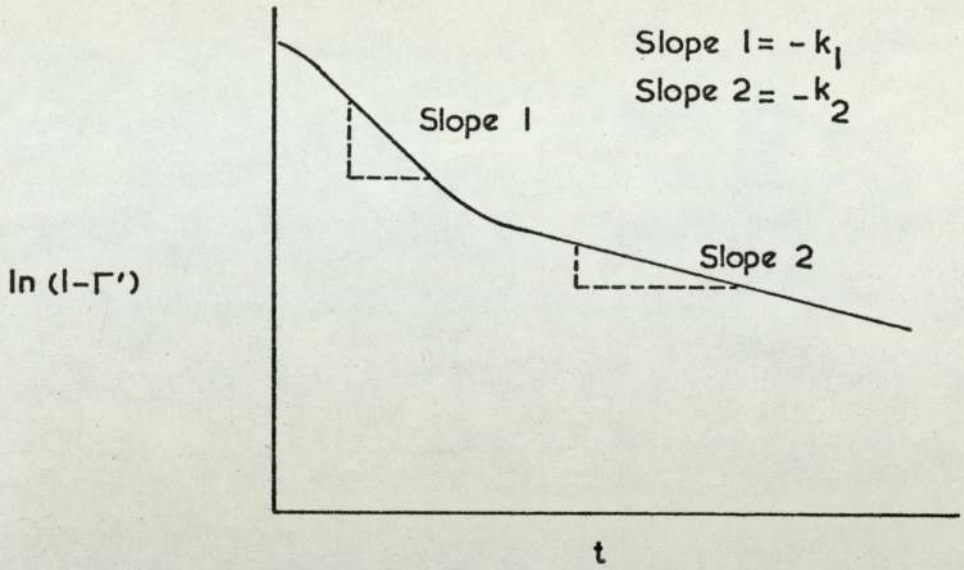

Figure 5.16 Estimation of Parameters k_1 and k_2 from Experimental Data.

slowing down in the probe response during calibration tests. The simplest two region, two-layer model of the system involves three empirical parameters but estimates of two of these can be made without great difficulty (see figures 5.16 and 5.17).

The model involves use of the equation

$$\Gamma' = 1 - 2\sum_{n=1}^{\infty}(-1)^n \left\{ A_1 e^{-n^2\Theta} + (1 - A_1)\, e^{-n^2 z\Theta} \right\} \qquad (5.2)$$

where $\Theta = k_1 t$ and $z = \frac{k_2}{k_1}$, and where k_1, k_2 and A_1 are the paramters required to describe the probe response. Some theoretical curves plotted by the above authors and based on the above equation suggest that for the Chark electrode $A_1 = 0.8$, although some variation of this parameter with temperature is possible. Estimates of k_1 and k_2 can be made by plotting ln $(1 - \Gamma')$ against time and measuring the slopes of the first and second parts of the curve. It should be noted that in their later paper (9) the authors suggest that a model based on Equation (5.2) is only satisfactory for the range of $(1 - \Gamma')$ between 0.99 and

0.07.

Finally, consideration was given to the effect of start-up procedures during both probe calibration and tests to estimate $k_L a$ values. The errors incurred are considered to be small when compared to the overall system response characteristics.

When the estimation of $k_L a$ values was considered it was noted that the most widely used methods for evaluating the parameters of the oxygen electrode responses are regression methods and the Method of Moments.[9] In using regression methods it is necessary to have a model to describe the probe behaviour: it is for this reason that the two-region, two-layer model has been given consideration. However, the method of moments has the advantage of simplicity since it is based on measuring the difference in areas under the response curves: it can be seen that with this method it is not necessary to have a detailed mathematical model to describe the probe response. The method is illustrated in figure 5.17. The area between the curves can be found either using a planimeter or by calculating the area beneath each curve using a convenient numerical method, for example the Trapezoidal Rule. The major difficulty with this method concerns estimates at high values of t: a linear extrapolation in this region is probably of sufficient accuracy when using the 0th. moment, i.e. the area under the $(1 - \Gamma)$ vs. t curve. In most cases the tail contributes about 5 - 10% of the total area. Typical results using this method are shown in figures 5.21 to 5.25. The raw data for these graphs are shown in figure 5.26. The same data have also been presented in the form $\ln (1 - \Gamma)$ vs. t for direct comparison (figures 5.27 to 5.31)

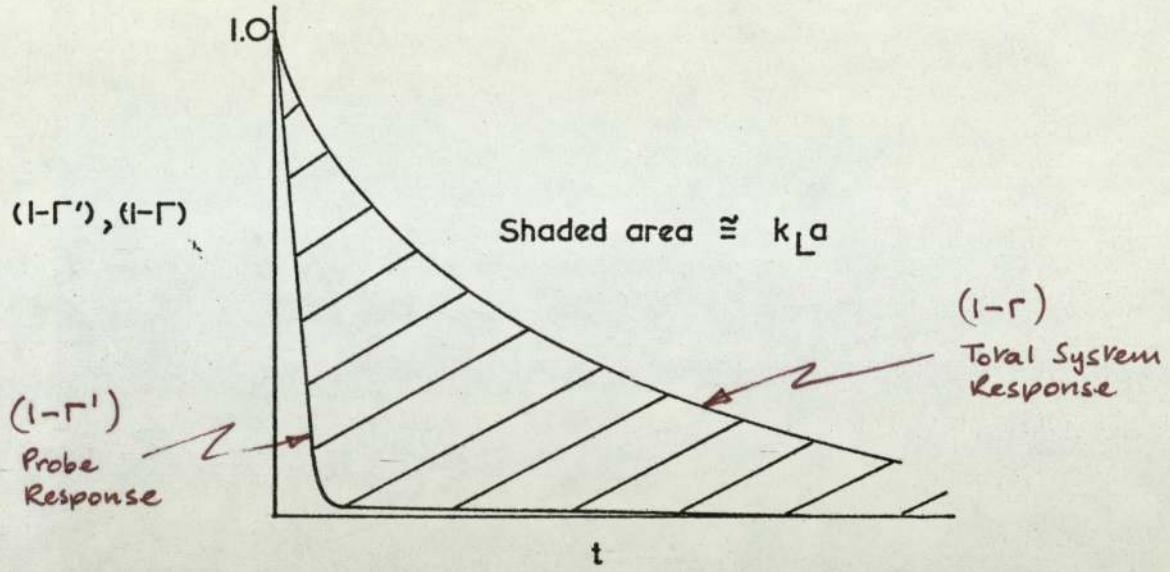

Figure 5.17 Method of Moments for the Estimation of $k_L a$. (9)

5.2.2. Temperature Calibration of the Oxygen Electrode.

The Chark electrode was also calibrated at different operating temperatures. This was done by immersing the electrode in a bath of aerated water and gradually increasing the temperature of the bath (see figures 5.32 to 5.34).

5.2.3. The Two Phase System.

Estimated values of the overall mass transfer coefficient ($k_L a$) for the air-water system using the 102 mm diameter column are shown in figures 5.35 and 5.36. A range of temperatures between 25 and 35°C was used, and fig 5.36 shows the dependence of $k_L a$ on T.

Mass transfer coefficients have also been estimated in the two phase air-MISM system. The effects of sugar concentration and the antifoams Silcolapse and P2000 are illustrated in figures 5.37 to 5.39.

5.2.4 The Three Phase System.

Information recorded during an actual fermentation is shown in figures 5.40 to 5.42. This information includes the saturated oxygen concentration, pH, dry weight, holdup and overall mass-transfer coefficient: all parameters are plotted versus time. Figure 5.41 is a repeat of figure 5.15 but it is included for ease of comparison with other data in this section.

Noting that

$$k_L a\ (c^* - c_p^*) - Rx = 0 \qquad (5.3)$$

under pseudo steady-state conditions, it is possible to estimate values for Rx and R using the above dry weight and mass-transfer information: figure 5.43 shows a plot of these parameters versus time.

The fermentation, which lasted a total of three days, was also recorded photographically. Figure 5.44 shows three general photographs taken at the beginning of each day. The photographs making up figures 5.45 to 5.50 show aggregates and the aggregate-air dispersion within the fermenter.

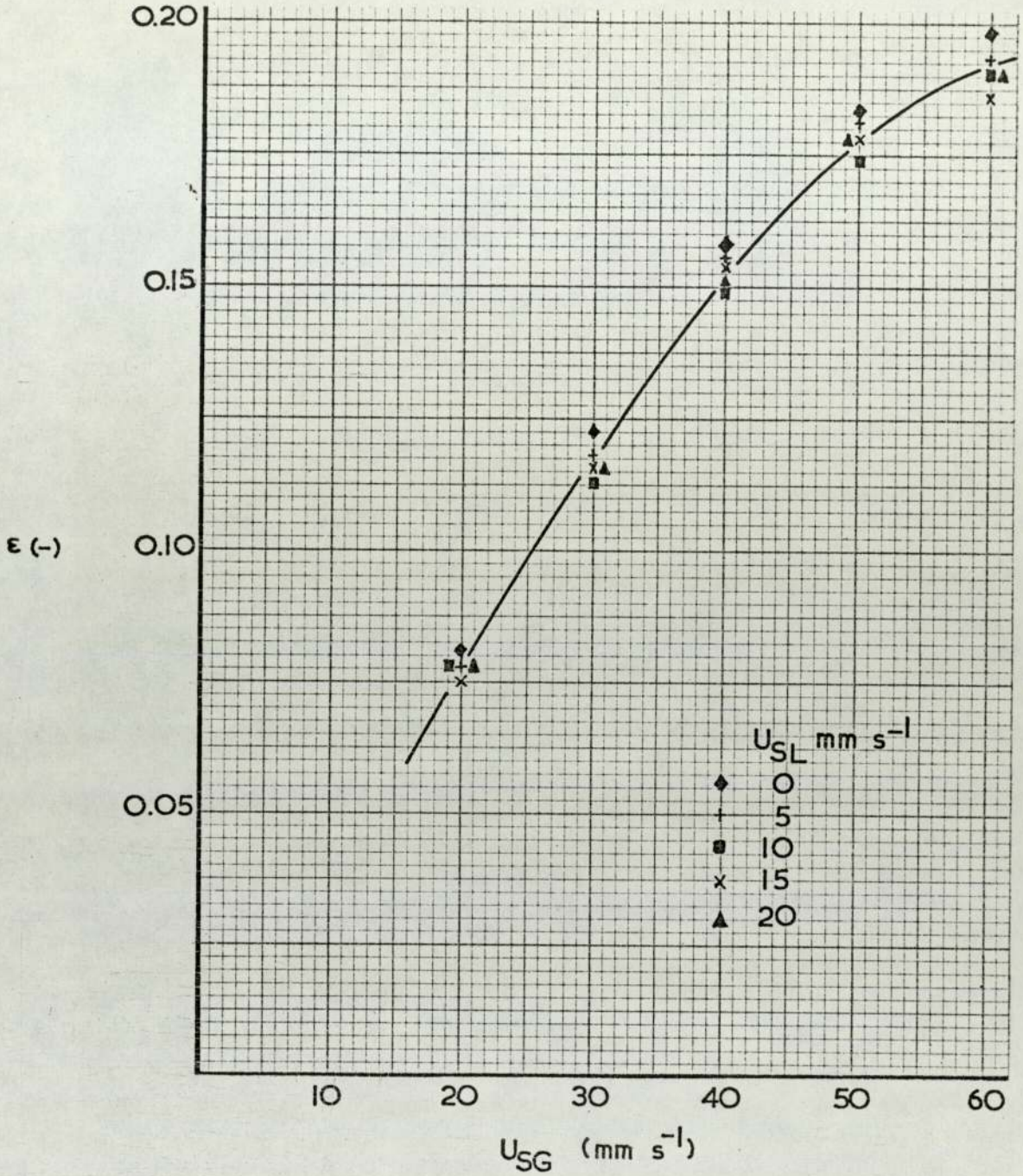

Figure 5.1 Gas Holdup vs. Superficial Gas Velocity

Column	152 mm
System	Air-Water
Temperature	Ambient

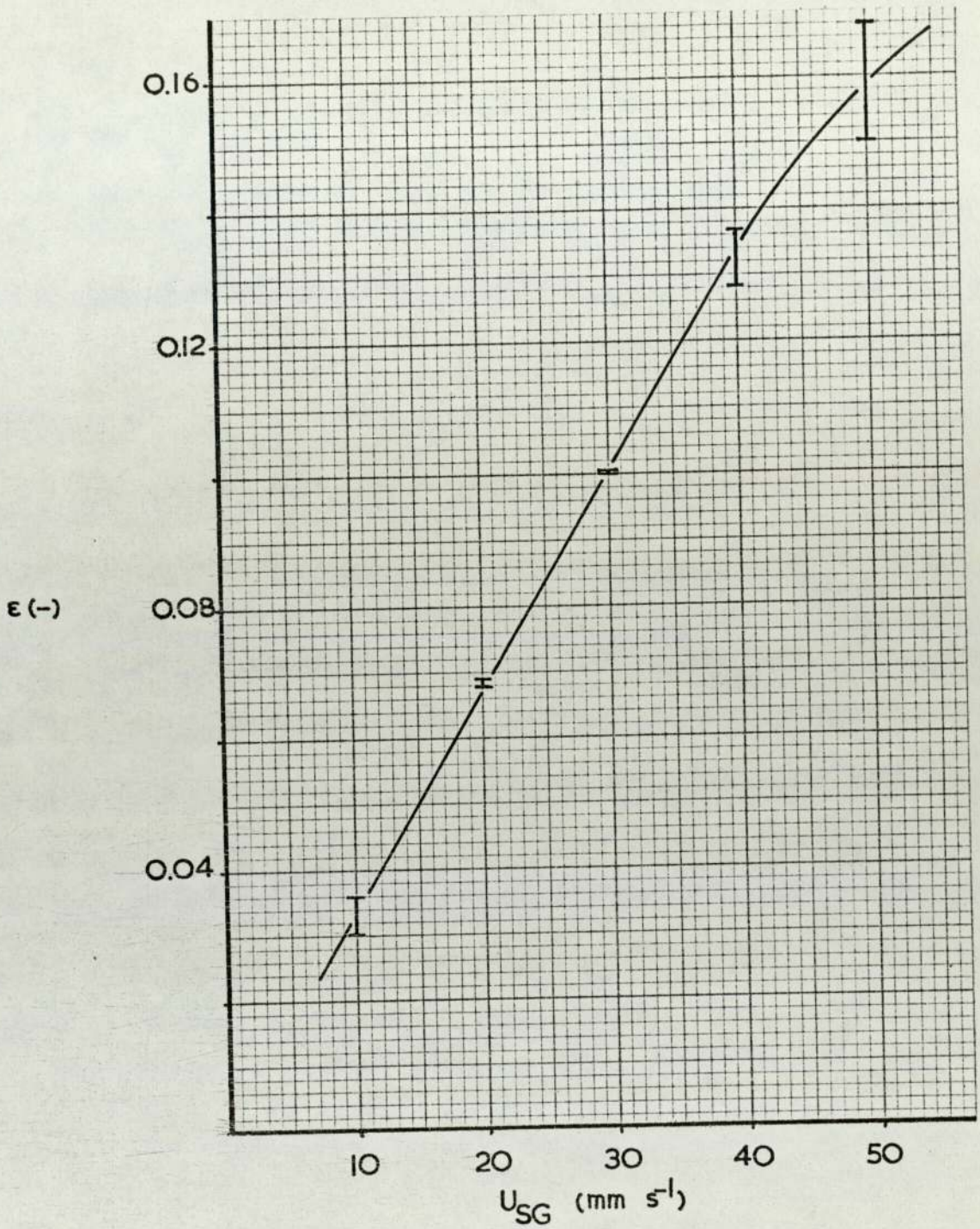

Figure 5.2 Gas Holdup vs. Superficial Gas Velocity

Column	102 mm
System	Air-Water
Temperature	25-35 °C

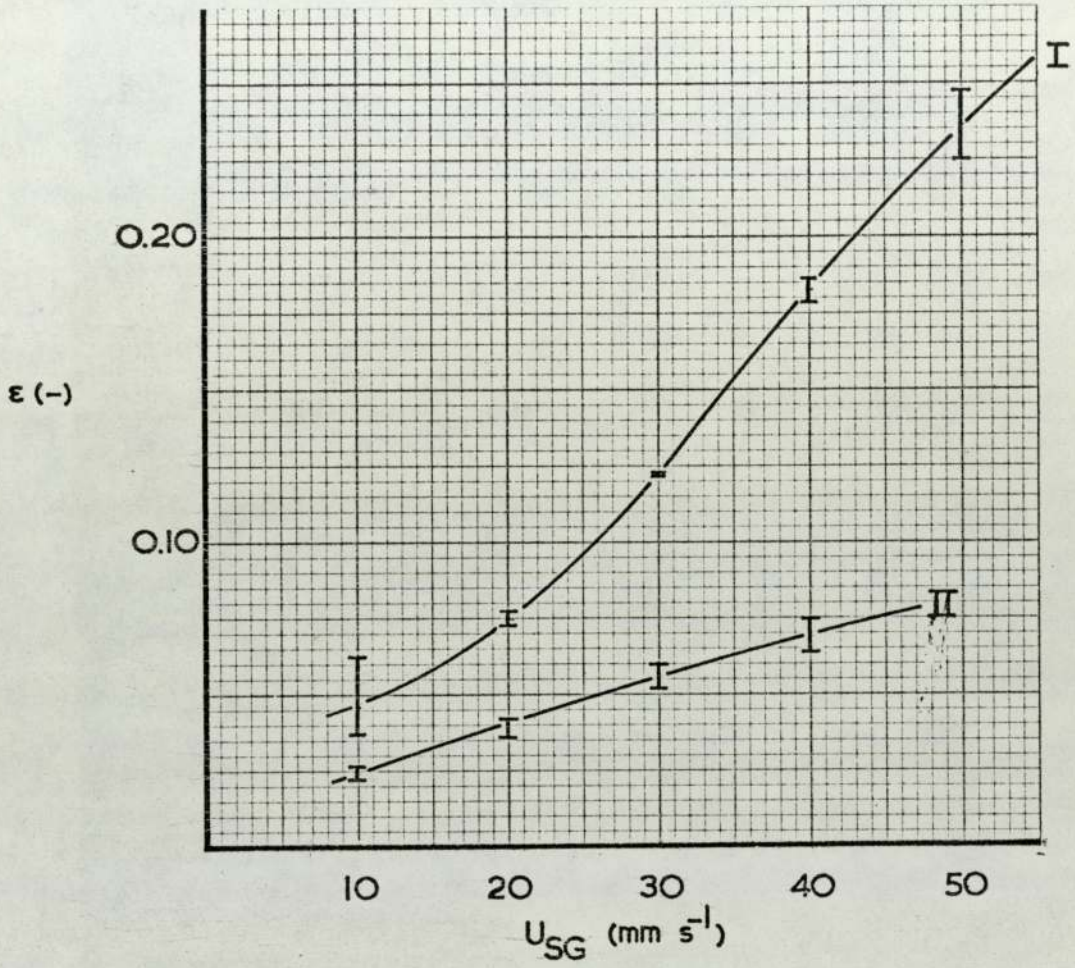

Figure 5.3 Gas Holdup vs. Superficial Gas Velocity

Column	102 mm
System	I Air-M1SM
	II Air-M1SM-Silcolapse
Temperature	30 °C

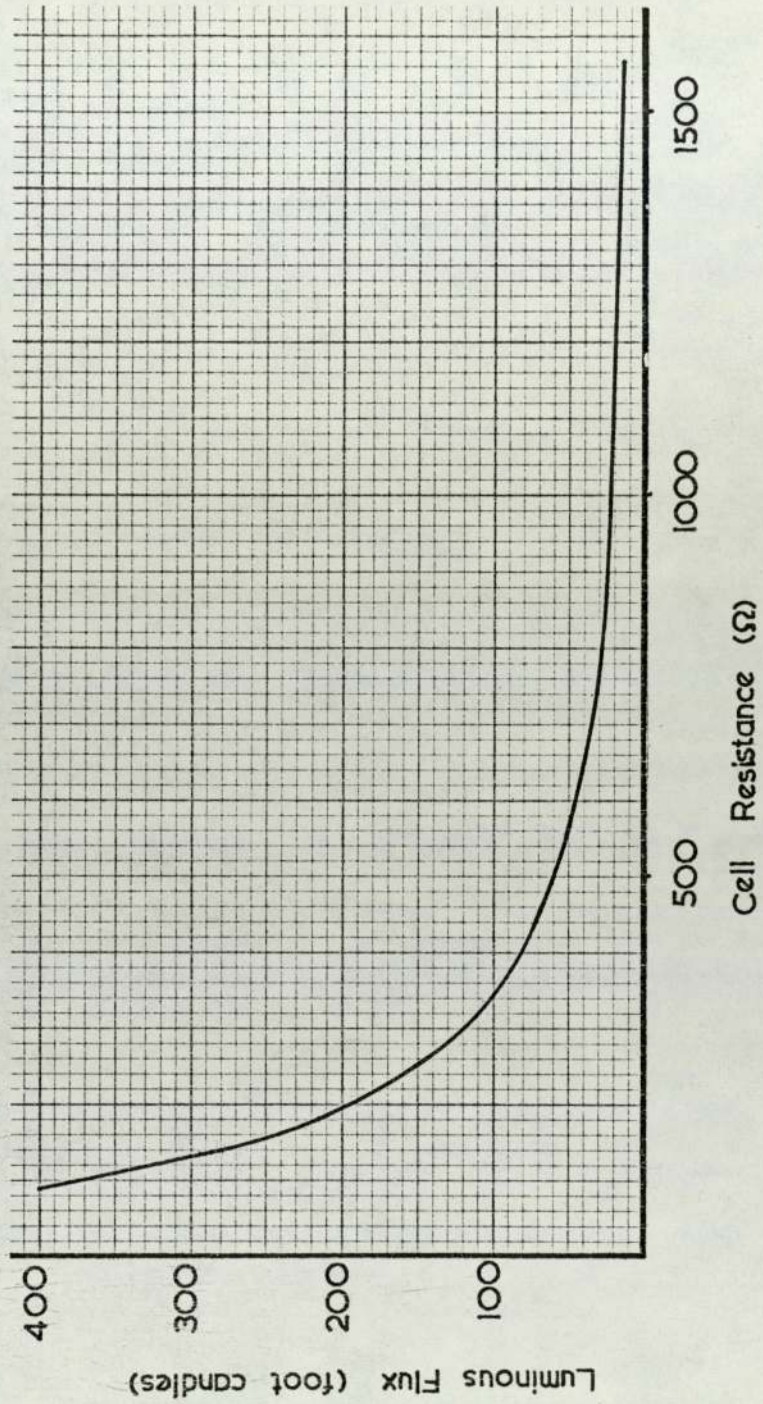

Figure 5.4 Photocell Calibration

Luminous Flux vs. Cell Resistance

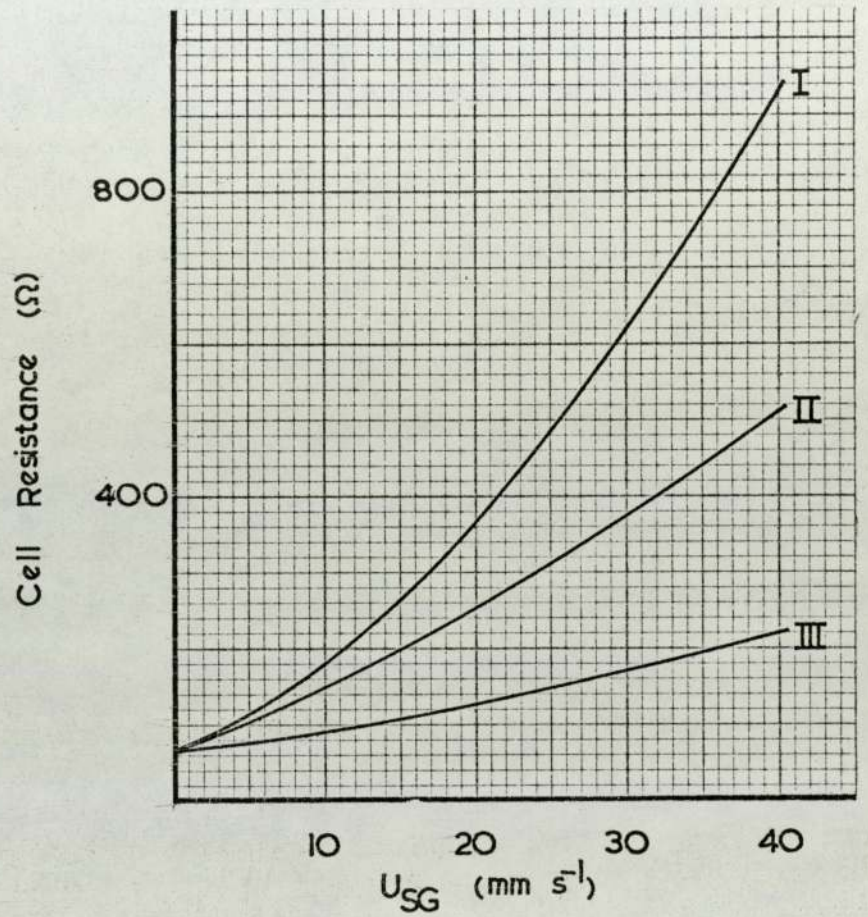

Figure 5.5 Gas Holdup - Light Transmittence Method. Photocell Resistance vs. Superficial Gas Velocity

Column	102 mm
System	I Air-Water-P2000
	II Air-Water
	III Air-Water Silcolapse
Temperature	30 °C

Figure 5.6

U_{SG} 10 mm s^{-1} U_{SG} 20 mm s^{-1}

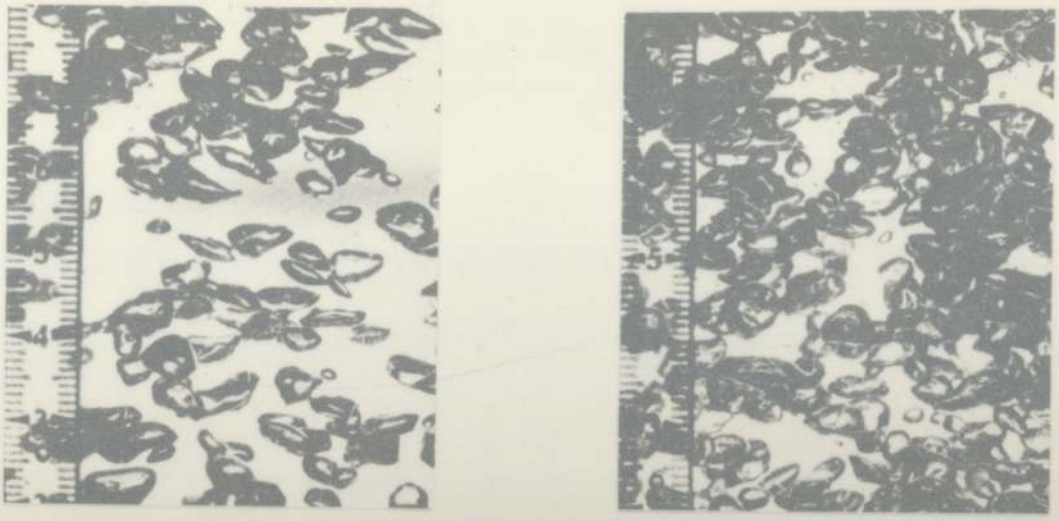

Air-Water System

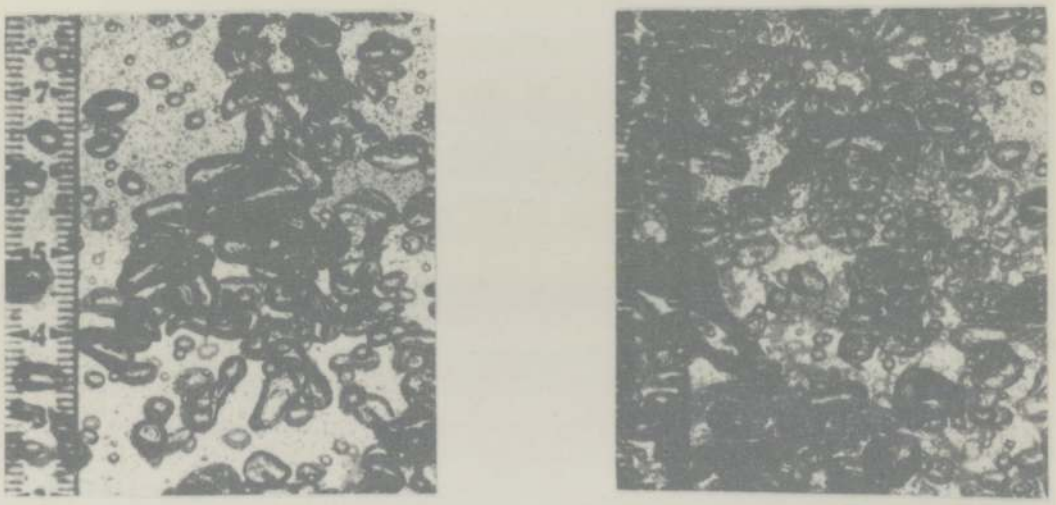

Air-Water-P2000

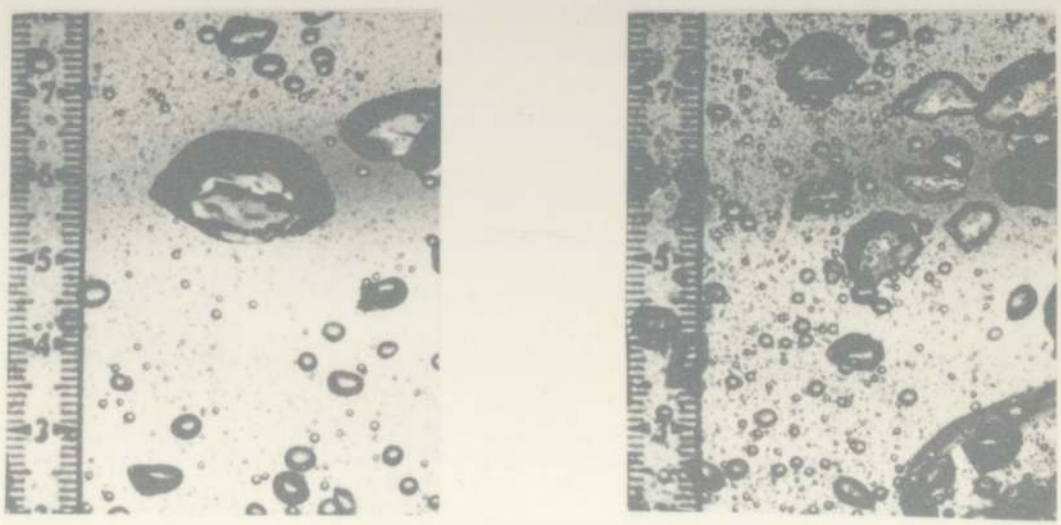

Air-Water-Silcolapse

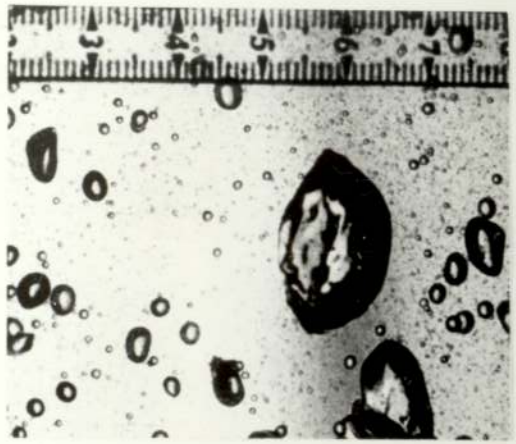

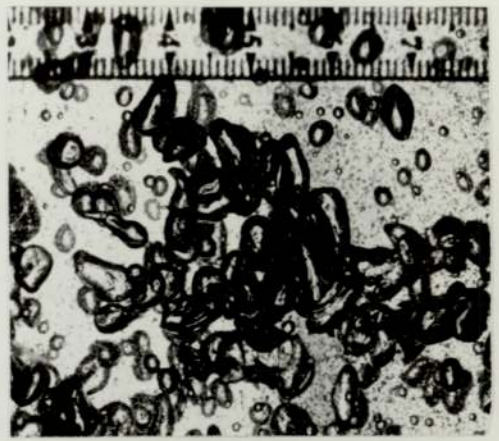

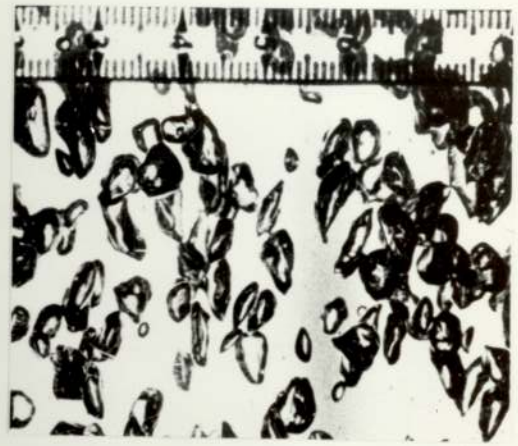

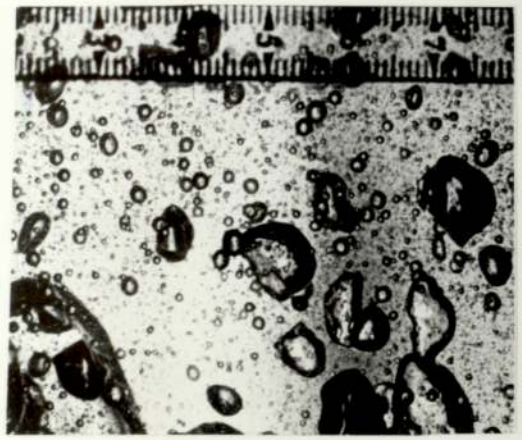

Figure 5.7

U_{SG} 30 mm s^{-1} U_{SG} 30 mm s^{-1}

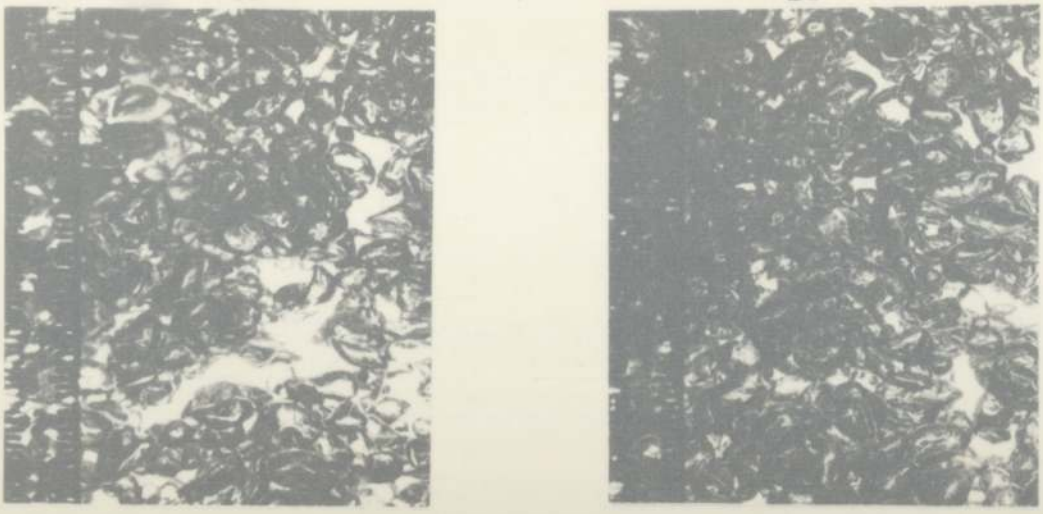

Air-Water System

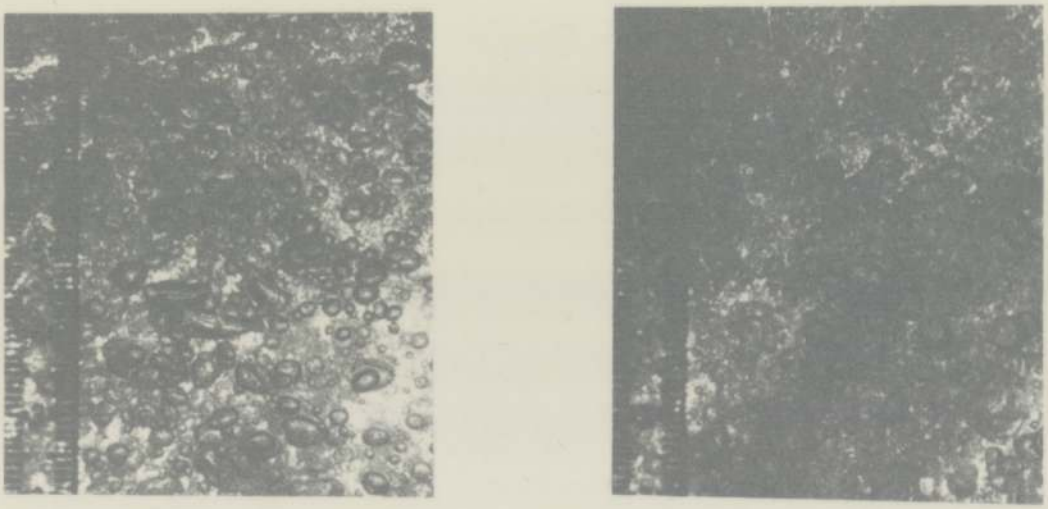

Air- Water-P2000

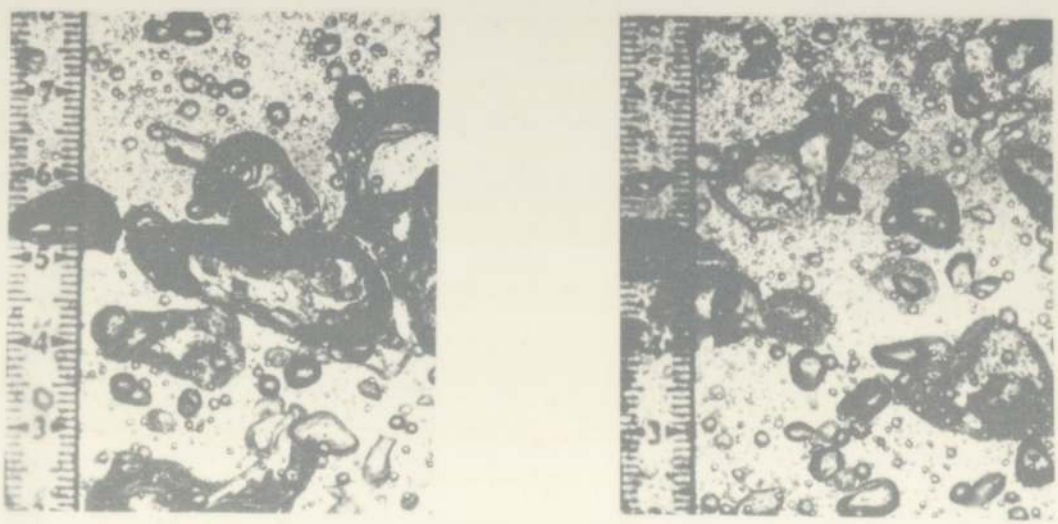

Air- Water-Silcolapse

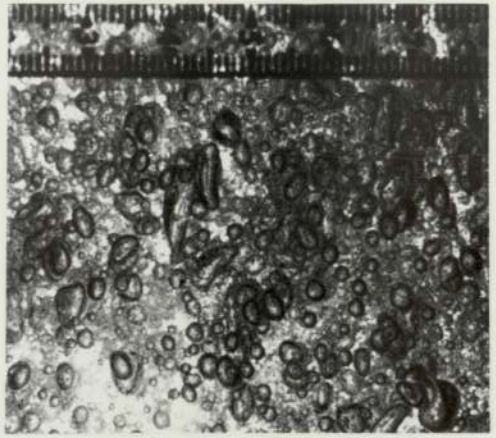

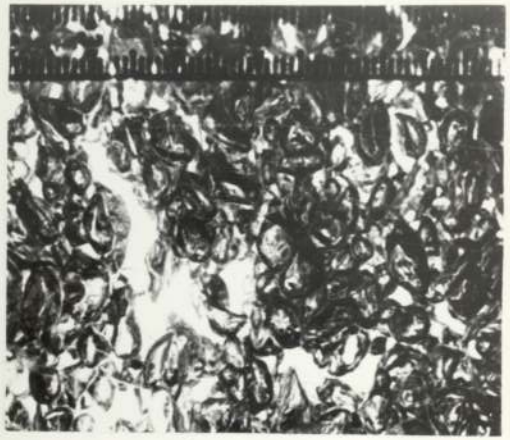

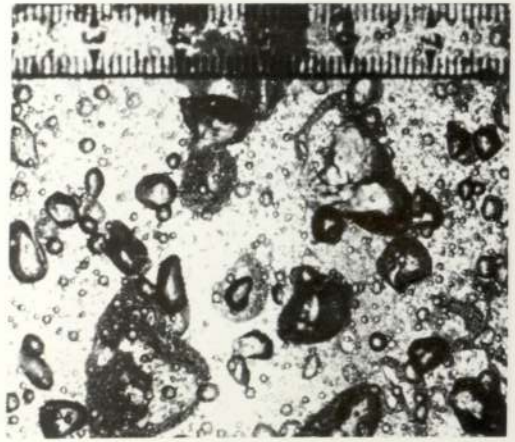

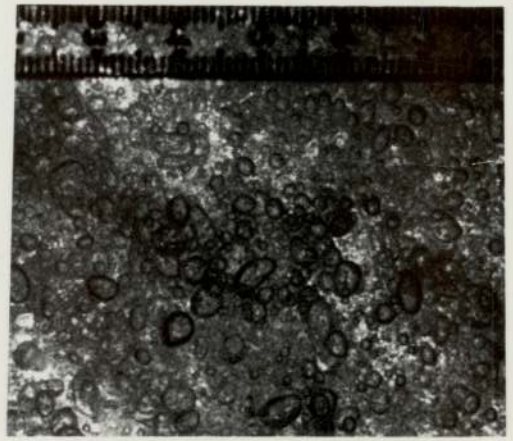

Figure 5.8

U_{SG} 10 mm s^{-1} U_{SG} 20 mm s^{-1}

Air- 0.5% M1SM

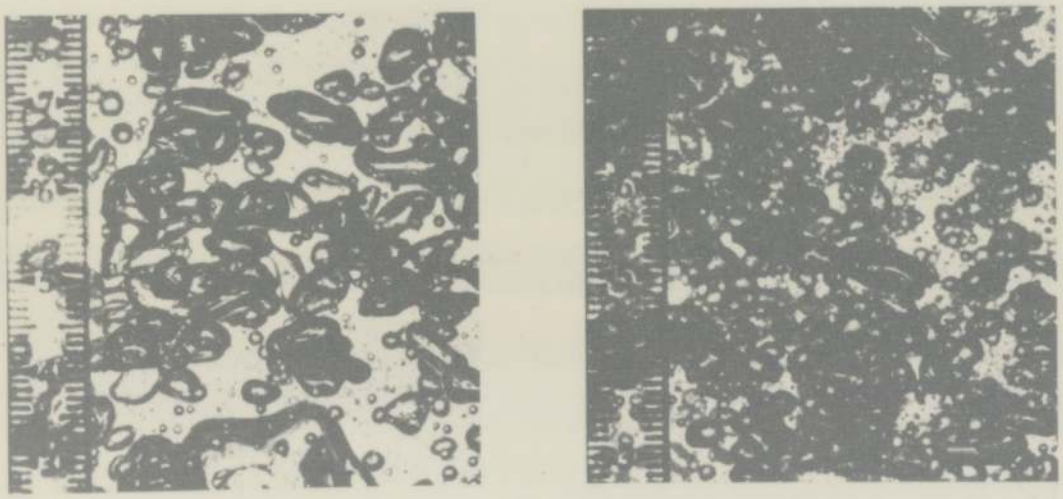

Air- 0.5% M1SM-P2000

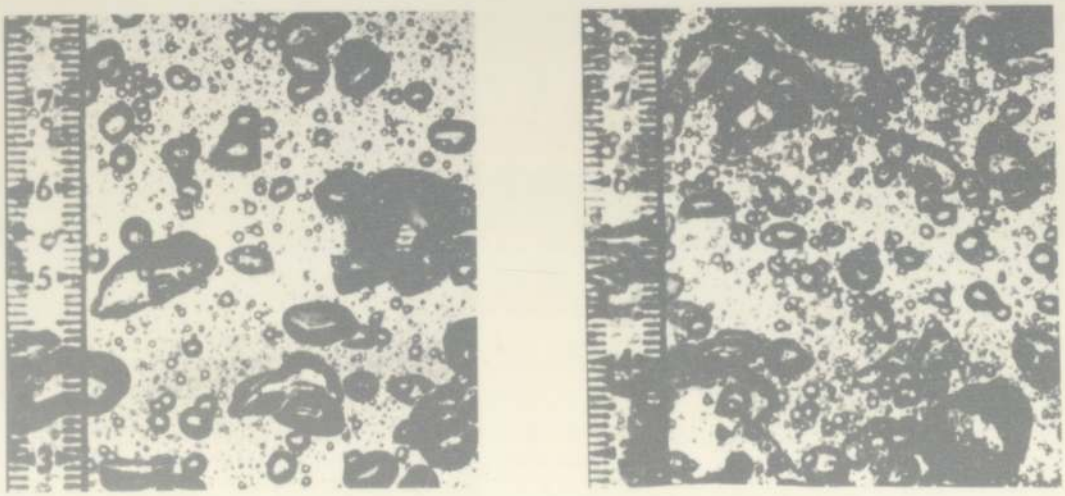

Air- 0.5% M1SM-Silcolapse

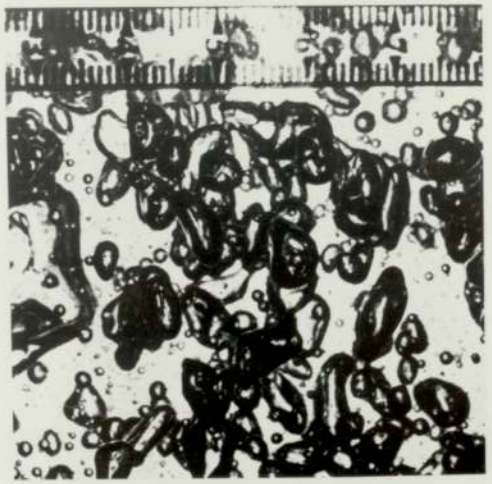

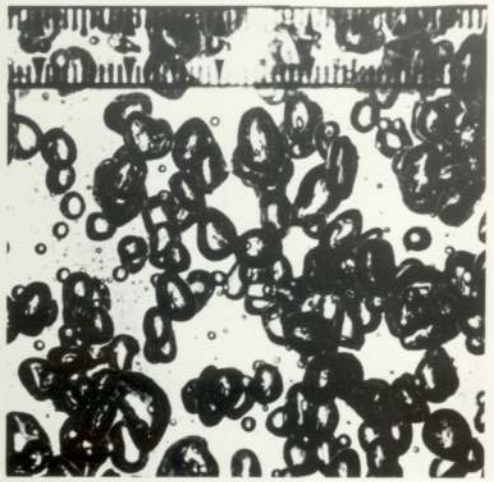

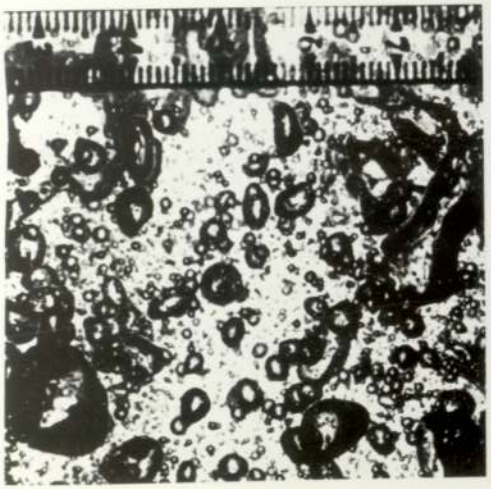

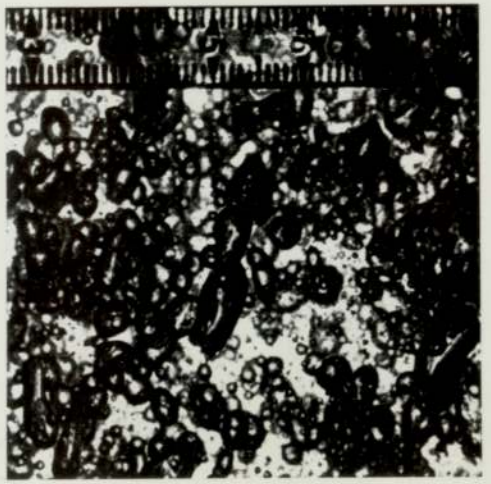

Figure 5.9

U_{SG} 30 mm s^{-1} U_{SG} 40 mm s^{-1}

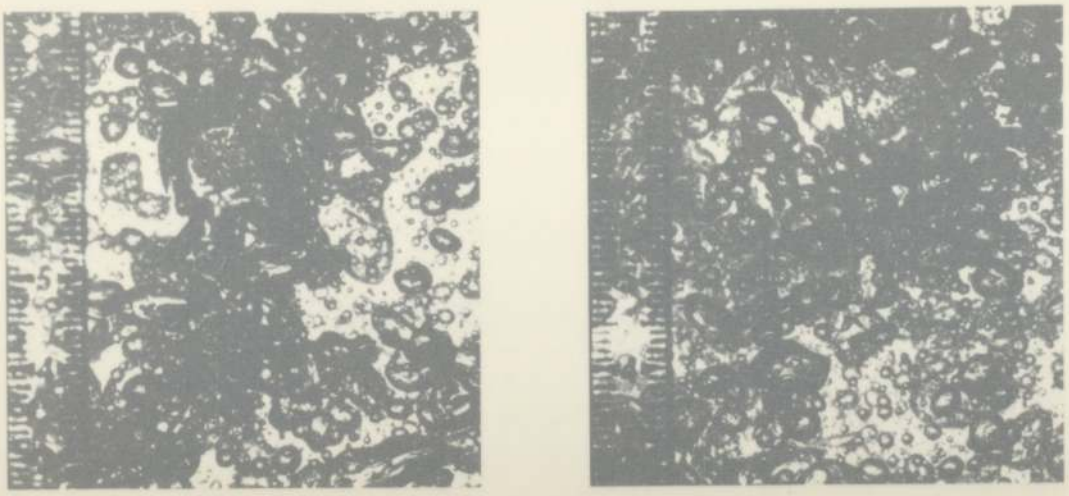

Air- 0.5% M1SM

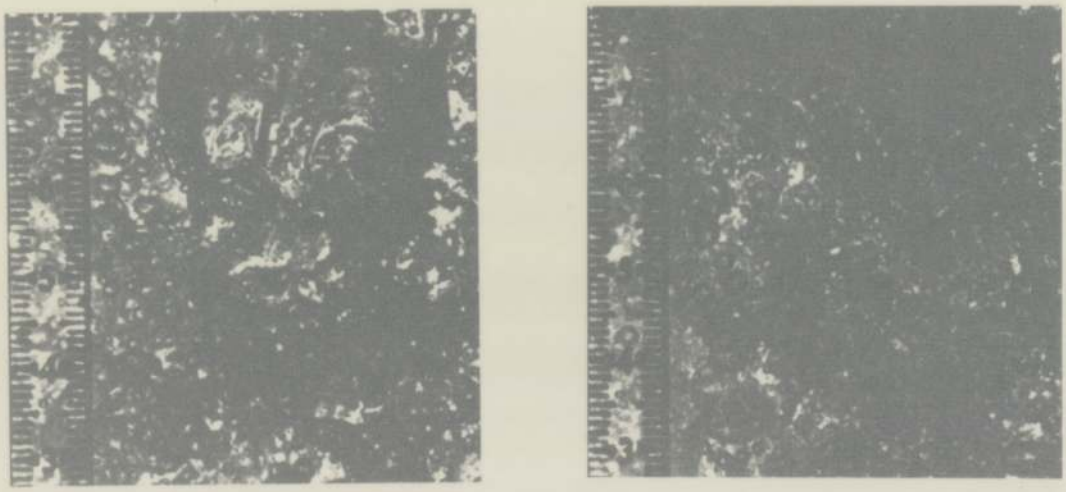

Air- 0.5% M1SM-P2000

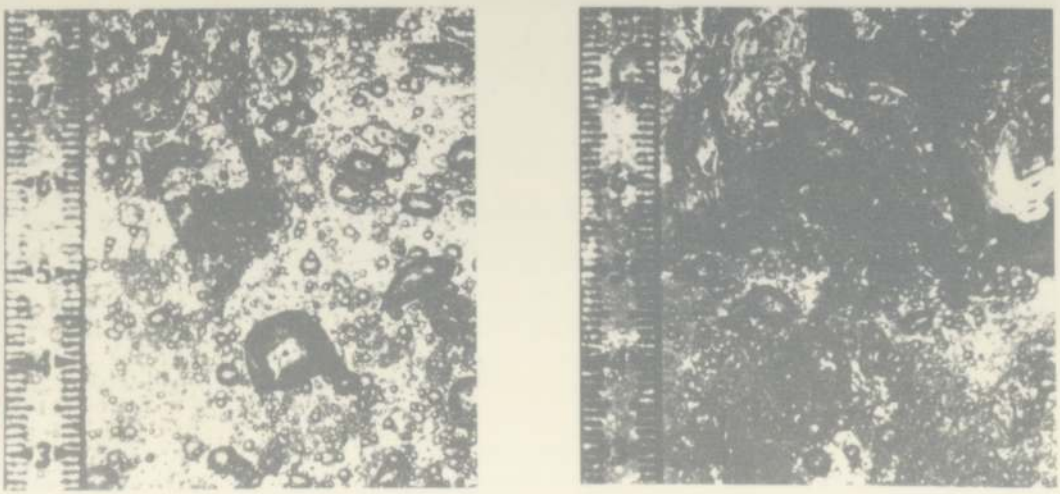

Air- 0.5% M1SM-Silcolapse

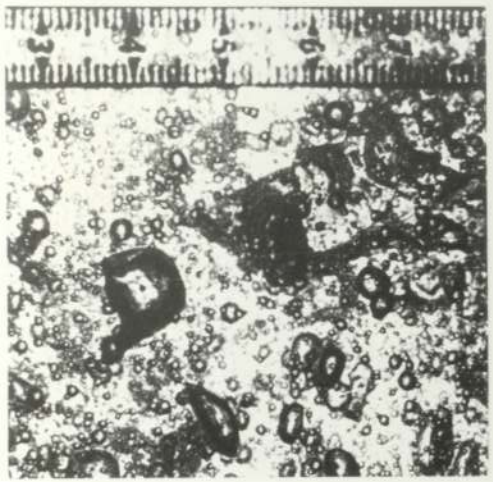

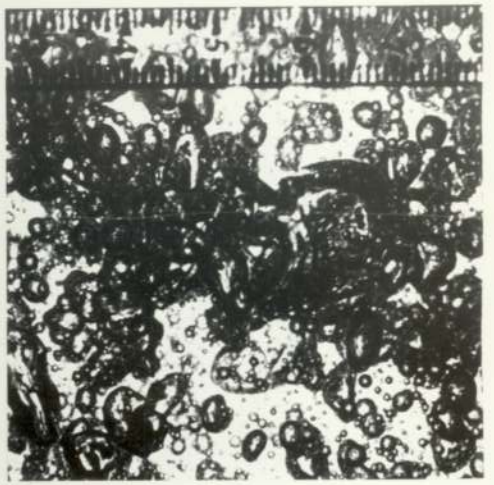

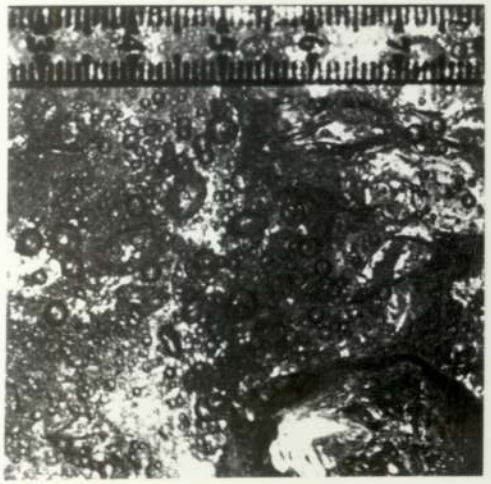

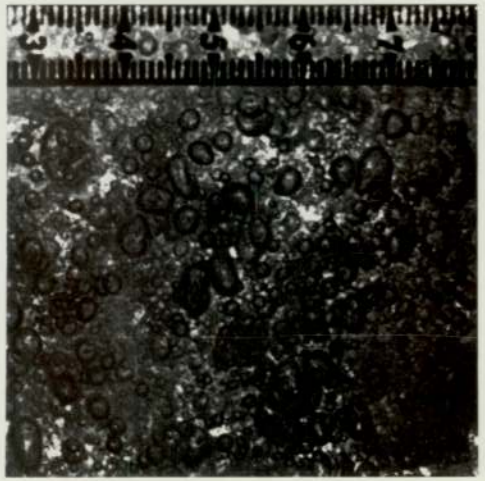

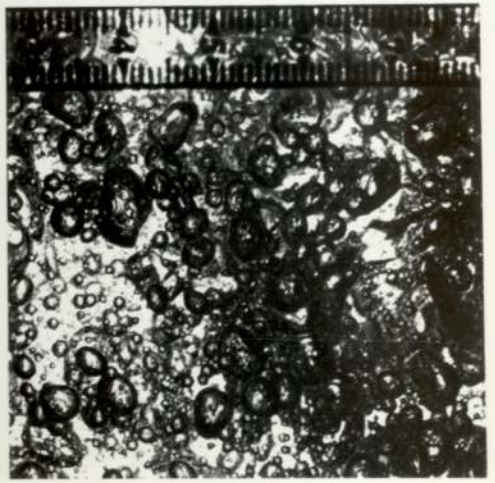

Figure 5.10

U_{SG} 10 mm s^{-1} U_{SG} 20 mm s^{-1}

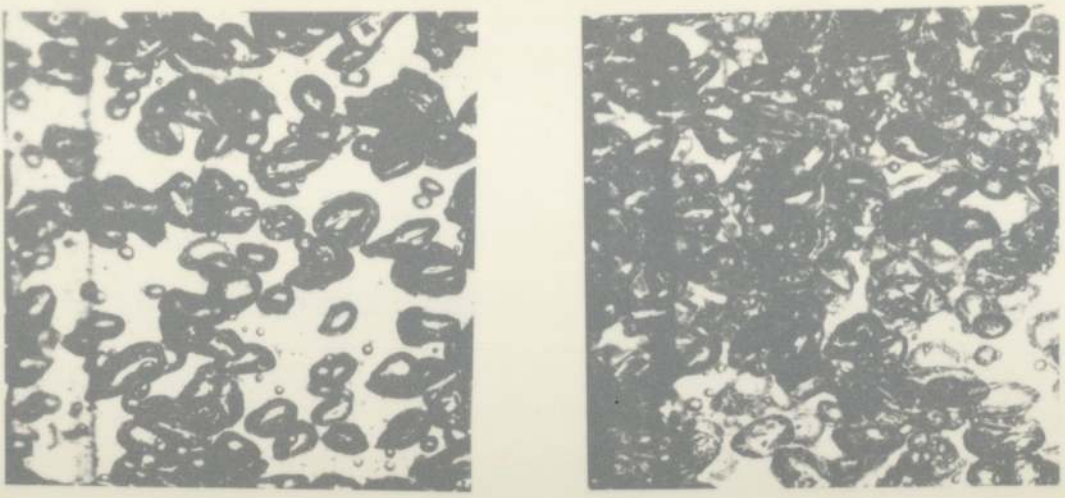

Air- 2.75% M1SM

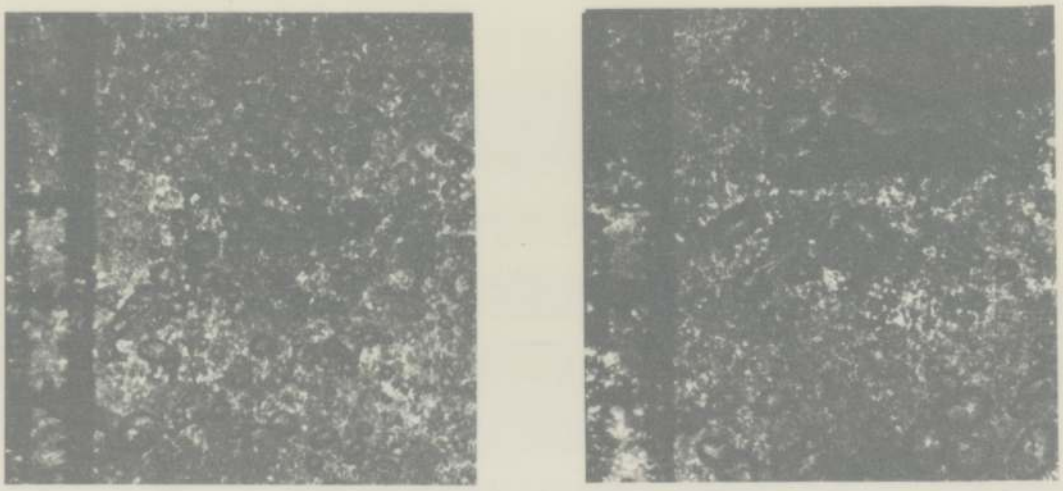

Air- 2.75% M1SM-P2000

Air- 2.75% M1SM-Silcolapse

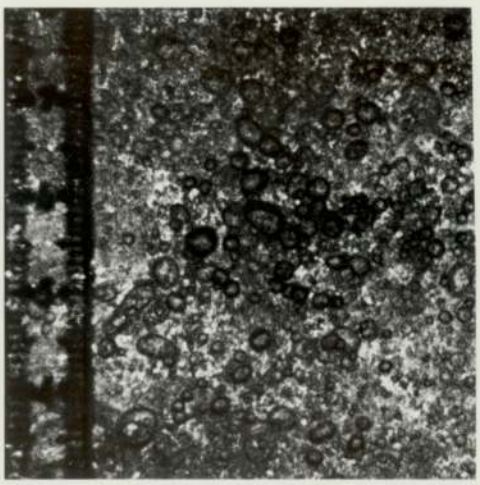

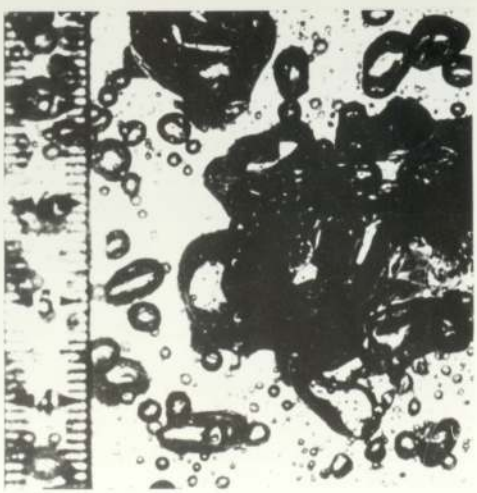

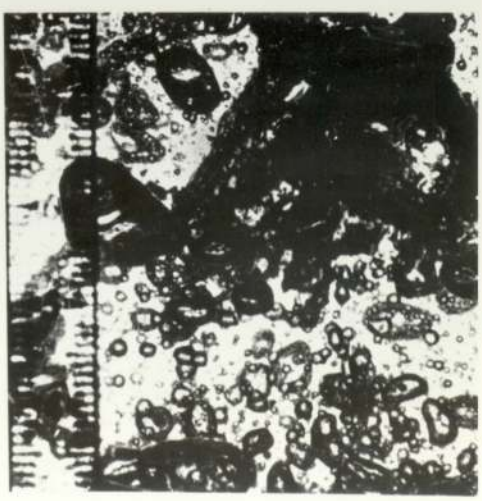

Figure 5.11

U_{SG} 30 mm s^{-1} U_{SG} 40 mm s^{-1}

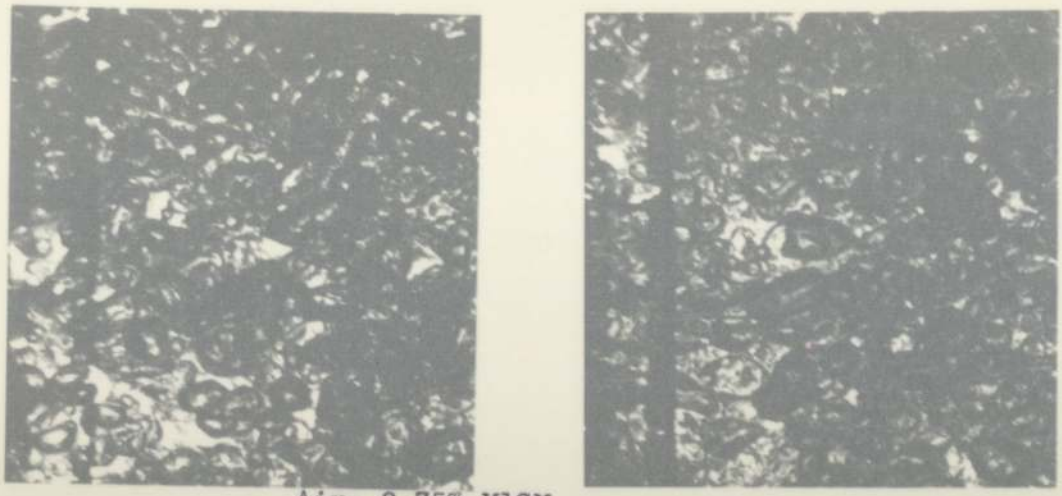

Air- 2.75% M1SM

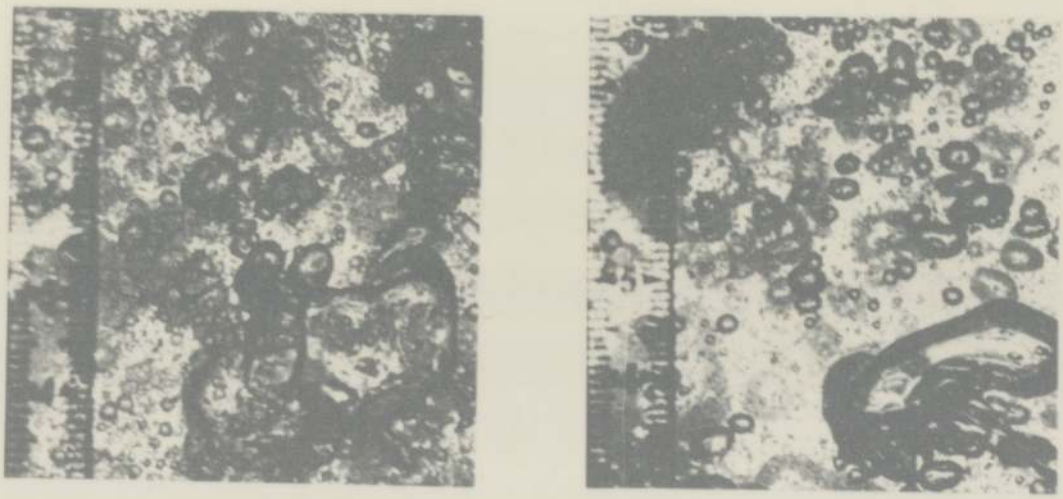

Air- 2.75% M1SM-P2000

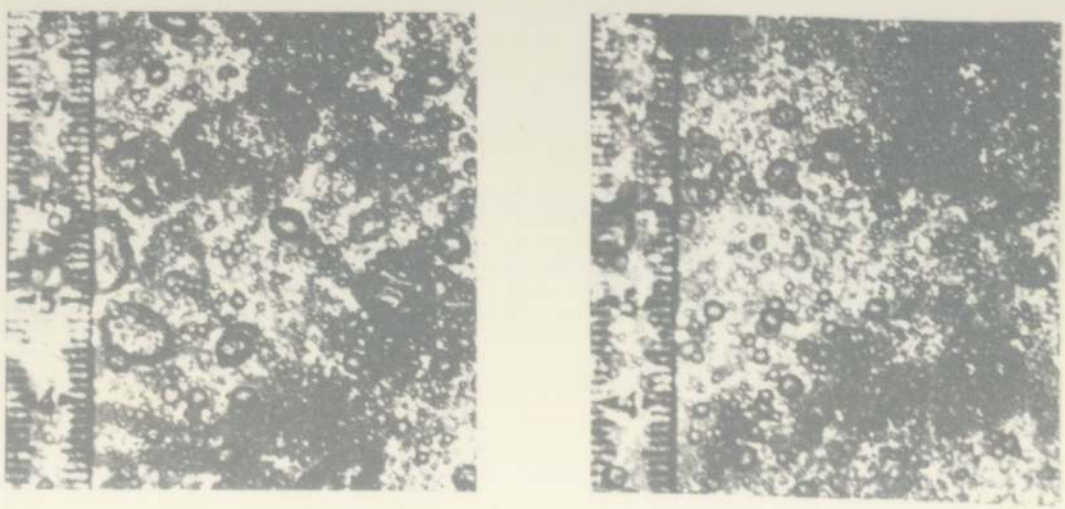

Air- 2.75% M1SM-Silcolapse

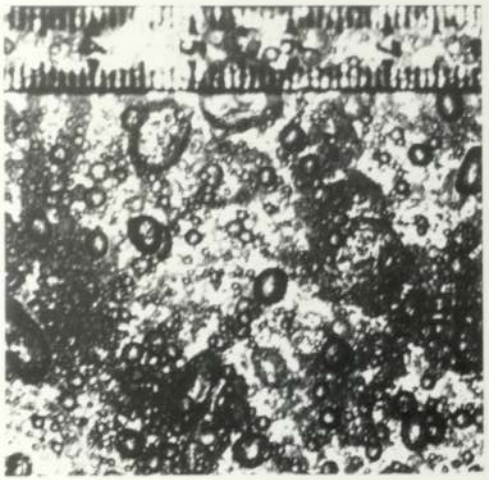

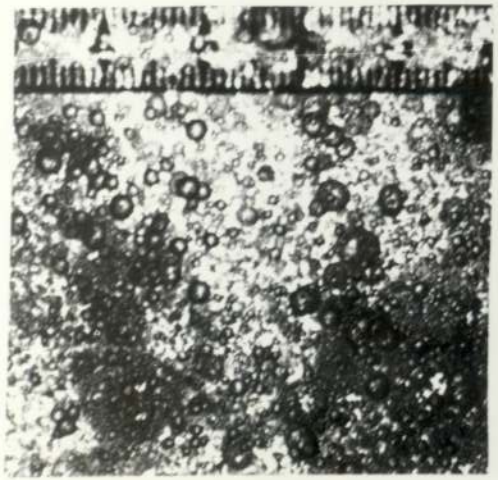

Figure 5.12

U_{SG} 10 mm s^{-1} U_{SG} 20 mm s^{-1}

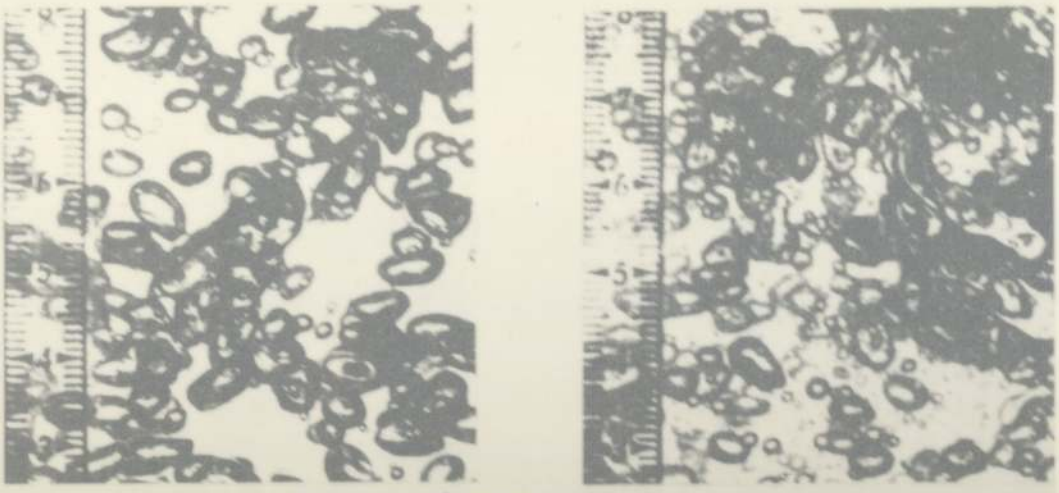

Air- 5.0% M1SM

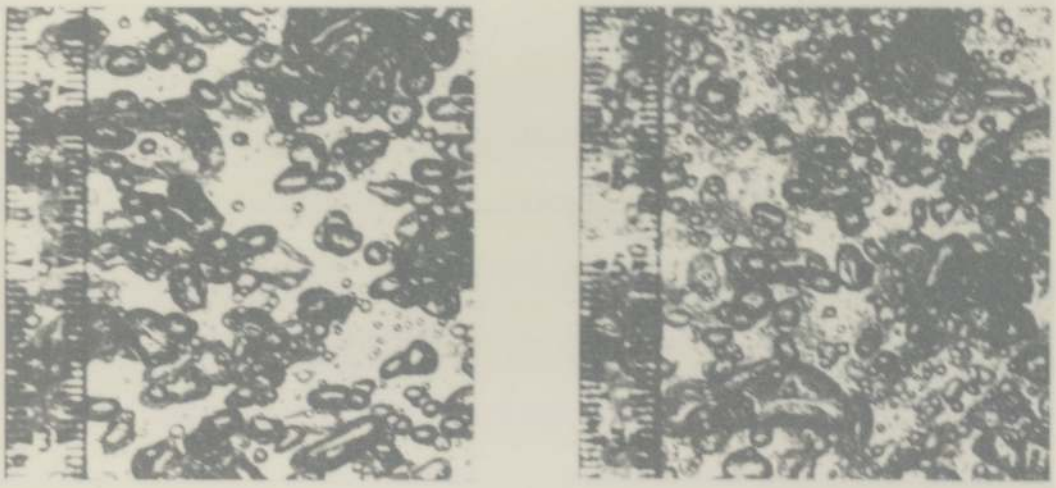

Air- 5.0% M1SM-P2000

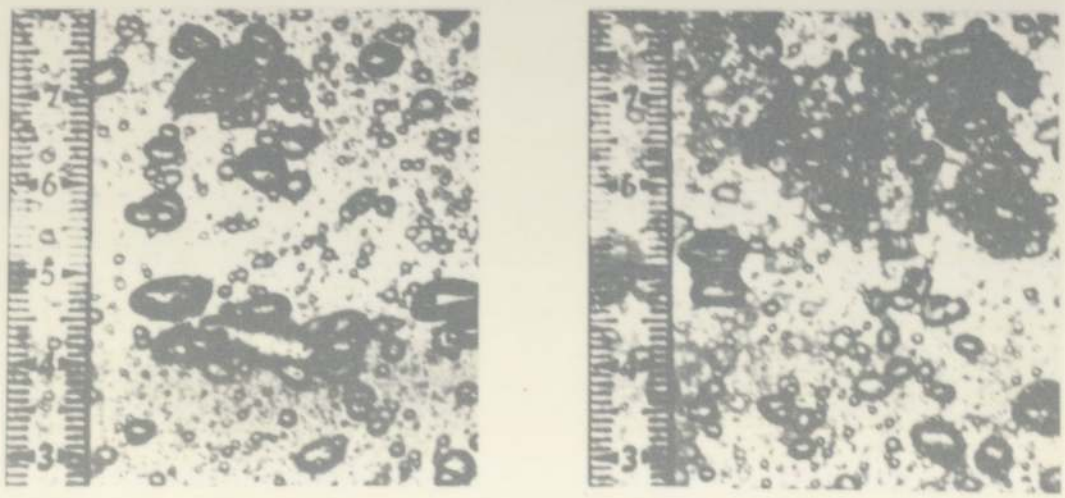

Air- 5.0% M1SM-Silcolapse

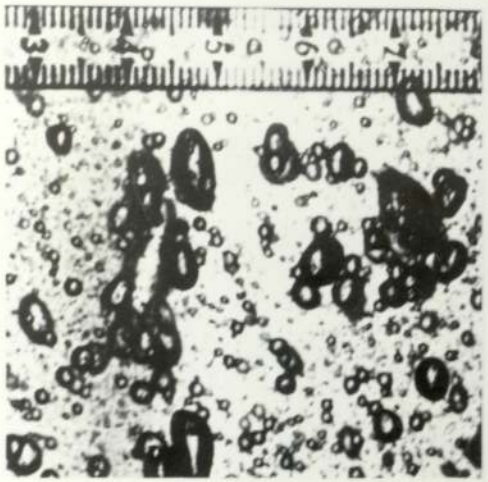

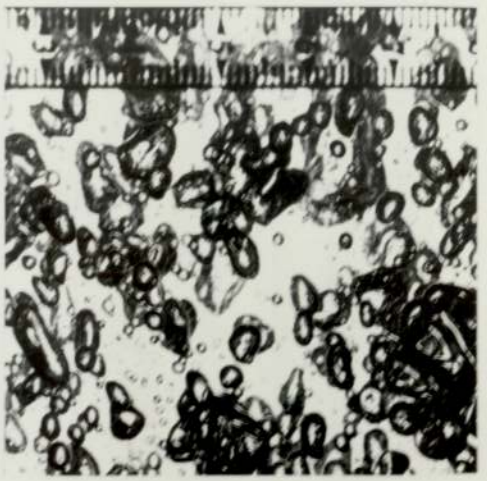

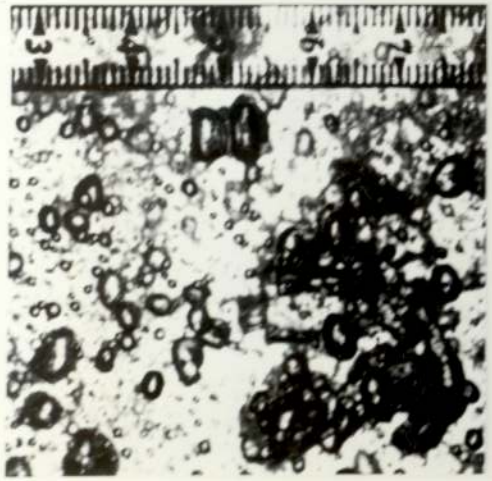

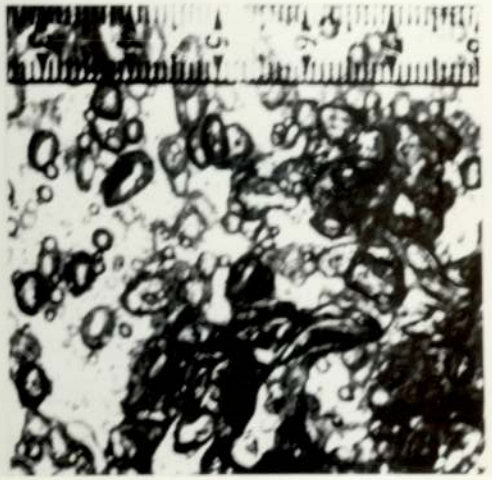

Figure 5.13

U_{SG} 30 mm s^{-1} U_{SG} 40 mm s^{-1}

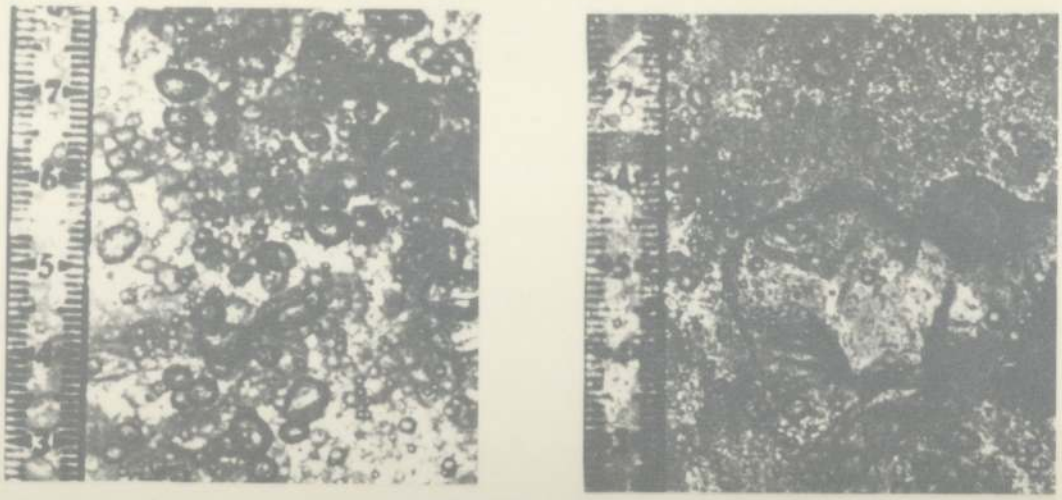

Air 5.0% M1SM

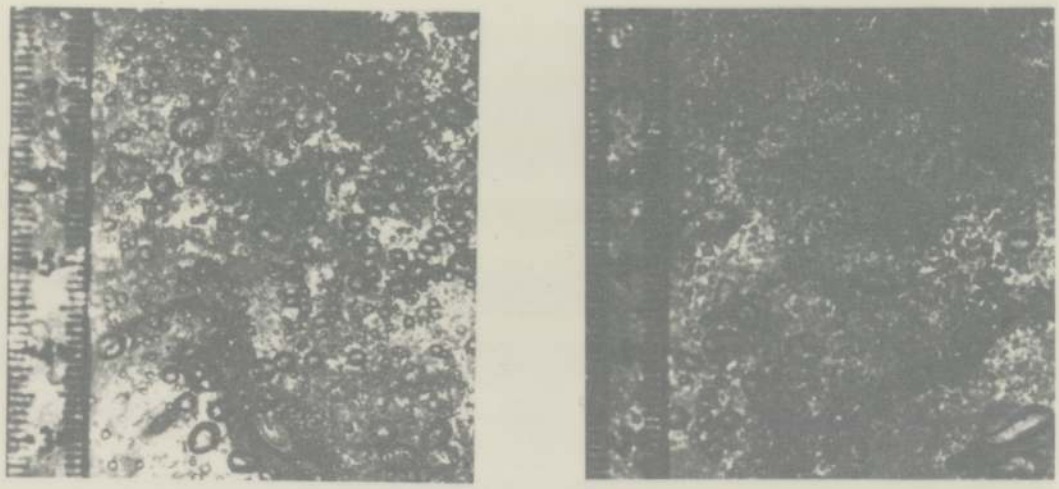

Air- 5.0% M1SM-P2000

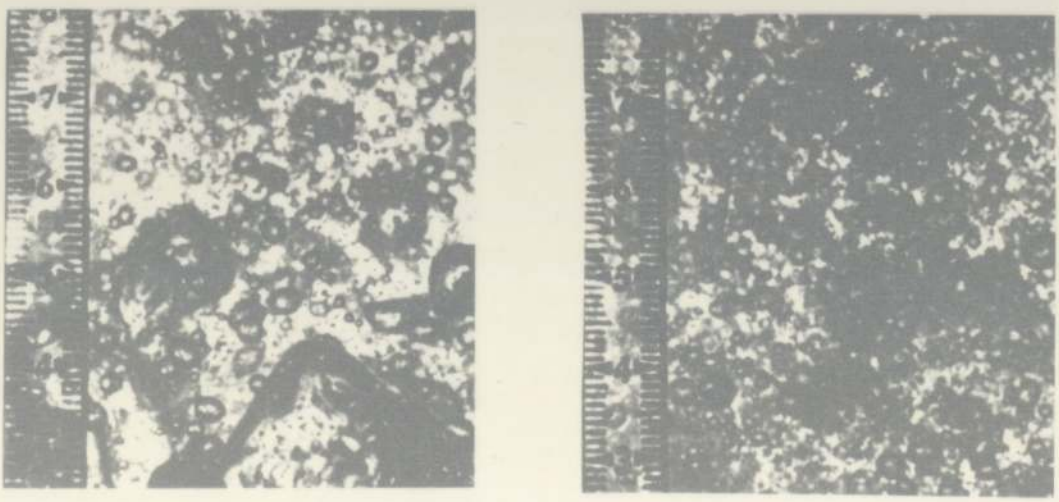

Air- 5.0% M1SM-Silcolapse

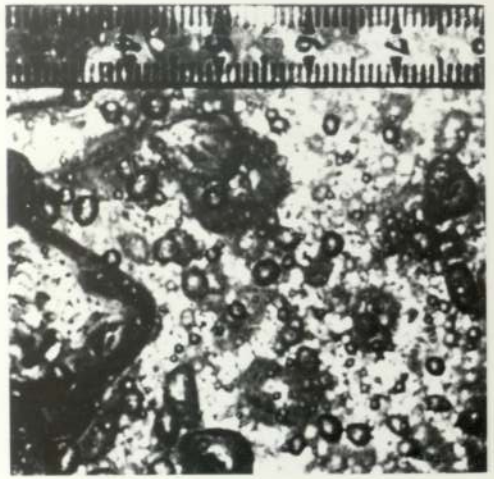

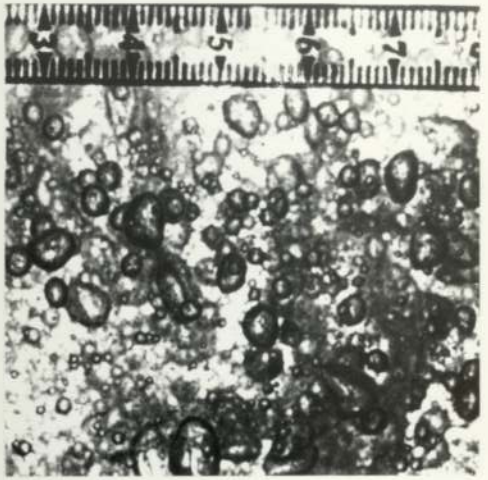
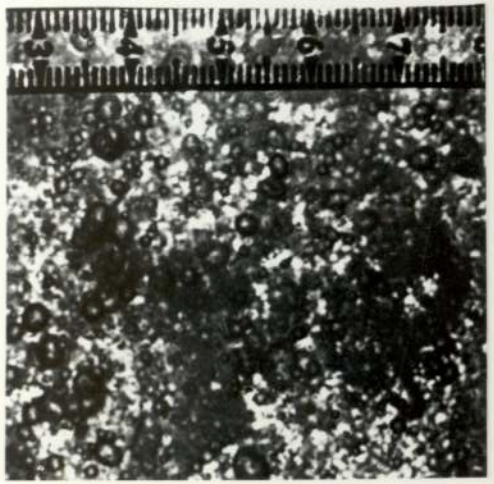
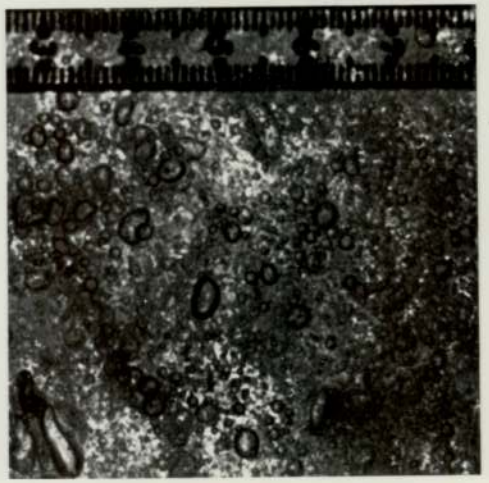


Figure 5.14 Ionic Bubbles in M1SM Solutions

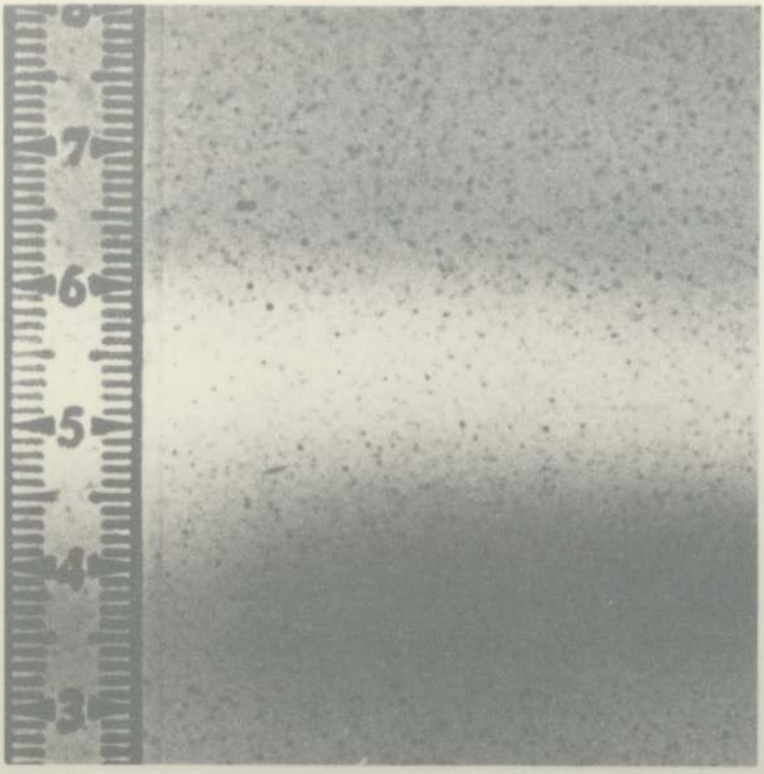

U_{SG} 10 mm s^{-1}

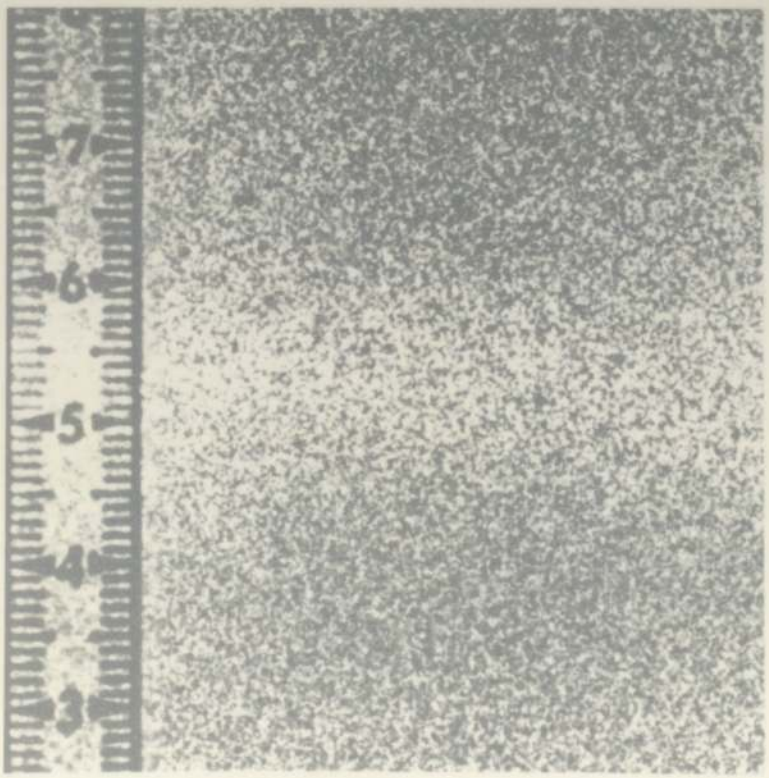

U_{SG} 40 mm s^{-1}

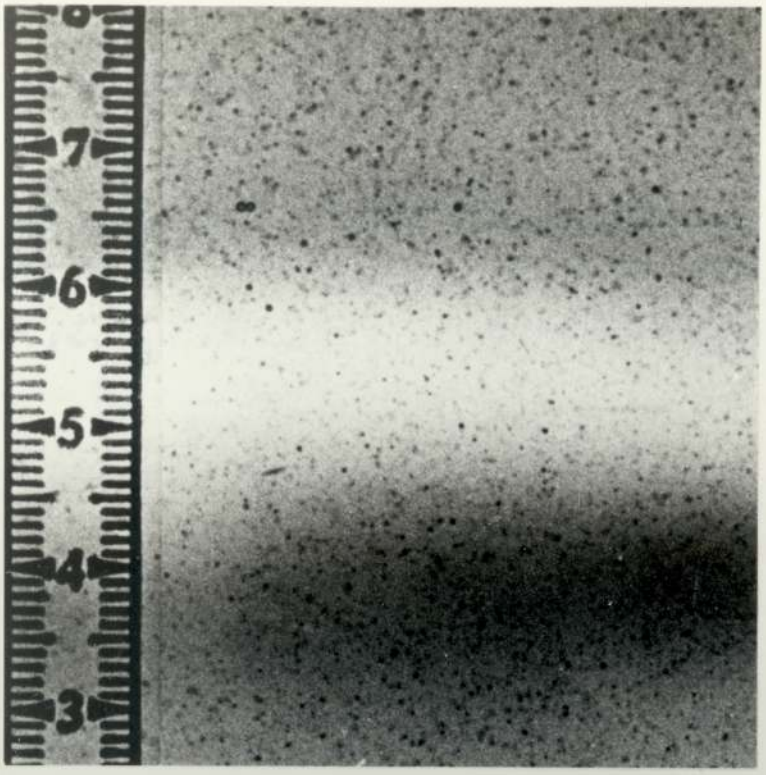
7
6
5
4
3

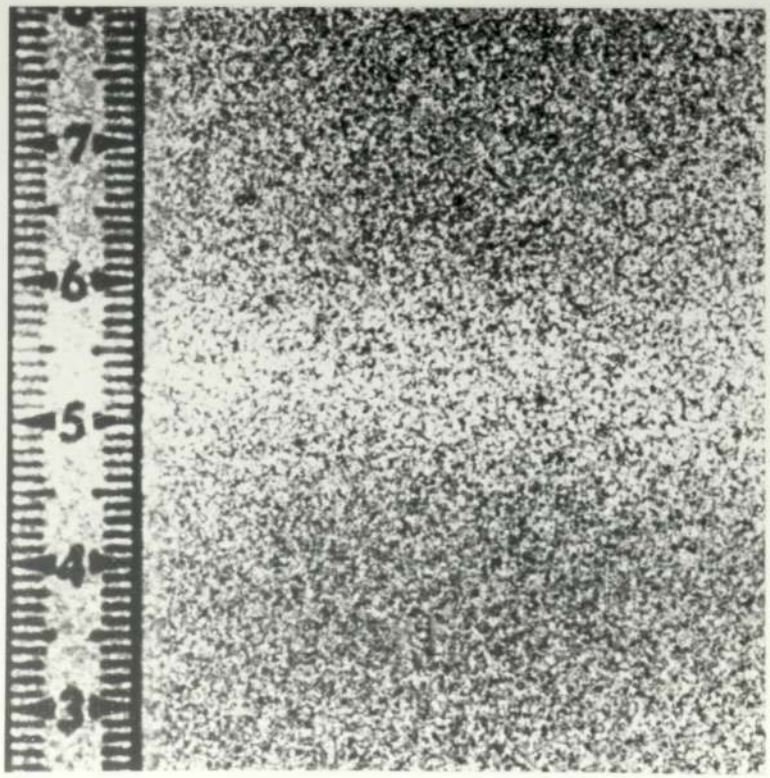
7
6
5
4
3

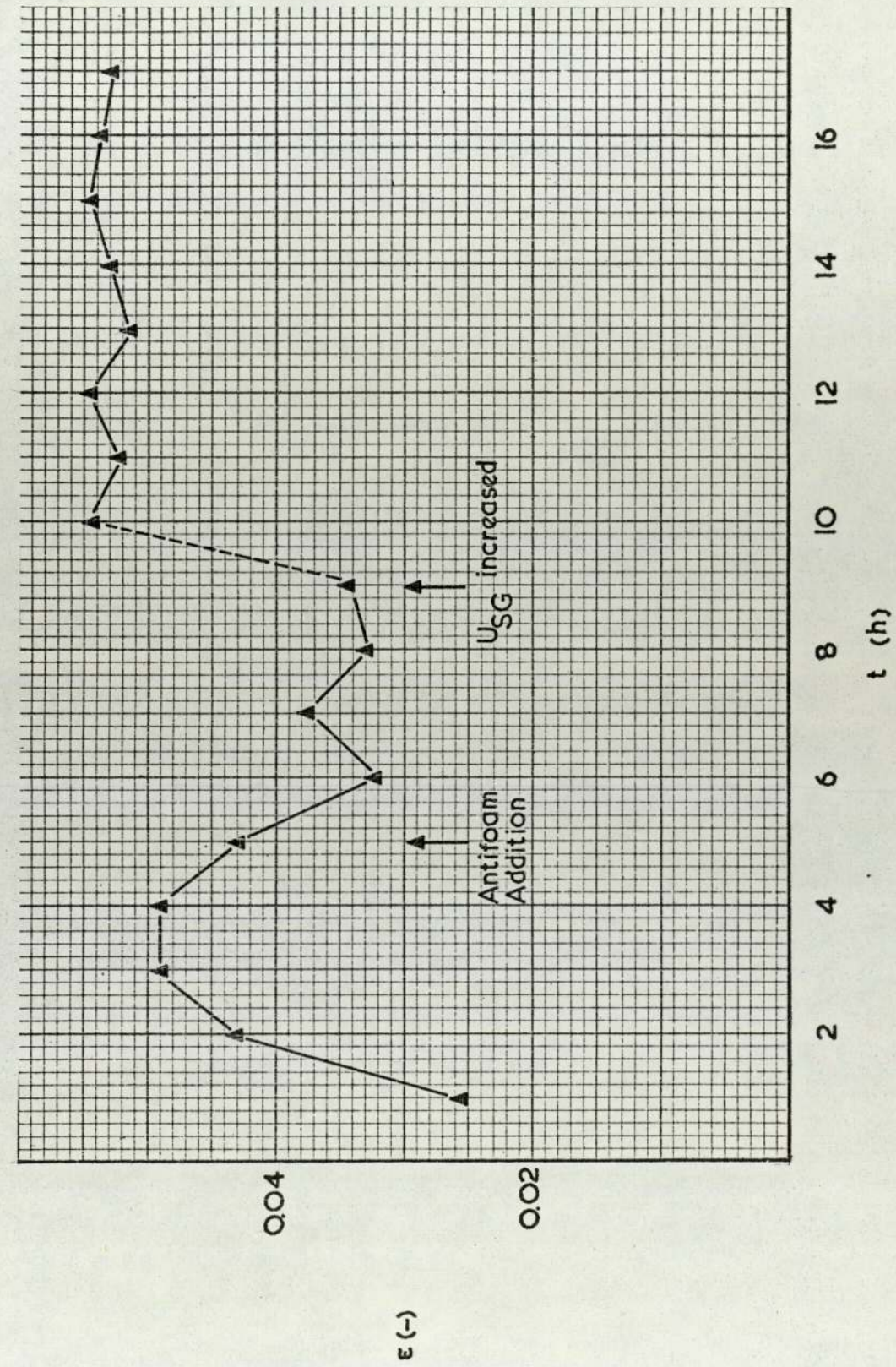

Figure 5.15 Gas Holdup During an Aspergillus niger Fermentation

Figure 5.18 Typical Probe Calibration Traces

Chark Electrode

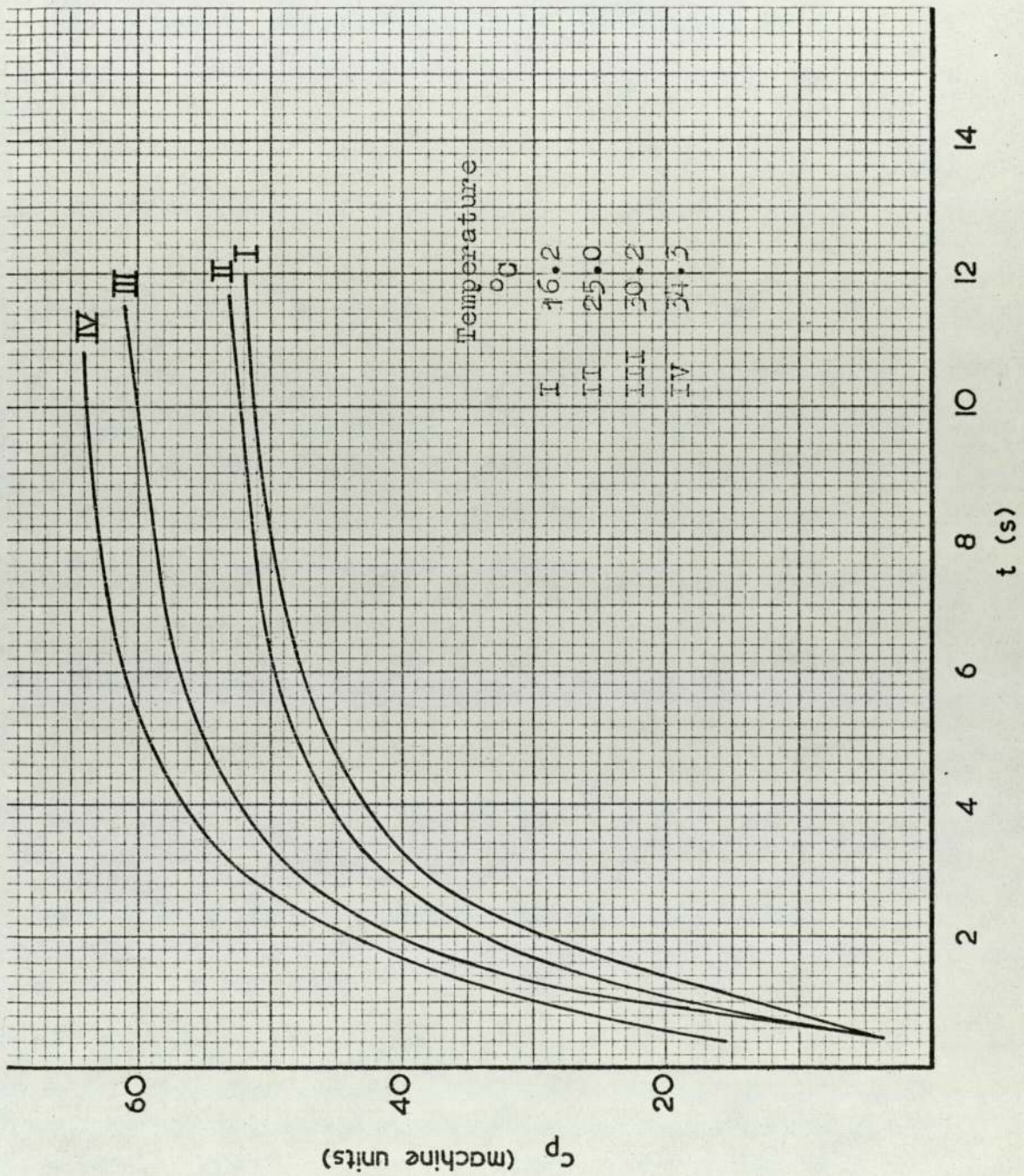

Figure 5.19 Normalised Form of Data Presented in Figure 5.18

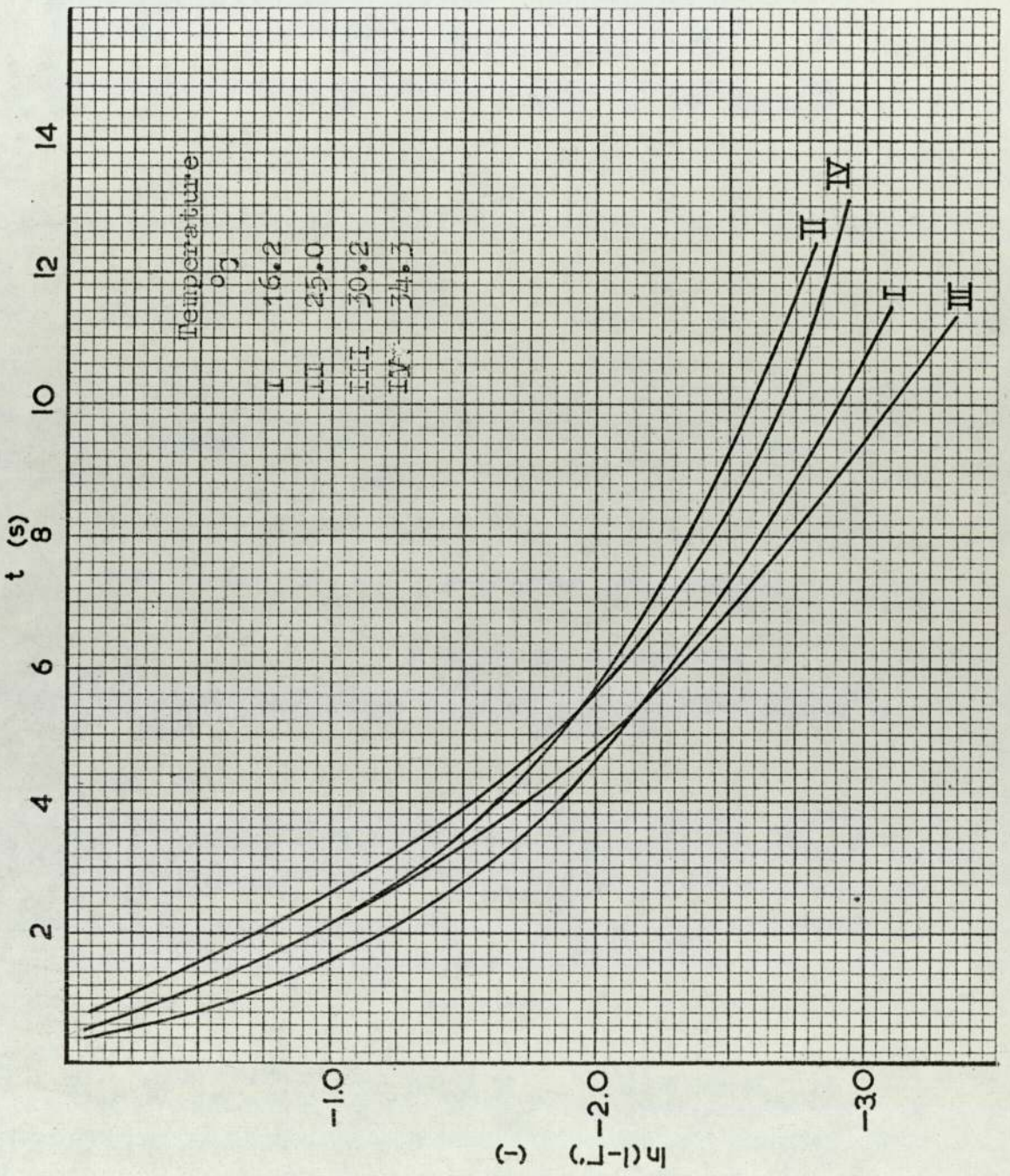

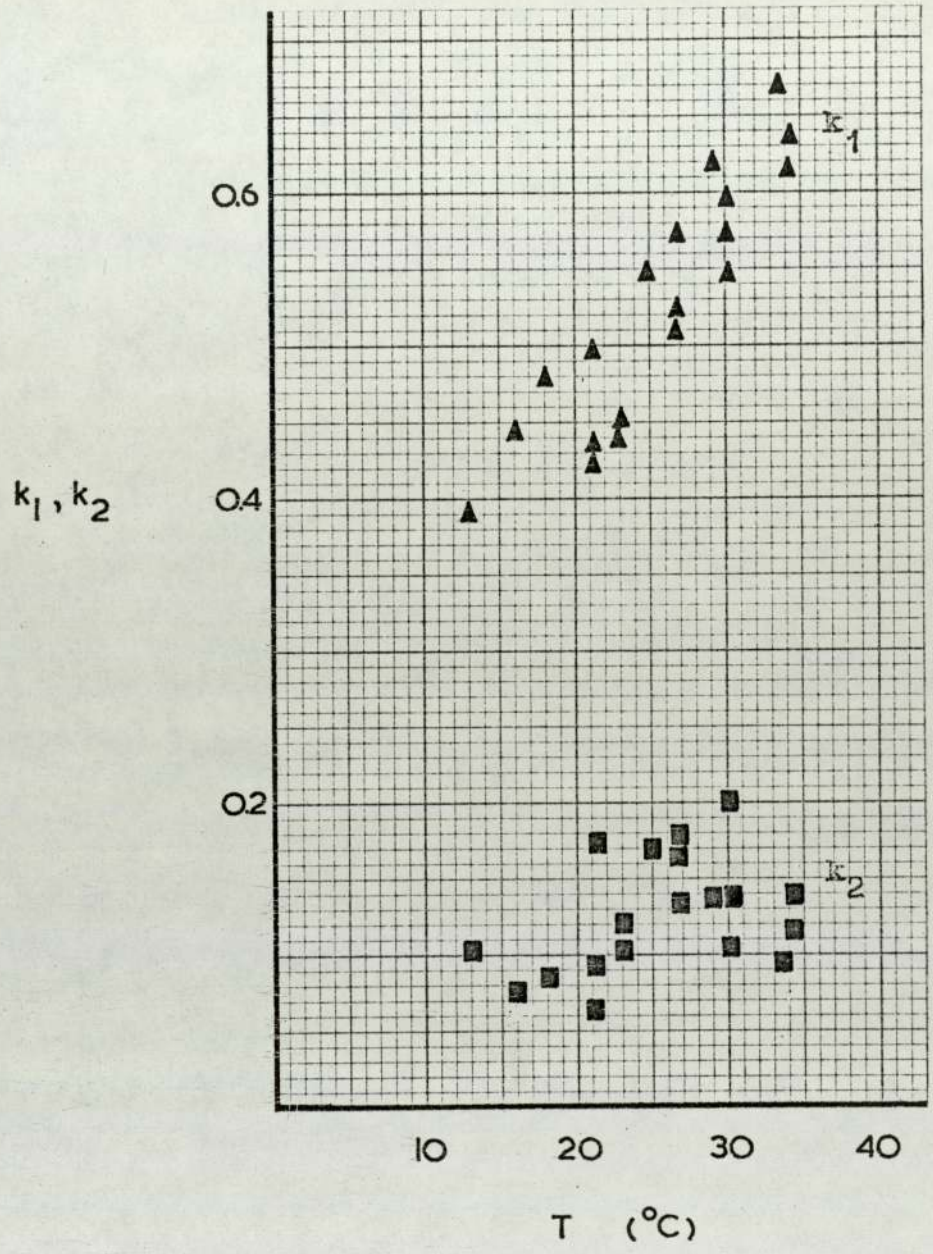

Figure 5.20 Temperature Dependence of Parameters k_1 and k_2 Estimated from Experimental Results

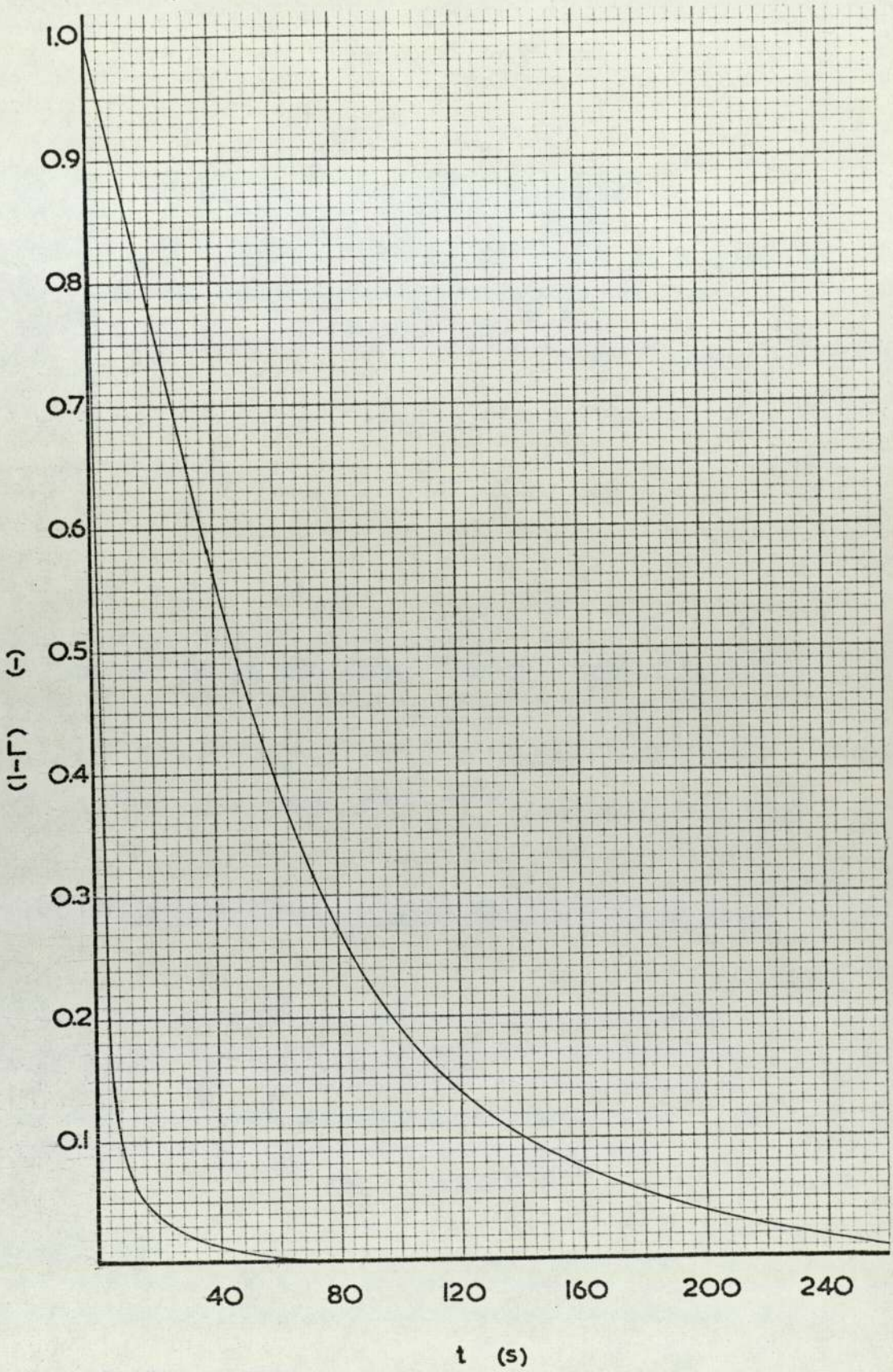

Figure 5.21 Estimation of $k_L a$ Using Method of Moments

$U_{SG} = 10$ mm s^{-1}

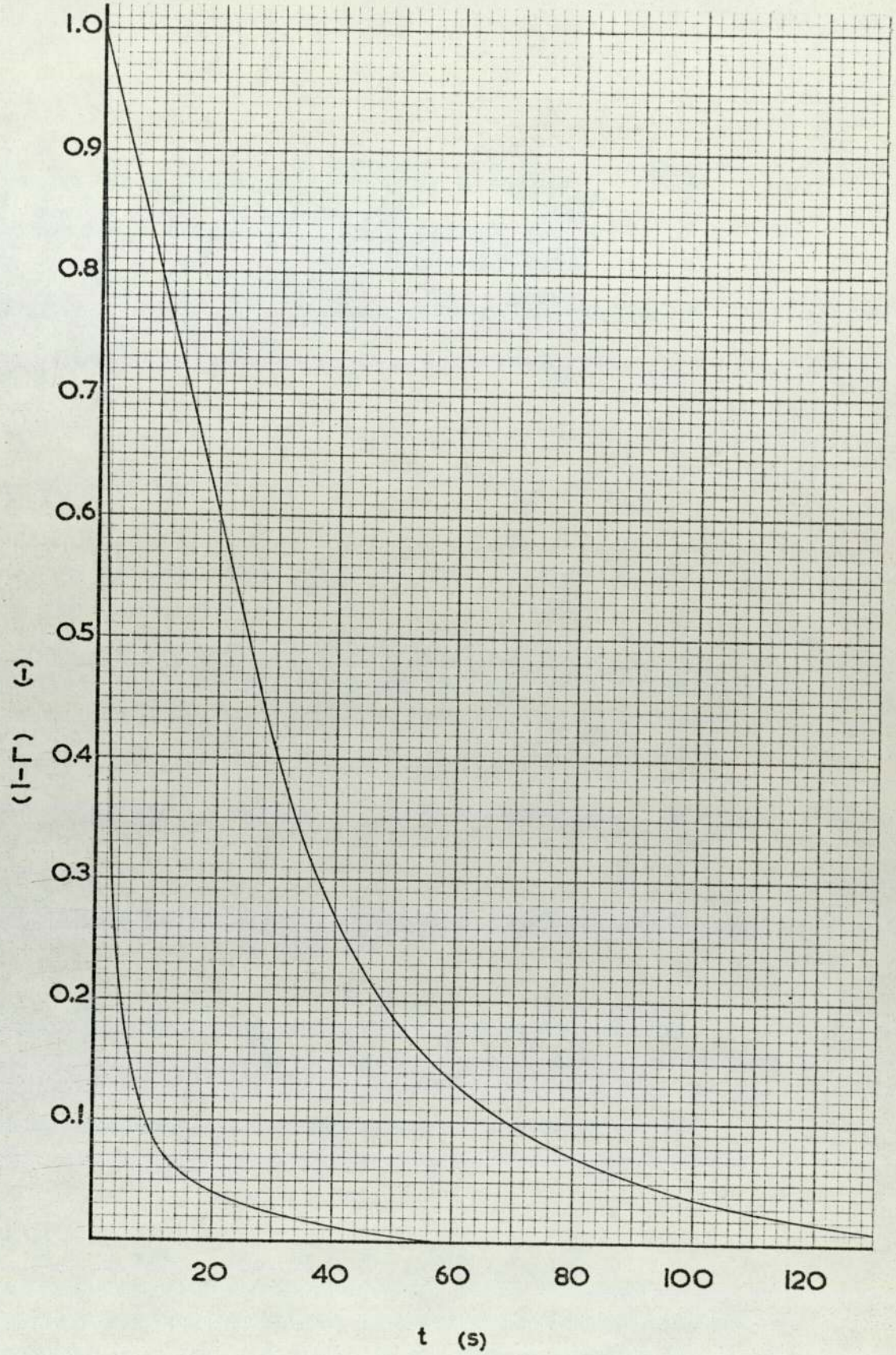

Figure 5.22 Estimation of $k_L a$ Using Method of Moments

$U_{SG} = 20$ mm s^{-1}

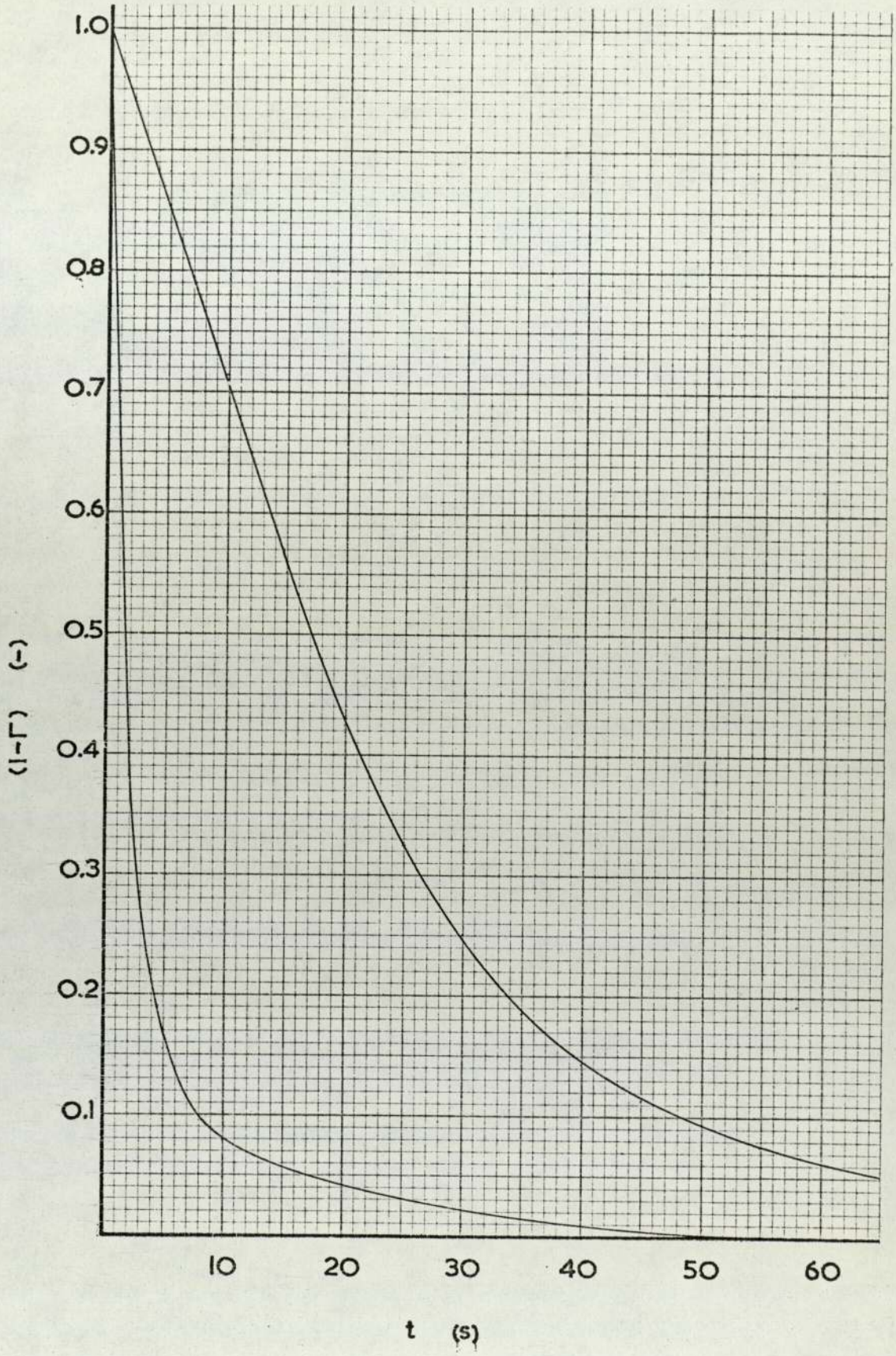

Figure 5.23 Estimation of $k_L a$ Using Method of Moments

$U_{SG} = 30$ mm s^{-1}

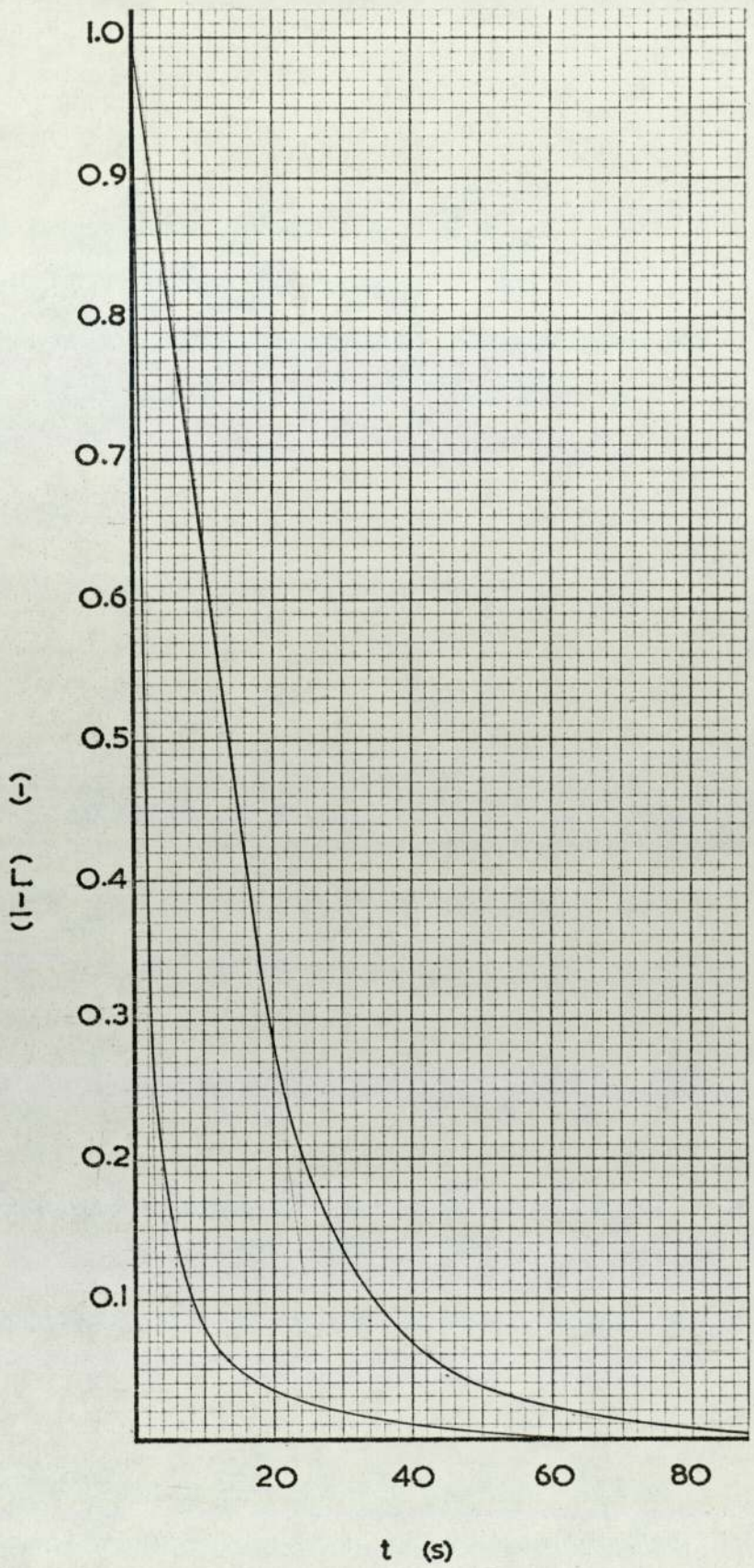

Figure 5.24 Estimation of $k_L a$ Using Method of Moments

$U_{SG} = 40$ mm s^{-1}

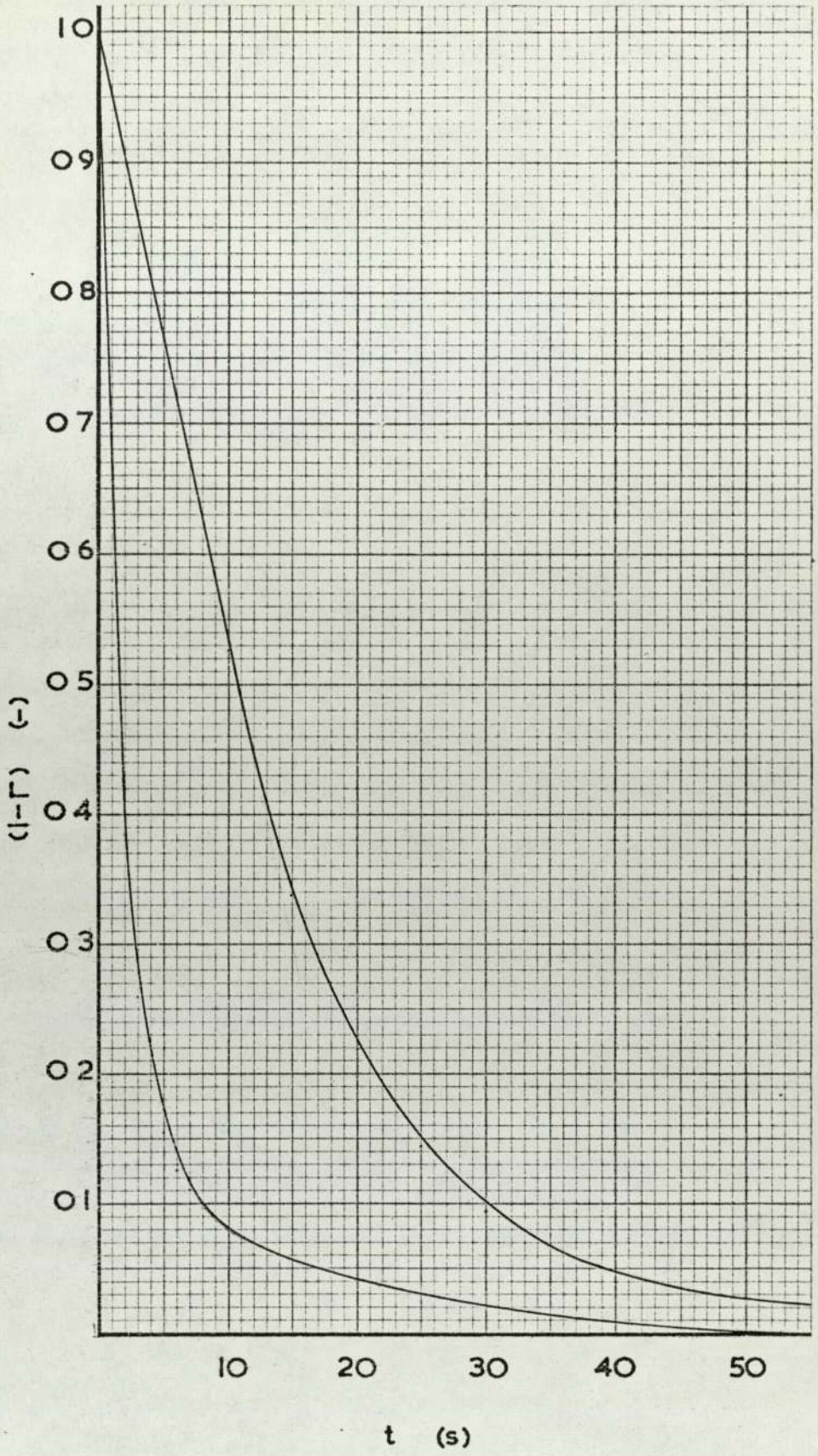

Figure 5.25 Estimation of $k_L a$ Using Method of Moments

$U_{SG} = 50$ mm s^{-1}

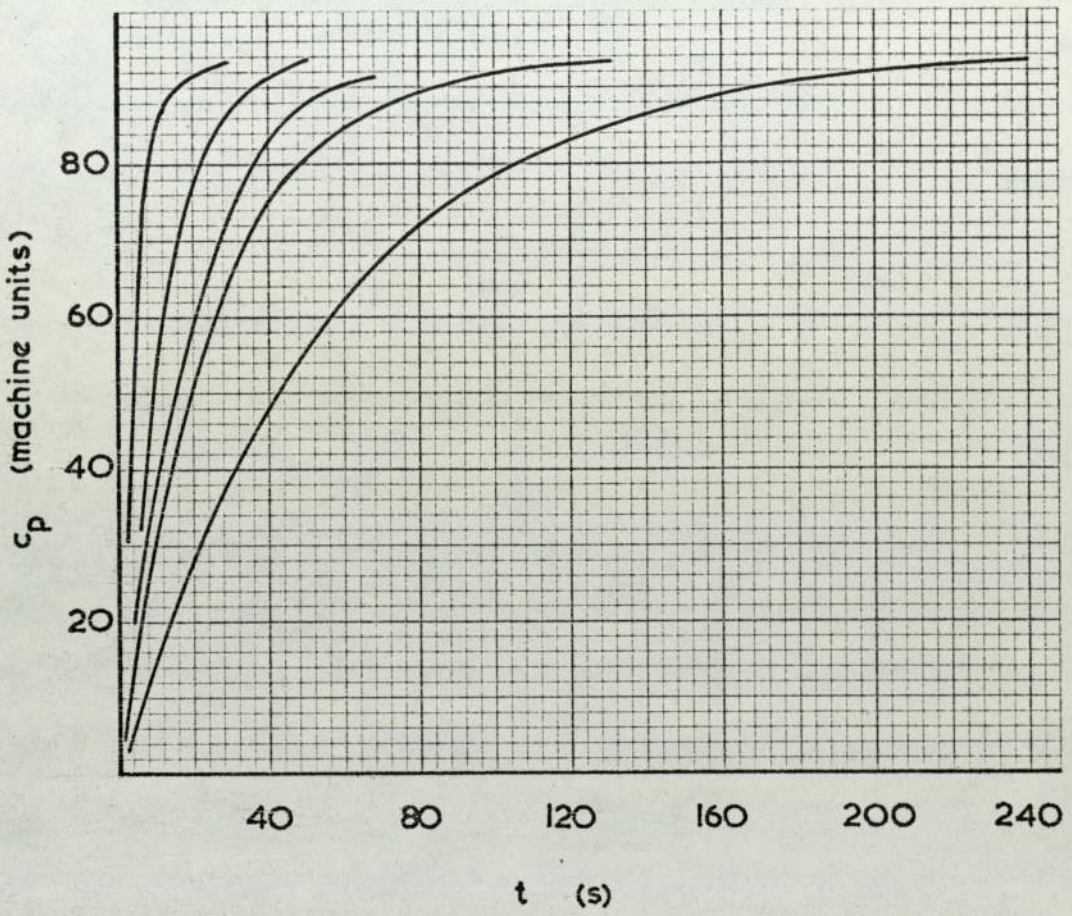

Figure 5.26 Experimental Traces Used in the Preparation of Figures 5.21-5.25 and 5.27-5.31

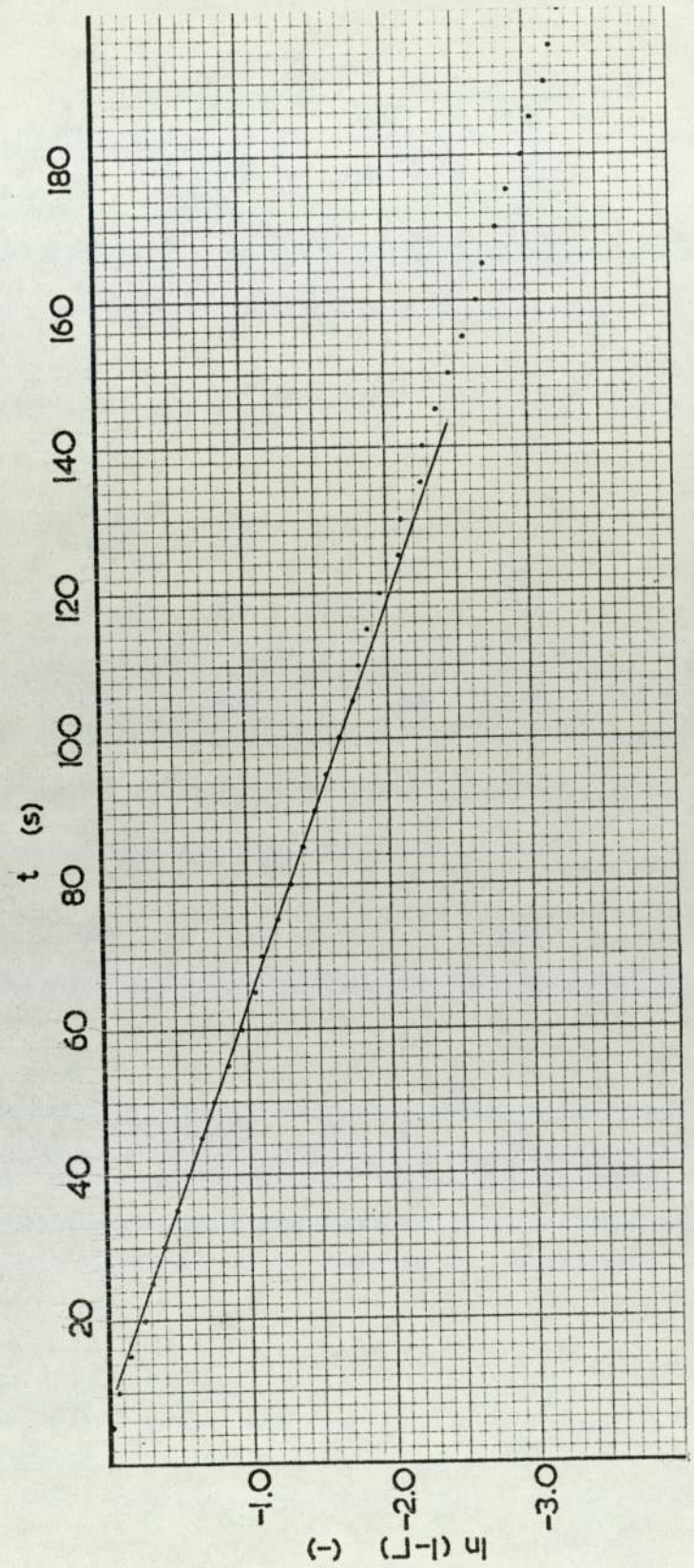

Figure 5.27 Estimation of $k_L a$ from a Plot of the Normalised Experimental Data

$U_{SG} = 10$ mm s^{-1}

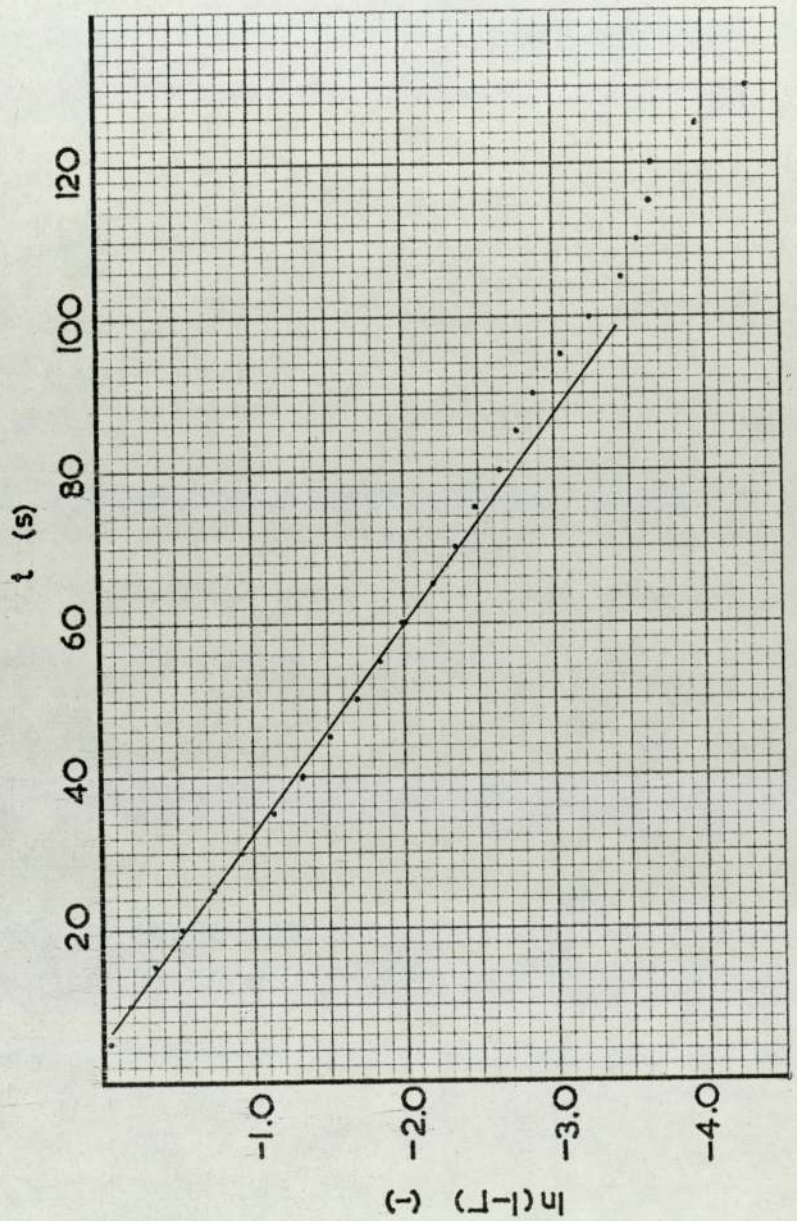

Figure 5.28 Estimation of $k_L a$ from a Plot of the Normalised Experimental Data

U_{SG} = 20 mm s^{-1}

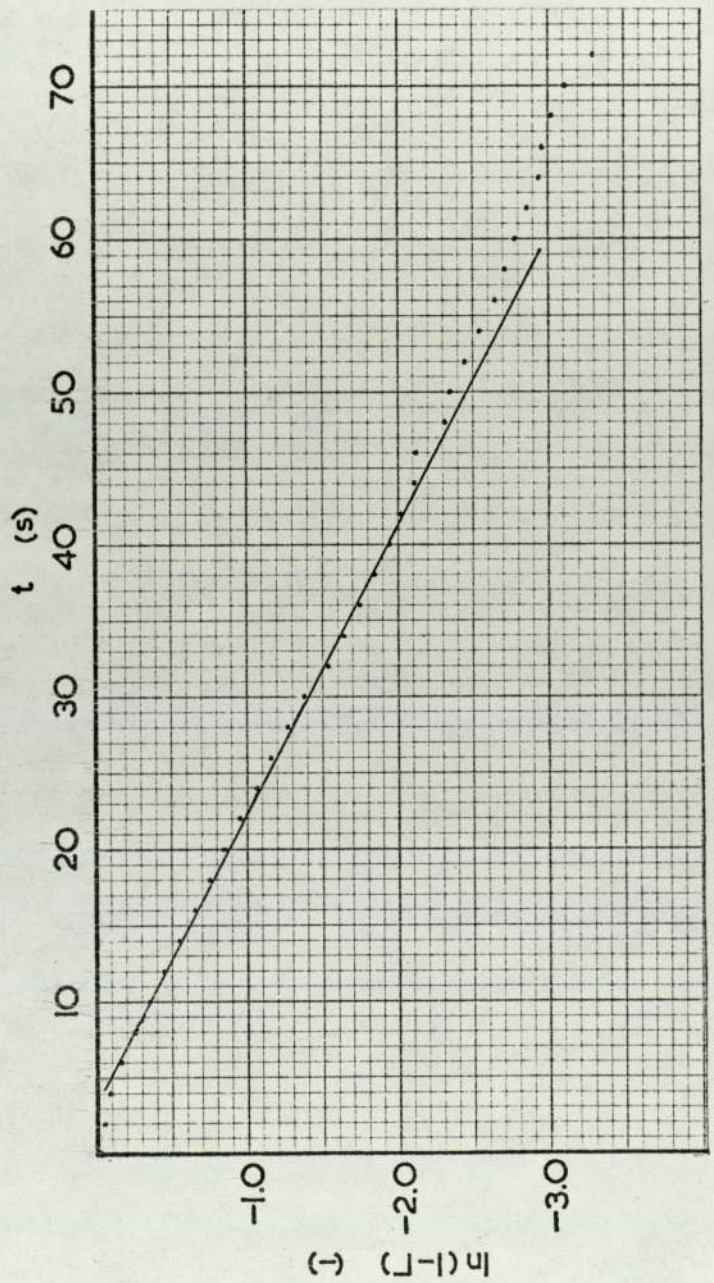

Figure 5.29 Estimation of $k_L a$ from a Plot of the Normalised Experimental Data

$U_{SG} = 30$ mm s^{-1}

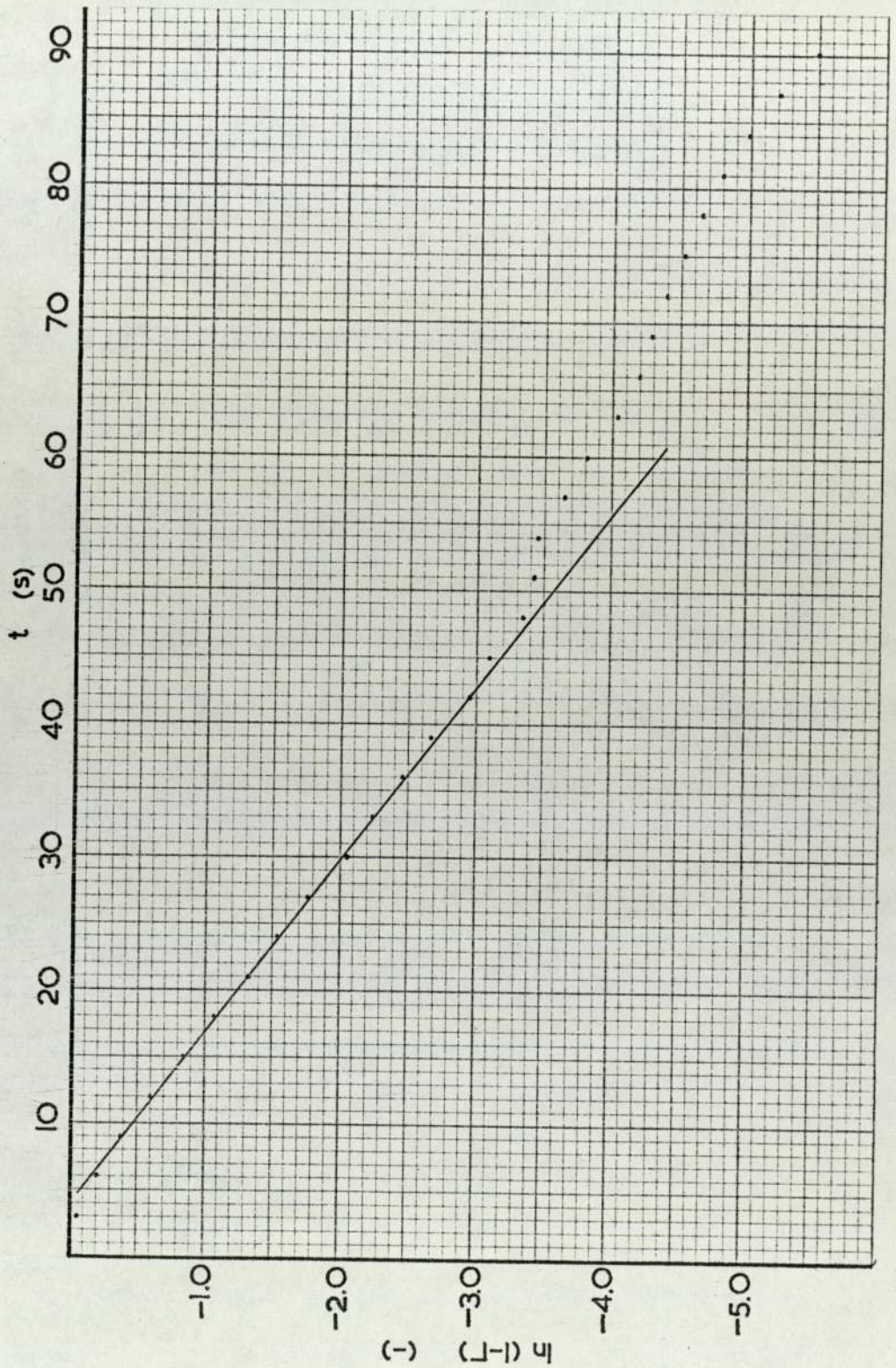

Figure 5.30 Estimation of $k_L a$ from a Plot of the Normalised Experimental Data

$U_{SG} = 40$ mm s^{-1}

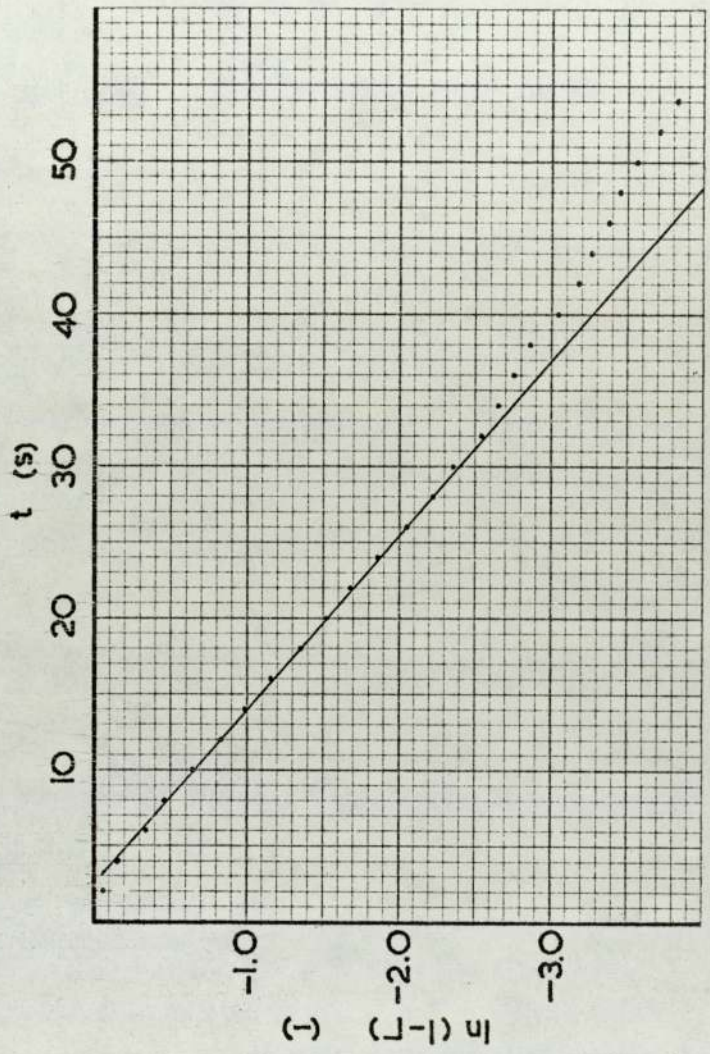

Figure 5.31 Estimation of $k_L a$ from a Plot of the Normalised Experimental Data

$U_{SG} = 50$ mm s^{-1}

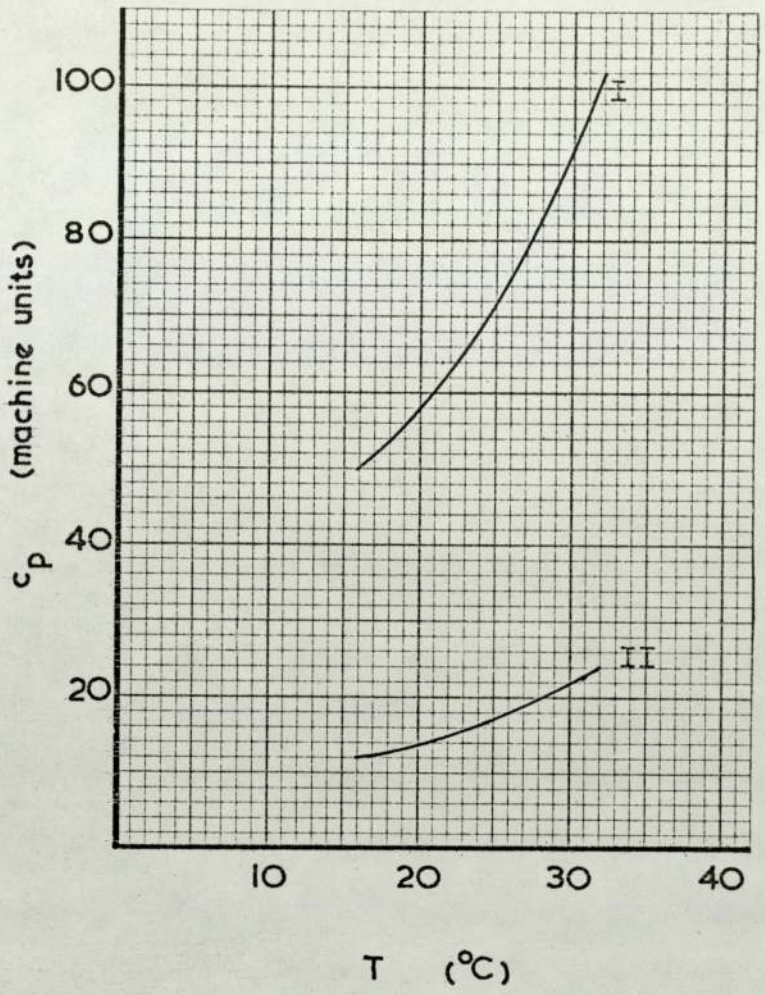

Figure 5.32 Temperature Calibration of the Chark Oxygen Electrode

Curves I and II are at different amplifications

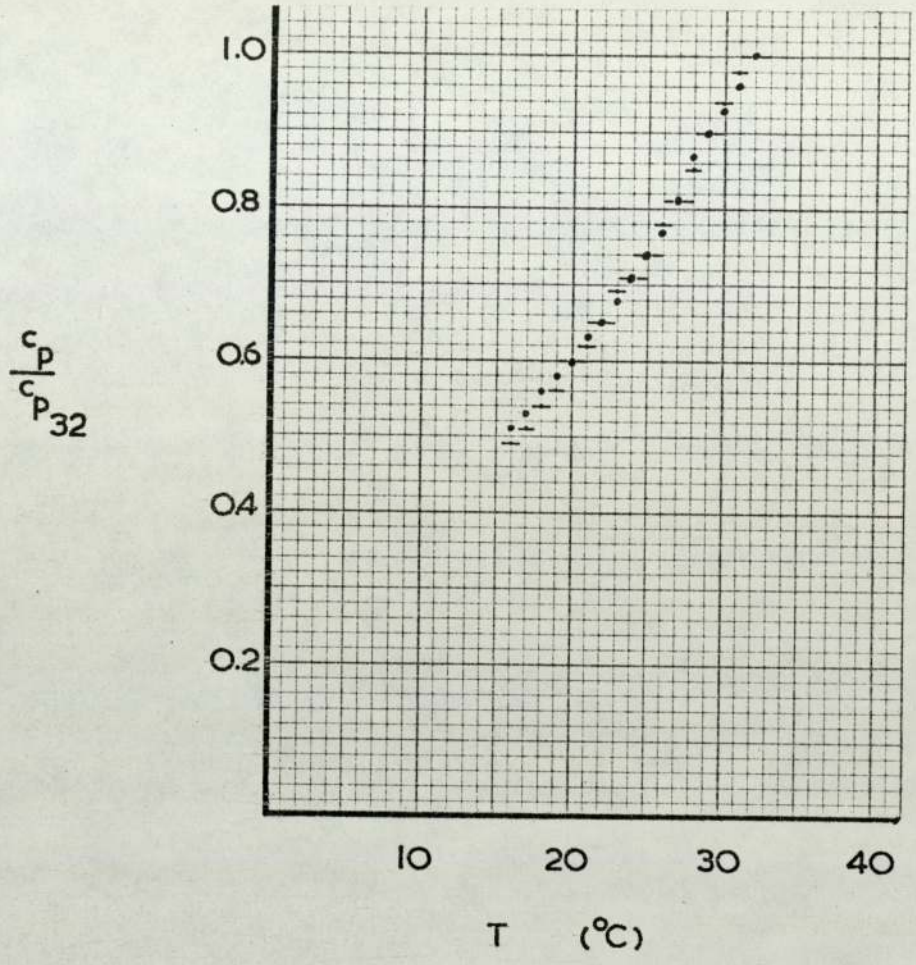

Figure 5.33 Temperature Calibration of the Chark Oxygen Electrode - Normalised Experimental Data vs. Temperature

- Data set I
. Data set II

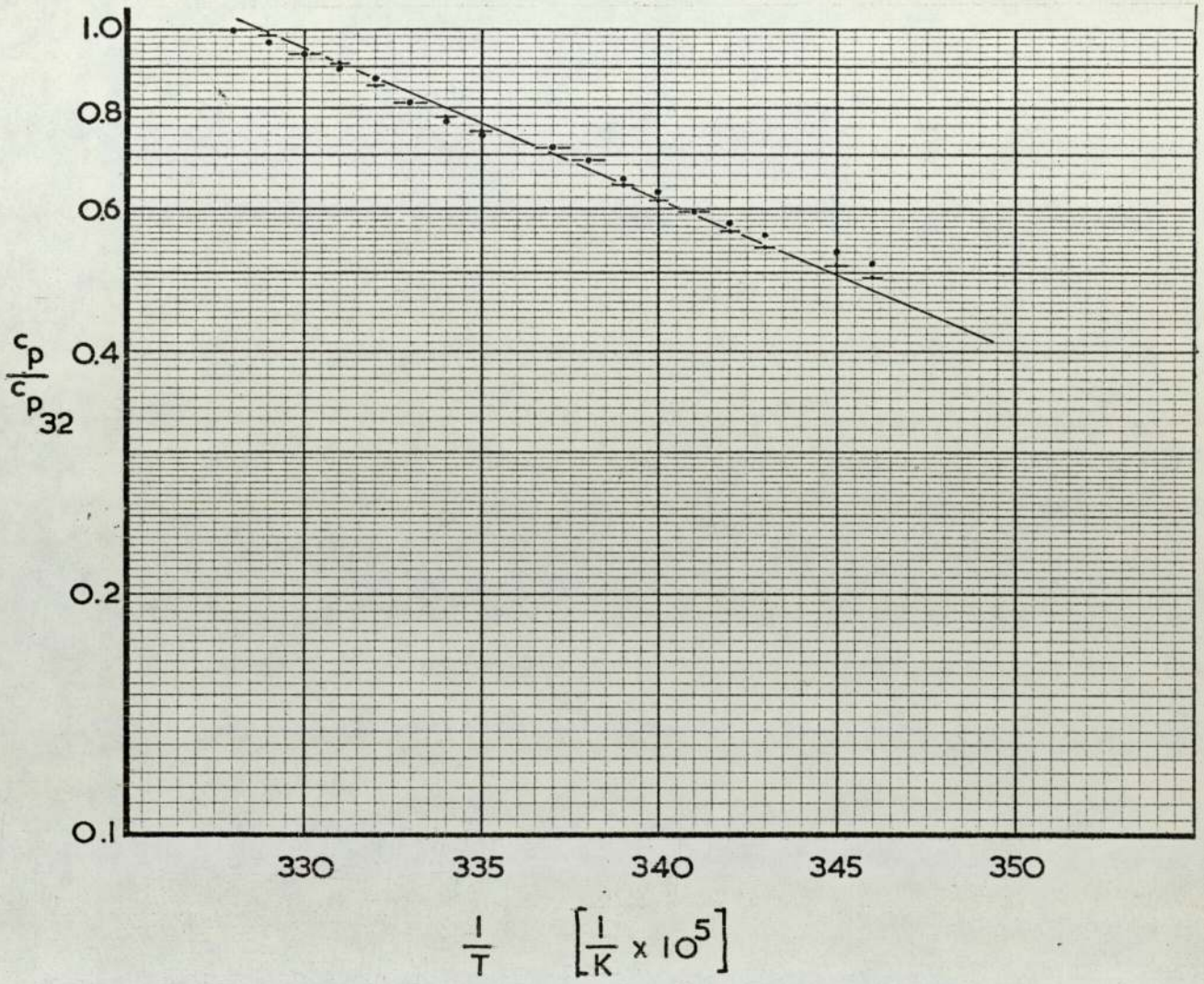

Figure 5.34 Temperature Calibration of the Chark Oxygen Electrode - Log_e(Normalised Experimental Response) vs. 1/(Absolute Temperature of the System)

- Data set I

. Data set II

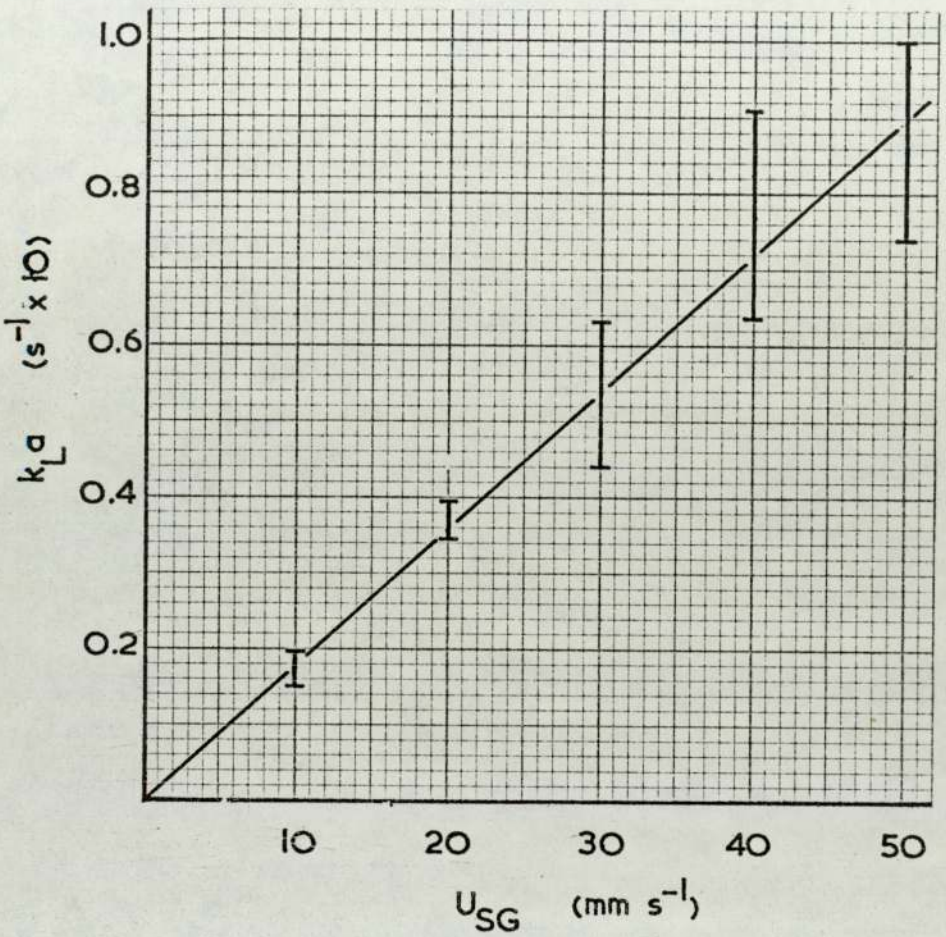

Figure 5.35 Estimated Values of the Overall Oxygen Mass-Transfer Coefficient in the Air-Water System

Column	102 mm
Temperature	25-35 °C

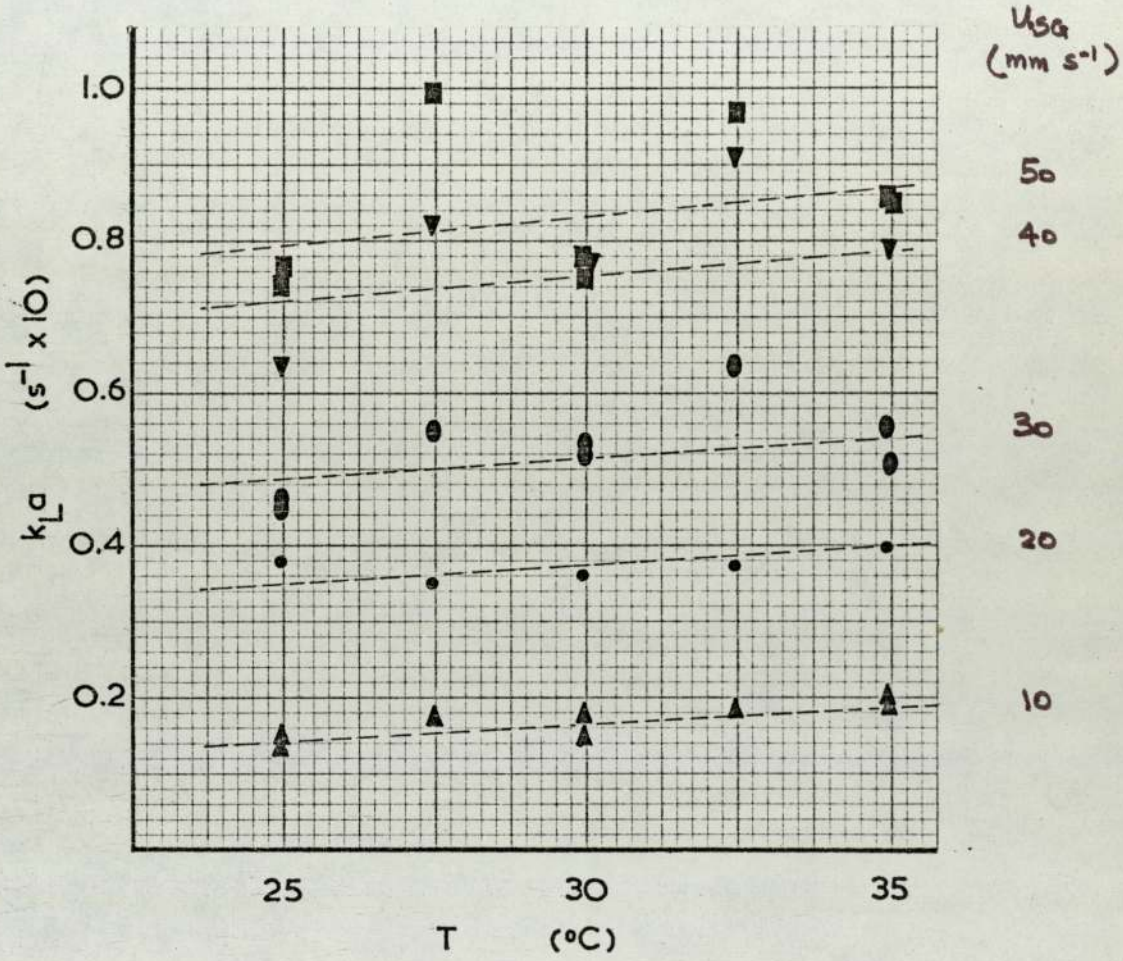

Figure 5.36 Temperature Dependence of k_La

Column 102 mm

System Air-Water

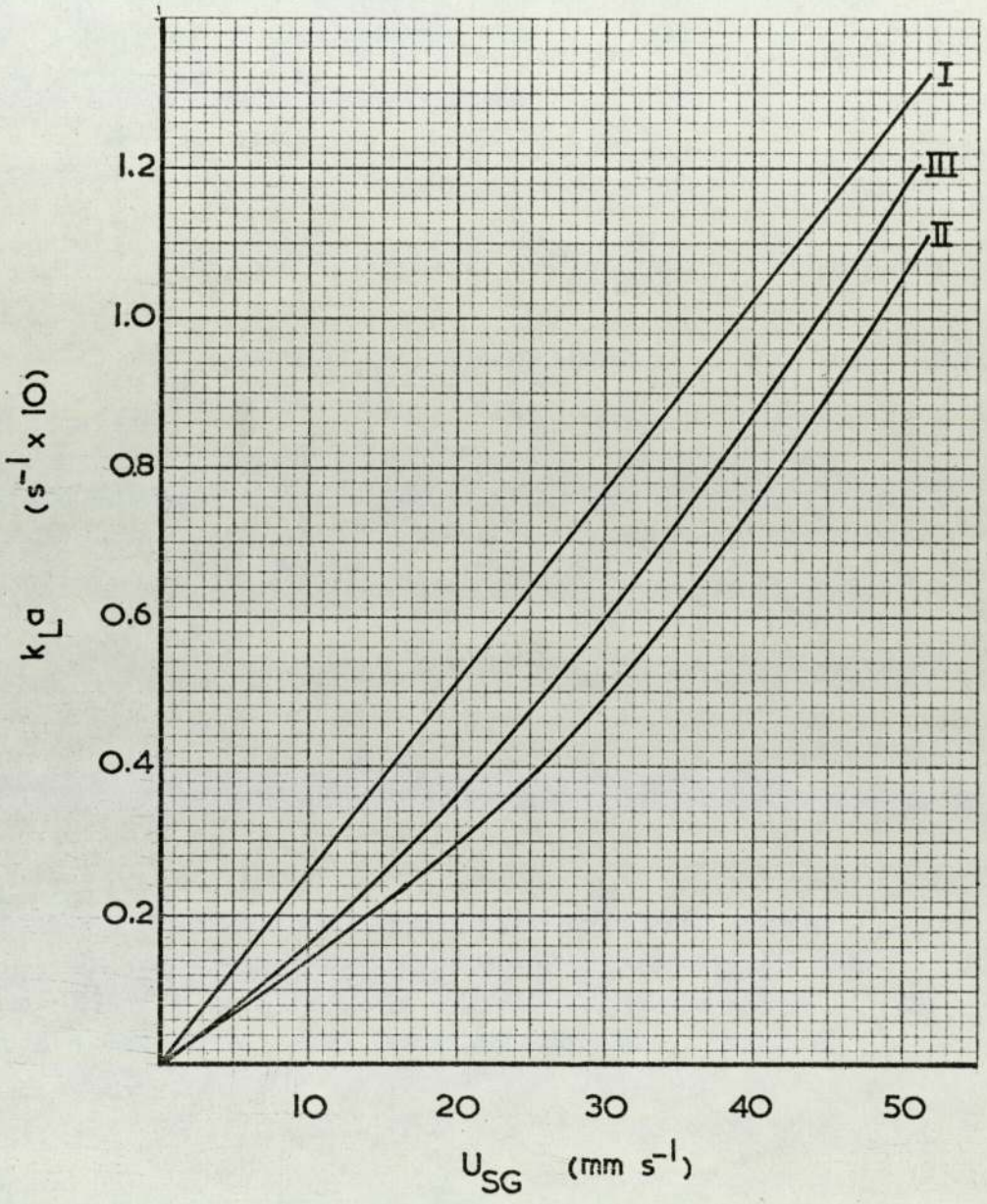

Figure 5.37 Oxygen Mass-Tranafer Coefficients in M1SM Solutions

I 0.5% M1SM
II 2.75% M1SM
III 5.0% M1SM

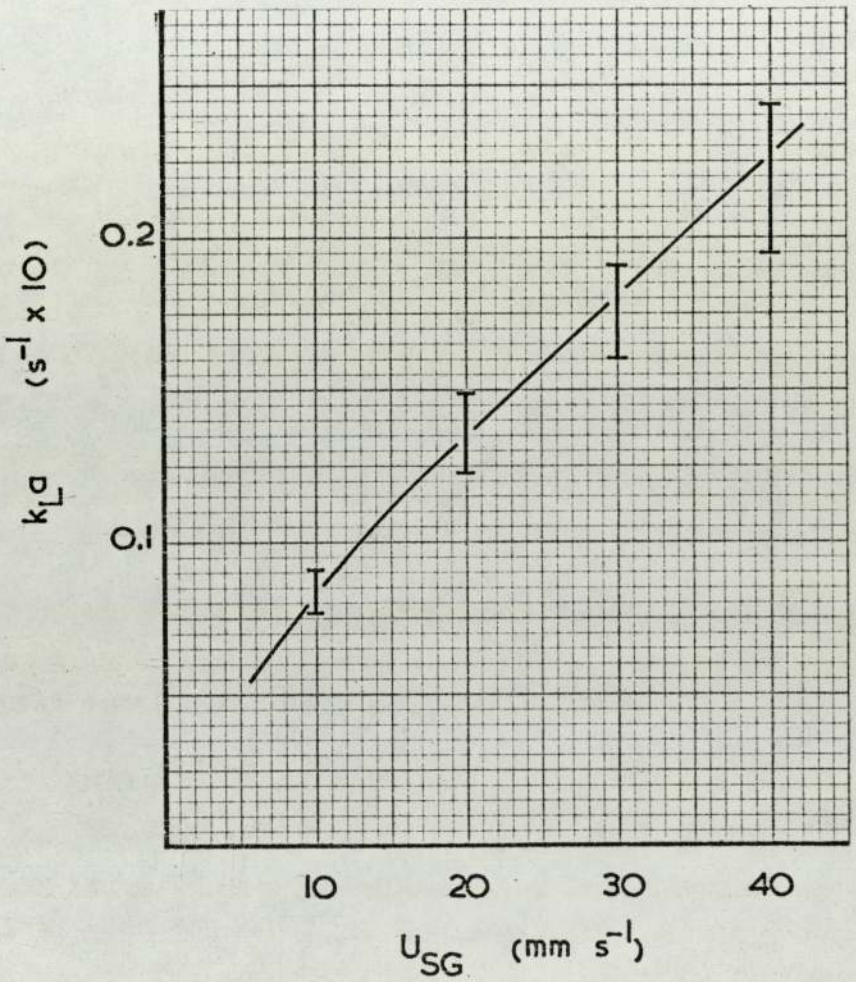

Figure 5.38 Effect of Anti-foams on the Mass-Transfer Coefficient

1. Silcolapse

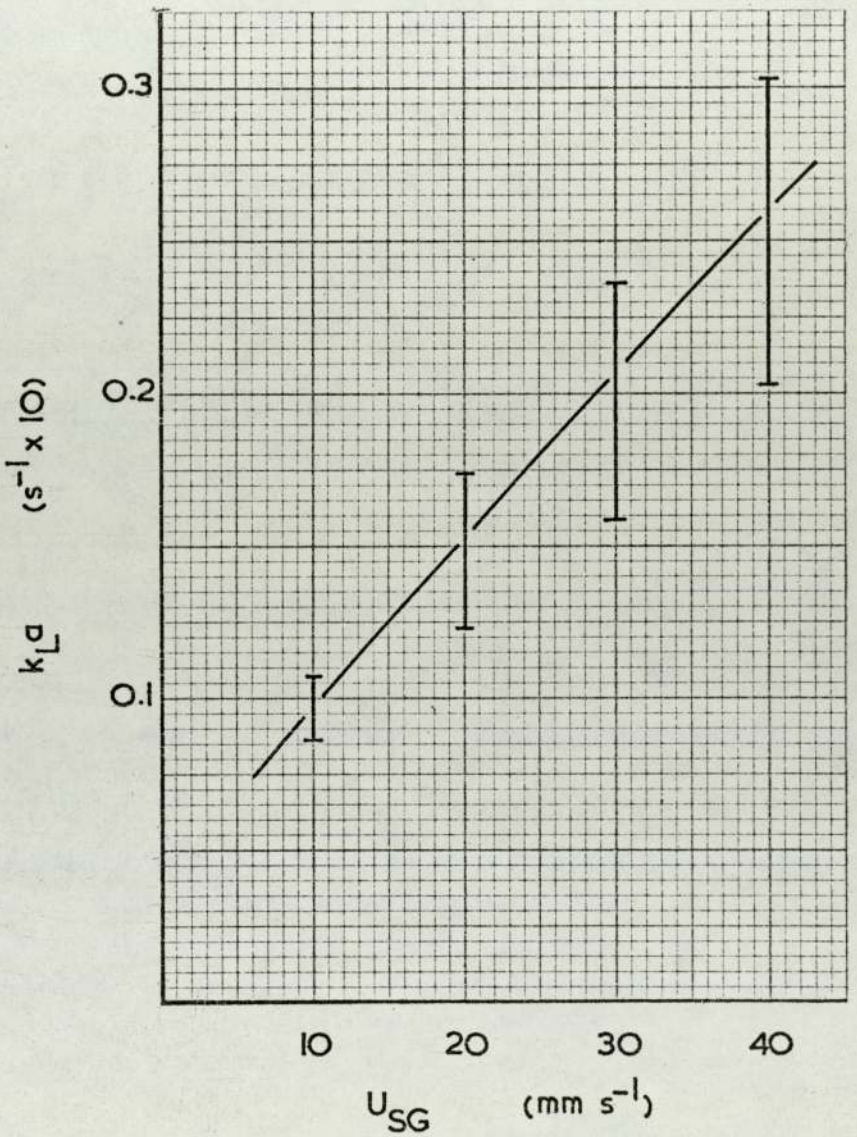

Figure 5.39 Effect of Anti-foams on the Mass-Transfer Coefficient

2. P2000

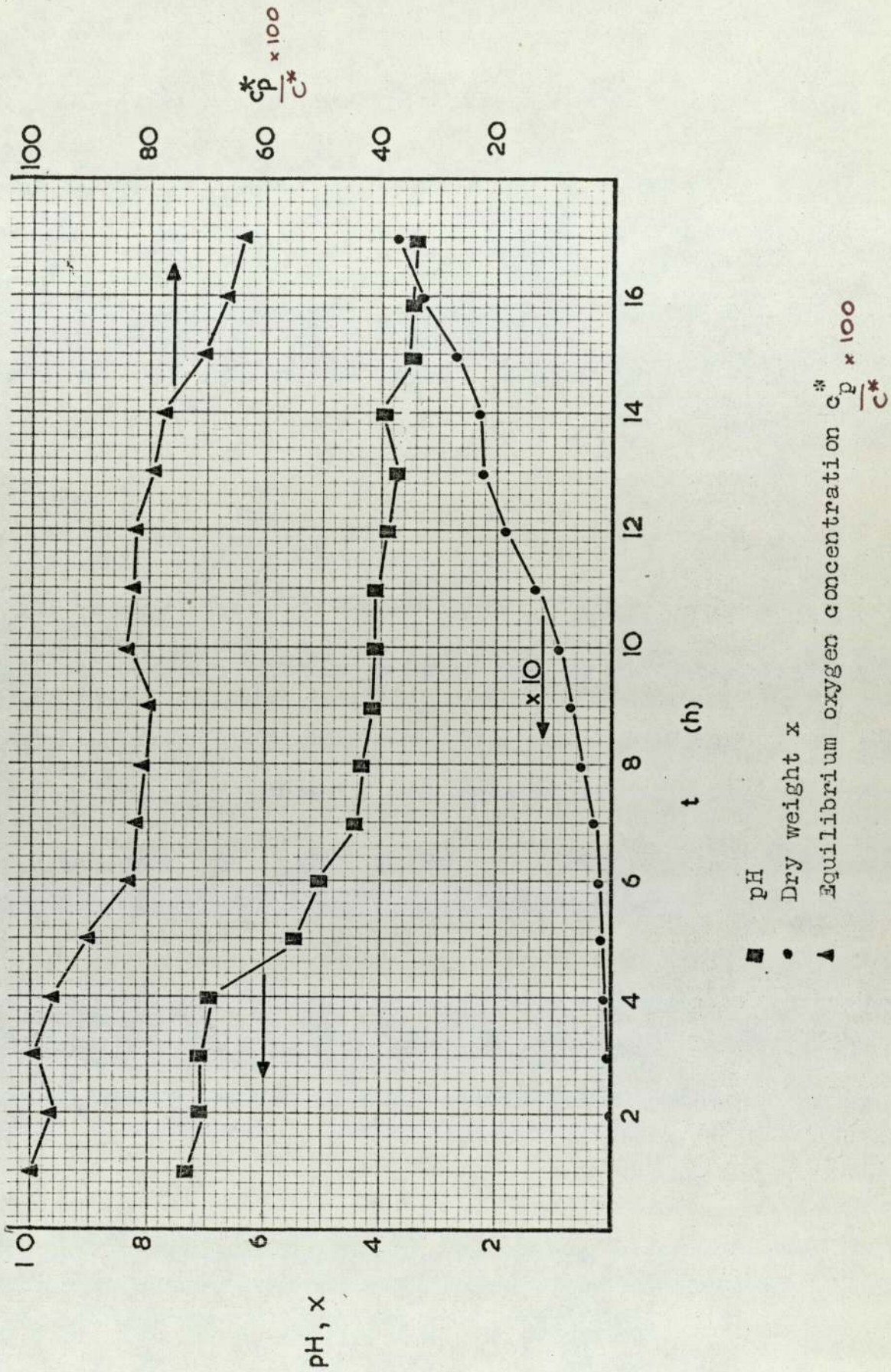

Figure 5.40 Variation of Parameters During a Fermentation

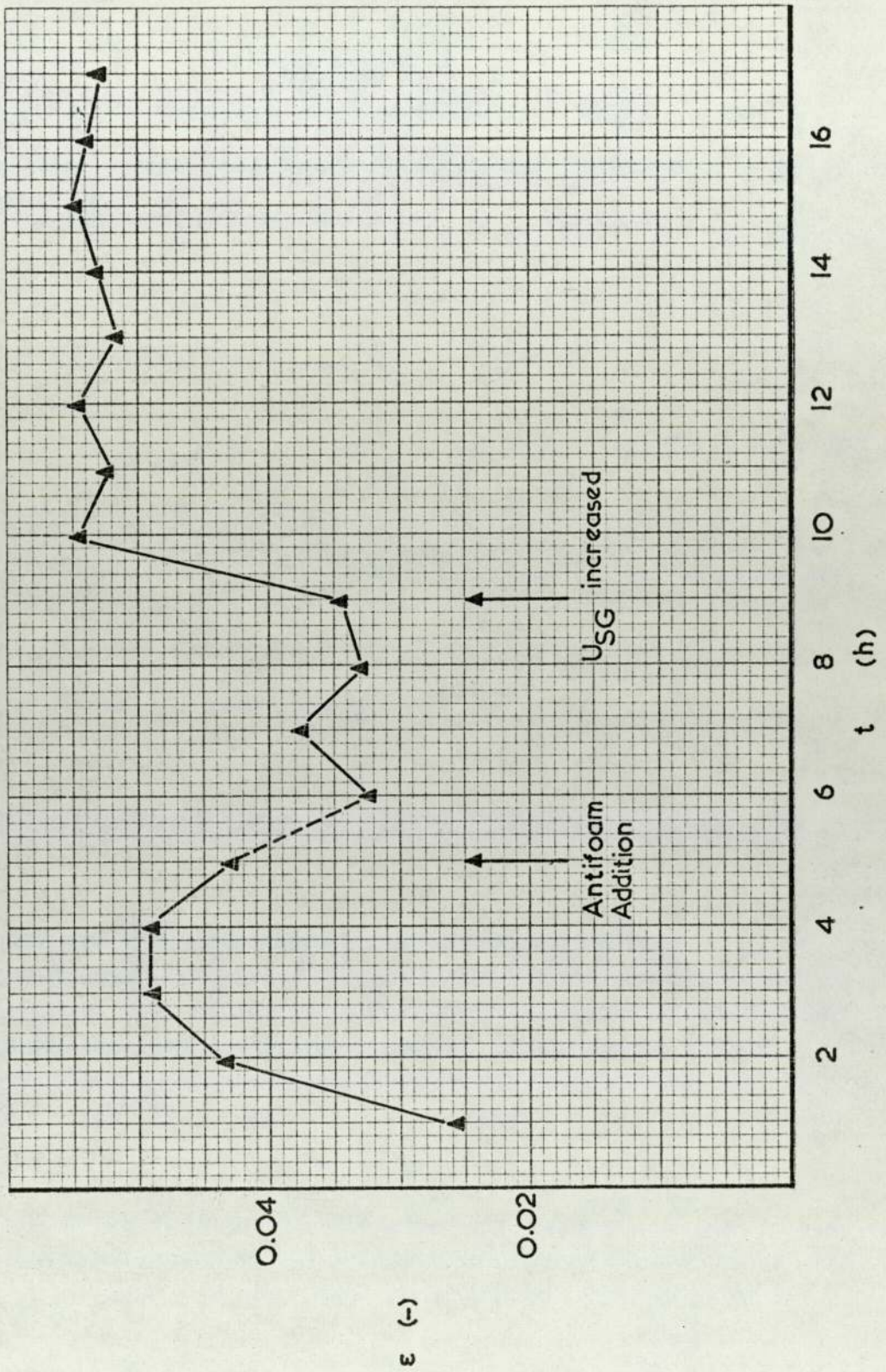

Figure 5.41 Gas Holdup During an Aspergillus niger Fermentation

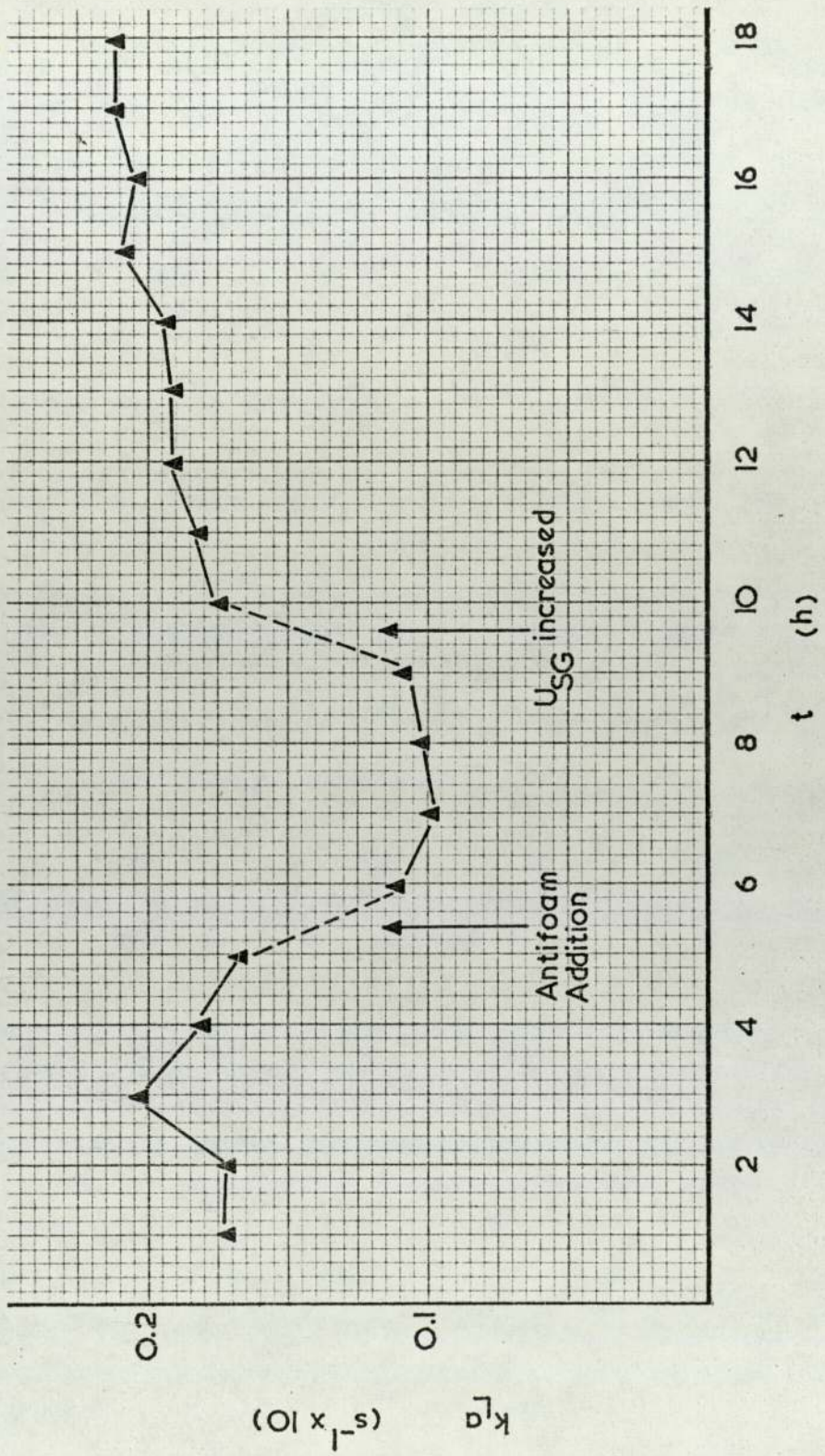

Figure 5.42 Variation of k_La During an Aspergillus niger Fermentation

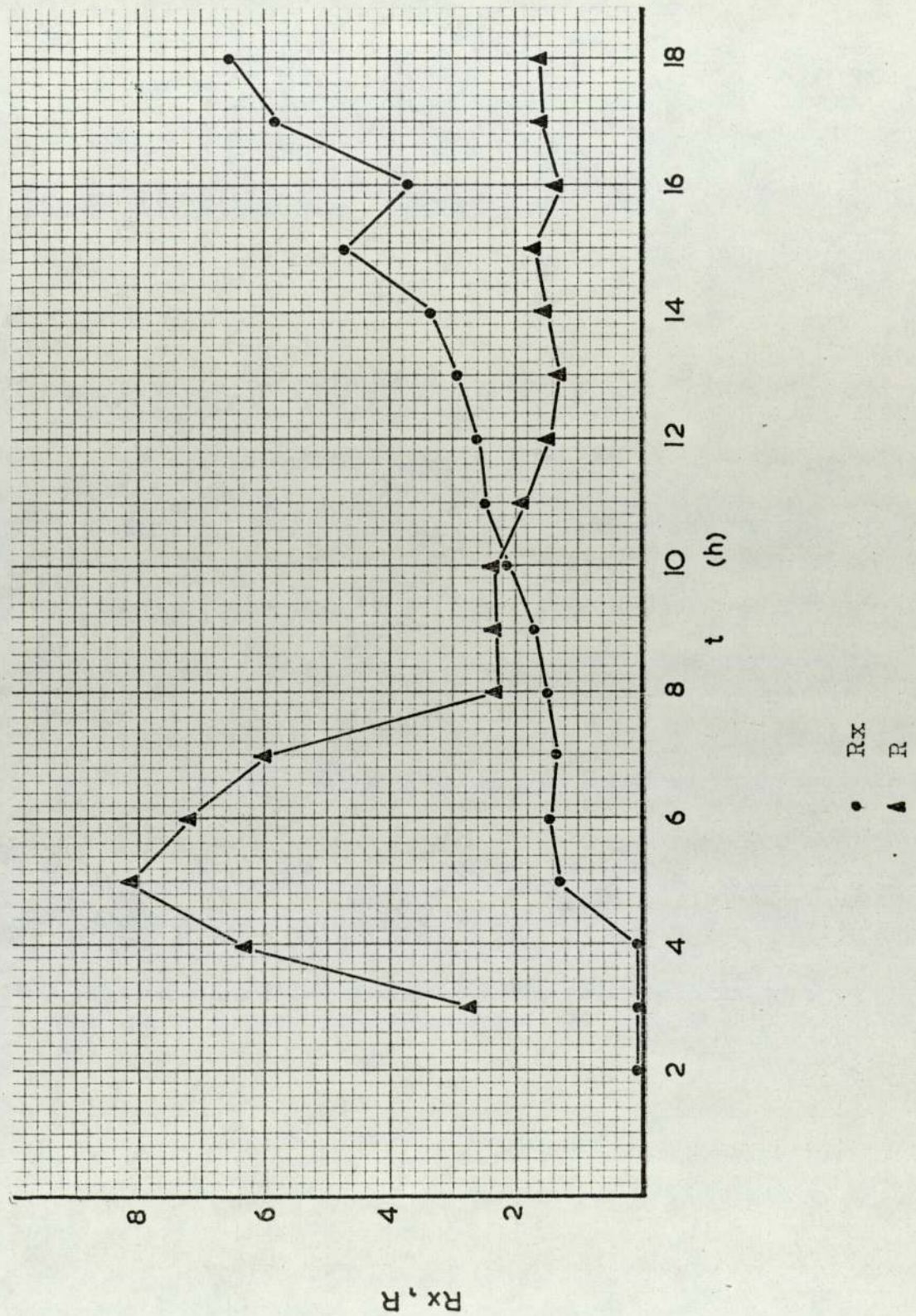

Figure 5.43 Calculated Values of the Micro-organism Respiratory Rate During an Aspergillus niger Fermentation

Figure 5.44 General Photographs of the 3 Day Fermentation

A. niger+Air A.niger Pellets

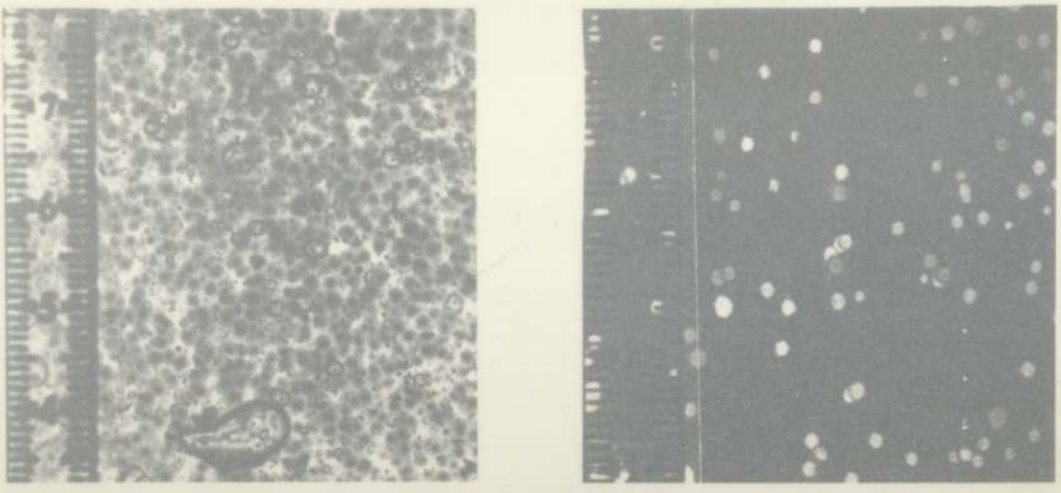

t = 24 hrs.

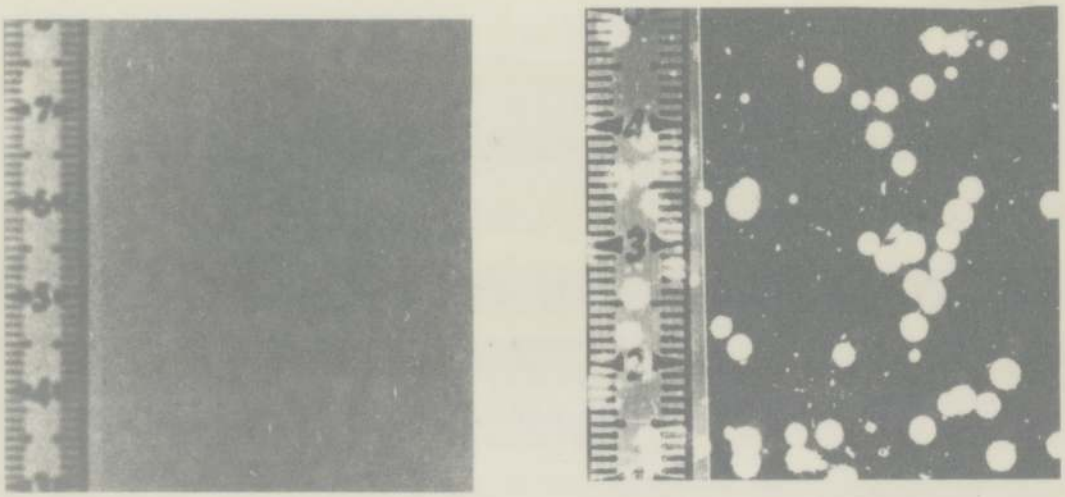

t = 48 hrs.

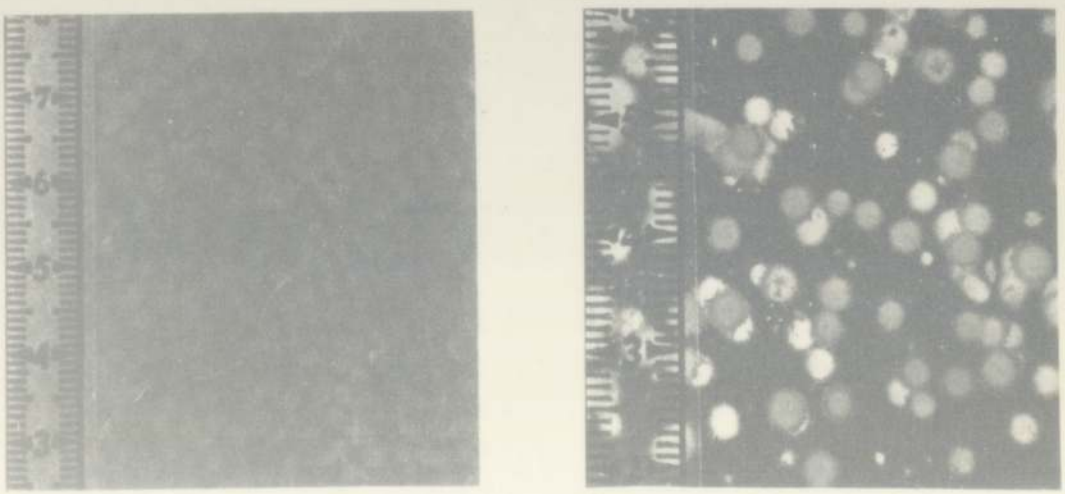

t = 72 hrs.

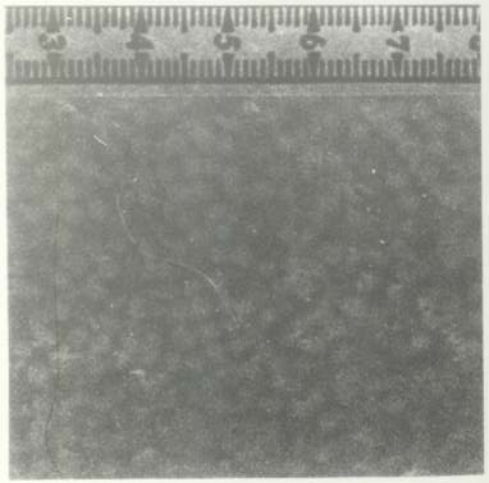

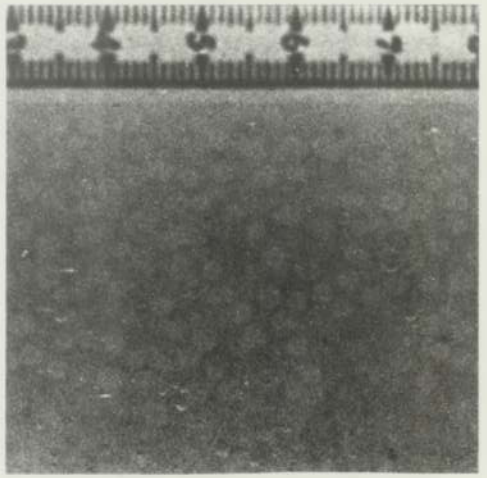

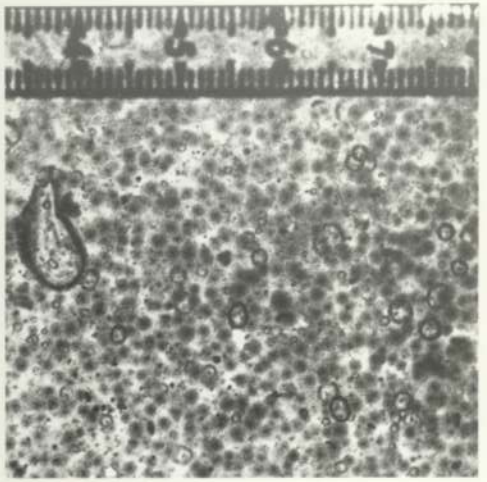

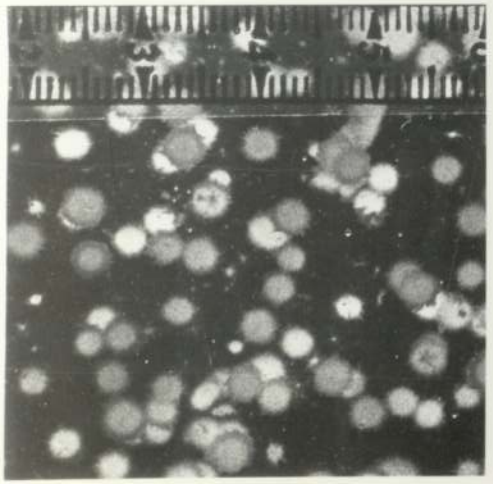

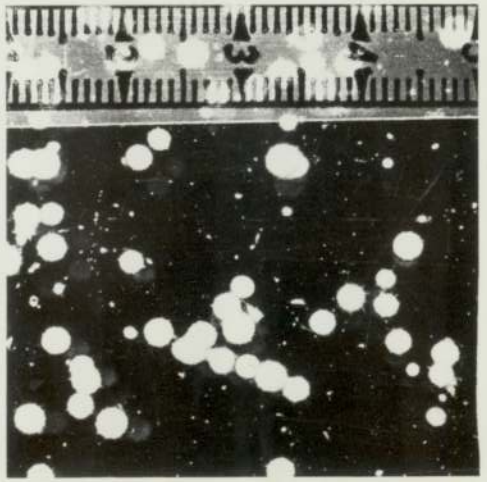

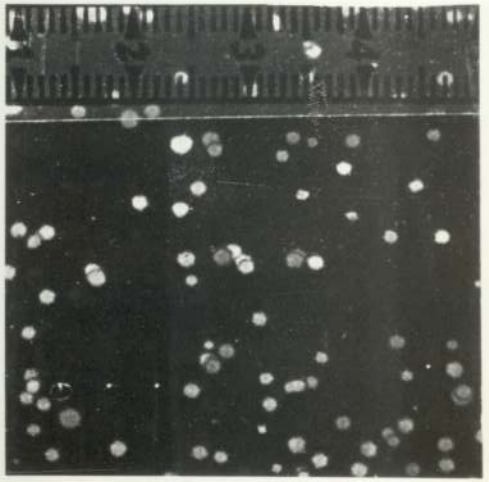

Figure 5.45 An *A. niger* Fermentation

A. niger Pellets | Air-Aggregate Dispersion

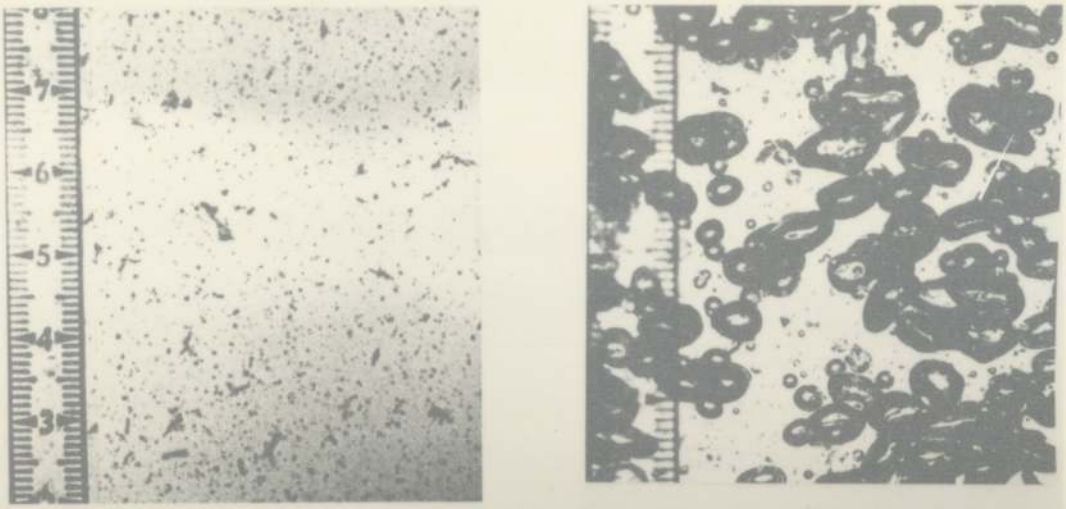

t = 1 hr.

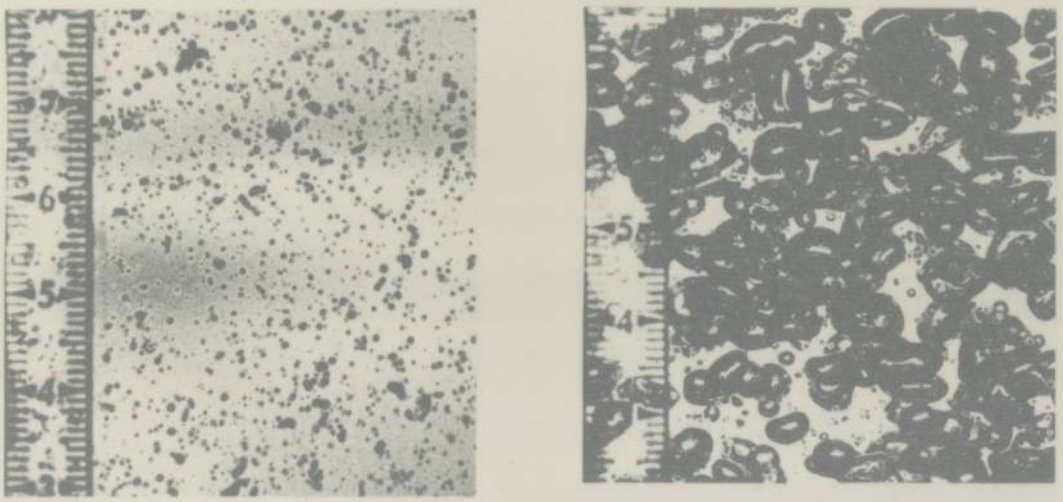

t = 2 hrs.

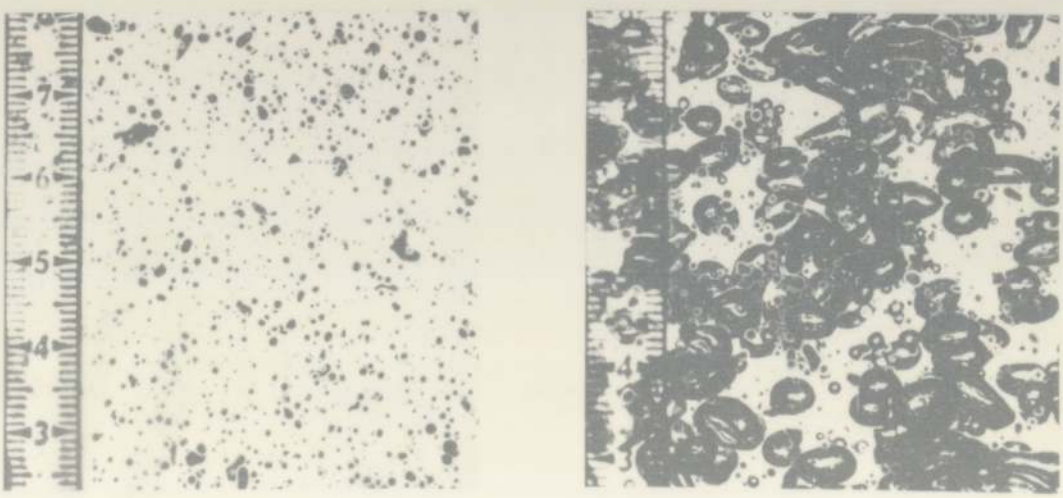

t = 3 hrs.

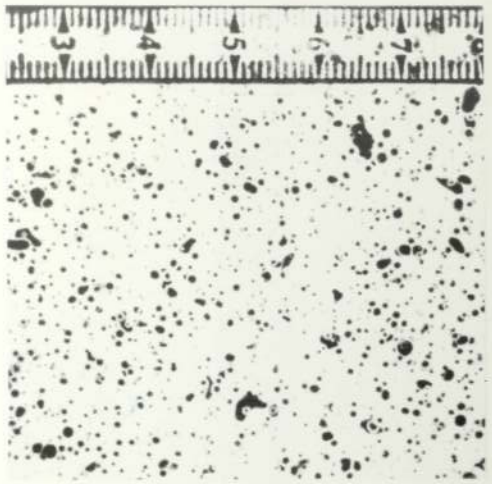

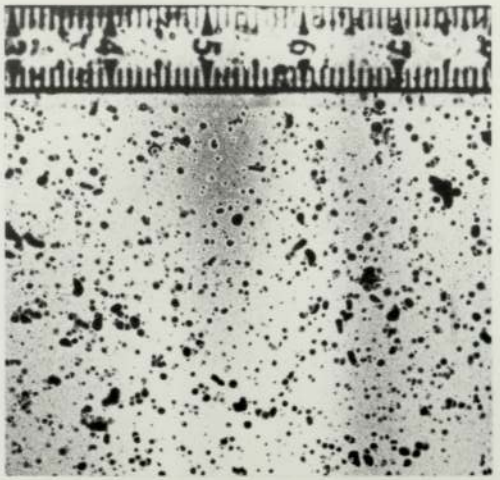

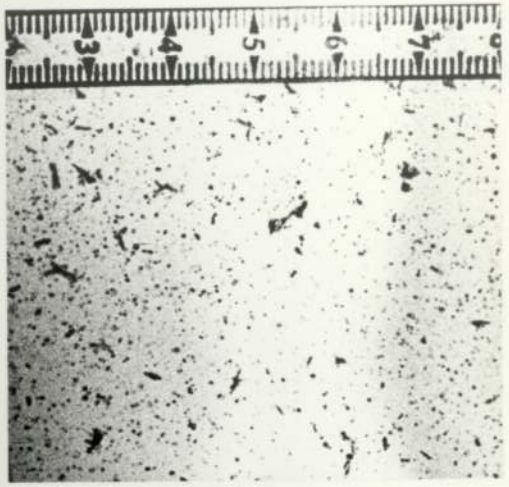

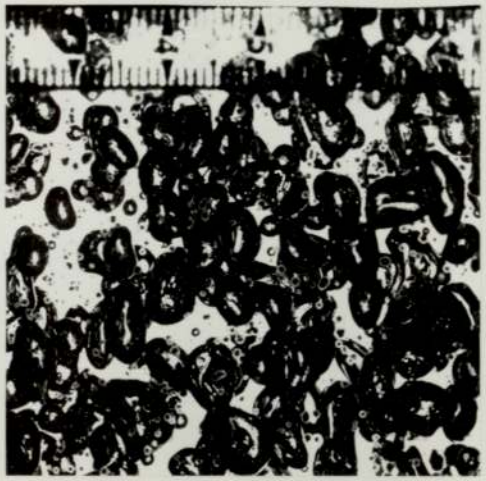

Figure 5.46 An A.niger Fermentation

A.niger Pellets

Air-Aggregate Dispersion

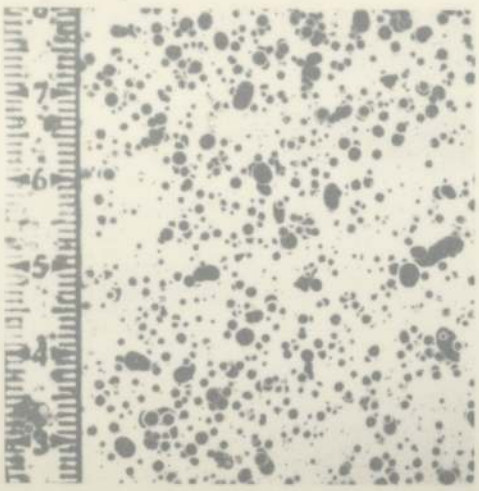

t = 4 hrs.

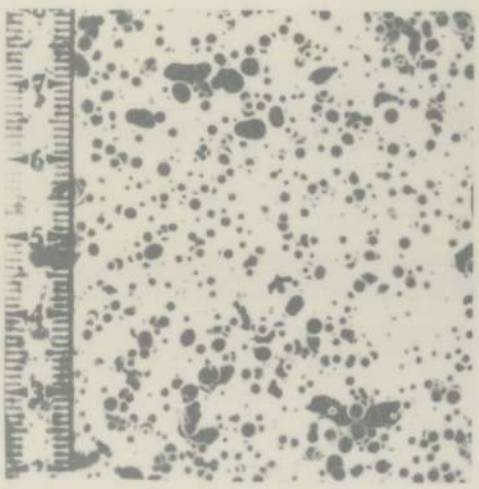

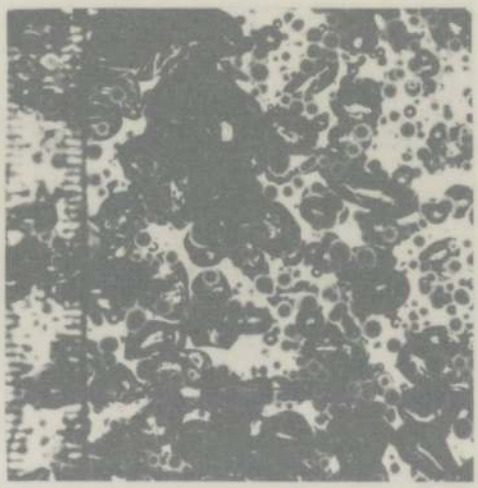

t = 5 hrs.

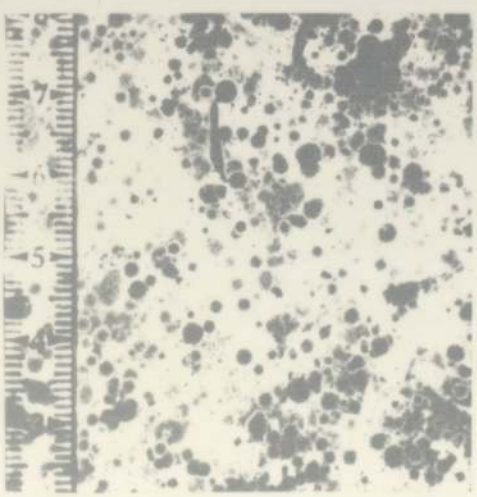

t = 6 hrs.

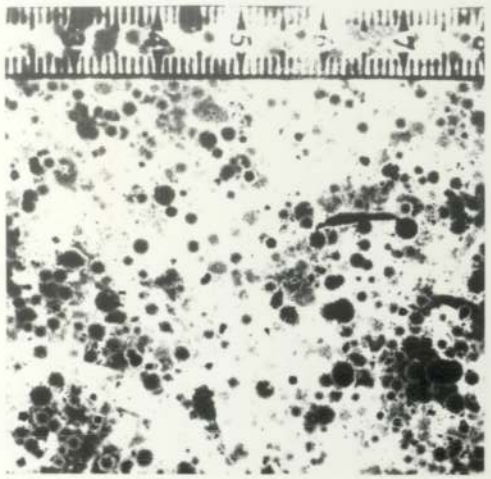

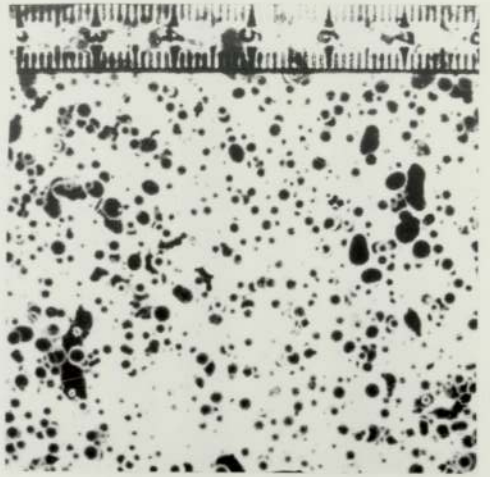

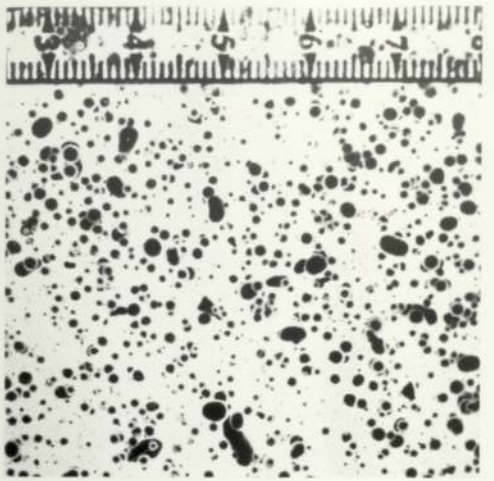

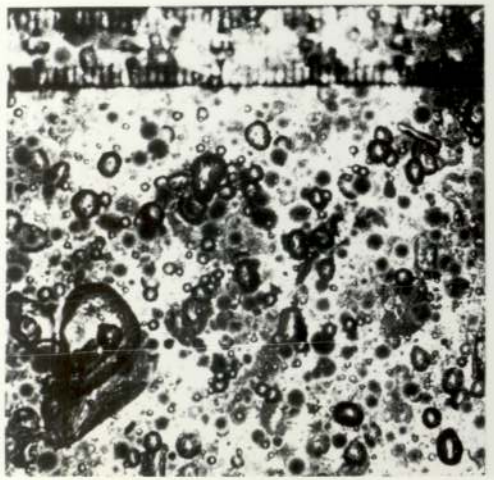

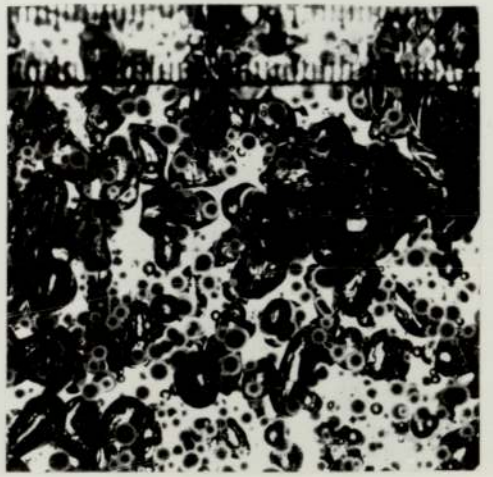

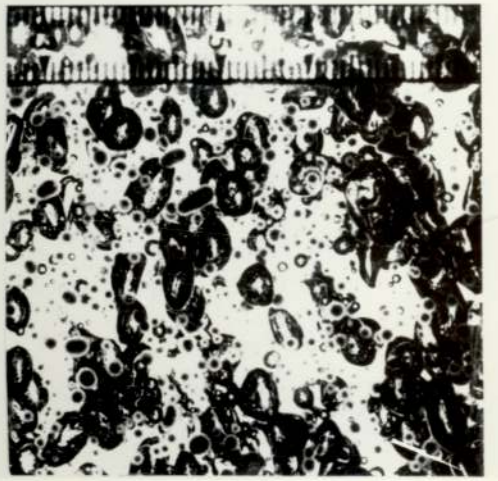

Figure 5.47 An *A.niger* Fermentation

A.niger Pellets | Air-Aggregate Dispersion

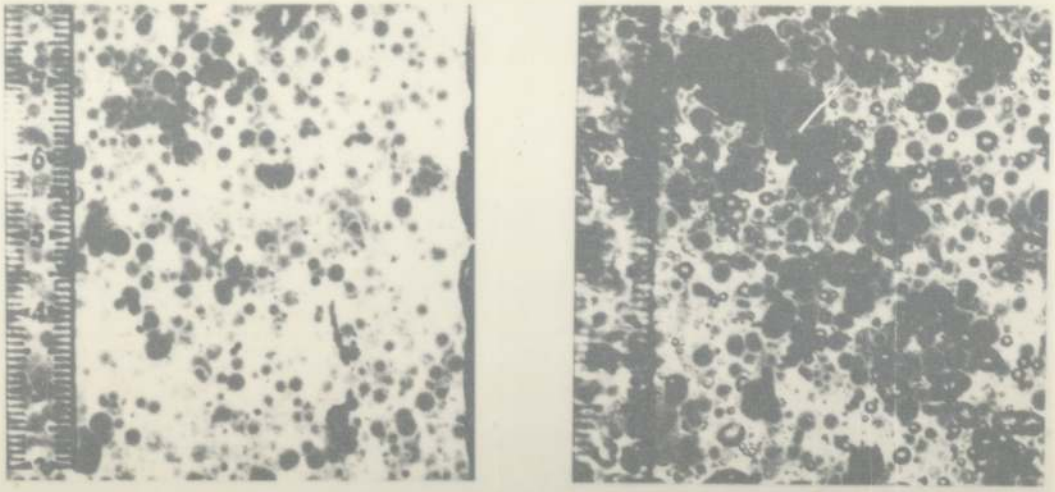

t = 7 hrs.

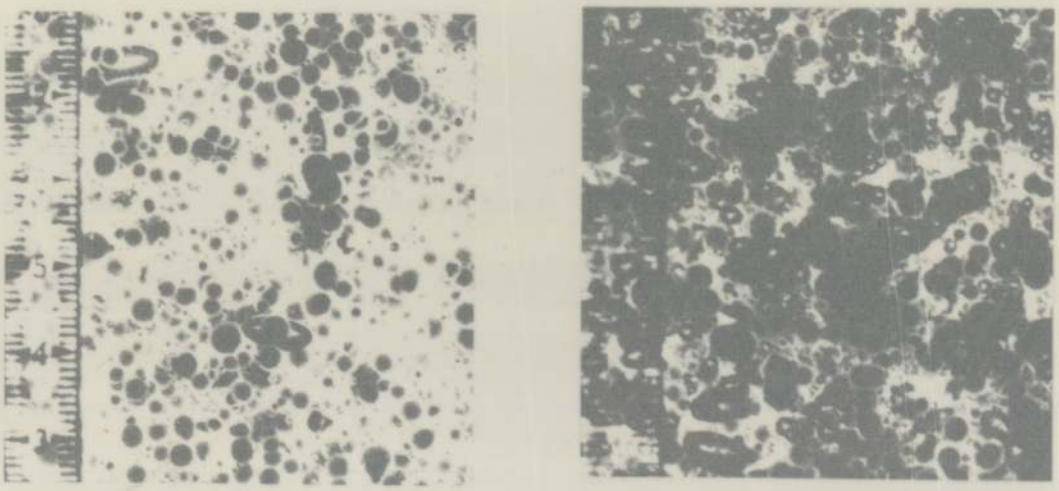

t = 8 hrs.

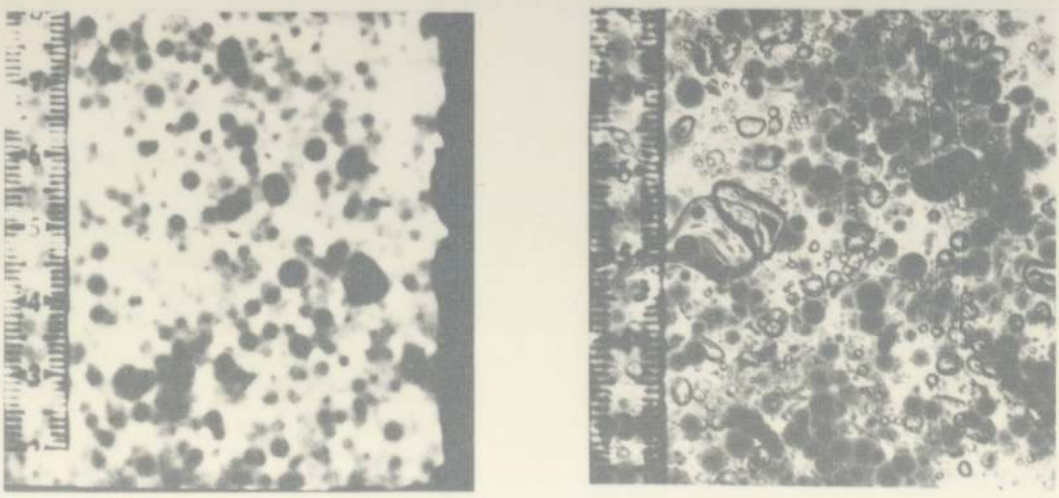

t = 9 hrs.

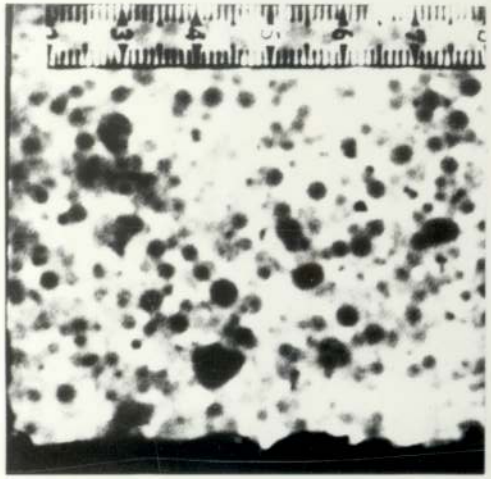

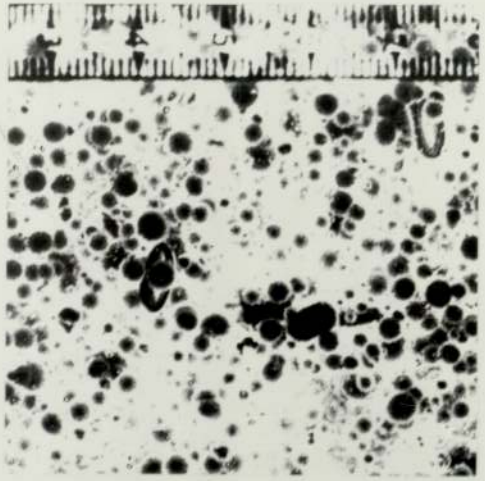

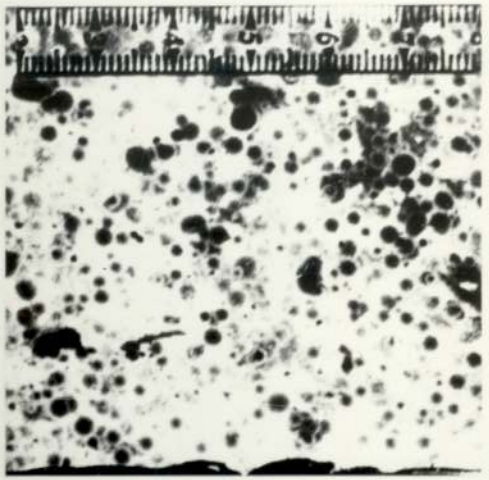

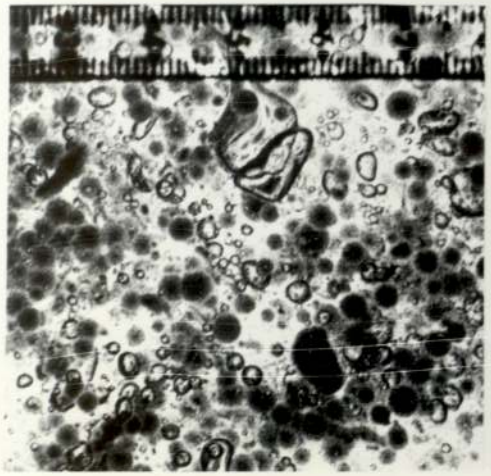

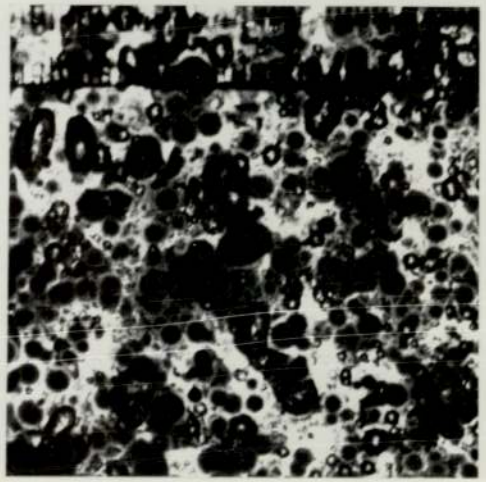

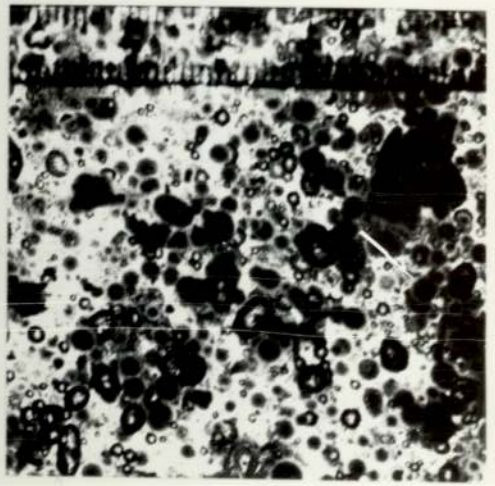

Figure 5.48 An *A.niger* Fermentation

A.niger Pellets | Air-Aggregate Dispersion

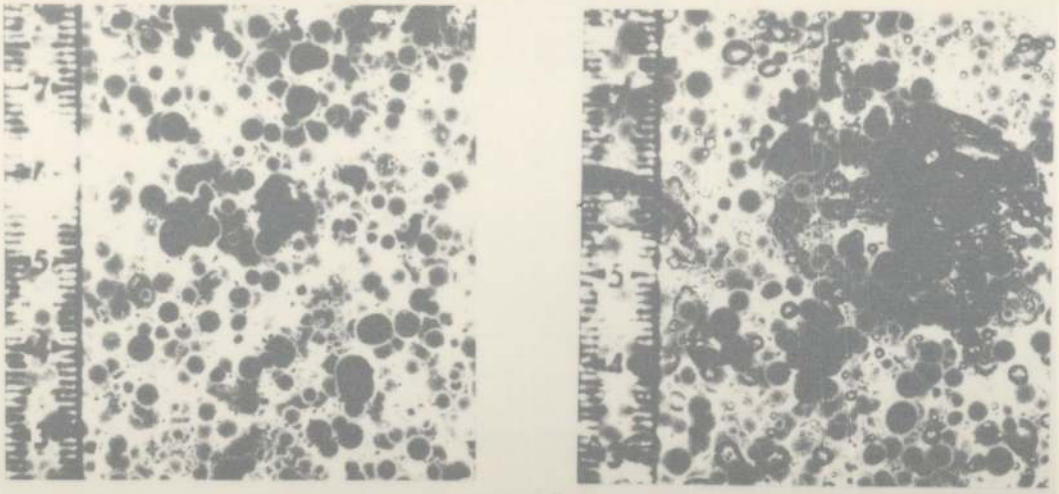

t = 10 hrs

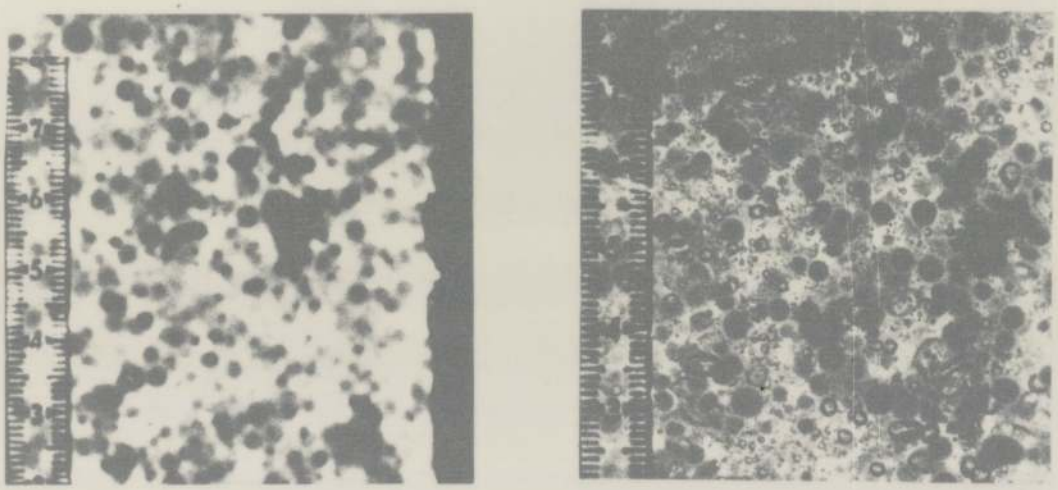

t = 11 hrs.

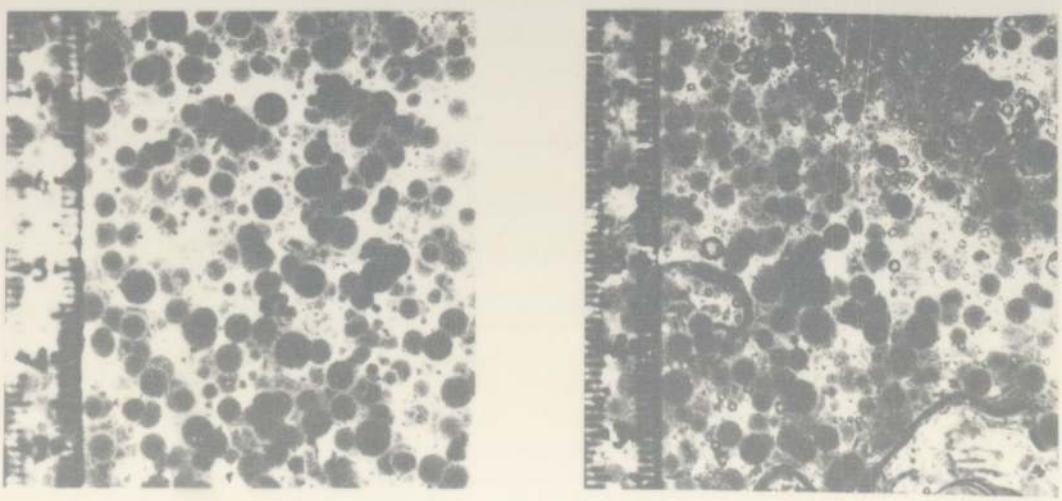

t = 12 hrs.

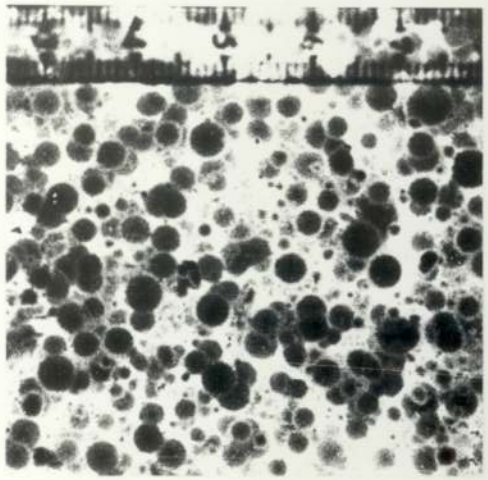

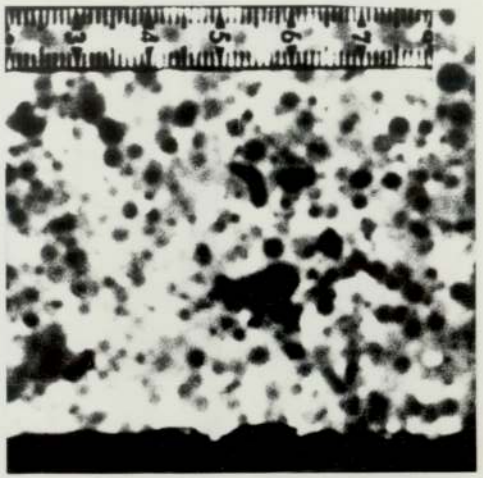

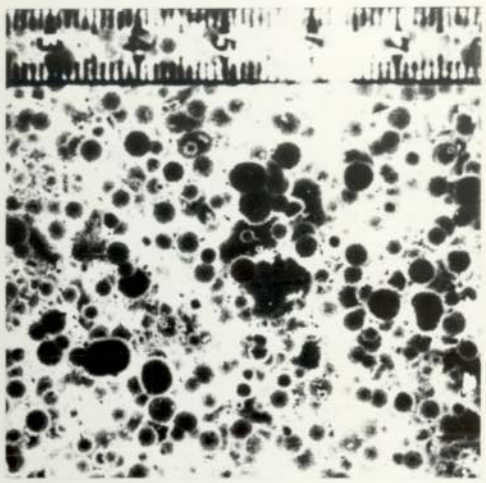

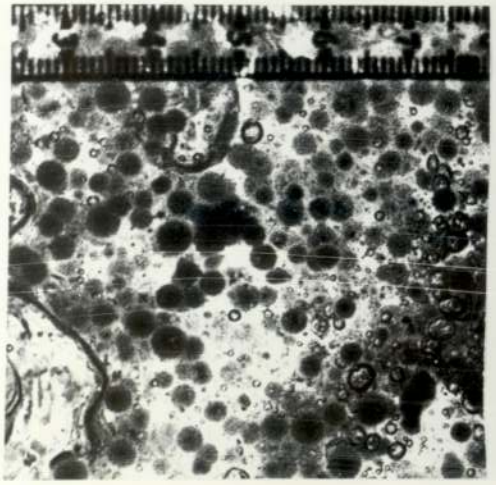

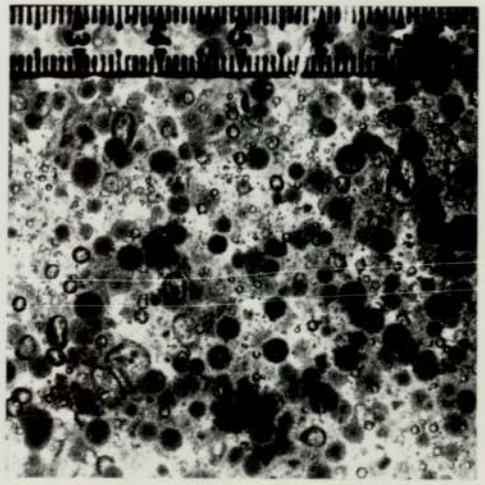

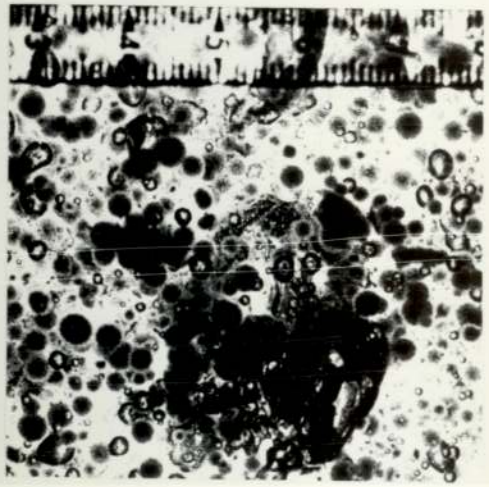

Figure 5.49 An *A.niger* Fermentation

A.niger Pellets | Air-Aggregate Dispersion

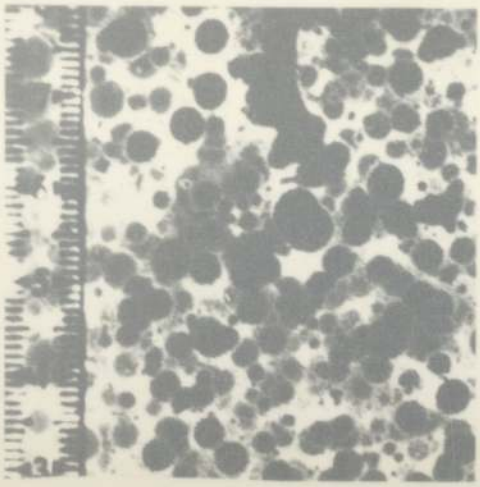

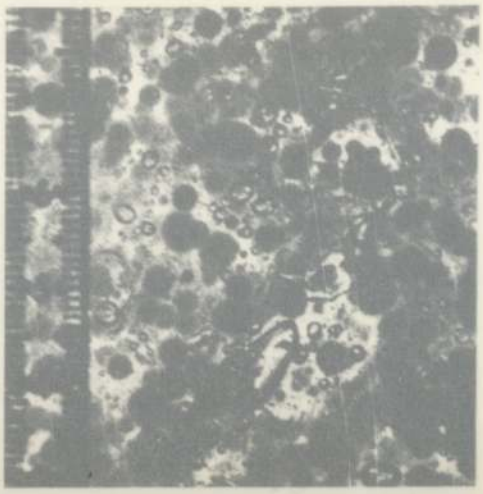

t = 13 hrs.

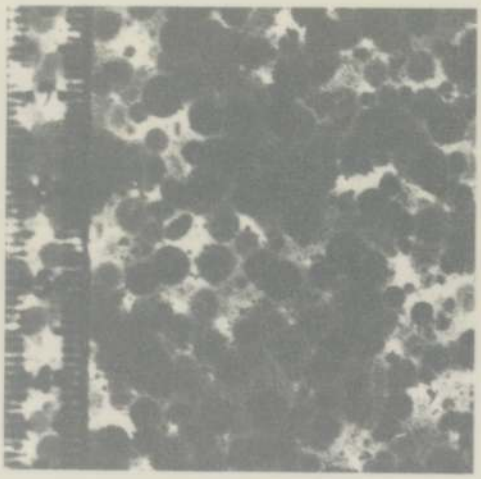

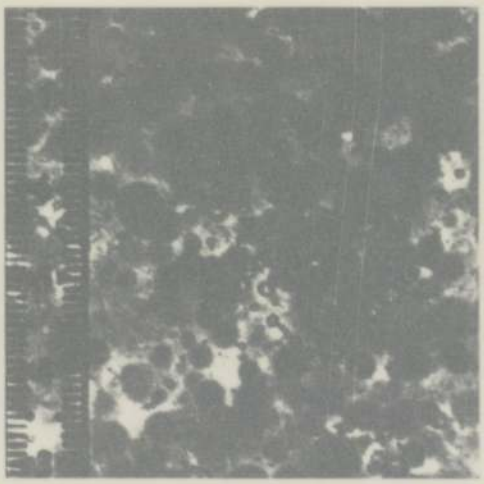

t = 14 hrs.

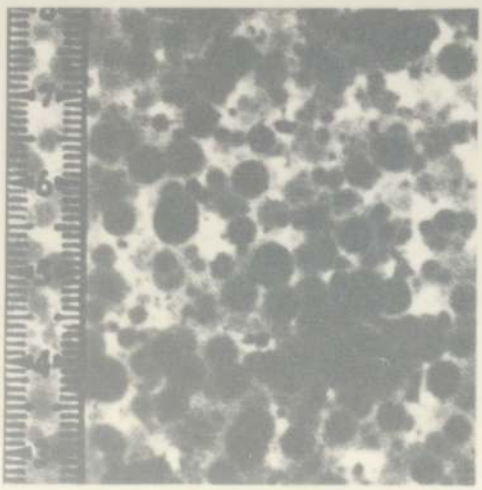

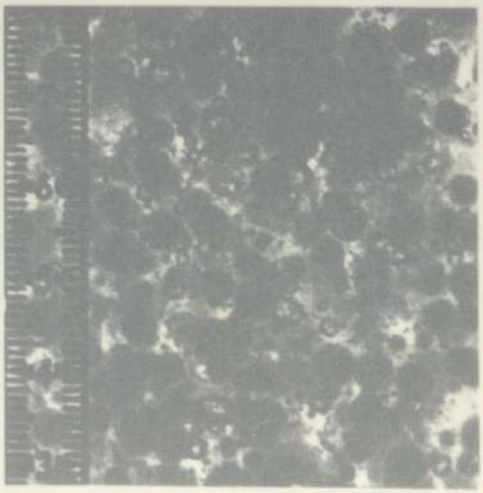

t = 15 hrs.

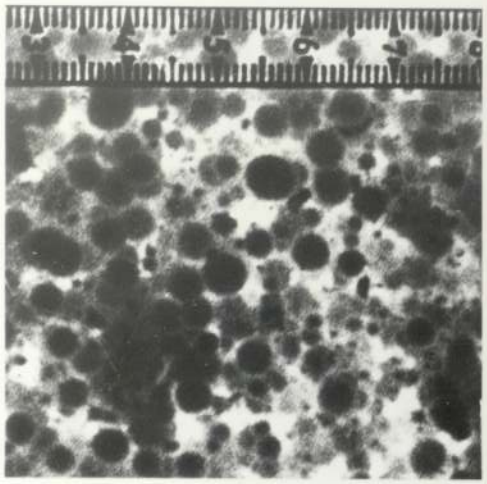

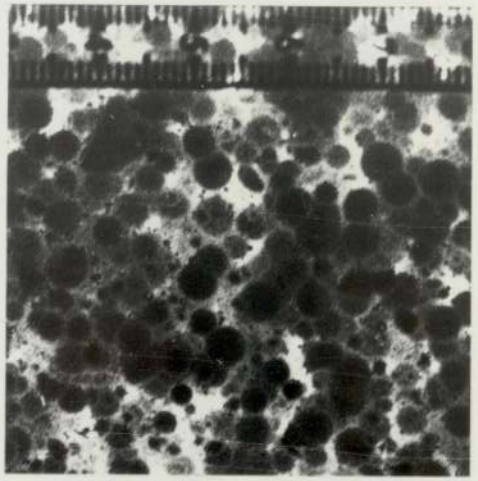

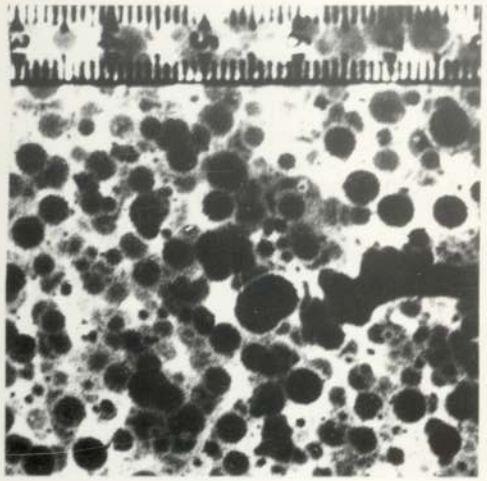

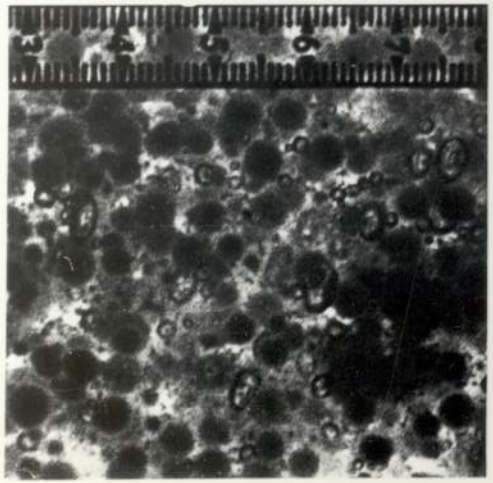

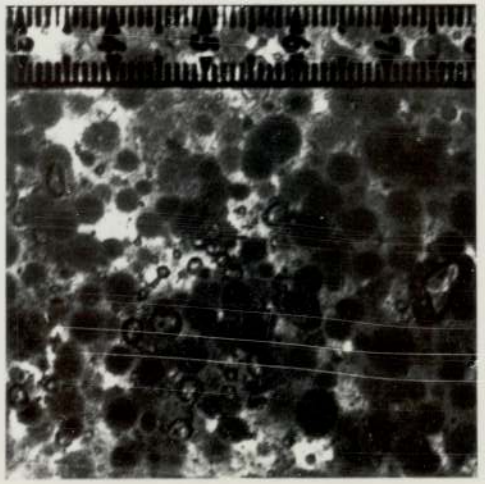

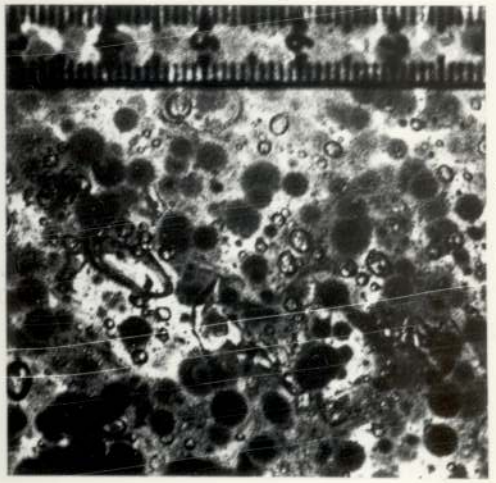

Figure 5.50 An *A.niger* Fermentation

A.niger Pellets | Air-Aggregate Dispersion

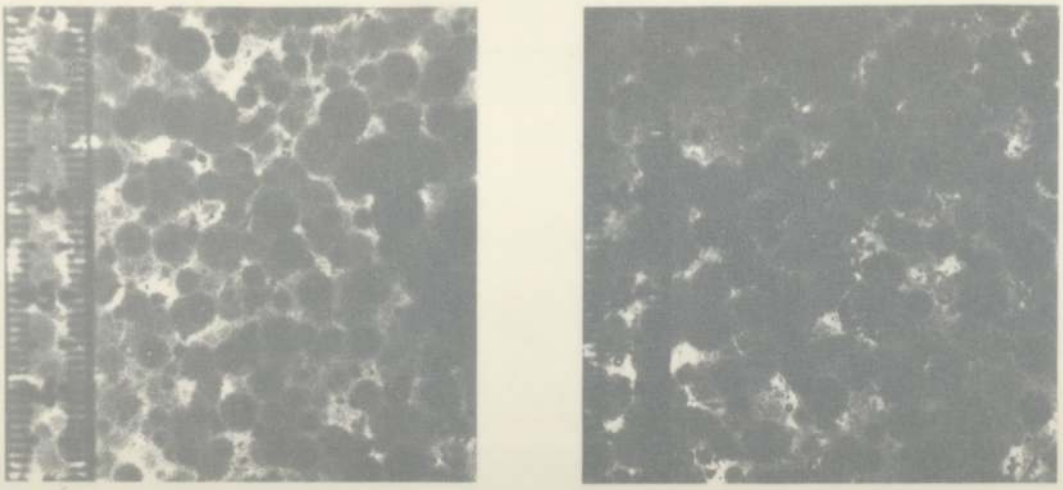

t = 16 hrs.

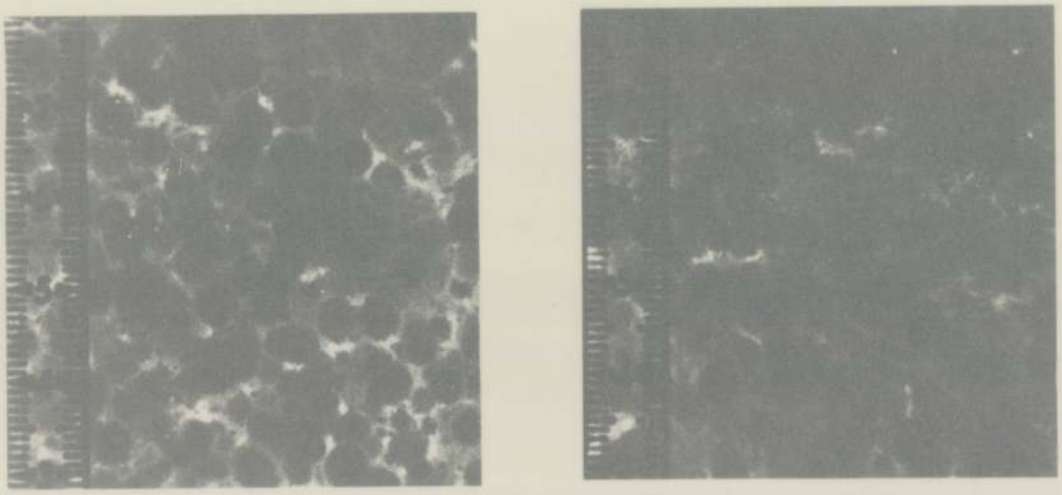

t = 17 hrs.

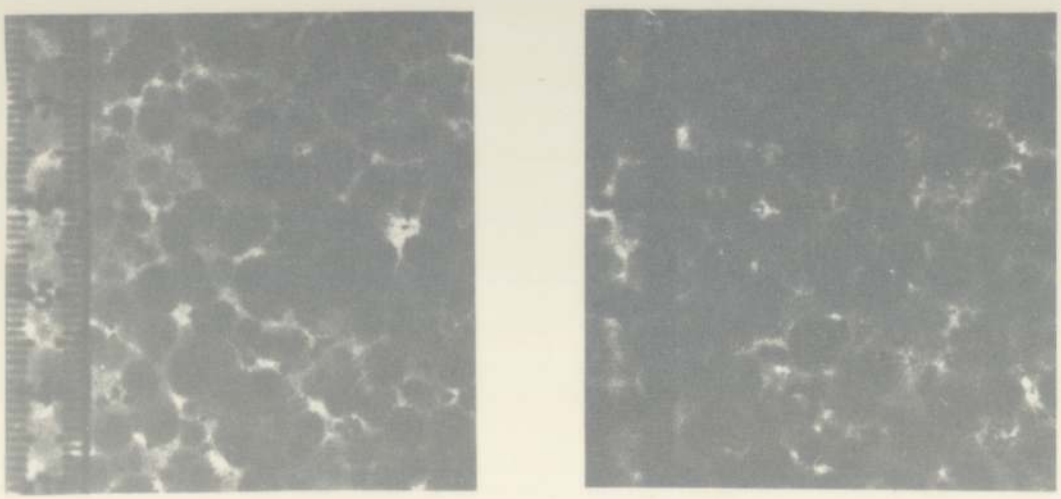

t = 18 hrs.

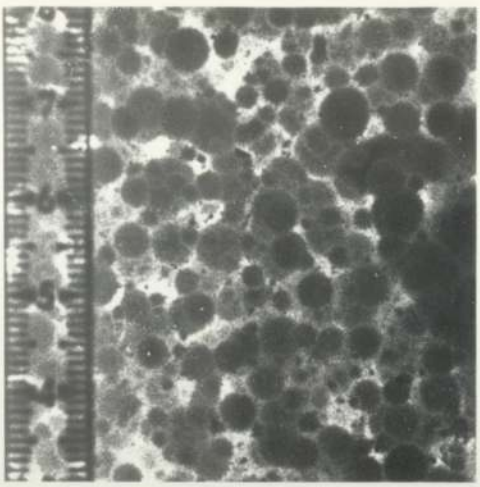

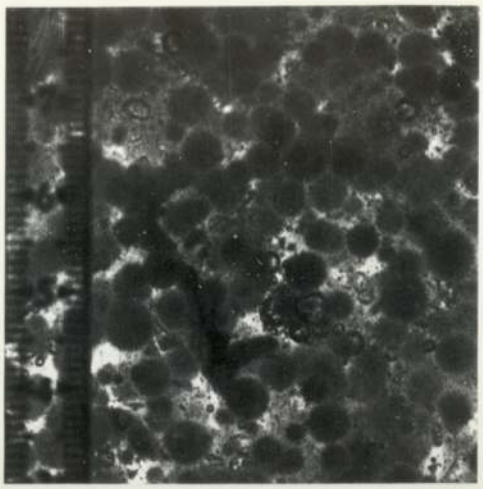

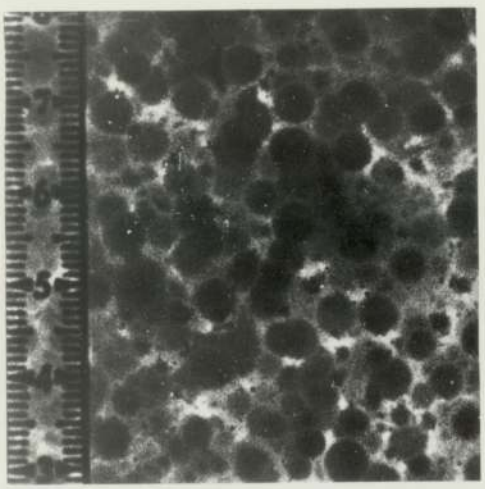

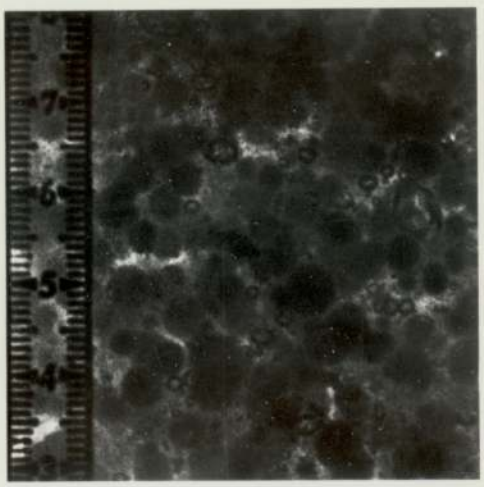

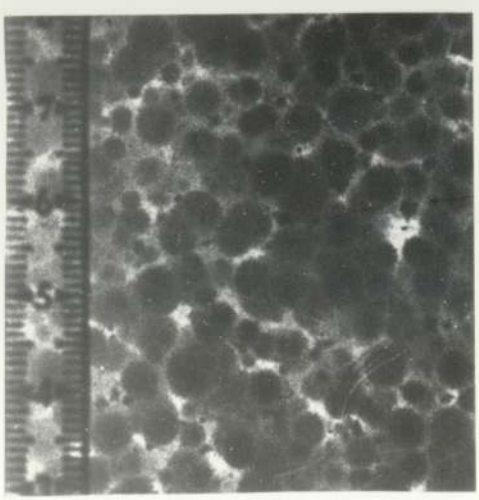

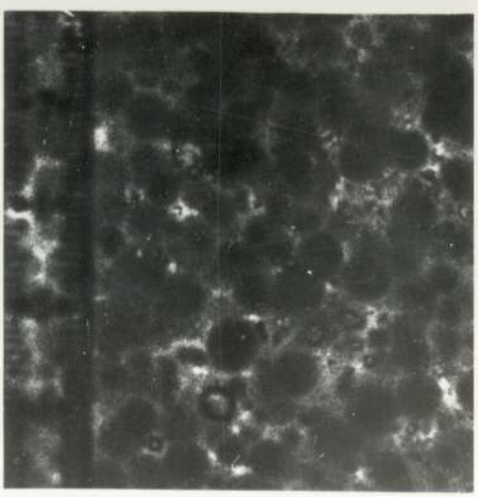

Nomenclature (Section 5)

Symbol	Explanation	Units
A_1, k_1, k_2	parameters required to describe the oxygen electrode response	
c	concentration of oxygen in the liquid phase	g/l
c_p	oxygen concentration detected by the oxygen electrode	g/l
c^*	equilibrium concentration of oxygen in the liquid phase	g/l
c_p^*	equilibrium oxygen concentration detected by electrode under pseudo steady state conditions	g/l
$k_L a$	overall oxygen mass-transfer coefficient	s^{-1}
R	respiratory rate of the micro-organism	$(g\ O_2)/(g\ org)s$
t	time	s
x	micro-organism dry weight	g/l
z	(k_2/k_1)	

Greek

ϵ	gas holdup	-
θ	$(k_1 . t)$	
Γ	normalised probe response following a step change in the oxygen concentration in the gas phase	-
Γ'	normalised probe response following a step change in the oxygen concentration in the liquid phase	-

References (Section 5)

(1) HEINEKEN, F.G., Biotechnol. Bioeng., 12, 145 (1970)

(2) LINEK, V., Biotechnol. Bioeng., 14, 285 (1972)

(3) CALDERBANK, P.H., Trans. Inst. Chem. Engrs., 37, 173 (1959)

(4) VOTRUKA, J. and SOBOTKA, M., Biotechnol. Bioeng., 18, 1815 (1976)

(5) VOTRUKA, J., SOBOTKA, M. and PROKOP, A., Biotechnol. Bioeng., 19, 435 (1977)

(6) LINEK, V. and VACEK, V., Biotechnol. Bioeng., 18, 1537 (1976)

(7) CRANK, J., "The Mathematics of Diffusion", 2nd. Ed., Oxford University Press (1975)

(8) LINEK, V. and BENES, P., Biotechnol. Bioeng., 19, 741 (1977)

(9) LINEK, V. and BENES, P., Biotechnol. Bioeng., 20, 903 (1978)

6. DISCUSSION

6 Discussion.

6.1 Gas Holdup.

The Manometric Technique.

Gas holdup measurements using the air-water system were made in two columns of different diameters. The results obtained with the 152 mm column (figure 5.1) also include those from experiments in which the superficial liquid velocity was varied. Whilst the effect of this parameter can be shown statistically to be significant, the diagram illustrates that the effect of the superficial gas velocity was far greater. Similar work was then done with M1SM solutions of various concentrations in the 102 mm column (figure 5.3); the effect of antifoam was also considered. Gas holdup in M1SM solutions was found to be slightly higher than the value obtained in pure water; the effect of varying concentrations was however small. Silcolapse even at low concentrations reduced the holdup figure further to approximately 50% of that obtained in the M1SM solutions.

For the bubbly-flow regime it was found that the gas holdup may roughly be expressed in terms of the superficial gas velocity, viz :

$$\varepsilon = q\, U_{SG} \qquad (1)$$

The estimated values of the constant, q, for this work are compared with those of Shayegan-Salek (1) in table 6.1: the data presented show good agreement. Results obtained using the 102 mm diameter column are smaller than those predicted from the work of Shayegan-Salek due to the construction of the gas distributer. In this work with the 102 mm column a perforated phase distributer was used whereas Shayegan-Salek

Table 6.1 - q Values for the Estimation of Gas Hold-up.

Column d.	System	This work	Shayegan-Salek
76	Air-water	-	0.0048
102	" "	0.0034	-
152	" "	0.0039	0.0040
305	" "	-	0.0034
102	Air-MlSM	0.0049	-
152	Air-wort		0.0043
102	Air-MlSM-Silcolapse	0.0008	-
152	Air-wort-Silcolapse	-	0.0018

Note units : q in s/mm
U_{sc} in mm/s

used a sintered glass distributer; the latter produced smaller bubble diameters and higher bubble densities.

The bubbly-flow regime existed in the 152 mm diameter column up to gas velocities of approximately 35 mm s^{-1}; the regime extended a little further, to approximately 40 mm s^{-1}, in the smaller 102 mm column. At higher gas velocities bubble coalescense occurred and the slugs so formed, because of their greater size and velocity, passed more quickly through the column.

Light Transmittance Method.

After calibration of the selenium resistance cell versus luminous flux, the variation of resistance with superficial gas velocity in air-water dispersions was measured. It was noted that the resistance varied between approximately 100 and 500 Ω over the range of gas velocities used and up to 800 Ω in the presence of the antifoam

P2000. By comparison of these results with the calibration curve shown in figure 5.4 it can be seen that the resistance range falls in the most sensitive region of the cell response.

Having shown that the resistance varied continuously with gas velocity the method was used to study the effect of the anti-foams Silcolapse and P2000. It was found that whilst the values of gas holdup in solutions containing Silcolapse were smaller than in the same solutions without the anti-foam, solutions containing P2000 exhibited a reverse trend. This was confirmed by the photographs contained in figures 5.6 and 5.7 for the air water system and for M1SM solutions figures 5.8 to 5.13. The results suggest that the anti-foams Silcolapse and P2000 have different modes of action. Measurements show that P2000 reduces the surface tension of the liquid medium, and this is indicative of the high spreading characteristics of such anti-foams. Silcolapse, on the other hand, does not appear to reduce the bulk surface tension to any significant extent. It is effective because it reduces intermolecular cohesive forces and does not contribute to surface viscosity or rigidity.

The experiments using the light transmittance technique were very easy to perform and illustrate that light transmission is a possible way of measuring bubble densities. Calderbank (2) and Lockett and Safekourdi (3) performed similar experiments using a parallel beam of light. Further work is, however, required before the method can be used for a detailed examination of this system. This is particularly true in the three-phase fermentation system. Here it was found that with the light source and detector mounted either side of the column the mycelium concentration soon became too dense for light to be transmitted through the dispersion at all. At low mycelium concentrations, however,

it was possible to measure differences in the levels of light transmitted with changes in the concentration of the growing micro-organism. This was done during a short interruption of aeration, suggesting that the technique, after further development, may also be useful for estimating dry weight concentrations. Apparatus similar to that of Calderbank,(see figure 3.2), may be more successful for these measurements but with the light source and detector inserted through the wall of the column: this would provide a much shorter path through the dispersion and increase the possibility of detection.

Again refering to figures 5.6 and 5.7 the air-water system produces bubble dispersions which have a fairly uniform size distribution. The individual bubbles have a smooth exterior but appear twisted and mis-shapen. The bubble density increases as the gas velocity increases and at 40 mm s^{-1} there is no sign of the formation of gas slugs.

In systems containing P2000 the bubble size distribution widens. Bubbles with diameters of several millimetres can be seen against a background of "ionic bubbles" with diameters of much less than 1 mm. The larger bubbles appear more rigid than in the air-water system and less mis-shapen. The bubble density again increases with increasing superficial gas velocity: there is no formation of gas slugs at 40 mm s^{-1}, but the range of bubble diameters leads to higher bubble densities and gas holdups.

The introduction of Silcolapse into a system causes the formation of gas slugs even at gas velocities of 10 mm s^{-1}. The slugs are smooth in appearance but evidence exists that the surfaces are "wrinkled". Again the overall dispersion contains a wide range of bubble sizes and is seen against a background of "ionic" bubbles.

The density of the "ionic" bubble-dispersion is illustrated in figure 5.14. These photographs were taken during an interruption in aeration. The larger bubbles because of their higher rise velocities quickly leave the smaller bubbles behind in the fermenter. The photographs clearly show the range of densities which occured at different superficial gas velocities.

Holdup in the Three-Phase System.

The results obtained from the measurement of holdup in a three phase system (figure 5.15) are similar to those obtained for the two phase system at identical superficial gas velocities. Following start up, the gas holdup quickly rose to 5%. The onset of germination of the spores, which occured after approximately four hours, led to a decrease but this was partially masked by the addition of Silcolapse five hours into the fermentation. A new level of 3.5% was then found until the superficial gas velocity was increased to 20 mm s^{-1} after nine hours. A constant value of 5.5% was then achieved for the remainder of the experiment. The interaction between gas holdup and other variables is discussed later in the section.

6.2 Oxygen Mass-Transfer.

6.2.1. Probe Calibration Response to a Step Change in Oxygen Concentration.

Figure 5.18 shows four typical traces obtained at different temperatures for the response of a Chark electrode to a step change in dissolved oxygen concentration. Although the traces appear to be affected by the operating temperature, the curves have similar slopes and reach equilibrium values after similar periods of time. This is

confirmed by the presentation of this data in a normalised form (figure 5.19). Within the limits of experimental accuracy the plots presented in the latter figure appear to be almost identical.

These curves also highlight the difficulty of measurement at start-up and at high values of t. At start-up, the concentration is altering so rapidly that during the first second or so it is difficult to obtain an accurate record: hence the curves do not pass through the origin. At the other end of the curve the fall in concentration is so slow that it is difficult to make estimates of the change that has occurred over small time periods.

As mentioned in section 5, a two-region, two-layer model for the membrane-electrolyte-electrode system was used to account for the probe response characteristics. Two of the constants for this model, k_1 and k_2, can be estimated from a semi-log plot of the normalised results. These constants have been estimated for the calibration experiments conducted during the course of this work, and they are presented as a function of temperature in figure 5.20. Both k_1 and k_2 increase with increasing temperature although k_1 is affected to a greater degree than k_2.

6.2.2. Direct Calibration of the Probe Response versus Temperature.

On increasing the temperature of oxygen saturated aerated water, the indicated output from the Chark oxygen electrode (immersed, in the water) was found to increase. Now oxygen is only sparingly soluble in water (4), and the dependence of the saturated dissolved oxygen concentration on temperature is an inverse function as described by:

$$c^* = \frac{0.468}{31.6 + T} \quad g/l. \qquad (2)$$

for $4 < T^{\circ}C < 33$

The increase in output is therefore not due to a change in c^{*}.

To test the effect of amplification of the meter the experiment was repeated at different amplifier settings. At first sight this leads to different experimental traces (see figure 5.32). Again, however, when the data are normalised, i.e. the response at any temperature is divided by a suitably chosen reference figure, and replotted (see figure 5.33) the responses at different amplifications are very similiar. In this work the response at $32^{\circ}C$ was used as the reference value because this is the maximum temperature that was used at both amplifier settings.

As already mentioned in section 3, Vincent (5) expressed the temperature dependence of the output figure of an oxygen electrode in the form

$$I_T = A\, e^{-\frac{J}{T}} \qquad (3)$$

where I_T is the signal current and A and J are constants. For a polyetheylene membrane he calculated a value of J of approximately 4500 K. A value of J has been calculated for this work from figure 5.34; here the normalised results have been presented on a semi-log plot versus values of the reciprocal of the absolute temperature. A line has been fitted to all of the data points by using a Least Squares Method. The slope of this line, which is equivalant to -J, has been calculated to be 4318 K, which is in good agreement with the value quoted by Vincent.

6.2.3. Analysis of Experimental Results for $k_L a$.

The experimental results for the two-phase systems have been

analysed in two ways. Firstly, the traces have been plotted in normalised form, the areas below the curves calculated and corrected as specified in the Method of Moments (see section 5). Five typical traces have been included (see figures 5.21 to 5.25) using the raw data shown in figure 5.26. Secondly, semi-log plots of the normalised data against time were prepared (see figures 5.27 to 5.31). Using the Method of Moments it is necessary to have probe calibration data at the correct temperature, and the analysis involves the calculation of the areas below two curves: this latter part of the analysis procedure is time-consuming and subject to errors due to the estimation of the areas for the tail of the curves. Estimates of this area show that 5-10 % of the curve is contained in the tail. Using the second method to assess k_La, plots of ln $(1-\Gamma)$ vs t were quickly drawn without reference to any other measurements. The central portion of this type of curve was found, in all the cases considered, to be a good approximation to a straight line. The two ends of this type of plot were curved and can be attributed to system lags at low values of t and to the slow probe response at large values of t. The initial curved portion arose from the fact that a finite time was required for the air bubbles to rise through the fermenter at start-up: this occurred in plug-flow fashion. As described previously, experiments to assess k_La involved de-oxygenating the system using oxygen free nitrogen followed by re-aeration. At change-over the nitrogen bubbles could be seen moving through system and separated from the following air bubbles by a small volume of bubble-free liquid. At large values of t, where the concentration difference and the driving force between the phases was small, the oxygen electrode's response was very slow and errors could not be avoided.

According to Heineken and Linek's original model (6,7) if the curved portion of these plots are ignored and the probe response time is small enough the slope of the straight portion should be a good approximation to k_La. This can also be seen from the later model of

Linek and Vacek. Here, if the slowly responding zones of the probe are neglected:

$$G = 1 - A_1\left\{\frac{\pi\sqrt{B_1}}{\sin\pi\sqrt{B_1}}\, e^{-B_1 k_1 t} + 2\sum_{n=1}^{\infty}(-1)\,\frac{e^{-n^2 k_1 t}}{\left(\frac{n^2}{B_1} - 1\right)}\right\} \qquad (4)$$

where $B_1 = \frac{k_L a}{k_1}$ and k_1 is the calibration constant for the fast response region of the probe. Taking a typical value of B_1 for the Chark electrode to be 0.1:

$$\frac{\pi\sqrt{B_1}}{\sin\pi\sqrt{B_1}} = 1.19 \qquad (5)$$

and $e^{-k_1 t}$ will be small, even for t = 5 s.
Consequently

$$G = 1 - (A_1 \times 1.19\, e^{-k_L a t})$$

$$\text{or} \quad 1 - G = 1.19\, A_1 e^{-k_L a t} \qquad (6)$$

It should also be noted that when using a semi-log plot the constant $A_1 \times 1.19$ need not be known. A_1 has been estimated to be approximately 0.9 from the results of Linek and Vacek and so $A_1 \times 1.19$ will be close to 1.0.

Estimates of $k_L a$ using the two methods outlined above are summarised in Table 6.2 for 5 experiments. At superficial gas velocities of upto 30 mm s^{-1} the results obtained using both methods are comparable. The result obtained at a gas velocity of 40 mm s^{-1} appears to be spurious This is probably due to errors in the estimation of curve areas. It is assumed that it is the value obtained using the Method of Moments which is wrong due to the similarity between the values at 30 and 40 mm s^{-1} when compared to the smooth progression in $k_L a$ from the semi-log plots. However, at 50 mm s^{-1} there is again a 10% difference between the $k_L a$ values predicted by the two methods. Once more this may be due

Table 6.2 Comparison of $k_L a$ Values Calculated Using the Method of Moments and from a Plot of the Normalised Experimental Data.

U_{SG} (mm s^{-1})	$k_L a$ (s^{-1}) Method of Moments	$k_L a$ (s^{-1}) Normalised Plot
10.0	0.017	0.018
20.0	0.035	0.036
30.0	0.050	0.052
40.0	0.051	0.077
50.0	0.095	0.086

to inaccuracies in the estimation of areas. But at other velocities the k_La value predicted by the Method of Moments is smaller than that by the semi-log plot and in general it is thought that it is easier to over; rather than under- estimate areas. At the higher gas velocities it is probable that the contribution of the slowly changing section of the probe response is significant, which suggests that in this case the Method of Moments should be more accurate. With the two-region, two-layer model for the electrode this is equivalent to saying that k_2 becomes significant at superficial gas velocities greater than 40 mm s^{-1}.

In the fermentation system velocities of 40 mm s^{-1} and above would have caused slugging and washout of the micro-organisms. These velocities could therefore not be used. Because of this and for simplicity, results presented during the remainder of this work were based on the semi-log method of analysis. The reader should therefore be aware that k_La values quoted at superficial velocities greater than 40 mm s^{-1} may be subject to errors of up to 12% in addition to experimental errors.

6.2.4 Mass Transfer in the Two Phase System.

Air-Water System.

A summary of the k_La data estimates made in the air-water system is presented in figure 5.35. The spread in the results at superficial gas velocities of 30 mm s^{-1} and below (the bubbly region of gas flow) is due to the dependence of k_La and probe output on temperature. This is more clearly seen in figure 5.36 where the same data are shown as a function of temperature. Whilst the correlation with temperature is good in this region its effect is small when compared to that of the gas velocity. If the effect of temperature is neglected then for the

bubbly region:

$$k_L a \cong 0.0018 \quad U_{SG} \qquad s^{-1} \qquad (7)$$

At higher values of U_{SG} there is more scatter in the experimental results: this is due to the presence of gas slugs. In this region the experimental variation is far greater than the temperature effect, although there is a tendency for $k_L a$ to increase with temperature. If averages of the measured values are taken, these in-fact lie surprisingly close to values estimated from the correlation for the bubbly region.

Air-MISM Systems.

Similar results to those above have been presented in figure 5.37 for air-MISM systems. The temperature in this series of experiments was maintained at 30°C and three concentrations of the substrate were used. The effect of MISM concentration, in a similar manner to that of temperature, is small when compared to the effect of the superficial gas velocity. If the concentration effect is ignored, then using the mean of the experimental values :

$$k_L a = 0.0020 \; U_{SG} \; s^{-1} \quad (0 < U_{SG} < 30) \qquad (8)$$

and $$k_L a = (0.0285 \; U_{SG} - 0.255) \; s^{-1} \quad (30 < U_{SG}) \qquad (9)$$

Data from the present work are compared with $k_L a$ values summarised in the recent review of bubble column bio-reactors by Schugerl, Lucke and Oels (8) in figure 6.1. Results of Chang (9) and Deckwer et alia (10) are also included. Similar values to those obtained by the author have also been published by Yagi and Yoshida (11).

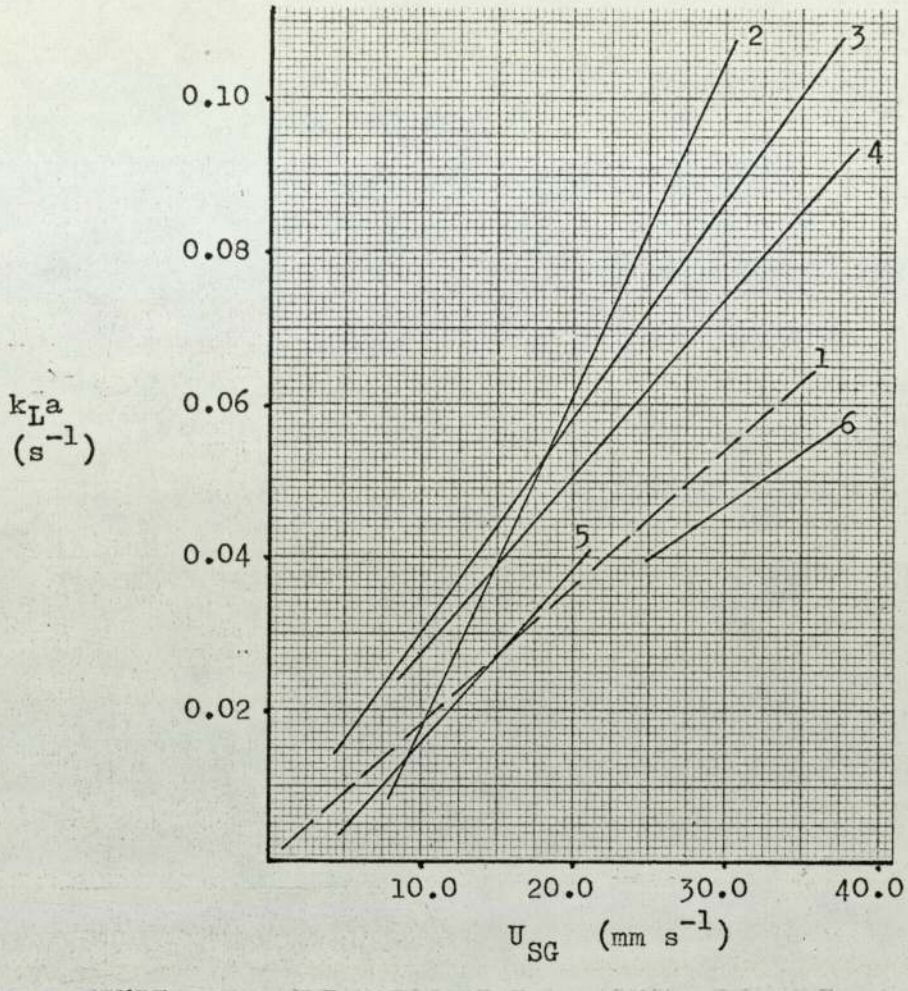

Figure 6.1 Comparison of k_La Values Obtained in This Work With Those of Other Authors

1 This Work - Tap Water and M1SM

2 Schugerl, Lucke and Oels - Tap Water (Sintered Plate Distributer

3 Schugerl, Lucke and Oels - 2% Glucose (Perforated Plate Distrib.)

4 Chang - Tap Water

5 Deckwer, Burckhart and Zoll - 3.37% Molasses

6 Yagi and Yoshida - Tap Water

The Effect of Anti-foams on the Behaviour of Air-MlSM Systems.

The addition of anti-foam, either Silcolapse or P2000, roughly halves the mass transfer coefficients when compared with those for the air-water or air-MlSM systems. However, the k_La values obtained with P2000 do appear to be marginally higher than those obtained with Silcolapse (see figure 5.38 and 5.39). This is perhaps due to the increase in the available surface area for transfer although the transfer of oxygen remains impeded. Effects of a similar order have been recorded by Phillips et alia (12) and Deindoerfer et alia (13) in stirred tank systems and by Yagi and Yoshida (11) with bubble columns.

It is apparent from photographs of systems containing the anti-foams (figures 5.6 and 5.7 are good examples) that P2000 and Silcolapse disperse foams by different mechanisms, as outlined earlier in this section.

6.2.5. The Three Phase System.

Figures 5.40 to 5.42 illustrate data obtained during the course of an Aspergillus niger fermentation which lasted a period of three days. Innoculation of the system with spores occurred at time equal to zero. Gas holdup and the mass transfer coefficient, obtained as outlined previously, quickly rose to a maximum value after two to three hours. After four hours, a change took place in the system: the saturated oxygen concentration began to fall, there was a sharp decrease in pH and the gas holdup and k_La values both dropped. Infact independent studies by other members of the Tower Fermenter Research Group at Aston (14,15) have confirmed that it is at this point that the spores germinate. After this point, apart from changes due to the addition of antifoam and an increase in the air flow-rate, the system behaved as expected. The saturated oxygen concentration and the pH

both fell at a constant rate, the gas holdup reaching a constant value of approximately 0.053 and the k_La value increasing slowly to 0.021 s^{-1} after 15 hours; there-after the k_La value remained constant. Following germination, the dry weight of organism in the system increased at an exponential rate.

Using the above information the respiratory rate of the organism was calculated from a simple mass balance, viz;

$$\frac{dc}{dt} = k_La\ (c^* - c_p^*) - Rx \qquad (10)$$

When the system is at steady-state, i.e. when oxygen absorption rate equals the rate of consumption by the organisms,

$$\frac{dc}{dt} = 0 \qquad (11)$$

and

$$Rx = k_La\ (c^* - c_p^*), \qquad (12)$$

where

$$c^* = c_p^* \Big|_{t=o} \qquad (13)$$

If it is assumed that the saturated oxygen concentration in MISM solutions is approximately the same as that in water, it is then possible to calculate Rx: then, using dry weight data and assuming that the organism present is 100% viable, R can be estimated. This has been done and the results are shown in figure 5.43. Whilst Rx increases during the course of the whole experiment the respiratory rate, R, passes through a peak at the time of germination and then quickly falls to a much lower constant value for the remainder of the fermentation. The respiratory rate of the organism at germination has been calculated to be 8.1×10^{-5} (g O_2)/(g org)s and the final constant value was approximately 1.6×10^{-5} (g O_2) / (g org) (s). Independant measurements by Morris (14), who used a Warburg respirometer,

gave values of 7.9×10^{-5} and 1.3×10^{-5} for the above conditions; these comparisons show that the method of analysis used can provide useful estimates of R.

Figures 5.45 to 5.50 show the microbial and bubble distributions as time progressed through the first eighteen hours of the three day fermentation. During the early stages the bubble distribution is similar to that which has already been seen in the two phase system. After five hours antifoam was introduced into the system and, after this point, gas slugs can be seen. As the series of photographs progresses the bubbles become smaller, 1-2 mm diameter, and gradually the mycellial pellets become so dense that it is difficult to detect the presence of the gas. At this stage the microbial pellets have increased to a diameter of approximately 3-4 mm.

Nomenclature (Section 6)

Symbol	Explanation	Units
A	constant	
A_1, k_1, k_2	parameters required to describe the oxygen electrode response	
c	concentration of oxygen in the liquid phase	g/l
c^*	equilibrium concentration of oxygen in the liquid phase	g/l
c_p^*	equilibrium oxygen concentraion detected by the electrode under pseudo steady state conditions	g/l
G	normalised probe response to a step change in oxygen concentration in the gas phase - Linek and Vacek	-
I_T	oxygen electrode signal current at temperature T	mA
J	constant	
k_La	overall oxygen mass-transfer coefficient	s^{-1}
q	constant in gas holdup correlation	s/mm
R	micro-organism respiration rate	$(g\ O_2)/(g\ org)\ s$
t	time	s
T	absolute temperature	K
U_{SG}	superficial gas velocity	mm/s
x	micro-organism dry weight	g/l

Greek

ε	gas holdup	-
Γ	normalised probe response following a step change in the oxygen concentration in the gas phase - this work	-
Γ'	normalised probe response following a step change in the oxygen concentration in the liquid phase	-

References (Section 6)

(1) SHAYEGAN-SALEK, J., Ph.D. Thesis, University of Aston in Birmingham (1974)

(2) CALDERBANK, P.H., "Mixing", Vol. 2, Eds. UHL,V.W. and GRAY, J.B., Academic Press (1967)

(3) LOCKETT, M.J. and SAFEKOURDI, A.A., A.I.Ch.E.J., 23, 395 (1977)

(4) MONTGOMERY, H.A.C., THOM, N.S. and COCKBURN, A., J. Appl. Chem., 14, 280 (1964)

(5) VINCENT, A., Process Biochem., April, 19 '1974)

(6) HEINEKEN, F.G., Biotechnol. Bioeng., 12, 145 (1970)

(7) LINEK, V., Biotechnol. Bioeng., 14, 285 (1972)

(8) SCHUGERL, K., LUCKE, J. and OELS, U., Adv. Biochem. Eng., 7, 1 (1977)

(9) CHANG, C.L., Doctoral Thesis, Technical University, Berlin (1968)

(10) DECKWER, W.D., BURCKHART, R. and ZOLL, G., Chem. Eng. Sci., 29, 2177 (1974)

(11) YAGI, H. and YOSHIDA, F., J. Ferment. Technol., 52, 905 (1974)

(12) PHILLIPS, K.L., SPENCER, J.F.T., SALLAUS, H.R. and ROXBURGH, J.M., J. Biochem. Microbiol. Technol. and Eng., 2, 81, (1960)

(13) DEINDOERFER, F.H. and GADEN, E.L., Appl. Microbiol., 3, 253 (1955)

(14) MORRIS, G.G., Ph.D. Thesis, University of Aston in Birmingham (1972)

(15) WEBB, C., Private Communication

7. CONCLUSIONS AND RECOMMENDATIONS FOR FUTURE WORK

7. Conclusions and Recommendations for Future Work.

7.1 Conclusions.

7.1.1 Gas Hold-up.

The major factor affecting gas hold-up is the superficial gas velocity. In most cases an estimate of the gas hold-up may be obtained from the correlation:

$$\epsilon = q \cdot U_{SG}$$

were q is a constant depending on the type of system being used and the column diameter. Typical values of this constant are given in table 6.1.

Anti-foams operate in several ways and may cause an increase or a decrease in the gas hold-up depending on the type used. Of those used in this work P2000 reduces the surface tension of the liquid medium and results in an increase in hold-up over that of the simple liquid medium. Conversely, Silcolapse, which reduces the intermolecular cohesive forces, has been found to decrease gas hold-up due to the formation of gas slugs.

Photographs have shown that the bubble size distribution in particular two-phase systems is fairly constant as U_{SG} is increased. However, the introduction of salts and sugars into the system leads to the formation of very small "ionic bubbles". The bubble size and degree of distortion is dependent on the system used.

7.1.2 Oxygen Mass-Transfer.

The behaviour of a fast response oxygen electrode, may be described by a three-parameter model. However, it is more convenient to analyse results using the Method of Moments, which merely involves the graphical (or numerical) integration of two response curves. In some cases, when the probe response is fast enough, a plot of $\ln(1-\Gamma)$ versus t yields a curve which has a straight central region. An estimate of k_La may be obtained from the slope of this central portion, but such estimates have been shown to be subject to errors of upto 12%.

Again, as with gas hold-up, the most important parameter affecting oxygen mass-transfer in a tower system is superficial gas velocity. Estimates for k_La may be made in terms of this parameter. In a 102 mm diameter column for the air-water system

$$k_La = 0.0018\ U_{SG} \qquad s^{-1}$$

for all values of U_{SG}. In air-MISM systems the correlation used depends on the turbulence of the system. In the bubbly region ($0<U_{SG}<30$)

$$k_La = 0.0020\ U_{SG} \qquad s^{-1}$$

for the turbulent region,

$$k_La = (0.0285\ U_{SG} - 0.255) \qquad s^{-1}$$

Antifoams, both P2000 and Silcolapse, have been shown to reduce the values obtained from the above correlations by approximately 50%.

In the three-phase fermentation system, using MISM and A.niger,

once the biomass concentration is established the $k_L a$ value is fairly constant at a value of approximately 0.02 s^{-1} (with U_{SG} = 20 mm s^{-1}).

The results obtained in this work have been shown to be comparable with those of several other workers. A direct comparison is given in figure 6.1.

7.1.3. Growth of Aspergillus niger.

During the course of an A.niger fermentation the gas holdup and mass-transfer coefficient quickly rise to a maximum. After four hours, at germination, a change takes place in the system. This results in a fall in the saturated oxygen concentration, system pH, gas holdup and mass transfer coefficient; the mass transfer coefficient later rises slowly to a constant value of 0.021 s^{-1}.

The respiratory rate of the organism can be calculated from the experimental data. Two values, one at germination and the other which prevailed during the fermentation from 12 hours onwards, have been estimated: the respective values are 8.1×10^{-5} (g O_2)/(g org)(s) and 1.6×10^{-5} (g O_2)/(g org)(s).

7.2. Recommendations for Future Work.

Consideration of the following areas would help in the evaluation and design of tower fermenters as efficient fermentation systems.

7.2.1. Gas Holdup.

1. Development of a light attenuation technique for tower fermentation systems should be pursued: it will be necessary to use

probes within the fermenter to decrease the path length of the light beam through the system.

2. A basic study of the interfacial phenomena affecting bubble size and stability, particularly in the presence of anti-foams, should be carried out.

7.2.2. Oxygen Mass-Transfer.

1. There is a need for a major review of recently published work.

2. Fast response electrodes provide a valuable tool for studying mass transfer, but further work on the evaluation of the properties of electrode membranes and on modelling of the dynamic response characteristics is required.

3. A critical review of methods for measuring $k_L a$ values would be of value.

7.2.3. Fermenter Design and Performance.

1. The gas hold-up and $k_L a$ results obtained in this work should be used to assess the performance of existing tower fermenters (from laboratory to industrial scale) and should be useful in the design of new systems.

2. The measurement techniques for hold-up and $k_L a$ should help in the assessment of fermenter performance.

Nomenclature (Section 7)

Symbol	Explanation	Units
$k_L a$	overall oxygen mass-transfer coefficient	s^{-1}
q	constant	
t	time	s
U_{SG}	superficial gas velocity	$mm\ s^{-1}$

Greek

ε	gas hold-up	-
Γ	normalised probe response following a step change in the oxygen concentration in the gas phase	-

APPENDIX 1

5.0% M1SM Recipe.

	kg
Sucrose	1.0
$(NH_4)_2SO_4$	0.1974
NaH_2PO_4	0.010
Yeast Extract	0.010
KCl	0.005
$MgSO_4$	0.002
$CaCl_2$	0.001

The above ingredients were dissolved in warm water and made upto 20 l. For M1SM solutions of other concentrations this solution was diluted futher with water.

Detailed Solution of Heineken's Model for a Membrane Covered Oxygen Electrode.

Basis: Carslaw and Jaeger, "Conduction of Heat in Solids", 2nd. Edition. 1959 p.102

$$\frac{\partial c}{\partial t} = D \frac{\partial^2 c}{\partial x^2} \qquad (0 < x < d)$$

$c = \phi(t)$ at $x = 0$; $c = f(x)$ at $t = 0$

$c = 0$ at $x = d$

Put $c = u + w$

where $\frac{\partial u}{\partial t} = D \frac{\partial^2 u}{\partial x^2}$

$u = f(x)$ at $t = 0$; $u = 0$ at $x = 0, d$

(Eq. 1) $$u = \frac{2}{d} \sum_{1}^{\infty} e^{-\frac{D\pi^2 n^2 t}{d^2}} \cdot \sin \frac{n\pi x}{d} \int_0^d \sin \frac{n\pi x'}{d} \cdot f(x') \cdot dx'$$

When $f(x) = c_1 \left(1 - \frac{x}{d}\right)$

$$u = \frac{2}{d} \sum_{1}^{\infty} e^{-\frac{D\pi^2 n^2 t}{d^2}} \cdot \sin \frac{n\pi x}{d} \cdot \frac{c_1 d}{n\pi}$$

For w $\frac{\partial w}{\partial t} = D \frac{\partial^2 w}{\partial x^2}$

$w = 0$ at $t = 0$; $w = \phi(t)$ at $x = 0$

$w = 0$ at $x = d$

(Eq. 2) $$w = \frac{2D\pi}{d^2} \sum_{1}^{\infty} n \cdot \sin \frac{n\pi x}{d} \cdot e^{-\frac{D\pi^2 n^2 t}{d^2}} \int_0^t \phi(\lambda) \cdot e^{\frac{Dn^2\pi^2 x}{d^2}} \cdot d\lambda$$

Laplace Transform Method $\frac{\partial c}{\partial t} = D \frac{\partial^2 c}{\partial x^2}$

$c = c_1 \left(1 - \frac{x}{d}\right)$ at $t = 0$; $c = 0$ at $x = 0$

$$c = c^{o}\,(1 - e^{-\beta t}) \qquad \text{at } x = 0$$

(Eq. 3) $$\bar{c} = \left[\left(\frac{c^{o} - c'}{s}\right) - \left(\frac{c^{o}}{s + \beta}\right)\right] \cdot \left(\frac{\sinh \sqrt{\frac{s}{D}}\,(d - x)}{\sinh \sqrt{\frac{s}{D}}\; d}\right) + \frac{c_1}{s}\left(1 - \frac{x}{d}\right)$$

Inversion: $$\frac{\sinh b\sqrt{s}}{s \sinh a\sqrt{s}} = \frac{b}{a} + \frac{2}{\pi} \sum_{1}^{\infty} \frac{(-1)^n}{n} \cdot \sin \frac{n\pi b}{a} \cdot e^{-\frac{n^2\pi^2 t}{a^2}}$$

$$\bar{c} = \frac{c_1}{s}\left(1 - \frac{x}{d}\right) + \left[\frac{c^{o}}{(s + \beta)} - c_1\right] \frac{F(s)}{s}$$

where $$F(s) = \frac{\sinh \sqrt{\frac{s}{D}}\,(d - x)}{\sinh \sqrt{\frac{s}{D}} \cdot d}$$

(Eq. 4) $$c = c_1\left(1 - \frac{x}{d}\right) + c_1\left(1 - \frac{x}{d}\right) - c_1 \frac{2}{\pi} \sum_{1}^{n} \frac{(-1)^n}{n} \sin \frac{n\pi(d - x)}{d} \cdot e^{-\alpha}$$

$$+ c^{o}\left(\frac{d - x}{d}\right)(1 - e^{-\beta t}) + \frac{2}{\pi} \sum_{1}^{n} \frac{(-1)^n}{n} \cdot \sin \frac{n\pi(d - x)}{d} \cdot \frac{\beta c^{o}}{(\beta - \alpha)}$$

$$\cdot (e^{-\alpha t} - e^{-\beta t})$$

where $$\alpha = \frac{n^2\pi^2 D}{d^2}$$

From Eq. 1 and Eq.2 using $f(x) = c_1\left(1 - \frac{x}{d}\right)$

and $\phi(t) = c^{o}(1 - e^{-\beta t})$

$$c = c_1 \frac{2}{\pi} \sum_{1}^{\infty} \frac{1}{n} \cdot e^{-\alpha t} \cdot \sin \frac{n\pi x}{d} + c^{o} \frac{2}{\pi} \sum_{1}^{\infty} \frac{1}{n} \cdot \sin \frac{n\pi x}{d} \cdot (1 - e^{-\beta t})$$

$$- c^{o} \frac{2}{\pi} \sum_{1}^{\infty} \frac{1}{n} \cdot \sin \frac{n\pi x}{d} \cdot \frac{\beta}{(\alpha - \beta)} \cdot (e^{-\beta t} - e^{-\alpha t})$$

Note: $$\sum_{1}^{\infty} \frac{1}{n} \cdot \sin \frac{n\pi x}{d} = \sin z + \frac{1}{2} \sin 2z + \frac{1}{3} \sin 3z + \ldots$$

$$= \frac{1}{2}(\pi - z)$$

where $z = \frac{\pi x}{d}$

(Eq. 5) $$c = c_1 \frac{2}{\pi} \sum_1^\infty \frac{1}{n} \cdot e^{-\alpha t} \cdot \sin \frac{n\pi x}{d} + c^o \frac{2}{\pi} (1 - e^{-\beta t}) \cdot \frac{1}{2} (\pi - \frac{\pi x}{d})$$

$$- c^o \frac{2}{\pi} \sum_1^\infty \frac{1}{n} \cdot \sin \frac{n\pi x}{d} \cdot \frac{\beta}{(\alpha - \beta)} \cdot (e^{-\beta t} - e^{-\alpha t})$$

Now $$\sin(n\pi - n\pi\tfrac{x}{d}) \equiv \sin(n\pi).\cos(n\pi\tfrac{x}{d}) - \cos(n\pi).\sin(n\pi\tfrac{x}{d})$$

or $$\sin n\pi(1 - \tfrac{x}{d}) \equiv - (-1)^n . \sin(n\pi\tfrac{x}{d})$$

Hence Eq. 5 can be written:

$$c = - c_1 \frac{2}{\pi} \sum_1^\infty (-1)^n \cdot e^{-\alpha t} \cdot \sin n\pi(1 - \tfrac{x}{d}) + c^o (1 - \tfrac{x}{d}).(1 - e^{-\beta t})$$

$$+ c^o \frac{2}{\pi} \sum_1^\infty \frac{(-1)^n}{n} \cdot \sin n\pi(1 - \tfrac{x}{d}) \cdot \frac{\beta}{(\beta - \alpha)} \cdot (e^{-\alpha t} - e^{-\beta t})$$

Solution:

(Eq. 6) $$c = - c_1 \frac{2}{\pi} \sum_1^\infty \frac{(-1)^n}{n} \cdot \sin n\pi(1 - \tfrac{x}{d}) \cdot e^{- \frac{n^2\pi^2 Dt}{d^2}}$$

$$+ c^o (1 - \tfrac{x}{d}) \cdot (1 - e^{-\beta t})$$

$$+ c^o \frac{2}{\pi} \sum_1^\infty \frac{(-1)^n}{n} \cdot \sin n\pi(1 - \tfrac{x}{d}) \cdot \frac{\beta}{(\beta - \frac{n^2\pi^2 D}{d^2})} \cdot (e^{- \frac{n^2\pi^2 Dt}{d^2}}$$

$$- e^{-\beta t})$$

Check on limits:

For finite values of t:

$x = 0$: $c = c^o (1 - e^{-\beta t})$

$x = d$: $c = 0$

Boundary conditions

At $t = 0$: $$c = - c_1 \frac{2}{\pi} \sum_1^\infty \frac{(-1)^n}{n} \cdot \sin n\pi(1 - \tfrac{x}{d})$$

Since $\sin y - \frac{\sin 2y}{2} + \frac{\sin 3y}{3} - \dots = \frac{y}{3}$,

$c = c_1 (1 - \frac{x}{d})$ Initial condition

At $t = \infty$: $c = c^o (1 - \frac{x}{d})$ Expected solution

All these conditions are met.

For the case where $f(x) = 0$ (or $c_1 = 0$) and $\phi(t) = c^o$ (or $\beta \to \alpha$)

$$c = c^o (1 - \frac{x}{d}) + c^o \frac{2}{\pi} \sum_1^\infty \frac{(-1)^n}{n} \cdot \sin n\pi(1 - \frac{x}{d}) \cdot e^{-\frac{n^2\pi^2 Dt}{d^2}}$$

Instrument Response.

Assume $I = G(-DAm \left.\frac{\partial c}{\partial x}\right|_{x=d})$

From Eq. 6

(Eq. 8)
$$\frac{\partial c}{\partial x} = - c_1 \frac{2}{\pi} \sum_1^\infty \frac{(-1)^n}{n} \cdot \cos n\pi(1 - \frac{x}{d}) \cdot - \frac{n\pi}{d} \cdot e^{-\alpha t}$$
$$+ c^o (- \frac{1}{d}) \cdot (1 - e^{-\beta t})$$
$$+ c^o \frac{2}{\pi} \sum_1^\infty \frac{(-1)^n}{n} \cdot \cos n\pi(1 - \frac{x}{d}) \cdot (- \frac{n\pi}{d}) \cdot \frac{\beta}{(\beta - \alpha)} \cdot$$
$$\cdot (e^{-\alpha t} - e^{-\beta t})$$

At $x = d$:

(Eq. 9)
$$\left.\frac{\partial c}{\partial x}\right|_{x=d} = c_1 \frac{2}{d} \sum_1^\infty (-1)^n \cdot e^{-\alpha t} - \frac{c^o}{d} \cdot (1 - e^{-\beta t})$$
$$- c^o \frac{2}{d} \sum_1^\infty (-1)^n \cdot \frac{\beta}{(\beta - \alpha)} \cdot (e^{-\alpha t} - e^{-\beta t})$$

Check on limits:

As $t \to 0$:

$$\left.\frac{\partial c}{\partial x}\right|_{x=d} \Rightarrow c_1 \ldots 2 \cdot (-1)^n \cdot e^{-\alpha t}$$

$$- e^{-z} + e^{-4z} - e^{-9z} = -\frac{1}{z} \quad \text{as} \quad e^{-z} \Rightarrow 1$$

$$\therefore \left.\frac{\partial c}{\partial x}\right|_{x=d} = -\frac{c_1}{d}$$

As $t \to \infty$:

$$\left.\frac{\partial c}{\partial x}\right|_{x=d} \Rightarrow -\frac{c^o}{d}$$

For the general case where

$$\frac{\partial c}{\partial x} = c_1 \ldots 2 \cdot \sum_1^{\infty} (-1)^n \cdot \cos n\pi\left(1 - \frac{x}{d}\right) \cdot e^{-\alpha t}$$

$$+ c^o \left(-\frac{1}{d}\right) \cdot (1 - e^{-\beta t}) + c^o \cdot 2 \cdot \sum_1^{\infty} (-1)^n \cdot \cos n\pi\left(1 - \frac{x}{d}\right)$$

$$\cdot \frac{\beta}{(\beta - \alpha)} \cdot (e^{-\alpha t} - e^{-\beta t})$$

As $t \to \infty$: $\frac{\partial c}{\partial x} \Rightarrow -\frac{c^o}{d}$

and as $t \to 0$: $\frac{\partial c}{\partial x} \Rightarrow -\frac{c_1}{d}$

Alternative form for Eq. 9

$$\operatorname{cosec} y = \frac{1}{y} + \sum_1^{\infty} \frac{(-1)^n \cdot 2y}{y^2 - n^2\pi^2} \qquad \text{for} \quad y \neq n\pi$$

$$\left.\frac{\partial c}{\partial x}\right|_{x=d} = c_1 \cdot \frac{2}{d} \cdot \sum_1^{\infty} (-1)^n \cdot e^{-\alpha t} - \frac{c^o}{d} + \frac{c^o}{d} \cdot e^{-\beta t}$$

$$- c^o \cdot \frac{2}{d} \cdot \sum_1^\infty (-1)^n \cdot \frac{\beta}{(\beta - \alpha)} \cdot e^{-\alpha t}$$

$$+ \frac{c^o}{d} \cdot e^{-\beta t} \cdot (w \cdot \operatorname{cosec} w - 1)$$

where $w = \sqrt{\frac{\beta}{D}} \cdot d$

$$I = G\left(-DAm \cdot \left.\frac{\partial c}{\partial x}\right|_{x=d}\right)$$

(Eq. 10)
$$= GAm\, D \cdot \left[- c_1 \cdot \frac{2}{d} \cdot \sum_1^\infty (-1)^n \cdot e^{-\frac{n^2\pi^2 Dt}{d^2}} \right.$$

$$+ c^o \cdot \frac{2}{d} \cdot \sum_1^\infty (-1)^n \cdot \frac{\beta}{(\beta - \frac{n^2\pi^2 D}{d^2})} \cdot e^{-\frac{n^2\pi^2 Dt}{d^2}}$$

$$\left. + \frac{c^o}{d} \cdot \left(1 - \frac{\sqrt{\frac{\beta}{D}} \cdot d}{\sin \sqrt{\frac{\beta}{D}} \cdot d} \cdot e^{-\beta t}\right) \right]$$

If $c_1 = 0$, ie. there is no oxygen in the membrane at $t = 0$

(Eq. 11)
$$I = G.Am. \frac{Dc^o}{d} \cdot \left[2 \cdot \sum_1^\infty (-1)^n \cdot \frac{\beta}{(\beta - \frac{n^2\pi^2 D}{d^2})} \cdot e^{-\frac{n^2\pi^2 Dt}{d^2}} \right.$$

$$\left. + \left(1 - \frac{\sqrt{\frac{\beta}{D}} \cdot d}{\sin \sqrt{\frac{\beta}{D}} \cdot d}\right) \cdot e^{-\beta t} \right]$$

This equation is identical to that used by Heineken and Linek. Eq. 11 can also be written

$$I = G.Am. \frac{D}{d} c^o \cdot \left[1 - e^{-\beta t} + 2 \cdot \sum_1^\infty (-1)^n \cdot \frac{\beta}{(\beta - \frac{n^2\pi^2 D}{d^2})} \cdot \right.$$

$$\left. \cdot \left(e^{-\frac{n^2\pi^2 Dt}{d^2}} - e^{-\beta t}\right) \right]$$

APPENDIX 2

Summary of gas hold-up results with 152 mm column.

U_{SL}	U_{SG}	h_1	h_2	h_3	h_4	ε
0	2.0	26.6	30.1	33.8	37.6	0.080
0	3.0	22.1	27.5	33.2	39.1	0.123
0	4.0	18.0	24.6	32.1	39.9	0.159
0	5.0	13.2	20.9	29.7	38.4	0.183
0	6.0	8.2	17.2	26.0	35.7	0.199
0.5	2.0	36.0	39.4	43.1	46.8	0.078
0.5	3.0	28.1	33.3	38.5	44.4	0.118
0.5	4.0	21.1	27.7	34.9	42.3	0.154
0.5	5.0	15.3	23.2	31.9	40.4	0.182
0.5	6.0	14.5	23.0	32.2	41.1	0.193
1.0	2.0	36.6	40.0	43.7	47.4	0.078
1.0	3.0	29.5	34.4	39.7	45.2	0.114
1.0	4.0	21.6	28.7	35.5	42.3	0.150
1.0	5.0	16.4	23.8	32.0	40.4	0.174
1.0	6.0	14.5	23.2	31.9	40.8	0.191
1.5	2.0	36.9	40.5	43.9	47.3	0.075
1.5	3.0	28.8	33.8	39.2	44.8	0.116
1.5	4.0	21.4	28.2	35.3	42.4	0.152
1.5	5.0	16.3	24.0	32.3	40.8	0.178
1.5	6.0	15.8	24.5	33.1	41.5	0.186
2.0	2.0	37.1	40.6	44.2	47.9	0.078
2.0	3.0	29.3	34.5	39.7	45.3	0.116
2.0	4.0	22.6	29.8	36.1	43.4	0.151
2.0	5.0	17.4	24.8	33.2	41.9	0.178
2.0	6.0	15.7	24.1	33.3	41.9	0.190

U_{SG} = Superficial gas velocity (cm s^{-1})
U_{SL} = Superficial liquid velocity (cm s^{-1})
h_i = i th. manometer level (mm)
ε = Average gas hold-up (-)

Summary of gas hold-up results with 102 mm column.

U_{SG}	T	ε
1.0	25.0	0.031
1.0	27.5	0.033
1.0	30.0	0.033
1.0	32.5	0.036
1.0	35.0	0.034
2.0	25.0	0.068
2.0	27.5	0.067
2.0	30.0	0.069
2.0	32.5	0.069
2.0	35.0	0.068
3.0	25.0	0.100
3.0	27.5	0.101
3.0	30.0	0.101
3.0	32.5	0.100
3.0	35.0	0.100
4.0	25.0	0.137
4.0	27.5	0.134
4.0	30.0	0.137
4.0	32.5	0.135
4.0	35.0	0.128
5.0	25.0	0.168
5.0	27.5	0.162
5.0	30.0	0.157
5.0	32.5	0.155
5.0	35.0	0.150

U_{SG} = Superficial gas velocity (cm s^{-1})
T = Temperature (^{o}C)
ε = Average gas hold-up (-)

Oxygen Mass-Transfer Studies Using Fast Response Oxygen Electrodes

Introduction

The following is a collection of experimental data which was gathered during the course of the series of experiments to determine the rate of oxygen mass-transfer in a tower fermenter.

Appart from the Temperature Calibration Results the information consists of a series of points read from the experimental traces at given time intervals. The "Maximum value" refered to is equivalent to the equilibrium dissolved oxygen concentration detected by the electrode (c_p^*). The "Minimum value" was the minimum detected concentration and was not necessarily equal to zero.

In order to "Normalise" the data the following equation was used:

$$\Gamma' = \left(\frac{x \quad - \text{min. value}}{\text{max. value} - \text{min. value}} \right)$$

where "x" is the value of the experimental point being considered.

The above equation is for the probe calibration experiments. In mass-transfer studies Γ' becomes Γ.

Probe calibration.

Experiment number	1
No. of points	22
Temperature (°C)	21.4
Time interval (s)	0.5
Maximum value	60.3
Minimum value	3.5

	7.4	17.9	27.5	34.0	38.7
41.8	44.5	46.7	48.1	49.5	50.5
51.4	52.3	53.0	53.7	54.2	54.7
55.2	55.8	56.1	56.5	56.6	

Experiment number	2
No. of points	34
Temperature (°C)	21.4
Time interval (s)	0.5
Maximum value	59.0
Minimum value	2.3

	6.4	17.1	26.1	32.9	37.7
40.9	43.5	45.5	47.0	48.2	49.4
50.2	51.0	51.6	52.2	53.0	53.5
53.8	54.0	54.2	54.4	54.6	55.0
55.2	55.5	55.8	56.0	56.2	56.4
56.6	56.7	56.8	56.9	57.0	

Experiment number	3
No. of points	20
Temperature (°C)	23.1
Time interval (s)	0.5
Maximum value	59.0
Minimum value	1.7

	5.2	16.5	26.7	33.5	37.9
41.0	43.8	45.9	47.2	48.6	49.5
50.1	51.7	52.2	52.5	52.9	53.1
53.6	53.9				

Experiment number	4
No. of points	26
Temperature (°C)	23.1
Time interval (s)	0.5
Maximum value	59.0
Minimum value	0.5

	2.6	11.3	22.6	30.7	36.0
39.9	42.6	44.7	46.1	47.3	48.5
49.6	50.5	51.1	51.9	52.3	52.7
52.9	53.2	53.7	54.0	54.2	54.5
54.8	54.9	55.0			

Experiment number	5
No. of points	23
Temperature (°C)	27.0
Time interval (s)	0.5
Maximum value	64.1
Minimum value	0.2

	4.9	18.0	30.2	38.9	43.1
46.2	48.9	50.7	51.9	53.2	54.1
55.7	56.9	57.5	58.0	58.2	58.8
59.2	60.0	60.5	61.0	61.2	61.5

Experiment number	6
No. of points	23
Temperature (°C)	27.0
Time interval (s)	0.5
Maximum value	68.0
Minimum value	4.3

	10.2	23.8	34.0	41.7	47.8
51.8	54.1	56.0	57.8	58.9	59.9
60.8	61.5	62.1	62.9	63.0	63.6
64.0	64.3	64.8	65.0	65.2	65.4

Experiment number	7
No. of points	24
Temperature (°C)	30.2
Time interval (s)	0.5
Maximum value	65.0
Minimum value	0.2

	4.5	21.9	33.7	40.2	45.0
48.2	50.5	52.4	53.9	55.0	56.0
56.9	57.7	57.9	58.1	58.8	59.0
59.2	59.5	59.9	60.1	60.5	60.9
61.0					

Experiment number	8
No. of points	21
Temperature (°C)	30.2
Time interval (s)	0.5
Maximum value	68.0
Minimum value	4.7

	5.5	19.9	34.8	42.7	47.4
50.8	52.9	54.8	56.2	58.0	59.1
60.3	61.2	62.0	62.7	63.1	63.3
63.7	64.2	64.7	65.0		

Experiment number	9
No. of points	22
Temperature (°C)	34.3
Time interval (s)	0.5
Maximum value	68.0
Minimum value	4.0

	18.0	35.2	43.8	48.8	52.1
54.8	56.8	58.1	58.9	58.7	60.6
61.8	62.1	62.7	63.1	63.2	63.3
63.7	64.1	64.5	64.9	65.0	

Experiment number	10
No. of points	26
Temperature (°C)	13.1
Time interval (s)	0.5
Maximum value	48.0
Minimum value	4.0

	6.6	12.7	19.2	24.7	28.9
32.2	34.9	36.9	38.4	39.7	40.8
41.6	42.3	43.0	43.3	43.9	44.1
44.6	44.8	45.0	45.2	45.4	45.6
45.8	45.9	46.0			

Experiment number	11
No. of points	18
Temperature (°C)	34.3
Time interval (s)	0.5
Maximum value	68.0
Minimum value	3.8

	9.7	23.8	36.1	44.7	49.1
52.2	54.2	56.2	58.2	59.2	60.3
61.3	61.5	61.8	62.0	62.2	62.5
63.2					

Experiment number	12
No. of points	31
Temperature (°C)	16.2
Time interval (s)	0.5
Maximum value	55.2
Minimum value	2.3

	4.6	13.0	22.0	29.5	34.8
38.8	41.8	44.0	45.5	46.8	47.8
48.7	49.2	49.8	50.1	50.7	51.0
51.2	51.4	51.6	51.8	51.9	52.0
52.1	52.2	52.3	52.4	52.5	52.6
52.7	52.8				

Experiment number	13
No. of points	24
Temperature (°C)	18.2
Time interval (s)	0.5
Maximum value	55.0
Minimum value	2.6

	3.0	11.1	21.0	28.8	34.5
38.6	41.7	43.8	45.3	46.7	47.7
48.5	49.1	49.7	50.1	50.6	51.0
51.1	51.2	51.3	51.5	51.7	51.9
52.0					

Experiment number	14
No. of points	27
Temperature (°C)	21.3
Time interval (s)	0.5
Maximum value	55.7
Minimum value	1.2

	3.7	13.8	24.0	31.3	36.8
40.3	43.0	45.0	46.7	47.8	48.6
49.2	49.8	50.2	50.8	51.0	51.2
51.7	51.9	52.1	52.3	52.5	52.6
52.7	52.8	52.9	53.0		

Experiment number	15
No. of points	24
Temperature (°C)	25.0
Time interval (s)	0.5
Maximum value	55.0
Minimum value	1.2

	5.3	18.0	27.5	34.1	38.2
41.7	44.9	45.5	46.9	47.9	48.9
49.7	50.1	50.7	51.0	51.3	51.6
52.0	52.1	52.3	52.6	52.9	53.0
53.2					

Experiment number	16
No. of points	27
Temperature (°C)	26.9
Time interval (s)	0.5
Maximum value	51.7
Minimum value	1.3

	9.8	20.8	28.0	33.0	36.8
39.4	41.2	42.8	44.0	45.0	45.9
46.4	46.9	47.2	47.8	48.0	48.4
48.8	48.9	49.0	49.1	49.2	49.5
49.6	49.8	49.9	50.0		

Experiment number	17
No. of points	27
Temperature (°C)	29.3
Time interval (s)	0.5
Maximum value	50.0
Minimum value	1.0

	4.0	17.7	25.5	33.0	36.5
38.9	40.6	42.1	43.2	44.1	44.8
45.3	45.9	46.1	46.4	46.6	46.8
47.1	47.4	47.5	47.7	47.8	48.0
48.1	48.2	48.3	48.5		

Experiment number	18
No. of points	30
Temperature (°C)	30.2
Time interval (s)	0.5
Maximum value	49.0
Minimum value	1.0

	8.0	20.8	28.0	32.3	35.5
37.5	39.2	40.6	41.7	42.3	43.2
44.0	44.4	45.0	45.1	45.3	45.9
46.1	46.2	46.3	46.5	46.7	46.9
47.0	47.1	47.2	47.3	47.5	47.7
47.8					

Experiment number	19
No. of points	20
Temperature (^{o}C)	33.8
Time interval (s)	0.5
Maximum value	56.7
Minimum value	1.0

	5.0	22.0	32.3	37.7	41.0
43.5	49.4	46.3	47.9	48.9	49.8
50.3	51.0	51.3	52.0	52.3	52.5
52.7	52.8	53.0			

Temperature calibration of Chark electrode.

T	Amplification 1		Amplification 2	
	c_p	$\frac{c_p}{c_{p32}}$	c_p	$\frac{c_p}{c_{p32}}$
16.0	12.0	0.513	49.8	0.491
17.0	12.4	0.530	51.8	0.510
18.0	13.0	0.556	54.5	0.537
19.0	13.5	0.577	57.1	0.563
20.0	14.0	0.598	60.4	0.595
21.0	14.7	0.628	62.5	0.616
22.0	15.3	0.654	65.7	0.647
23.0	16.0	0.684	69.9	0.689
24.0	16.7	0.714	72.2	0.711
25.0	17.3	0.739	75.4	0.743
26.0	18.0	0.796	79.1	0.779
27.0	19.0	0.812	82.6	0.814
28.0	20.3	0.868	86.8	0.855
29.0	21.0	0.897	91.8	0.904
30.0	21.8	0.932	95.0	0.936
31.0	22.5	0.962	99.6	0.981
32.0	23.4	1.000	101.5	1.000
33.0	24.1	1.030	-	-
34.0	25.4	1.085	-	-
35.0	26.6	1.137	-	-
36.0	27.2	1.162	-	-

T = Temperature (^{o}C)

c_p = Dissolved oxygen meter reading (machine units)

Air-water system.

Experiment number		1			
No. of points		48			
Temperature (°C)		25.0	U_{SG} (mm s^{-1})		10
Time interval (s)		5.0			
Maximum value		92.7			
Minimum value		9.7			
	11.8	16.4	22.4	27.2	32.5
37.3	41.4	45.1	48.9	52.8	55.5
58.9	60.9	63.4	65.7	67.3	69.6
71.4	73.2	74.2	75.1	76.3	77.8
78.7	79.8	80.7	81.3	82.5	83.0
83.8	84.3	85.1	85.6	86.5	86.6
86.8	87.3	87.9	88.1	88.5	88.6
89.0	89.1	89.4	89.5	89.8	89.9
90.1					

Experiment number		2			
No. of points		39			
Temperature (°C)		25.0	U_{SG} (mm s^{-1})		10
Time interval (s)		5.0			
Maximum value		93.3			
Minimum value		11.3			
	12.2	16.2	19.8	25.2	30.1
35.0	39.3	43.4	47.3	51.1	57.3
60.2	62.8	65.1	67.2	69.1	70.9
72.9	74.1	75.5	76.9	77.9	79.3
80.3	80.8	81.7	82.4	83.1	84.0
84.6	85.2	85.9	86.1	86.7	87.2
87.8	87.9	88.0	88.4		

Experiment number		3			
No.of points		36			
Temperature (^{o}C)		35.0	U_{SG} (mm s^{-1})		10
Time interval		5.0			
Maximum value		96.5			
Minimum value		9.0			
	11.8	17.3	23.5	30.0	37.2
42.5	47.4	51.6	56.5	59.0	62.8
66.2	69.2	71.9	73.2	75.1	77.5
79.2	80.8	81.9	83.2	84.3	85.2
86.3	87.0	87.6	88.1	88.8	89.2
89.7	90.4	90.9	91.2	91.4	92.1
92.7					

Experiment number		4			
No. of points		35			
Temperature (^{o}C)		35.0	U_{SG} (mm s^{-1})		10
Time interval (s)		5.0			
Maximum value		97.2			
Minimum value		11.0			
	13.5	19.4	25.6	32.4	38.2
42.9	48.3	53.5	58.1	62.9	66.3
69.3	72.4	74.2	76.2	78.2	79.7
81.2	82.7	84.1	85.1	86.5	87.0
88.3	89.0	89.1	89.9	90.2	90.7
91.3	91.9	92.2	92.7	93.1	93.6

Experiment number		5			
No. of points		68			
Temperature (°C)		25.0	U_{SG} (mm s^{-1})		30
Time interval (s)		1.0			
Maximum value		97.6			
Minimum value		10.5			

	11.0	12.0	13.3	15.1	17.6
20.1	22.7	25.8	28.9	31.5	34.2
36.4	39.1	41.2	43.6	45.9	48.4
50.5	52.5	54.7	56.5	58.2	59.8
61.3	62.9	64.7	66.1	67.7	69.2
70.3	71.3	72.7	73.8	74.6	75.6
76.7	77.8	78.5	79.7	80.4	81.4
82.3	83.1	83.7	84.2	84.5	85.0
85.6	86.1	86.4	86.9	87.6	87.8
88.0	88.6	89.0	89.4	89.5	89.7
90.1	90.2	90.3	90.5	90.8	91.0
91.2	91.6	92.1			

Experiment number		6			
No. of points		67			
Temperature (°C)		25.0	U_{SG} (mm s^{-1})		30
Time interval (s)		1.0			
Maximum value		96.9			
Minimum value		12.7			

	13.3	15.1	17.0	19.3	22.0
24.9	27.5	30.2	32.8	35.1	37.7
40.2	42.6	44.9	47.1	49.7	52.0
53.8	55.5	57.4	59.3	61.0	62.4
64.2	65.4	67.1	68.7	70.0	71.2
72.3	73.2	74.4	75.6	76.8	77.6
78.3	79.3	80.1	80.9	81.5	82.2
82.8	83.3	83.8	84.2	84.8	85.3
86.0	86.3	86.8	87.2	87.5	87.8
88.1	88.5	88.8	89.2	89.4	89.6
89.8	89.9	90.1	90.4	90.6	90.9
91.0	91.5				

Experiment number		7			
No. of points		76			
Temperature (^{o}C)		35.0	U_{SG} (mm s^{-1})		30
Time interval (s)		1.0			
Maximum value		99.8			
Minimum value		10.7			

	11.4	13.4	16.1	19.2	23.2
26.6	29.9	33.5	36.5	39.3	43.1
45.9	48.3	50.8	53.4	56.2	59.2
61.2	63.3	65.7	67.6	69.3	70.8
72.4	73.8	75.2	76.6	77.3	78.5
80.0	80.9	81.6	82.2	83.2	84.1
84.8	85.5	86.1	86.9	87.3	88.0
88.5	89.1	89.5	89.8	90.1	90.5
90.9	91.3	91.7	91.9	92.1	92.2
92.3	92.6	92.8	93.0	93.2	93.5
93.7	94.1	94.3	94.5	94.7	95.0
95.2	95.3	95.5	95.6	95.7	95.8
95.9	96.0	96.1	96.2	96.3	

Experiment number		8			
No. of points		75			
Temperature (°C)		35.0	U_{SG} (mm s^{-1})		30
Time interval (s)		1.0			
Maximum value		98.6			
Minimum value		11.4			

	11.7	13.5	15.7	18.6	21.4
24.9	28.7	31.8	35.2	38.5	41.5
44.2	46.8	50.1	52.3	55.1	57.6
59.9	62.2	64.5	66.4	68.1	69.7
71.3	72.6	73.7	75.0	76.3	77.6
79.0	80.2	81.0	81.9	82.7	83.3
84.2	85.1	85.8	86.1	86.6	87.2
87.7	88.0	88.4	89.1	89.5	89.9
90.3	90.5	90.8	91.1	91.4	91.7
91.9	92.1	92.5	92.7	92.9	93.0
93.2	93.5	93.6	93.8	94.0	94.1
94.2	94.3	94.5	94.8	94.9	95.0
95.1	95.2	95.3	95.5		

Experiment number		9			
No. of points		49			
Temperature (°C)		25.0	U_{SG} (mm s^{-1})		50
Time interval (s)		1.0			
Maximum value		96.8			
Minimum value		13.0			

	13.8	16.2	19.8	23.7	27.0
30.5	34.5	38.4	43.0	47.0	50.4
53.5	56.8	59.7	62.5	65.1	67.3
69.8	71.8	73.7	75.6	77.1	78.6
80.0	81.2	82.2	83.4	84.5	85.3
86.2	86.7	87.5	88.1	88.8	89.4
90.0	90.2	90.6	90.9	91.2	91.9
92.2	92.4	92.7	93.1	93.2	93.7
94.1	94.2				

Experiment number		10			
No. of points		52			
Temperature (°C)		25.0	U_{SG} (mm s^{-1})		50
Time interval (s)		1.0			
Maximum value		91.8			
Minimum value		15.0			

	15.6	17.9	20.4	24.0	28.0
31.1	35.0	38.8	42.5	45.7	49.0
51.9	54.9	57.6	60.2	62.4	64.6
66.4	68.4	70.5	72.1	73.6	75.0
76.2	77.2	78.2	79.1	80.0	80.9
81.7	82.2	82.9	83.3	84.0	84.4
85.0	85.2	85.6	85.9	86.2	86.7
87.0	87.2	87.5	87.8	88.1	88.2
88.4	88.5	88.6	88.9	89.1	

Experiment number		11			
No. of points		54			
Temperature (°C)		35.0	U_{SG} (mm s^{-1})		50
Time interval (s)		1.0			
Maximum value		95.9			
Minimum value		14.0			
	15.6	18.3	22.1	27.0	32.0
36.8	40.6	44.8	48.7	52.7	56.8
60.0	62.8	65.6	68.2	70.6	72.7
74.7	76.4	77.9	79.3	80.7	82.2
83.3	84.2	85.2	85.9	87.0	87.7
88.2	88.8	89.4	90.0	90.2	90.3
90.7	90.9	91.2	91.8	92.0	92.2
92.5	92.6	92.8	93.0	93.1	93.2
93.3	93.4	93.6	93.8	93.9	94.0
94.1					

Experiment number		12			
No. of points		49			
Temperature (°C)		35.0	U_{SG} (mm s^{-1})		50
Time interval (s)		1.0			
Maximum value		95.7			
Minimum value		14.8			
	15.8	18.1	22.4	27.1	32.3
36.2	39.4	45.0	49.2	52.5	56.5
60.0	63.1	66.0	68.4	70.4	72.5
74.5	76.3	77.9	79.3	80.6	81.9
82.6	83.8	84.8	85.6	86.4	87.2
87.8	88.3	88.9	89.2	89.5	89.9
90.2	90.3	90.7	91.1	91.5	91.9
92.0	92.1	92.3	92.6	93.2	93.6
93.7	93.9				

Experiment number		13			
No. of points		48			
Temperature (°C)		30.0	U_{SG} (mm s^{-1})		10
Time interval (s)		5.0			
Maximum value		95.3			
Minimum value		10.0			
	11.1	15.9	21.8	28.6	32.8
38.0	42.9	47.3	51.7	55.4	59.0
62.5	65.1	67.2	70.2	72.2	74.2
75.9	77.6	79.3	80.5	81.2	82.2
83.4	84.8	85.0	86.1	86.5	87.3
88.0	88.8	89.4	89.6	90.1	90.5
91.0	91.2	91.6	91.8	92.0	92.1
92.2	92.5	92.7	93.0	93.1	93.3
93.7					

Experiment number		14			
No. of points		46			
Temperature (°C)		30.0	U_{SG} (mm s^{-1})		10
Time interval (s)		5.0			
Maximum value		92.6			
Minimum value		11.0			
	11.8	14.9	20.8	25.9	31.3
36.4	41.2	49.5	50.0	53.2	57.0
59.7	62.3	64.9	67.2	69.3	71.3
72.9	74.7	75.6	76.6	77.7	79.0
80.1	80.8	80.9	82.5	83.2	83.6
84.0	84.5	85.3	85.6	86.2	86.3
86.8	87.2	87.5	87.9	88.5	88.7
88.9	89.2	89.5	89.7	89.8	

Experiment number		15			
No. of points		73			
Temperature (°C)		30.0	U_{SG} (mm s^{-1})		30
Time interval (s)		1.0			
Maximum value		94.2			
Minimum value		10.2			

	11.0	12.7	15.0	17.3	20.1
23.3	25.8	28.8	31.5	34.2	37.2
40.1	43.0	45.3	47.8	50.2	52.3
54.2	56.4	58.3	60.0	61.7	63.7
65.3	66.9	68.2	69.7	70.8	72.2
73.1	74.0	76.1	77.1	77.8	78.5
79.4	80.1	80.9	81.8	82.1	82.6
83.1	83.4	84.0	84.6	85.0	85.8
85.9	86.1	86.3	86.7	86.9	87.2
87.5	87.8	88.2	88.4	88.6	88.8
89.0	89.2	89.4	89.6	89.7	89.8
89.9	90.0	90.1	90.4	90.5	90.8
91.1	91.2				

Experiment number		16			
No. of points		75			
Temperature (°C)		30.0	U_{SG} (mm s^{-1})		30
Time interval (s)		1.0			
Maximum value		94.8			
Minimum value		11.0			

	12.6	13.9	17.2	19.8	23.0
25.9	29.1	32.2	34.4	37.3	40.2
43.1	45.6	48.3	51.2	53.3	55.0
57.2	59.2	61.1	62.7	64.2	65.8
67.2	68.6	70.1	71.4	72.8	73.8
74.8	75.9	76.7	77.6	78.2	79.1
79.8	80.5	81.2	81.9	82.6	83.2
83.8	84.5	84.9	85.2	85.8	86.2
86.4	86.9	87.2	87.3	87.6	87.8
88.2	88.7	88.9	89.1	89.2	89.3
89.4	89.5	89.8	90.1	90.4	90.6
90.9	91.1	91.2	91.4	91.6	91.9
92.1	92.2	92.3	92.4		

Experiment number		17			
No. of points		50			
Temperature (°C)		30.0	U_{SG} (mm s^{-1})		50
Time interval (s)		1.0			
Maximum value		99.0			
Minimum value		14.0			
	14.3	17.4	20.8	25.7	30.5
34.5	38.8	42.9	46.9	50.4	54.3
58.0	61.1	63.5	66.4	69.1	71.7
73.8	76.0	77.8	79.2	81.0	82.1
83.5	84.7	85.7	86.4	87.3	88.2
89.0	89.8	90.5	91.1	91.7	92.1
92.3	92.8	93.2	93.5	93.7	94.1
94.2	94.8	94.9	95.0	95.1	95.2
95.5	95.6	95.8			

Experiment number		18			
No. of points		52			
Temperature (°C)		30.0	U_{SG} (mm s^{-1})		50
Time interval (s)		1.0			
Maximum value		98.9			
Minimum value		14.2			
	15.0	18.1	23.2	27.4	32.1
36.0	40.3	45.0	49.0	52.2	55.4
58.7	61.5	64.8	67.6	70.0	72.2
74.2	76.1	77.7	79.2	80.5	82.3
83.3	84.3	85.6	86.3	87.6	88.2
88.9	89.7	90.2	90.6	91.5	91.9
92.0	92.2	92.9	93.5	93.8	94.0
94.2	94.3	94.6	94.8	95.0	95.1
95.3	95.6	95.9	96.0	96.1	

Experiment number		19			
No. of points		43			
Temperature (°C)		25.0	U_{SG} (mm s^{-1})		20
Time interval (s)		3.0			
Maximum value		95.3			
Minimum value		10.5			
	21.4	26.1	30,8	36.2	41.2
46.4	51.2	55.8	59.8	63.8	67.0
70.0	72.7	74.8	77.1	79.2	81.1
82.7	84.2	85.7	86.7	87.7	88.3
89.2	89.8	90.2	91.2	91.7	92.2
92.7	93.0	93.2	93.3	93.8	94.0
94.2	94.3	94.6	94.7	94.8	95.0
95.1	95.2				

Experiment number		20			
No. of points		20			
Temperature (°C)		25.0	U_{SG} (mm s^{-1})		40
Time interval (s)		3.0			
Maximum value		93.0			
Minimum value		21.3			
	25.1	35.2	44.8	54.3	62.8
63.7	68.8	73.6	76.8	80.0	82.5
84.7	86.2	87.4	88.2	88.9	89.9
90.3	91.1	91.3			

Experiment number		21			
No. of points		27			
Temperature (°C)		27.5	U_{SG} (mm s^{-1})		10
Time interval (s)		10.0			
Maximum value		91.2			
Minimum value		20.9			
	26.7	37.3	45.7	52.8	60.3
65.2	70.0	72.7	75.6	77.8	80.0
81.9	83.4	84.4	85.9	86.8	87.4
88.1	88.2	88.3	88.4	88.8	89.3
89.9	90.2	90.5	90.8		

Experiment number		22			
No. of points		24			
Temperature (°C)		27.5	U_{SG} (mm s^{-1})		20
Time interval (s)		5.0			
Maximum value		91.5			
Minimum value		19.5			
	23.9	32.8	41.3	50.8	57.3
63.2	67.8	72.3	75.2	77.8	80.1
81.8	83.3	84.3	85.4	86.2	86.7
87.8	88.5	88.8	89.6	89.7	89.8
89.9					

Experiment number		23			
No. of points		35			
Temperature (°C)		27.5	U_{SG} (mm s^{-1})		30
Time interval (s)		3.0			
Maximum value		95.0			
Minimum value		20.8			
	23.0	29.0	37.2	45.2	53.1
59.0	65.2	69.8	73.7	77.5	80.1
82.3	84.1	85.9	87.2	88.3	89.2
89.7	90.2	90.5	90.9	91.3	91.7
92.0	92.4	92.7	92.8	92.9	93.0
93.2	93.5	93.7	93.8	94.0	94.2

Experiment number		24			
No.of points		28			
Temperature (°C)		27.5	U_{SG} (mm s^{-1})		40
Time interval (s)		3.0			
Maximum value		94.0			
Minimum value		21.1			
	26.9	37.3	48.4	58.2	66.7
72.8	77.9	81.4	84.0	86.3	88.0
89.3	90.2	90.9	91.6	91.9	92.2
92.4	92.8	92.9	93.0	93.1	93.2
93.4	93.5	93.6	93.7	93.8	

Experiment number		25			
No. of points		26			
Temperature (°C)		27.5	U_{SG} (mm s^{-1})		50
Time interval (s)		2.0			
Maximum value		92.4			
Minimum value		19.8			
	24.7	33.3	42.5	50.0	57.2
63.5	68.9	73.2	77.0	80.0	82.5
84.2	85.2	86.8	87.7	88.7	89.2
89.8	90.2	90.6	91.2	91.6	91.9
92.0	92.1				

Experiment number		26			
No. of points		26			
Temperature (°C)		30.0	U_{SG} (mm s^{-1})		20
Time interval (s)		5.0			
Maximum value		94.9			
Minimum value		20.9			
	23.1	32.8	42.0	50.8	59.2
65.5	71.1	75.2	78.5	81.2	83.2
85.0	86.7	87.8	88.7	89.6	90.2
90.7	91.4	92.0	92.6	92.8	92.9
93.0	93.5	93.9			

Experiment number		27			
No. of points		30			
Temperature (°C)		30.0	U_{SG} (mm s^{-1})		40
Time interval (s)		3.0			
Maximum value		93.2			
Minimum value		20.0			
	22.9	33.3	43.0	52.9	61.2
68.1	73.6	77.3	80.7	83.7	85.3
87.0	88.2	89.4	89.9	90.6	90.8
90.9	91.3	91.6	91.9	92.1	92.2
92.3	92.4	92.5	92.6	92.7	92.8
92.9					

Experiment number		28			
No. of points		29			
Temperature (°C)		32.5	U_{SG} (mm s^{-1})		10
Time interval (s)		10.0			
Maximum value		90.3			
Minimum value		21.3			
	21.9	31.8	41.6	50.0	56.8
62.3	67.5	71.0	74.4	77.1	79.2
80.4	82.6	83.7	84.6	85.6	86.2
86.8	87.2	87.7	88.2	88.3	88.7
89.2	89.3	89.4	89.7	89.8	90.2

Experiment number		29			
No. of points		30			
Temperature (°C)		32.5	U_{SG} (mm s^{-1})		20
Time interval (s)		5.0			
Maximum value		92.8			
Minimum value		20.1			
	21.8	31.2	40.6	49.3	57.2
63.2	67.8	73.0	76.0	79.3	80.9
83.0	84.6	86.0	87.3	87.6	88.6
88.8	89.3	89.9	90.2	90.8	90.9
91.2	91.3	91.4	91.5	91.8	91.9
92.0					

Experiment number		30			
No. of points		41			
Temperature (°C)		32.5	U_{SG} (mm s^{-1})		30
Time interval (s)		2.0			
Maximum value		96.5			
Minimum value		23.1			
	24.5	30.6	36.2	42.5	46.7
52.7	57.2	62.3	66.7	70.1	73.0
75.7	78.0	80.0	82.1	83.8	85.1
86.6	87.9	89.0	89.8	90.6	91.3
91.7	92.2	92.8	93.1	93.3	93.9
94.2	94.8	95.1	95.3	95.4	95.6
95.7	95.8	95.9	96.0	96.1	96.2

Experiment number		31			
No. of points		30			
Temperature (°C)		32.5	U_{SG} (mm s^{-1})		40
Time interval (s)		2.0			
Maximum value		92.9			
Minimum value		20.0			
	24.1	31.5	39.3	47.6	54.8
60.8	66.1	70.5	74.0	77.7	80.0
82.3	84.0	85.6	86.7	87.9	88.9
89.7	90.2	90.5	90.6	91.1	91.3
91.7	91.8	92.1	92.3	92.4	92.7
92.8					

Experiment number		32			
No. of points		30			
Temperature (°C)		32.5	U_{SG} (mm s^{-1})		50
Time interval (s)		2.0			
Maximum value		93.2			
Minimum value		20.0			
	23.9	32.8	40.8	49.3	56.8
63.4	68.9	73.3	76.9	79.9	82.2
84.0	85.9	87.1	87.9	89.0	89.5
89.9	90.1	90.3	91.2	91.4	91.5
91.9	92.1	92.2	92.3	92.8	92.9
93.0					

Experiment number		33			
No. of points		43			
Temperature (°C)		35.0	U_{SG} (mm s^{-1})		20
Time interval (s)		3.0			
Maximum value		92.3			
Minimum value		20.6			
	23.3	29.3	35.7	41.8	47.5
52.3	57.1	61.0	64.7	68.1	70.8
73.0	75.2	77.1	78.5	79.9	81.4
82.7	83.8	84.3	85.0	85.9	86.2
86.8	87.5	87.8	88.2	88.6	89.2
89.5	89.6	89.8	90.0	90.1	90.2
90.4	90.5	90.6	90.8	91.0	91.2
91.3	91.8				

Experiment number		34			
No. of points		36			
Temperature (°C)		35.0	U_{SG} (mm s^{-1})		40
Time interval (s)		2.0			
Maximum value		92.0			
Minimum value		20.3			
	23.1	30.7	38.1	46.2	52.8
59.5	64.0	68.0	72.0	74.9	77.2
79.3	81.2	82.8	84.1	85.1	86.1
87.3	88.0	88.4	88.9	89.4	90.0
90.3	90.5	90.8	90.9	91.0	91.1
91.2	91.3	91.4	91.5	91.6	91.7
91.8					

Air-0.5% MISM.

Experiment number		1			
No. of points		32			
Temperature (°C)		30.0	U_{SG} (mm s^{-1})		10
Time interval (s)		5.0			
Maximum value		98.3			
Minimum value		31.7			
	32.2	36.4	43.7	50.2	57.0
62.1	66.4	71.1	74.8	78.0	80.3
82.2	84.3	86.0	86.9	88.5	89.3
89.9	90.5	91.0	91.3	92.1	92.7
93.2	93.4	93.9	94.2	94.7	94.8
94.9	95.1	95.3			

Experiment number		2			
No. of points		40			
Temperature (°C)		30.0	U_{SG} (mm s^{-1})		20
Time interval (s)		2.0			
Maximum value		99.0			
Minimum value		32.3			
	33.7	37.0	42.3	47.1	52.3
57.5	61.7	65.6	69.8	72.9	75.5
78.2	80.5	82.4	84.3	86.0	87.4
88.3	89.3	90.2	90.9	91.7	92.2
92.9	93.3	93.8	94.2	94.5	94.9
95.2	95.6	95.8	96.1	96.2	93.6
96.4	96.5	96.8	96.9	97.0	

Experiment number		3			
No. of points		32			
Temperature (°C)		30.0	U_{SG} (mm s^{-1})		30
Time interval (s)		2.0			
Maximum value		99.3			
Minimum value		29.9			
	32.7	39.2	46.5	54.2	60.5
65.9	71.0	75.0	78.8	81.8	84.2
86.3	88.2	89.9	91.0	92.0	92.7
93.3	94.2	94.9	95.3	95.8	96.2
96.5	96.8	97.1	97.2	97.3	97.4
97.5	97.6	97.7			

Experiment number		4			
No. of points		40			
Temperature (°C)		30.0	U_{SG} (mm s^{-1})		40
Time interval (s)		1.0			
Maximum value		96.2			
Minimum value		28.7			
	29.8	32.5	37.0	42.0	46.4
50.8	54.8	59.0	63.9	67.3	70.2
73.0	76.0	78.5	80.2	81.6	83.0
84.1	85.1	85.9	86.8	87.5	88.2
88.7	89.2	89.8	90.2	90.9	91.3
91.7	91.9	92.2	92.4	92.6	92.9
93.0	93.1	93.2	93.3	93.5	

Experiment number		5			
No. of points		36			
Temperature (°C)		30.0	U_{SG} (mm s^{-1})		50
Time interval (s)		1.0			
Maximum value		94.2			
Minimum value		29.0			

	31.0	37.0	40.0	43.5	50.4
57.5	62.3	67.1	70.8	74.0	77.1
79.7	81.2	82.8	84.2	85.5	86.6
87.5	88.3	88.9	89.5	90.1	90.3
90.7	91.0	91.2	91.3	91.4	91.5
91.7	91.8	91.9	92.0	92.1	92.2
92.3					

Air-2.75% M1SM.

Experiment number		1			
No. of points		48			
Temperature (°C)		30.0	U_{SG} (mm s^{-1})		10
Time interval (s)		5.0			
Maximum value		92.0			
Minimum value		16.5			
	17.8	22.0	27.1	31.5	36.2
40.4	44.0	47.9	51.1	54.2	56.9
59.6	62.3	64.4	66.2	67.8	69.4
71.0	72.3	73.6	74.7	75.8	76.8
77.7	78.6	79.6	80.3	81.2	81.9
82.4	83.0	83.3	83.8	84.3	84.9
85.2	85.4	85.7	85.9	86.1	86.6
87.0	87.2	87.5	87.8	88.0	88.2
88.4					

Experiment number		2			
No. of points		36			
Temperature (°C)		30.0	U_{SG} (mm s^{-1})		20
Time interval (s)		4.0			
Maximum value		92.3			
Minimum value		16.9			
	21.1	29.2	36.8	43.1	49.2
54.8	59.2	62.9	66.8	69.3	71.7
74.0	75.8	77.2	79.4	80.7	81.8
82.3	82.8	83.2	83.9	84.9	85.3
85.9	86.7	86.9	87.1	87.2	87.7
88.0	88.2	88.3	88.5	88.8	89.0
89.2					

Experiment number		3			
No. of points		36			
Temperature (°C)		30.0	U_{SG} (mm s^{-1})		30
Time interval (s)		2.0			
Maximum value		92.7			
Minimum value		16.8			
	19.3	23.2	28.0	33.1	39.3
45.0	48.8	52.2	55.5	58.5	61.6
64.3	67.0	69.5	71.4	73.0	75.0
76.5	78.0	79.2	80.2	81.4	82.7
83.6	84.3	85.2	85.8	86.5	87.0
87.3	87.4	87.6	87.7	87.8	87.9
88.0					

Experiment number		4			
No. of points		33			
Temperature (°C)		30.0	U_{SG} (mm s^{-1})		40
Time interval (s)		2.0			
Maximum value		94.8			
Minimum value		15.4			
	17.9	27.5	34.2	41.8	48.4
54.9	61.2	65.5	69.8	73.3	76.7
79.3	81.7	83.5	85.1	86.7	87.8
88.5	89.2	89.8	90.4	90.9	91.1
91.3	91.4	91.8	92.0	92.2	92.3
92.4	92.6	92.8	92.9		

Experiment number		5			
No. of points		24			
Temperature (^{o}C)		30.0	U_{SG} (mm s^{-1})		50
Time interval (s)		2.0			
Maximum value		90.0			
Minimum value		14.8			
	21.0	32.2	39.0	50.0	58.8
64.5	69.4	73.2	76.2	79.0	81.3
82.6	84.0	85.3	86.2	86.5	87.1
87.2	87.3	87.4	87.8	88.2	88.4
88.6					

Air-5.0% MISM.

Experiment number		1			
No. of points		34			
Temperature (°C)		30.0	U_{SG} (mm s^{-1})		10
Time interval (s)		5.0			
Maximum value		89.4			
Minimum value		28.2			
	20.5	25.2	29.5	33.8	38.0
41.5	44.8	48.3	51.2	53.5	57.1
59.5	62.1	64.0	66.2	67.7	69.1
70.5	72.2	72.7	73.8	75.2	76.2
76.8	78.1	79.3	79.6	80.4	81.5
82.7	82.8	84.0	84.2	85.0	

Experiment number		2			
No. of points		28			
Temperature (°C)		30.0	U_{SG} (mm s^{-1})		20
Time interval (s)		4.0			
Maximum value		83.3			
Minimum value		15.2			
	23.4	30.1	36.2	42.3	47.5
52.2	56.2	59.5	63.2	65.3	67.9
70.0	71.8	73.2	74.6	75.8	76.8
77.7	78.4	79.2	79.8	80.3	80.8
81.2	81.7	82.1	82.3	82.6	

Experiment number		3			
No. of points		40			
Temperature (^{o}C)		30.0	U_{SG} (mm s^{-1})		30
Time interval (s)		2.0			
Maximum value		92.6			
Minimum value		25.9			
	18.8	23.0	29.0	35.0	40.2
46.0	51.2	55.8	59.1	62.8	66.3
69.2	71.4	74.0	76.2	77.9	79.3
80.7	82.0	83,2	84.2	85.1	85.9
86.6	87.3	87.9	88.3	88.6	89.0
89.3	89.8	90.2	90.4	90.8	91.1
91.3	91.5	91.7	91.8	91.9	

Experiment number		4			
No. of points		28			
Temperature (^{o}C)		30.0	U_{SG} (mm s^{-1})		40
Time interval (s)		2.0			
Maximum value		93.2			
Minimum value		17.1			
	21.2	26.5	33.8	40.7	48.2
55.1	61.6	66.0	70.0	73.3	76.5
79.3	81.6	83.5	85.2	86.5	87.6
88.5	89.2	89.8	90.2	90.5	90.9
91.2	91.3	91.6	91.9	92.0	

Experiment number		5			
No. of points		40			
Temperature (°C)		93.8	U_{SG} (mm s^{-1})		50
Time interval (s)		1.0			
Maximum value		93.8			
Minimum value		16.8			

	19.3	24.2	29.6	34.0	36.9
41.3	46.5	52.1	56.3	60.1	64.9
68.1	71.0	73.6	75.6	77.8	79.5
81.0	82.4	84.0	84.1	85.9	86.8
87.5	88.0	89.2	90.2	90.5	90.9
91.3	91.5	91.6	91.8	92.0	92.2
92.3	92.4	92.5	92.8	93.2	

Air-0.5% MlSM-Silcolapse.

Experiment number		1			
No. of points		48			
Temperature (^{o}C)		30.0	U_{SG} (mm s^{-1})		10
Time interval (s)		10.0			
Maximum value		90.9			
Minimum value		11.2			
	14.4	18.9	24.1	29.0	33.3
38.0	41.2	44.9	48.8	52.1	54.9
57.7	60.0	62.3	64.2	66.4	68.3
70.2	71.9	73.4	75.0	76.2	77.8
78.8	79.9	80.2	80.9	81.7	82.8
83.4	84.2	84.7	85.3	85.5	86.0
86.3	86.8	87.2	87.3	87.8	88.0
88.3	88.7	89.0	89.2	89.3	89.4
89.5					

Experiment number		2			
No. of points		36			
Temperature (^{o}C)		30.0	U_{SG} (mm s^{-1})		20
Time interval (s)		10.0			
Maximum value		89.0			
Minimum value		10.6			
	17.2	24.3	32.1	38.3	44.0
49.5	54.3	58.5	62.3	65.8	68.4
71.0	73.3	75.3	77.5	78.8	80.0
81.3	82.5	82.9	84.0	84.7	85.1
85.9	86.5	86.8	87.1	87.3	87.5
87.7	88.0	88.2	88.4	88.5	88.6
88.7					

Experiment number		3			
No. of points		26			
Temperature (°C)		30.0	U_{SG} (mm s^{-1})		30
Time interval (s)		10.0			
Maximum value		92.0			
Minimum value		12.2			
	14.8	24.9	35.1	45.0	52.9
59.6	65.0	69.5	73.3	76.4	79.1
81.6	83.3	85.1	86.3	87.1	87.8
88.7	89.3	90.1	90.8	91.2	91.3
91.4	91.7	91.9			

Experiment number		4			
No. of points		35			
Temperature (°C)		30.0	U_{SG} (mm s^{-1})		40
Time interval (s)		5.0			
Maximum value		93.0			
Minimum value		10.8			
	11.9	17.5	25.0	31.5	38.2
44.3	49.6	54.3	58.6	62.8	66.2
69.3	72.0	74.5	76.8	78.5	80.2
81.6	82.8	84.0	84.8	85.8	86.8
87.7	88.4	89.1	89.6	90.0	90.2
90.8	91.2	91.5	91.6	91.8	92.0

Air-2.75% MISM-silcolapse.

Experiment number		1			
No. of points		40			
Temperature (°C)		30.0	U_{SG} (mm s^{-1})		10
Time interval (s)		10.0			
Maximum value		92.1			
Minimum value		20.3			
	20.8	24.3	28.2	32.1	36.1
40.2	43.6	47.2	50.2	53.0	56.0
58.7	61.3	63.7	66.1	67.5	69.0
71.1	72.7	74.0	75.3	76.4	77.9
79.2	80.2	81.1	82.2	83.1	83.8
84.3	85.2	85.6	86.6	86.8	87.3
87.5	88.0	88.2	88.7	89.0	

Experiment number		2			
No. of points		32			
Temperature (°C)		30.0	U_{SG} (mm s^{-1})		20
Time interval (s)		10.0			
Maximum value		91.8			
Minimum value		21.1			
	27.6	33.6	40.1	45.6	50.5
55.3	59.3	63.2	66.7	69.6	72.1
74.7	76.8	78.3	80.0	81.5	82.9
83.5	84.7	85.8	86.4	87.3	87.9
88.3	88.7	89.3	89.7	90.0	90.2
90.5	90.7	90.8			

Experiment number		3			
No. of points		40			
Temperature (°C)		30.0	U_{SG} (mm s^{-1})		30
Time interval (s)		5.0			
Maximum value		91.0			
Minimum value		19.3			
	21.9	25.2	29.3	33.8	37.8
42.3	45.4	49.1	52.2	55.1	57.8
60.6	63.1	65.2	67.4	68.6	70.6
72.2	74.1	75.0	76.2	77.8	78.7
79.7	80.2	81.2	81.8	82.5	83.2
83.8	84.5	85.1	85.6	85.9	86.3
86.9	87.1	87.3	87.6	88.2	

Experiment number		4			
No. of points		36			
Temperature (°C)		30.0	U_{SG} (mm s^{-1})		40
Time interval (s)		5.0			
Maximum value		90.1			
Minimum value		19.1			
	20.1	24.8	29.7	35.1	40.3
44.5	49.4	52.9	57.1	59.9	62.8
65.2	67.5	69.6	71.3	73.7	74.4
76.2	77.7	78.4	79.8	80.4	81.6
82.1	83.1	83.6	84.0	84.5	86.5
87.0	87.6	87.8			

Air-5.0% M1SM-Silcolapse.

Experiment number		1			
No. of points		36			
Temperature (°C)		30.0	U_{SG} (mm s^{-1})		10
Time interval (s)		10.0			
Maximum value		92.9			
Minimum value		16.9			
	16.8	21.8	27.2	32.3	37.4
41.9	46.6	50.5	54.3	57.1	60.1
63.6	66.0	68.3	70.2	72.2	73.9
75.8	77.2	77.4	79.6	81.3	82.4
83.4	84.1	84.8	85.8	86.2	87.2
87.7	88.2	88.3	89.0	89.4	89.9
90.2					

Experiment number		2			
No. of points		48			
Temperature (°C)		30.0	U_{SG} (mm s^{-1})		20
Time interval (s)		5.0			
Maximum value		94.0			
Minimum value		16.8			
	19.2	23.8	28.2	32.9	36.8
40.4	44.0	47.9	51.0	53.9	56.7
59.3	62.0	64.3	66.3	68.3	70.1
71.4	72.9	74.8	76.3	77.9	79.3
80.8	82.0	82.8	84.0	84.8	85.3
86.0	86.5	87.0	87.3	87.6	87.9
88.3	89.0	89.2	89.9	90.2	90.4
90.8	91.0	91.2	91.4	91.7	91.9
92.1					

Experiment number		3			
No. of points		40			
Temperature (°C)		30.0	U_{SG} (mm s^{-1})		30
Time interval (s)		5.0			
Maximum value		94.7			
Minimum value		15.8			
	18.4	23.8	29.2	25.0	40.6
45.9	50.3	55.3	58.5	62.0	64.8
67.2	69.9	72.2	74.3	76.6	78.1
79.8	81.1	82.2	83.1	84.1	85.2
86.0	86.7	87.3	88.1	88.3	89.2
89.8	90.2	90.7	91.2	91.3	91.7
92.0	92.2	92.6	92.8	92.9	

Experiment number		4			
No. of points		36			
Temperature (°C)		30.0	U_{SG} (mm s^{-1})		40
Time interval (s)		5.0			
Maximum value		94.0			
Minimum value		16.5			
	21.1	28.0	34.8	41.6	49.0
53.8	59.1	63.6	67.0	70.2	72.7
75.4	77.5	79.3	81.0	82.3	83.6
85.0	85.8	86.6	87.5	88.0	88.5
89.1	89.7	90.2	90.6	90.8	91.3
91.5	91.9	92.2	92.3	92.5	92.7
92.9					

Air-0.5% M1SM-P2000.

Experiment number		1			
No. of points		38			
Temperature (°C)		30.0	U_{SG} (mm s^{-1})		10
Time interval (s)		10.0			
Maximum value		92.8			
Minimum value		16.2			
	20.3	25.8	31.4	36.5	42.0
46.6	51.1	54.9	58.8	62.2	65.3
68.0	70.3	72.3	74.9	76.7	78.2
79.8	80.9	82.5	83.8	84.9	85.6
86.3	87.1	87.5	88.0	88.8	89.1
89.5	90.0	90.2	90.7	91.0	91.2
91.3	91.4	91.5			

Experiment number		2			
No. of points		44			
Temperature (°C)		30.0	U_{SG} (mm s^{-1})		20
Time interval (s)		5.0			
Maximum value		90.0			
Minimum value		16.2			
	18.6	22.7	27.1	32.0	34.8
39.6	43.8	47.8	51.1	53.6	56.3
59.1	61.9	64.1	66.0	68.1	69.7
71.1	73.0	74.5	76.9	77.2	78.2
79.3	80.3	81.2	81.5	82.7	83.2
83.8	84.3	85.0	85.5	85.9	86.2
86.6	86.7	87.2	87.8	88.1	88.2
88.3	88.5	88.6			

Experiment number		3			
No. of points		34			
Temperature (°C)		30.0	U_{SG} (mm s^{-1})		30
Time interval (s)		5.0			
Maximum value		91.0			
Minimum value		15.2			
	19.3	25.1	30.8	36.3	42.5
47.1	51.8	56.4	59.8	63.0	65.9
68.6	71.2	73.3	75.3	76.6	78.3
80.0	81.2	82.5	83.5	84.3	85.2
85.8	86.3	87.0	87.2	87.7	87.8
88.5	89.0	89.2	89.3	89.5	

Experiment number		4			
No. of points		32			
Temperature (°C)		30.0	U_{SG} (mm s^{-1})		40
Time interval (s)		5.0			
Maximum value		89.5			
Minimum value		16.3			
	19.9	26.8	34.2	41.7	48.0
54.1	59.0	63.2	66.9	70.1	73.0
75.1	77.2	78.8	80.5	81.9	82.7
83.9	84.7	85.3	85.7	86.3	86.8
86.9	87.1	87.6	87.9	88.0	88.2
88.3	88.5	88.6			

Air-2.75% M1SM-P2000.

Experiment number		1			
No. of points		40			
Temperature (°C)		30.0	U_{SG} (mm s^{-1})		10
Time interval (s)		10.0			
Maximum value		90.3			
Minimum value		15.1			
	19.2	23.7	28.1	32.5	36.7
40.8	44.7	48.3	51.3	54.5	57.2
59.8	62.5	64.7	67.0	68.4	70.6
72.2	73.9	75.2	76.6	77.3	78.4
79.5	80.6	81.3	82.2	83.0	83.6
84.3	84.9	85.1	85.8	86.2	86.4
87.1	87.4	87.8	87.9	88.2	

Experiment number		2			
No of points		32			
Temperature (°C)		30.0	U_{SG} (mm s^{-1})		20
Time interval (s)		10.0			
Maximum value		92.2			
Minimum value		16.2			
	17.6	24.8	31.6	38.3	45.1
51.4	56.3	60.3	64.4	67.7	70.1
72.8	75.2	77.0	78.7	80.4	81.2
82.7	83.8	84.8	85.9	86.4	87.2
87.6	88.2	88.4	89.0	89.3	89.7
90.0	90.2	90.3			

Experiment number		3			
No. of points		48			
Temperature (°C)		30.0	U_{SG} (mm s^{-1})		30
Time interval (s)		5.0			
Maximum value		92.0			
Minimum value		15.3			
	17.2	21.0	26.6	30.6	36.4
40.6	45.8	49.4	53.2	56.3	59.2
61.7	63.9	66.0	67.6	69.7	71.4
72.7	74.6	75.4	77.1	78.1	78.8
79.8	80.5	81.6	82.3	83.1	84.0
84.8	84.9	85.3	85.6	86.3	86.4
86.8	87.2	87.3	87.8	88.0	88.3
88.4	88.6	88.9	89.0	89.2	89.3
89.4					

Experiment number		4			
No. of points		42			
Temperature (°C)		30.0	U_{SG} (mm s^{-1})		40
Time interval (s)		5.0			
Maximum value		91.0			
Minimum value		15.2			
	20.3	28.8	33.0	39.2	44.7
49.4	53.7	57.7	61.1	64.0	67.4
69.1	70.2	72.6	74.3	76.0	77.2
78.3	79.4	80.1	81.3	82.1	82.7
83.2	83.9	84.4	84.8	85.2	85.7
85.8	86.2	86.7	87.2	87.3	87.4
87.9	88.0	88.3	88.6	88.8	88.9
89.0					

Air-5.0% MISM-P2000.

Experiment number		1			
No. of points		32			
Temperature (°C)		30.0	U_{SG} (mm s^{-1})		10
Time interval (s)		10.0			
Maximum value		89.2			
Minimum value		14.0			
	24.5	30.1	35.3	40.3	44.2
48.2	51.8	55.3	58.6	61.2	63.9
65.8	68.3	70.4	72.2	73.8	75.2
76.5	77.1	78.6	79.3	80.6	81.4
82.1	82.8	83.2	84.3	84.8	84.9
85.2	85.8	86.0			

Experiment number		2			
No. of points		26			
Temperature (°C)		30.0	U_{SG} (mm s^{-1})		20
Time interval (s)		10.0			
Maximum value		89.2			
Minimum value		15.1			
	22.2	31.0	40.2	47.2	53.2
58.6	62.7	66.3	70.0	73.2	75.2
77.3	79.0	80.5	81.3	83.0	83.6
84.2	85.2	85.6	86.2	86.7	87.2
87.8	87.9	88.0			

Experiment number		3			
No. of points		36			
Temperature (°C)		30.0	U_{SG} (mm s^{-1})		30
Time interval (s)		5.0			
Maximum value		88.3			
Minimum value		13.9			
	17.2	23.8	30.0	35.7	41.2
46.4	52.0	55.8	59.1	62.5	64.9
68.0	70.0	71.9	73.5	75.3	76.5
77.5	79.1	79.8	80.7	81.4	82.1
82.7	83.2	83.7	84.5	84.8	85.2
85.8	85.9	86.2	86.4	86.7	87.0
87.1					

Experiment number		4			
No. of points		30			
Temperature (°C)		30.0	U_{SG} (mm s^{-1})		40
Time interval (s)		5.0			
Maximum value		87.8			
Minimum value		13.0			
	15.8	23.9	32.2	39.9	46.4
51.6	56.3	60.9	64.6	67.9	70.5
72.6	74.3	75.9	77.2	78.5	79.7
80.6	81.4	82.2	83.0	83.5	84.1
84.7	85.2	85.3	85.5	85.8	86.0
86.2					

Three-phase run.

Experiment number		1			
No. of points		43			
Temperature (°C)		30.0	U_{SG} (mm s^{-1})		1
Time interval (s)		5.0			
Maximum value		101.0			
Minimum value		9.4			
	11.1	16.0	22.3	28.0	33.8
38.2	43.6	48.2	52.8	56.3	59.9
63.1	66.6	69.3	71.8	74.3	76.9
78.6	80.7	82.3	83.8	85.2	86.1
87.4	88.7	89.7	90.1	91.3	92.5
92.6	93.3	94.1	94.2	95.2	95.7
96.1	96.6	97.0	97.4	97.7	97.8
97.9	98.0				

Experiment number		2			
No. of points		45			
Temperature (°C)		30.0	U_{SG} (mm s^{-1})		10
Time interval (s)		5.0			
Maximum value		96.1			
Minimum value		9.7			
	11.7	17.5	22.8	28.8	34.2
39.1	43.8	48.3	52.3	55.7	59.0
62.4	65.2	68.0	70.3	72.0	74.1
76.2	77.8	79.2	80.6	81.3	82.9
83.9	84.7	85.5	86.5	87.1	87.6
88.2	88.7	89.3	89.9	90.1	90.2
90.8	91.0	91.8	91.9	92.6	92.8
92.9	93.1	93.3	93.9		

Experiment number		3			
No. of points		37			
Temperature (°C)		30.5	U_{SG} (mm s^{-1})		10
Time interval (s)		5.0			
Maximum value		98.7			
Minimum value		16.2			
	18.0	23.7	29.4	36.8	41.7
47.7	52.6	57.1	60.9	65.0	68.5
71.3	74.2	76.2	78.5	80.8	82.5
83.9	85.3	86.3	88.0	88.8	90.3
90.9	91.0	92.6	92.7	92.9	93.5
93.9	94.0	94.9	95.0	95.1	95.5
96.0	96.4				

Experiment number		4			
No. of points		40			
Temperature (°C)		30.0	U_{SG} (mm s^{-1})		10
Time interval (s)		5.0			
Maximum value		96.5			
Minimum value		10.2			
	11.6	17.4	23.7	29.1	35.3
40.3	46.3	51.0	55.1	58.3	62.3
65.2	67.9	70.2	72.1	74.3	76.2
78.1	79.3	80.8	82.4	83.3	84.3
85.0	86.1	87.0	87.6	88.3	89.2
89.4	90.2	90.7	90.8	91.2	91.6
91.9	92.3	92.6	93.1	93.2	

Experiment number		5			
No. of points		42			
Temperature (°C)		30.0	U_{SG} (mm s^{-1})		10
Time interval (s)		5.0			
Maximum value		90.0			
Minimum value		10.1			
	13.8	18.7	24.3	30.8	36.9
41.3	46.0	50.8	54.1	58.0	61.1
64.0	66.6	68.8	70.4	72.3	73.8
75.1	76.7	77.2	78.3	79.2	80.4
81.2	82.0	82.6	82.9	83.4	84.2
84.3	85.0	85.3	85.6	86.0	86.4
86.8	86.9	87.0	87.3	87.5	87.8
88.2					

Experiment number		6			
No. of points		56			
Temperature (°C)		30.0	U_{SG} (mm s^{-1})		10
Time interval (s)		5.0			
Maximum value		82.0			
Minimum value		10.3			
	12.7	15.1	17.4	20.8	23.7
26.6	30.0	33.0	35.3	38.2	40.7
42.6	44.8	47.3	48.9	50.7	52.8
53.8	55.7	57.0	58.0	59.2	60.6
61.6	62.8	63.4	64.8	65.3	66.2
67.0	67.9	68.6	68.8	69.8	70.2
70.8	71.5	71.6	72.6	72.9	73.1
73.8	74.3	74.4	75.0	75.3	75.4
76.0	76.3	76.7	77.0	77.2	77.3
77.7	77.8	78.0			

Experiment number		7			
No. of points		55			
Temperature (^{o}C)		30.0	U_{SG} (mm s^{-1})		10
Time interval (s)		5.0			
Maximum value		81.6			
Minimum value		9.8			
	10.3	12.9	15.4	19.0	21.6
24.3	27.9	29.8	33.0	36.4	38.3
40.6	42.4	45.0	46.8	49.2	50.5
57.8	53.9	55.0	56.7	57.8	59.2
60.4	61.0	62.3	63.3	64.3	65.2
65.8	66.8	67.8	68.0	68.4	68.9
69.6	70.4	71.1	71.2	71.6	72.2
72.7	73.1	73.2	74.1	74.2	74.3
74.8	75.2	75.5	75.6	75.8	76.1
76.2	76.8				

Experiment number		8			
No. of points		48			
Temperature (^{o}C)		30.0	U_{SG} (mm s^{-1})		10
Time interval (s)		5.0			
Maximum value		80.9			
Minimum value		9.2			
	11.3	13.5	16.0	19.7	22.8
25.6	28.6	31.1	34.0	36.2	38.3
41.1	43.1	44.8	46.2	48.3	50.0
51.6	53.2	54.6	55.5	57.0	57.9
59.2	60.5	61.2	62.2	62.9	63.4
64.8	65.3	66.1	66.6	67.4	67.9
68.7	69.4	69.9	70.1	70.2	71.2
71.8	72.1	72.2	72.7	73.1	73.3
73.9					

Experiment number		9			
No. of points		55			
Temperature (°C)		30.0	U_{SG} (mm s^{-1})		10
Time interval (s)		5.0			
Maximum value		79.1			
Minimum value		9.8			
	10.6	12.3	14.8	17.1	20.6
23.4	26.2	29.0	31.5	34.2	36.3
39.1	41.3	43.8	45.2	47.4	49.2
50.2	52.0	53.3	54.9	56.1	57.0
58.3	59.5	60.5	61.7	62.4	63.2
63.7	65.0	65.8	66.4	66.9	67.2
68.3	68.8	69.1	69.7	69.8	70.6
71.3	71.7	71.8	71.9	72.3	72.9
73.2	73.9	74.0	74.1	74.3	74.4
74.9	75.2				

Experiment number		10			
No. of points		46			
Temperature (°C)		29.0	U_{SG} (mm s^{-1})		20
Time interval (s)		5.0			
Maximum value		83.8			
Minimum value		12.3			
	12.7	15.8	20.0	24.3	28.7
33.3	38.0	41.6	46.2	49.1	52.6
55.8	57.3	60.0	62.1	64.1	65.7
67.3	68.3	69.9	71.1	72.3	73.1
73.7	74.2	74.9	75.8	76.3	77.0
77.5	78.2	78.4	78.9	79.1	79.3
79.8	80.2	80.3	80.6	80.9	81.2
81.3	81.6	81.8	81.9	82.0	

Experiment number		11			
No. of points		43			
Temperature (°C)		29.5	U_{SG} (mm s^{-1})		20
Time interval (s)		5.0			
Maximum value		82.1			
Minimum value		9.3			
	10.6	13.5	17.6	22.8	27.6
32.2	36.4	40.3	44.0	48.1	50.8
53.6	56.5	58.4	60.8	62.4	64.3
65.6	67.4	68.8	69.7	70.5	71.7
72.3	73.0	73.6	73.8	74.6	75.2
75.8	76.3	76.7	77.0	77.5	77.9
78.2	78.3	78.4	78.8	79.1	79.3
79.4	79.5				

Experiment number		12			
No. of points		39			
Temperature (°C)		30.0	U_{SG} (mm s^{-1})		20
Time interval		5.0			
Maximum value		82.1			
Minimum value		8.8			
	9.9	14.0	18.7	23.3	29.8
33.4	38.9	42.0	46.5	50.3	53.0
55.8	58.1	59.8	62.1	63.9	66.5
67.3	68.8	69.3	70.4	71.8	72.4
73.2	74.2	75.2	75.4	76.0	76.8
77.0	77.3	77.9	78.0	78.1	79.0
79.2	79.3	79.4	79.8		

Experiment number		13			
No. of points		29			
Temperature (^{o}C)		30.0	U_{SG} (mm s^{-1})		20
Time interval (s)		5.0			
Maximum value		79.8			
Minimum value		9.7			
	13.5	18.1	21.9	26.3	30.9
35.2	39.3	42.8	47.0	50.0	52.3
54.9	57.3	59.6	61.2	62.7	64.0
65.3	67.0	68.0	68.5	69.8	70.5
70.8	71.5	72.3	72.8	73.2	74.2

Experiment number		14			
No. of points		36			
Temperature (^{o}C)		30.0	U_{SG} (mm s^{-1})		20
Time interval (s)		5.0			
Maximum value		76.9			
Minimum value		9.3			
	12.8	18.1	22.2	26.8	31.1
36.7	39.5	42.8	46.2	49.0	51.5
54.2	56.7	58.5	60.1	61.7	63.1
64.0	64.8	66.3	67.2	68.2	69.0
69.6	70.2	71.0	71.4	71.7	72.1
72.2	72.5	72.9	73.2	73.3	74.0
74.2					

Experiment number		15			
No. of points		33			
Temperature (^{o}C)		30.0	U_{SG} (mm s^{-1})		20
Time interval (s)		5.0			
Maximum value		69.9			
Minimum value		8.2			
	11.2	14.5	18.6	22.0	27.0
30.4	35.0	38.7	42.3	45.0	47.2
49.5	51.2	53.2	55.1	56.0	57.6
58.8	60.1	60.3	61.8	62.2	63.2
63.8	64.0	64.2	64.7	65.6	65.8
66.2	66.5	66.8	66.9		

Experiment number		16			
No. of points		40			
Temperature (^{o}C)		30.0	U_{SG} (mm s^{-1})		20
Time interval (s)		5.0			
Maximum value		66.0			
Minimum value		8.2			
	9.6	12.6	16.6	20.5	24.2
27.9	32.8	35.3	38.8	41.8	44.2
46.2	48.1	49.8	51.3	52.7	54.0
55.0	56.1	57.0	58.0	58.8	59.4
60.2	60.8	61.3	61.7	62.0	62.2
62.6	62.8	63.0	63.5	63.9	64.0
64.1	64.2	64.3	64.6	64.8	

Experiment number		17			
No. of points		31			
Temperature (°C)		30.0	U_{SG} (mm s^{-1})		20
Time interval (s)		5.0			
Maximum value		62.7			
Minimum value		9.0			
	10.7	14.2	17.3	21.0	25.3
28.4	32.6	35.5	38.3	41.2	43.2
44.8	46.1	48.5	50.1	51.0	52.2
53.2	54.2	55.2	55.8	56.2	57.0
57.1	57.2	58.2	58.7	59.0	59.1
59.8	60.0				

Experiment number		18			
No. of points		29			
Temperature (°C)		30.0	U_{SG} (mm s^{-1})		20
Time interval (s)		5.0			
Maximum value		59.0			
Minimum value		9.0			
	11.2	14.2	17.2	21.7	23.9
27.1	30.8	33.7	36.3	38.8	40.7
43.0	44.4	46.0	47.1	48.1	49.4
50.3	51.2	52.3	53.4	54.0	54.1
54.7	55.0	55.1	55.2	55.4	56.2